EARTH RESOURCES TECHNOLOGY SATELLITE
FINAL REPORT

17. NASA DATA PROCESSING FACILITY STUDIES

PREPARED FOR

GODDARD SPACE FLIGHT CENTER
NATIONAL AERONAUTICS
AND SPACE ADMINISTRATION

UNDER CONTRACT NAS5-11260

TRW
SYSTEMS GROUP

IBM
FEDERAL
SYSTEMS
DIVISION

Itek
OPTICAL
SYSTEMS
DIVISION

EARTH RESOURCES TECHNOLOGY SATELLITE

FINAL REPORT

Volume 17. NASA Data Processing Facility Studies

April 17, 1970

prepared for

National Aeronautics and Space Administration
Goddard Space Flight Center

Contract NAS5-11260
item 5a

TRW Systems Group
One Space Park · Redondo Beach
Los Angeles County
California 90278

CONTENTS

CONTENTS (Continued)

1. Introduction

CONTENTS

1. INTRODUCTION

1.1 BASIC PROBLEMS TO BE STUDIED

The function of the NDPF is to accept data collected by ERTS and to present this data to users, in usable form, properly annotated, and as free as possible from the errors and anomalies introduced by the sensors and the data handling system. It also maintains a library of all past data and the means to retrieve further processes and reproduce them on request.

Even before the studies began there were a number of technical problems recognized.

- Internal picture distortions, because of the electronic imagery systems.

- Distortions in pictures, because of the spacecraft motions.

- Uncertainty in picture center, because of the spacecraft attitude uncertainties.

- The need to correlate all data, both imagery and DCS, with orbital data.

- Data management of the large volume of information collected.

In addition to these well known problems, there were a number of less known, but equally important, problems which range from the size film to be used through definition of digital techniques applicable to the correction of internal distortions.

The studies have been aimed to:

- Find and correct errors in the most cost effective manner.

- Ensure that data, which users want, can be retrieved when needed.

- Ensure that all data is properly formatted, annotated, and handled to provide the maximum utility to users.

- Optimize the overall NDPF from a cost/performance point of view, consistent with the flexibility requirements of a technology system.

- Determine the supporting requirements in storage/retrieval, data handling, and production control

1.2 STUDY DEFINITION CRITERIA

The specific study areas, as defined by the proposal and contract, are summarized in Volume 1. These may be grouped as follows:

- Identification of significant error sources and functions to be performed.

- Definition of various theoretical approaches to error correction.

- Specification of technologies required to implement solutions.

- Selection of optimal approaches.

In selecting the specific studies, and in performing them, these basic criteria served as guides:

a) The data collected by imagery must be reproducible with the maximum meaningful fidelity.

b) Where fidelity and cost conflict, the system must provide for various fidelity/cost options (from lowest cost to highest fidelity, with as many in-between points as practical).

c) Studies must provide parametric data to explore variations of the system design.

In addition to the studies on image processing, the subjects of information management, storage and retrieval, and production control have been examined. These functions are critical to the proper operation of the system.

1.3 SCOPE OF STUDIES

The studies described in the following sections provide the data required for system design. The studies do not, in general, describe the design; that task is accomplished in Volume 14.

The studies cover not only the techniques which will be used in the final system, but also include those techniques and devices which have been rejected; this provides the rationale upon which the selections of the final design have been made.

There are a few exceptions to this rule; e.g., in Section 2.8 the laser beam recorder selection is described; in Section 2.2, the UTM coordinate grid system is recommended.

In general, however, this volume provides the alternatives, performance, and problems of techniques upon which the final system tradeoff has been based.

2. Image Processing

CONTENTS

2. IMAGE PROCESSING

2.1 INTRODUCTION

One of the major aims of ERTS is to produce multispectral images from the data returned by the spacecraft electronic cameras. The latter have a number of known distortions; it is a key element of the study to identify the error sources, and to examine alternative means to correct these errors.

'The studies were initiated by defining the error sources. Because the most significant errors are geometric, a special set of studies has been performed on the extraction of reseau points.

Having defined the error sources and having determined the theoretical approach to error correction, two applicable technologies, digital and optical, are identified which provide the means to implement the correction algorithms. Studies were carried out on many constituent elements of each technology area.

Geodetic control, or the application of ground truth to obtain precise data on both picture location and spacecraft attitude, has received special attention, since it is proposed to use the information from a limited number of pictures to improve the overall system picture location accuracy.

Annotation has received particular attention since poorly annotated imagery complicates the job of the analysis unduly. Techniques for providing system photometric calibration also are included to enhance the quality of the output product.

The imagery is only as good as the device which is used to convert the electronic signals into exposed film. The relevant devices, election beam recorders (EBR) and laser beam recorders (LBR) have been studied from two points of view: the theoretical possibilities of the technology, and the performance of specific designs.

Among the techniques for correcting geometric distortions in RBV and MSS images, beam position modulation deserves attention. As indicated in Section 2.2 the essence of image correction requires the determination of two functions:

$$\Delta X = f_1 (XY)$$

$$\Delta Y = f_2 (XY)$$

which describe how to move each point in the image to remove the distortion. Once these functions are generated several candidate techniques for applying them exist. Optical means are discussed in Section 2.4 and digital techniques are discussed in Section 2.5. Here we are concerned with actually incrementing the sweep signals, so that the instantaneous value of the video wave train is written where it would be in the corrected image, rather than where it would be placed if the scans were perfectly linear.

To implement this approach requires an incremental sweep generator to supplement the normal linear sweep. It also requires a video reproducer capable of following the sweep position modulation and having sufficient inherent stability to preclude introducing a new set of distortions.

Included in the video reproducers which meet the needs of beam position modulation are electron beam recorders and cathode ray tubes. Laser beam recorders cannot be considered because of the difficulty of position modulating the laser beam. Analyses of the advantages and disadvantages of EBR's, LBR's and CRTS are presented in Section 2.8. which indicate that an LBR is the proper choice for converting ERTS video data to images. Thus, beam position modulation is dropped as a serious contender for geometric image correction. Other points supporting this decision are the lack of a digital tape as the by-product of the correction process and potential cosmetic problem if the distortions become too severe or too abrupt.

2.2 ERROR SOURCES AND CORRECTION TECHNIQUES ANALYSIS

The primary concern of ERTS is the capability of providing multispectral images. The user must be able to specify the location of the data recognized from the returned images. The output of the system is to be used by a diverse community of users who may be expected to use ground truth verifications of radiometric and geometric accuracy.

Radiometric accuracy in the two camera systems to be flown is achieved by calibration against the sun or a calibrated light source in the satellite. Geometric accuracy is achieved by calibration against a set of reseaux in one camera system and by using the best available ephemeris and attitude data in both camera systems.

The output images, compared either to a standard image or to a given performance measure, will contain errors. The errors in the images may be classified into groups:

1) Geometric: nonlinearity, pincushion, projection.

2) Radiometric: atmosphere, modulation transfer function, gamma, shading, channel noise

3) Reproduction: introduced between the received signal and the output image.

The image processing approach is to remove as much as possible of the first two groups, while introducing as few as possible in the third. The extent of the removal of image errors depends on knowledge of the error sources and the resources available to spend on a given image for correction. There will initially be a steep drop in error versus expenditure where the basic geometrical and radiometric errors are being removed, but the removal of the final errors (such as modulation transfer function and image motion) will be on a much flatter part of the performance curve and will be less cost effective. A balance must be reached. A second balance must be reached between error removal and speed of processing.

In this section, we present an analysis of the errors, categorized as projection errors, deviation between image and desired projection, RBV errors, MSS errors, coherent noise removal, and analysis of quantization.

2.2.1 Projection Errors and Coordinate Transform

The imagery from ERTS must be presented to users in some standard projection, which will permit ready comparison with other data on existing maps. This leads to a need to transform the image, for the difference between the image and the desired projection. The analysis of the effects involve:

- Terrain relief

- Scale factor: overall altitude change

- Desired map projection system.

Terrain relief effect is depicted in Figure 2.2-1, which shows the usual effect of mountains appearing to "lean out" at the edge of the picture. "A" is the true geodetic position of the mountain top, "C" is its apparent position due to terrain relief.
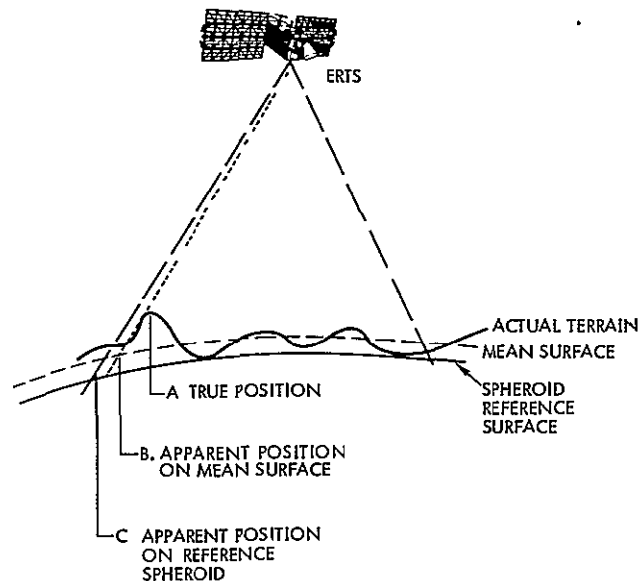
Figure 2.2-1

TERRAIN RELIEF EFFECT

If one passes a new surface, labeled "mean surface" in the figure, through the terrain, parallel to the reference spheroid, one obtains position "D", which has less displacement. Valleys on the other hand now "lean" inward.

One should note that terrain relief can exist for simply a high plateau with no mountain peaks. If one corrects to the mean surface, then the terrain errors vanish in this case. In any case, using the mean surface reduces the error, it completely eliminates bias, i.e., mean altitude variation, and reduces the RMS error by a factor of two.

The maximum magnitude of terrain error can be estimated as shown in Figure 2.2-2. The projection angle is 0.1 radian. For the highest mountains on earth, this leads to a maximum terrain error of 0.4 N mi, or roughly 2400 feet on the reference spheroid.
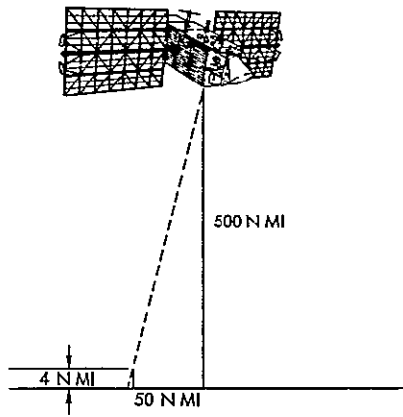
Figure 2.2-2

MAXIMUM TERRAIN RELIEF ERROR

By using a mean surface, this error is reduced significantly. Few, if any, peaks tower more than 2 N mi above the surrounding terrain. The mean surface deviation thus rarely exceeds 1 N mi; the resulting maximum terrain error is then 0.1 N mi, or 600 feet.

Since the highest mountains are not always right at the edge of the picture, they are found with equal probability across the picture, reducing the mean terrain error, in mountainous areas, to 300 feet.

In relatively flat areas, such as farming areas, altitude difference drops to perhaps 3000 feet, or ±1500 feet from a mean surface, reducing the maximum error to 150 feet, or the mean error to 75 feet. Care will be taken to annotate each picture which has been corrected to a mean

datum so that further correction by a user will be to the proper reference.

In summary, if terrain is modeled to provide a mean surface, the average terrain error ranges from 75 feet in smooth areas to 300 feet in rougher areas.

Spacecraft altitude changes, or changes in the reference surface, lead to magnification scale changes. The effect of such changes is to dilate or contract the image linearly.

2.2.1.1 Universal Transverse Mercator Coordinate System

There are many methods for projecting the earth's surface on representative planes. A representation of the earth cannot be projected directly on a plane and simultaneously retain all lines, distances, angles, and areas in true relation to one another.

The desirable characteristics of any projection are easily shown. To aid the choice of a map-projection type, maps can be grouped into the following primary categories:

1) An equal area projection to maintain a correct proportion between actual land areas and projected land areas at the expense of incorrectly represented land shapes.

2) A conformal projection that correctly represents the shape of smaller geographic features at the expense of changing scale over large expanses of land and water; this projection does not retain true shapes of large areas.

3) A projection that compromises between equal area and conformal, thereby minimizing misrepresentation of both size and shape.

4) An azimuthal projection that preserves a consistency of correct directions of all lines drawn from one point on the map.

For small areas or large scales, 1:250,000 to 1:20,000, the conformal or orthomorphic projection, Lambert conformal, is most commonly used by countries in the lower latitudes if they are not long, narrow, north-south oriented countries, e.g., Chile. For nautical purposes the Mercator projection method is used since angles, azimuths, are preserved best. For aerial navigation, large planning charts, and in polar areas,

the azimuthal projections, stereographic and gnomonic, are frequently used. States oriented in a north-south direction use the transverse Mercator method to reduce distortion.

The two principal projections used in the United States are the Lambert conformal and the universal transverse Mercator (UTM). Both are a series of projections over relatively narrow strips of several degrees so that the distortions are minimized. However, when a choice must be made between the two methods, additional complications arise. First, the grids chosen to be placed on these projections must be studied to determine if a choice is necessary based on the grid system. Second, our photograph is an orthographic projection, so we might need a projection that minimizes the differences between the photograph we have and the projection we want.

Each state in the United States has the responsibility for surveying property within its respective boundaries. Although the U. S. Coast and Geodetic Service gives accurate first-order survey lines, the states have designed their surveys to minimize the distortions within their boundaries. Furthermore, most states use an origin close to, but outside, their southwestern corner to ensure that all values are positive. Negative coordinates are possible for offshore islands of Florida, Puerto Rico, and Maine. Thirty-two states use Lambert conformal and 26 use universal transverse Mercator. Some states use more than one system, and the United States is divided into 131 projection and grid zones. Photographs that are 100 kilometers square will cross state boundaries so that processing of large amounts of data in such a variety of systems becomes inconceivable, even for such a small task as putting grid marks of several states on one photograph.

The U. S. Geological Survey and the U. S. Coast and Geodetic Service have set up a single system using three north-south bands and eight east-west strips, 24 zones of projection, that can be computerized. From these zones, any transverse Mercator state grid can be converted by changing the coordinate origin; a more lengthy calculation converts to the Lambert conformal state grid. However, with the accuracies expected for ERTS, the UTM can be equated to the Lambert for all practical purposes.

The UTM was chosen for several reasons. All federal charts are annotated with its grid and most state charts have the UTM, federal system, on their charts. All persons using a chart, including surveyors, are familiar with it, and may regard it as the only other grid system of universal use, the primary system being latitude and longitude.

The UTM is a cylindrical, conformal, transverse projection tangent to the earth at a specified meridian, like the equator of the mercator. The UTM is also called the Lambert orthomorphic projection since Lambert developed it also. Gauss and Kruger developed it independently and it is called the Gauss-Kruger minimal length distortion projection elsewhere. It is officially used for geodetic mapping in the Soviet Union, Germany, Great Britain and many former colonies, and for most federal surveys in the United States. Thus, UTM is recommended as the grid for ERTS.

2.2.1.2 Computation of UTM Coordinates for ERTS

The following procedure is used in computing UTM coordinates for ERTS.

a) Data

Entry data are the latitude and longitude of the center coordinate (principal point) and the heading of the spacecraft (ϕ, λ, α).

Locate the appropriate zone number and longitudinal value of its central meridian from a list of zone numbers, central meridians, and bounding meridians (see Table 2.2-1). For example, position λ 96° 02' W, ϕ 34° 15' N is in zone 14 with central meridian 99W.

Begin computations. Permanent stored data (Clarke 1866 spheroid) are:

a = semimajor axis of the spheroid = 6,378,206.4

b = semiminor axis of the spheroid = 6,356,585.36

e^2 = eccentricity = $(a^2 - b^2)/a^2$ = 0.00676817

k_o = 0.9996 (scale factor for UTM).

Table 2.2-1. Zone Numbers With Central and Bounding Meridians

Zone Number	Central Meridian	Bounding Meridians	Zone Number	Central Meridian	Bounding Meridians	Zone Number	Central Meridian	Bounding Meridians
1	177° W	180° 174° W	21	57° W	60° W 54° W	41	63° E	60° E 66° E
2	171° W	174° W 168° W	22	51° W	54° W 48° W	42	69° E	66° E 72° E
3	165° W	168° W 162° W	23	45	48° W 42° W	43	75° E	72° E 78° E
4	159° W	162° W 156° W	24	39° W	42° W 36° W	44	81° E	78° E 84° E
5	153° W	156° W 150° W	25	33° W	36° W 30° W	45	87° E	84° E 90° E
6	147° W	150° W 144° W	26	27° W	30° W 24° W	46	93° E	90° E 96° E
7	141° W	144° W 138° W	27	21° W	24° W 18° W	47	99° E	96° E 102° E
8	135° W	138° W 132° W	28	15° W	18° W 12° W	48	105° E	102° E 108° E
9	129° W	132° W 126° W	29	09° W	12° W 06° W	49	111° E	108° E 114° E
10	123° W	126° W 120° W	30	03° W	06° W 00°	50	117° E	114° E 120° E
11	117° W	120° W 114° W	31	03° E	00° 06° E	51	123° E	120° E 126° E
12	111° W	114° W 108° W	32	0)° E	06° E 12° E	52	129° E	126° E 132° E
13	105° W	108° W 102° W	33	15° E	12° E 18° E	53	135° E	132° E 138° E
14	99° W	102° W 96° W	34	21° E	18° E 24° E	54	141° E	138° E 144° E
15	93° W	96° W 90° W	35	27° E	24° E 30° E	55	147° E	144° E 150° E
16	87° W	90° W 84° W	36	33° E	30° E 36° E	56	153° E	150° E 156° E
17	81° W	84° W 78° W	37	39° E	36° E 42° E	57	159° E	156° E 162° E
18	75° W	78° W 72° W	38	45° E	42° E 48° E	58	165° E	162° E 168° E
19	69° W	72° W 66° W	39	51° E	48° E 54° E	59	171° E	168° E 174° E
20	63° W	66° W 60° W	40	57° E	54° E 60° E	60	177° E	174° E 180°

b) Additional notations are:

ϕ = latitude

λ = longitude

ϕ' = latitude at foot of perpendicular from the point to the central meridian

λ_o = longitude of origin (central meridian)

$\Delta\lambda$ = difference of longitude of point and central meridian
= $\lambda - \lambda_o$ in Eastern Hemisphere, $\lambda_o - \lambda$ in Western Hemisphere

f = flattening or ellipticity = $(a - b)/a$

e^2 = (eccentricity)^2 = $(a^2 - b^2)/a^2$

e'^2 = $(a^2 - b^2)/b^2 = e^2/1 - e^2$

n = $(a - b)/a + b$

ρ = radius of curvature on the meridian = $a(1 - e^2)/(1 - e^2 \sin^2 \phi)^{3/2}$

ν = radius of curvature in the prime vertical; also defined as the normal to the spheroid terminating at the minor axis = $a/(1 - e^2 \sin^2 \phi)^{1/2} = \rho (1 + e'^2 \cos^2 \phi)$

S = true meridianal distance from equator on the spheroid

K = scale factor at the working point on the projection

FN = false northing

FE = false easting

E' = grid distance from the central meridian (always positive)

N = grid northing

t = plane azimuth (measured from grid north) (grid azimuth)

T = projected geodetic azimuth (measured from grid north) (grid azimuth)

α = geodetic azimuth

C = convergence of the meridians, i. e., the angle between true north and grid north

p = $0.0001\Delta\lambda$

q = $0.000001E'$

The following formulas are used

$$(I) = Sk_o$$

where

$$(I) = k_o \left[a(1 - e^2) \left(A\phi - \frac{B}{2} \sin 2\phi + \frac{C}{4} \sin 4\phi - \frac{D}{6} \sin 6\phi \right. \right.$$

$$\left. \left. + \frac{E}{8} \sin 8\phi \right) \right]$$

where

$$A = 1 + \frac{3}{4}e^2 + \frac{45}{64}e^4 + \frac{175}{256}e^6 + \frac{11,025}{16,384}e^8 + \frac{43,659}{65,536}e^{10}$$

$$B = \frac{3}{4}e^2 + \frac{15}{64}e^4 + \frac{525}{512}e^6 + \frac{2,205}{2,048}e^8 + \frac{72,765}{65,536}e^{10}$$

$$C = \frac{15}{64}e^4 + \frac{105}{256}e^6 + \frac{2,205}{4,096}e^8 + \frac{10,395}{16,384}e^{10}$$

$$D = \frac{35}{512}e^6 + \frac{315}{2,048}e^8 + \frac{31,185}{131,072}e^{10}$$

$$E = \frac{315}{16,384}e^8 + \frac{3,465}{65,536}e^{10}$$

$$F = \frac{693}{131,072}e^{10}$$

$$(II) = \frac{\nu \sin \phi \cos \phi \sin^2 1''}{2} k_o 10^8$$

$$(III) = \frac{\sin^4 1'' \, \nu \, \sin \phi \cos^3 \phi}{24} (5 - \tan^2 \phi + 9e'^2 \cos^2 \phi$$

$$+ 4e'^4 \cos^4 \phi) K_o 10^{16}$$

$$A_6 = p^6 \frac{\sin^6 1'' \; \nu \; \sin \phi \; \cos^5 \phi}{720} (61 - 58 \tan^2 \phi + \tan^4 \phi$$

$$+ \; 270 e'^2 \cos^2 \phi - 330 e'^2 \sin^2 \phi)$$

$$N = (I) + (II)p^2 + (III)p^4 + A_6 \qquad \text{for points north of the equator}$$

$$N = 10,000,000 - [(I) + (II)p^2 \qquad \text{for points south of the equator}$$

$$+ \; (III)p^4 + A_6]$$

$$(IV) = \nu \cos \phi \sin 1'' k_o 10^4$$

$$(V) = \frac{\sin^3 1'' \; \nu \; \cos^3 \phi}{6} (1 - \tan^2 \phi + e'^2 \cos^2 \phi) k_o 10^{12}$$

$$B_5 = p^5 \frac{\sin^5 1'' \; \nu \; \cos^5 \phi}{120} (5 - 18 \tan^2 \phi + \tan^4 \phi$$

$$+ \; 14 e'^2 \cos^2 \phi - 58 e'^2 \sin^2 \phi) k_o 10^{20}$$

$$E = 5,000,000 \pm [(IV)p + (V)p^3 + B_5]$$

Note that plus refers to points east of a central meridian and minus refers to points west of the same meridian. The east and north figures are the UTM for a given zone. Further data is necessary for the complete grid zone designation.

For convenience, the world is divided into large geographical areas extending 6 degrees in longitude and 8 degrees in latitude. Each area is given an identification called the grid zone designation. These 6- by 8-degree areas are subdivided into 100,000-meter squares, based on the grid covering the area, with each square given a two-letter identification. Numerical references within these 100,000-meter squares are given to the desired accuracy in terms of the east and north grid coordinates of the point. Ordinarily, a reference is expressed only in numerical terms. When reporting beyond a 100,000-meter square and when reporting under certain other conditions, the reference is prefixed with the 100,000-meter

square two-letter identification. When reporting beyond the 6- by 8-degree geographical area, the reference is prefixed with the grid zone designation consisting of one number and one letter.

The area of the globe between 80 degrees north and 80 degrees south is divided into quadrilaterals 6 degrees east-west by 8 degrees north-south. The columns, 6 degrees wide, are identified by UTM grid zone numbers. The columns are numbered 1 through 60 consecutively, starting at the 180-degree meridian and proceeding easterly. The rows, 8 degrees high, are identified by letters. Starting at 80 degrees south and proceeding northward to 80 degrees north the rows are lettered consecutively C through X (with the letters I and O omitted). The designation, called the grid zone designation, of any 6 degrees east-west by 8 degrees north-south rectangle is determined by reading from the right up. The column designation, such as 3, is read first. The row designation, such as P, is read after the number. The result is 3P.

The computation has given UTM coordinates for the picture center. The grid divergence (difference from meridian or geodetic north and the grid or plane south) is needed. Additional notations are:

$\Delta \alpha$ = grid divergence or convergence of the meridians

α' = grid north

E' = $E \pm 500,000$ where the minus is used if E is larger, the plus if E is smaller

(XV) = $\tan \phi / \nu \sin 1'' \times 1/k_o \, 10^6$

q = $0.000001E'$

$\Delta \alpha$ = $q(XV)$ in arc-seconds with it added algebraically to geodetic azimuth which is the meridian line on the photograph.

This data, UTM east and north, the zone, and grid divergence allow the use of a protractor, dividers, pencil, and ruler to construct a UTM grid on any photograph in 1 or 2 minutes.

2.2.1.3 Equipment Tradeoffs for Geodetic Control Measurement Station

The accuracies required for the mensuration viewer coupled with the requirement that the full format be in view have restricted the number of mensuration viewers that can be considered. The accuracies needed to

satisfy the ground truth measurements and reseau measurement are approximately 6 microns over the 9-1/2-inch-square format. This accuracy requirement with the full format viewing plus the requirement for measuring the map information either at the same machine or a separate machine has pinpointed the search to a modified Optomechanism model 527-A.

This machine is a dual light strip comparator with monitorized film drives capable of handling both the 9-1/2- by 9-1/2-inch format and a dual 70-millimeter film format simultaneously. This comparator, when modified with direct coupled encoders and an automatic data logger tied to an IBM 526 summary punch station, lends itself to an efficient ground truth station. The accuracies required can be maintained with a calibration program in the computer.

The Mann model 422-F comparator, the Itek rear projection mensuration viewer, and the Computer Equipment Corporation coordinate digitizer were also considered.

The Mann unit was adequate for accuracies but did not allow full format viewing.

The Itek unit and the Computer Equipment Corporation equipment did not have the accuracy required.

2.2.2 RBV Errors

The error sources which produce unpleasant artifacts in the images can be listed as follows:

1) The readout spot is moving and not stationary: thus the output signal is the convolution of the spot, the channel impulse response and the image intensity function. Therefore, the video can suffer a photometric distortion if the bandwidth is not chosen correctly.

2) The shutter aperture time of the camera is such that the image is quantum limited and thus the video signal is corrupted by a signal dependent noise.

3) The RBV tubes are to be used in a storage mode and therefore the electron image will decay between exposures. The decay mechanism has two parts; one, lateral diffusion or leakage of the stored charge and secondly, leakage axially

through the storage surface. The first affects the resolution, the second is merely a gain control and is accommodated by RCA in the design. The quantum restriction in 2) means that the gain control approach may not be adequate. RCA claims that lateral diffusion is not a problem.

4) There will be noise entering the RBV and MSS signals from ground and power supply interferences. A secondary effect is that the electron lens in the RBV is very sensitive to power supply ripple and this ripple manifests itself in geometrical laying inaccuracies i.e., the spot will move from its desired position. Mesh noise will also be seen. The additive noise, the power supply noise and the mesh noise visibly affect the pictures by superimposing a coherent and a priori unpredictable pattern on the images. (Mesh noise is predictable but requires knowledge of the geometric errors). This pattern will be most visible in areas of uniform tone and may only be objectionable on close examination. ERTS imagery, it is to be hoped, will be scrutinized carefully. The additive noise should be coherent in time i.e., will be locked to the spacecraft clock as is the horizontal and vertical sync of the camera so that, although the interferences may become visible as a complex pattern, the temporal coherence is its outstanding characteristic. This is independent of tube geometry. Mesh noise on the other hand will appear as a geometric overlay on the image and will be distorted to the same extent as the images, since both are scanned through the same electron lens. Thus the mesh inteference will result in a small-deviation frequency modulated sine wave superimposed on the scan signal. Note, small deviation since, see later, the geometric distortion is small. If the deviation is small, the process of filtering the coherent noise will also remove the mesh noise.

5) The signal to noise ratio of the video signal is reduced by the magnetic video recording process. The signal to noise ratio is further reduced by quantization in the analog to digital converter. The choice of the analog to digital converter resolution must be made with the input signal to noise ratio and the further processing steps kept in mind.

6) There is a two pixel smear due to image motion. Since no image motion compensation is included in the satellite this effect should, if required, be removed by image processing.

7) The number of sampling points in the horizontal direction is under the control of the ground data processing facility and should be chosen to suit the information content of the video signal to eliminate errors due to undersampling.

8) Radiation darkening of the optics

9) Blemishes on the RBV tube face

10) Shading errors due to non-uniform response of the target

11) Gamma variation across the field

12) Modulation transfer function variation across the field

13) Sun angle

14) Registration errors between the three images.

2.2.2.1 RBV Distortion Correction Tradeoff Study

The ERTS RBV camera consists of three RCA return beam vidicon cameras which simultaneously photograph the same image in three corresponding spectral bands. A pattern of fiducial marks, or reseau, is interposed between each camera and the scene to provide a reference for estimation of the RBV camera distortion. The images taken by the three cameras are read out sequentially and transmitted to the ground data handling system, wherein the positions of the reseau points are determined for each. Based on these positions, the camera distortion is determined and the image subsequently corrected, either digitally or via analog means. It is the intent of this section to justify selection of the algorithms used to estimate the geometric image distortion caused by the RBV camera system. Tradeoffs will be made on the bases of error performance and computational requirements.

Error Performance of Distortion Correction Algorithms

The images generated by the RBV cameras will contain geometric distortions which are primarily a result of imperfect scanning by the electron beam of the RBV. Data link and tape recorder geometric errors will be negligible, with respect to the camera errors. In the camera, an optical system focuses an image on a faceplate, which is scanned by an electron beam and converted to a voltage train to be transmitted to and demodulated on the ground. Image distortion may arise through nonlinearities in the scanning beam path or scan rates. To obtain an estimate of this distortion, a known reseau grid (Figure 2.2-3) consisting of 81 evenly spaced fiducials in a 9 x 9 array is placed in front of the camera focal plane. By measuring the apparent reseau distortion, the camera distortion parameters may be estimated.
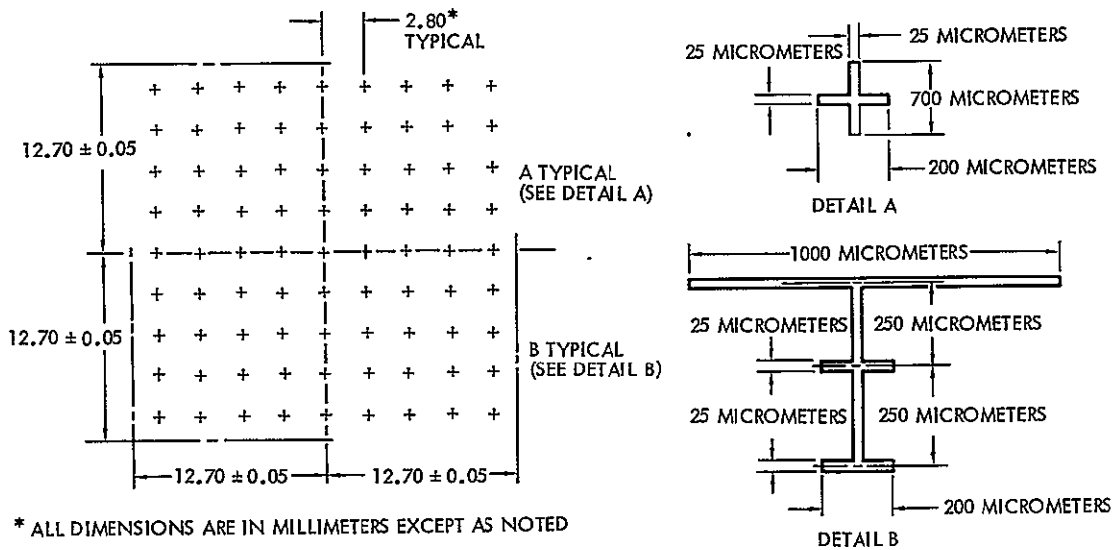
Figure 2.2-3

RESEAU ARRAY FORMAT

Typical sources of distortion may be modeled as follows. First, a coordinate system is defined, centered at the image plane and with coordinate axes x and y. Position displacements at a point (x, y) due to distortion are given by $\delta x(x, y)$ and $\delta y(x, y)$.

An image centering shift can result from incorrect deflection voltage bias or from misalignment and causes distortion terms of the form

$$\delta x = a_0 \qquad \delta y = b_0$$

The specifications call for a maximum centering error of 1 percent full scale.

Image size error can result from incorrect deflection gain and cause distortion terms of the form

$$\delta x = a_1 x \qquad \delta y = b_1 y$$

The specifications require these terms to be less than 1 percent full scale.

Skew distortions can arise from sources such as misaligned deflection coils and may be represented by terms of the form

$$\delta x = a_2 y \qquad \delta y = b_2 x$$

According to specifications, these terms should be less than 0.5 percent full scale.

Pincushion distortion can arise from magnetic field imperfections and gives terms of the form

$$\delta x = x \left[a_3 (x^2 + y^2) + a_4 (x^2 + y^2)^2 + \ldots \right]$$

$$\delta y = y \left[b_3 (x^2 + y^2) + b_4 (x^2 + y^2)^2 + \ldots \right]$$

Symmetric tangential distortion can be caused by the combined effect of unwanted radial electric fields and the axial focusing magnetic field and gives the terms of the form

$$\delta x = y \left[a_5 (x^2 + y^2) + a_6 (x^2 + y^2)^2 + \ldots \right]$$

$$\delta y = x \left[b_5 (x^2 + y^2) + b_6 (x^2 + y^2)^2 + \ldots \right]$$

Specifications call for the maximum "image distortion" to be less than 1 percent full scale. Since specifications for skew, size, and centering are quoted separately, we will assume "image distortion" refers to all other distortions including pincushion and tangential distortion.

The total effect of all of these sources of distortion becomes

$$\delta x = a_0 + a_1 x + a_2 y + a_3 x (x^2 + y^2) + a_4 x (x^2 + y^2)^2$$

$$+ a_5 y (x^2 + y^2) + a_6 y (x^2 + y^2)^2$$

$$\delta y = b_0 + b_1 y + b_2 x + b_3 y(x^2 + y^2) + b_4 y(x^2 + y^2)^2$$

$$+ b_5 x(x^2 + y^2) + b_6 x(x^2 + y^2)^2$$

where only the first two terms in pincushion and tangential have been included. No specifications could be found which give the stability of the distortions from picture to picture. This list of distortion terms is not exhaustive; quite possibly other sources of distortions will be found in the RBV. However, because these terms are not uncommon, they can serve as a specific test of proposed distortion correction schemes.

Thus, it can be assumed that the distortions present in the image are of the form

$$x + \delta x = f(x, y) + \nu$$

where f is a smoothly varying function and ν is random spatial noise. A similar equation exists for y distortion. The function f, which will be called the functional distortion, contains terms arising from all smooth distortion sources, such as those listed above. The spatial noise terms can arise from sources such as synch-jitter, beam jitter, beam pulling, and high frequency distortions. It is assumed that the noise is spatially uncorrelated so that

$$E(\nu_i, \nu_j) = \delta_{ij} \, \sigma_N^2$$

at points i and j. the values of δx_i for the reseau points are given as

$$\delta x_i = F(x_i, y_i) + \nu_i + m_i, \quad i = 1, 2, \ldots, N_R$$

where m_i represents the measurement error for the ith reseau point. It is further assumed that

$$E(m_i m_j) = \delta_{ij} \, \sigma_m^2 \quad \text{and} \quad E(\nu_i m_j) = 0$$

The reseau displacements are fit by an interpolation algorithm to determine the distortion elsewhere.

Four processing algorithms were considered based on the general image processing requirements of minimum error at reasonable processing cost with no image discontinuities caused by the algorithms. First, the distortion estimation algorithm tradeoffs will be discussed, followed by the correction implementation tradeoffs. The estimation algorithms considered were of two types: global polynomials, where a single set of parameters is used to model the distortion over the entire image; and interpolation algorithms, whereby the reseau grid is subdivided into smaller regions, each with its own set of distortion parameters. The global polynomial fits considered adequate for study are

1) Global Biquadratic Polynomial

$$\delta \tilde{x} = \sum_{i=0}^{2} \sum_{j=0}^{2} a_{ij} \, x^{i} \, y^{j}$$

    – parameters a_{ij} apply to entire image

2) Global Third-order Polynomial

$$\delta \tilde{x} = \sum_{i=0}^{3} \sum_{j=0}^{3-i} a_{ij} \, x^{i} y^{j}$$

    – parameters a_{ij} apply to entire image

The interpolation algorithms considered are

3) Bilinear Interpolation

$$\delta x = \sum_{i=0}^{1} \sum_{j=0}^{1} a_{ijk} \, x^{i} y^{j}$$

    – different parameters a_{ijk} depending on surrounding reseau points only

4) Biquadratic Interpolation

$$\delta \tilde{x} = \sum_{i=0}^{2} \sum_{j=0}^{2} a_{ijk} \, x^{i} y^{j}$$

    – different parameters a_{ijk} as above.

Utilization of the same algorithm throughout the image is deemed necessary to preclude image discontinuities.

In the piecewise-bilinear interpolation approach, a rectangle of four reseau points such as the four marked in Figure 2.2-4 are selected and the displacements of the reseau points are fitted with a function of the form 3) above.
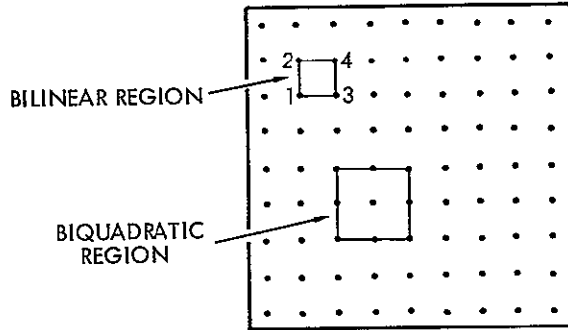
Figure 2.2-4

EXAMPLES OF PIECEWISE-BILINEAR AND PIECEWISE- BIQUADRATIC REGIONS

In piecewise-biquadratic interpolation, nine adjacent reseau points (see figure 2.2-4) are chosen and the nine reseau displacements at these points are used to determine a nine parameter function of the form 4). Sixteen of these regions span a 9 x 9 reseau. An internal point is corrected according to its regional biquadratic function and edge points are corrected by the fit function of the nearest region.

The processing algorithm models 1) through 4) can be written in matrix format as

$$\delta \tilde{x} = A(x, y) \underline{a}_m$$

where $\underline{a}_m$ contains the parameters a_{ij} and $A(x, y)$ the coefficients $x^i y^j$. The actual distortion δx also contains other terms such as first-order pincushion $x(x^2 + y^2) a_3$ and spatially uncorrelated noise v as discussed above. Thus,

$$\delta x(x, y) = [A(x, y) | N(x, y)] \begin{bmatrix} \underline{a}_m \\ \underline{a}_N \end{bmatrix} + v(x, y)$$

where $\delta x(x, y)$ is x-distortion at (x, y), $\underline{a}_N$ is the unmodelled distortion parameter, and $v(x, y)$ is the coefficient of $\underline{a}_N$ in the distortion. The distortion can be measured at each of the reseau points in each subregion for

2-21

the interpolation algorithms or at all 81 reseau points for the global polynomials and arranged as follows:

$$\delta x = [\underline{A} \mid \underline{N}] \begin{bmatrix} \underline{a}_m \\ \underline{a}_N \end{bmatrix} + \underline{v}$$

where

$$\delta\underline{x} \equiv \begin{bmatrix} \delta x(x_1, y_1) \\ \delta x(x_2, y_2) \\ \cdot \\ \cdot \\ \cdot \\ \delta x(x_N, y_N) \end{bmatrix} ; \quad \underline{A} \equiv \begin{bmatrix} A(x_1, y_1) \\ A(x_2, y_2) \\ \cdot \\ \cdot \\ \cdot \\ A(x_N, y_N) \end{bmatrix} ; \quad \underline{N} \equiv \begin{bmatrix} N(x_1, y_1) \\ N(x_2, y_2) \\ \cdot \\ \cdot \\ \cdot \\ N(x_N, y_N) \end{bmatrix} ; \quad \underline{V} \equiv \begin{bmatrix} V(x_1, y_1) + m_1 \\ V(x_2, y_2) + m_2 \\ \cdot \\ \cdot \\ \cdot \\ V(x_N, y_N) + m_N \end{bmatrix}$$

The distortion estimation equation based on the global polynomial models is given by

$$\delta\hat{x}(x, y) = A(x, y)\hat{\underline{a}}_m = A(x, y)(\underline{A}^T \underline{A})^{-1} \underline{A}^T \delta\underline{x}$$

which leaves a distortion estimation error $\varepsilon(x, y)$

$$\varepsilon(x, y) = \varepsilon_E(x, y) + \varepsilon_M(x, y)$$

where $\varepsilon_E(x, y)$ is the statistical error caused by the noise $v(x, y)$

$$\varepsilon_E(x, y) = A(x, y)(\underline{A}^T\underline{A})^{-1} \underline{A}^T \underline{v} - v(x, y)$$

and $\varepsilon_M(x, y)$ is the functional error caused by neglecting the terms $\underline{a}_N$ in the distortion estimation

$$\varepsilon_M(x, y) = K(x, y)\underline{a}_N$$

where

$$K(x, y) = A(x, y)(\underline{A}^T \underline{A})^{-1} \underline{A}^T \underline{N} - N(x, y)$$

The residual statistical error variance can be calculated as a function of σ_N^2 and σ_M^2 at image point (x, y) as

$$\sigma_x^2(x, y) = A(x, y)(\underline{A}^T \underline{A})^{-1} A^T(x, y)(\sigma_N^2 + \sigma_M^2) + \sigma_N^2$$

at points not coinciding with reseau points and

$$\sigma_x^2(x, y) = A(x, y)(\underline{A}^T \underline{A})^{-1} A^T(x, y)(\sigma_M^2 - \sigma_N^2) + \sigma_N^2$$

at reseau points due to correlation of $\underline{v}$ and $v(x, y)$ at these points. Similar equations apply to the interpolation algorithms. However, since the same number of parameters exist for the interpolation models as the number of reseau point measurements used, the parameters are exactly modelled and $(\underline{A}^T \underline{A})^{-1} \underline{A}^T$ can be replaced by $\underline{A}^{-1}$ in the error equations.

A digital computer study was made of the performance of these algorithms with respect to the variance of the spatially-uncorrelated distortions and reseau measurement errors.

$$\left(\sigma_N^2 + \sigma_M^2\right) \equiv \sigma_R^2$$

Flow charts depicting the structure of this computer program are shown in Figure 2.2-5. The results of this study are shown in Figures 2.2-6 through 2.2-12. Figure 2.2-6 presents the ratio of the standard deviation of the residual statistical error from reseau point distortion to σ_R for bilinear interpolation algorithm. The grid represents one quadrant of the image plane, the center of the image appearing in the upper left corner. Entries appear twice per reseau point spacing in the horizontal direction and four times per reseau point spacing in the vertical. The entries corresponding to reseau locations are encircled. Thus, it can be

seen that the statistical error in the far corner of the image has an uncertainty of 2.5 times the uncertainty of the reseau location due to measurement and random camera distortion. The grid is reproduced graphically in Figure 2.2-7 to demonstrate the increase in statistical uncertainty in the extrapolation region beyond the edge of the reseau grid.

Figures 2.2-8 and 2.2-9 show the same information for the biquadratic interpolation in the same format. Figure 2.2-10 represents the global biquadratic and Figures 2.2-11 and 2.2-12 represent the global third-order polynomial approaches.
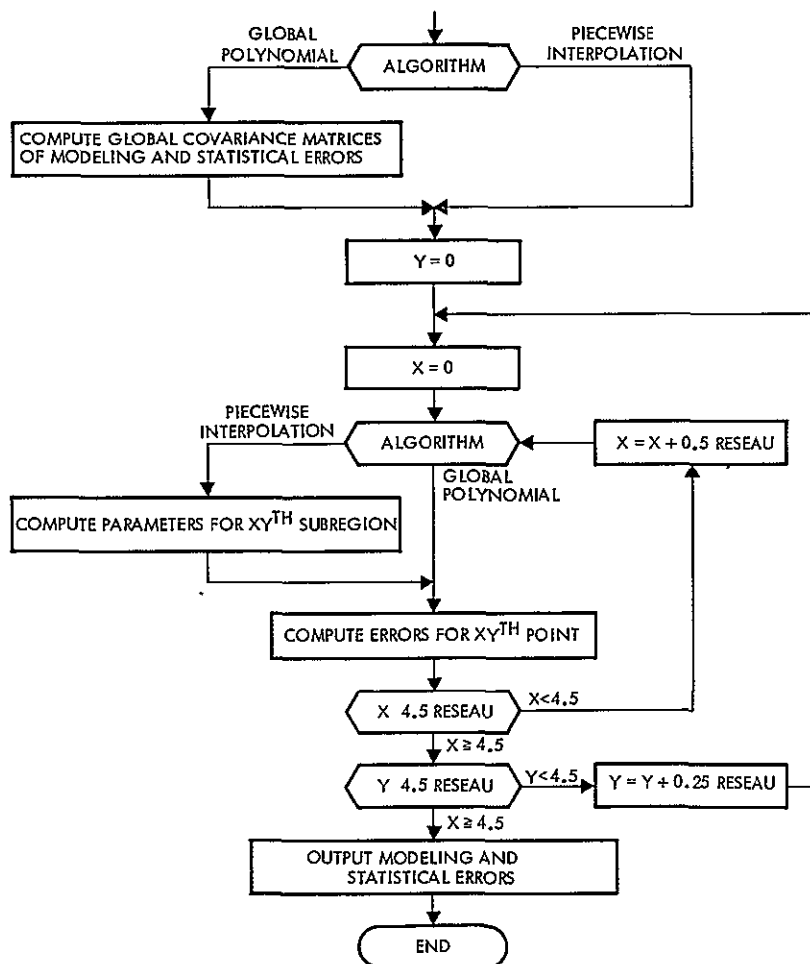
Figure 2.2-5

FLOW DIAGRAM FOR MODELLING AND STATISTICAL ERRORS over one quarter of image plane for global polynomial and piecewise interpolation algorithms.

Statistical

[1.000]	0.707	[1.000]	0.707	[1.000]	0.707	[1.000]	0.707	[1.000]	1.581
0.791	0.559	0.791	0.559	0.791	0.559	0.791	0.559	0.791	1.250
0.707	0.500	0.707	0.500	0.707	0.500	0.707	0.500	0.707	1.118
0.791	0.559	0.791	0.559	0.791	0.559	0.791	0.559	0.791	1.250
[1.000]	0.707	[1.000]	0.707	[1.000]	0.707	[1.000]	0.707	[1.000]	1.581
0.791	0.559	0.791	0.559	0.791	0.559	0.791	0.559	0.791	1.250
0.707	0.500	0.707	0.500	0.707	0.500	0.707	0.500	0.707	1.118
0.791	0.559	0.791	0.559	0.791	0.559	0.791	0.559	0.791	1.250
[1.000]	0.707	[1.000]	0.707	[1.000]	0.707	[1.000]	0.707	[1.000]	1.581
0.791	0.559	0.791	0.559	0.791	0.559	0.791	0.559	0.791	1.250
0.707	0.500	0.707	0.500	0.707	0.500	0.707	0.500	0.707	1.118
0.791	0.559	0.791	0.559	0.791	0.559	0.791	0.559	0.791	1.250
[1.000]	0.707	[1.000]	0.707	[1.000]	0.707	[1.000]	0.707	[1.000]	1.581
0.791	0.559	0.791	0.559	0.791	0.559	0.791	0.559	0.791	1.250
0.707	0.500	0.707	0.500	0.707	0.500	0.707	0.500	0.707	1.118
0.791	0.559	0.791	0.559	0.791	0.559	0.791	0.559	0.791	1.250
[1.000]	0.707	[1.000]	0.707	[1.000]	0.707	[1.000]	0.707	[1.000]	1.581
1.275	0.901	1.275	0.901	1.275	0.901	1.275	0.901	1.275	2.016
1.581	1.118	1.581	1.118	1.581	1.118	1.581	1.118	1.581	2.500

Figure 2.2-6

BILINEAR INTERPOLATION
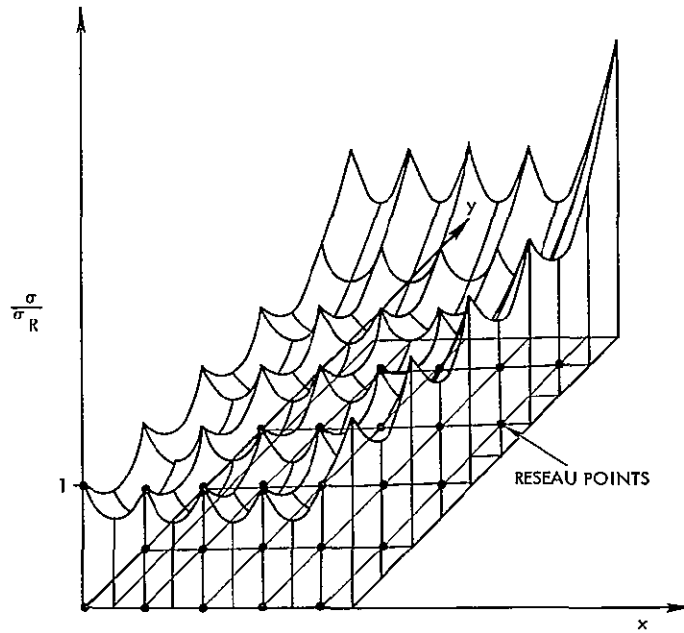
Figure 2.2-7

BILINEAR INTERPOLATION STATISTICAL ERROR

[1.000]	0.848	[1.000]	0.848	[1.000]	0.848	[1.000]	0.848	[1.000]	2.284
0.794	0.673	0.794	0.673	0.794	0.673	0.794	0.673	0.794	1.814
0.848	0.719	0.848	0.719	0.848	0.719	0.848	0.719	0.848	1.937
0.955	0.810	0.955	0.810	0.955	0.810	0.955	0.810	0.955	2.182
[1.000]	0.848	[1.000]	0.848	[1.000]	0.848	[1.000]	0.848	[1.000]	2.284
0.955	0.810	0.955	0.810	0.955	0.810	0.955	0.810	0.955	2.182
0.848	0.719	0.848	0.719	0.848	0.719	0.848	0.719	0.848	1.937
0.794	0.673	0.794	0.673	0.794	0.673	0.794	0.673	0.794	1.814
[1.000]	0.848	[1.000]	0.848	[1.000]	0.848	[1.000]	0.848	[1.000]	2.284
0.794	0.673	0.794	0.673	0.794	0.673	0.794	0.673	0.794	1.814
0.848	0.719	0.848	0.719	0.848	0.719	0.848	0.719	0.848	1.937
0.955	0.810	0.955	0.810	0.955	0.810	0.955	0.810	0.955	2.182
[1.000]	0.848	[1.000]	0.848	[1.000]	0.848	[1.000]	0.848	[1.000]	2.284
0.955	0.810	0.955	0.810	0.955	0.810	0.955	0.810	0.955	2.182
0.848	0.719	0.848	0.719	0.848	0.719	0.848	0.719	0.848	1.937
0.794	0.673	0.794	0.673	0.794	0.673	0.794	0.673	0.794	1.814
[1.000]	0.848	[1.000]	0.848	[1.000]	0.848	[1.000]	0.848	[1.000]	2.284
1.523	1.291	1.523	1.291	1.523	1.291	1.523	1.291	1.523	3.478
2.284	1.937	2.284	1.937	2.284	1.937	2.284	1.937	2.284	5.219

Figure 2.2-8

BIQUADRATIC INTERPOLATION

Figure 2.2-9

THE STATISTICAL FUNCTION $\sqrt{\sigma/\sigma_R}$ FOR THE PIECEWISE
biquadratic approach

Statistical

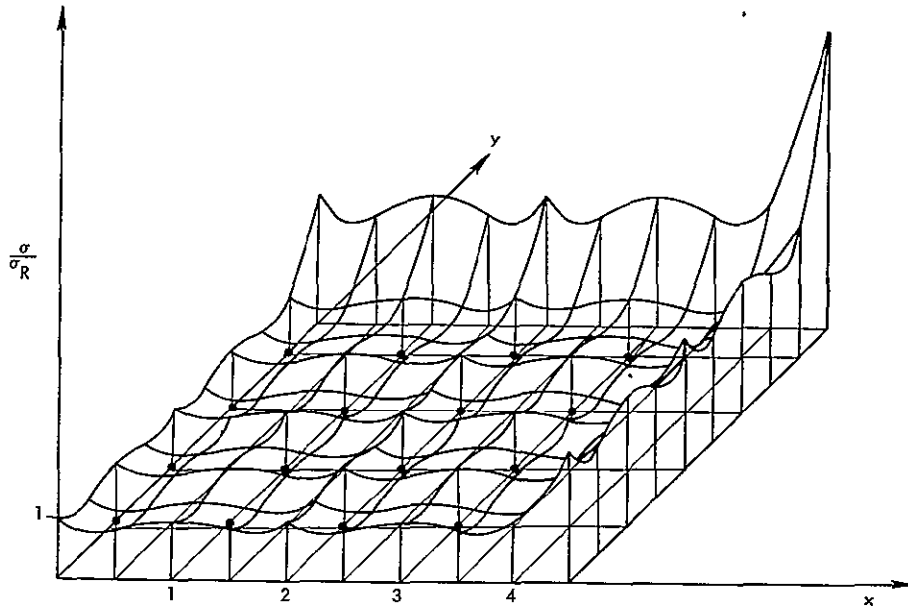|									
0.255	0.252	0.243	0.233	0.227	0.235	0.267	0.326	0.411	0.517
0.255	0.251	0.243	0.232	0.226	0.234	0.266	0.325	0.409	0.516
0.252	0.249	0.240	0.230	0.224	0.232	0.263	0.322	0.406	0.511
0.248	0.245	0.237	0.226	0.220	0.228	0.259	0.317	0.399	0.503
0.243	0.240	0.232	0.222	0.216	0.224	0.254	0.311	0.392	0.493
0.238	0.235	0.227	0.217	0.211	0.219	0.249	0.304	0.383	0.482
0.233	0.230	0.222	0.212	0.216	0.214	0.243	0.297	0.374	0.471
0.228	0.226	0.218	0.203	0.203	0.210	0.239	0.292	0.367	0.463
0.227	0.224	0.216	0.206	0.201	0.208	0.237	0.289	0.364	0.459
0.228	0.225	0.217	0.208	0.202	0.210	0.238	0.291	0.367	0.462
0.235	0.232	0.224	0.214	0.208	0.216	0.245	0.300	0.378	0.476
0.247	0.244	0.236	0.225	0.219	0.227	0.259	0.316	0.398	0.501
0.267	0.263	0.254	0.243	0.237	0.245	0.279	0.341	0.429	0.540
0.293	0.289	0.279	0.267	0.260	0.269	0.306	0.374	0.471	0.594
0.326	0.322	0.311	0.297	0.289	0.300	0.341	0.416	0.525	0.661
0.366	0.361	0.348	0.333	0.324	0.336	0.382	0.467	0.588	0.740
0.411	0.406	0.392	0.374	0.364	0.378	0.429	0.525	0.661	0.832
0.461	0.456	0.440	0.420	0.409	0.424	0.482	0.589	0.742	0.935
0.517	0.511	0.493	0.471	0.459	0.476	0.540	0.661	0.832	1.048

Figure 2.2-10

GLOBAL POLYNOMIAL, BIQUADRATIC

Statistical

0.211	0.217	0.231	0.247	0.259	0.265	0.272	0.303	0.387	0.542
0.212	0.218	0.232	0.248	0.260	0.265	0.273	0.304	0.388	0.543
0.217	0.222	0.236	0.251	0.262	0.267	0.274	0.305	0.389	0.544
0.223	0.228	0.241	0.255	0.265	0.269	0.276	0.307	0.391	0.547
0.231	0.236	0.247	0.260	0.269	0.272	0.278	0.309	0.394	0.550
0.239	0.243	0.254	0.265	0.273	0.275	0.280	0.311	0.397	0.554
0.247	0.251	0.260	0.270	0.276	0.277	0.282	0.313	0.400	0.559
0.254	0.257	0.265	0.274	0.278	0.278	0.283	0.315	0.404	0.565
0.259	0.262	0.269	0.276	0.279	0.278	0.283	0.317	0.409	0.573
0.262	0.265	0.271	0.277	0.279	0.277	0.283	0.320	0.415	0.582
0.265	0.267	0.272	0.277	0.278	0.277	0.284	0.324	0.424	0.595
0.267	0.269	0.274	0.278	0.279	0.278	0.288	0.332	0.436	0.611
0.272	0.274	0.278	0.282	0.283	0.284	0.297	0.346	0.455	0.632
0.283	0.285	0.289	0.292	0.294	0.298	0.316	0.370	0.481	0.661
0.303	0.305	0.309	0.313	0.317	0.324	0.346	0.404	0.518	0.699
0.337	0.339	0.343	0.348	0.354	0.365	0.392	0.454	0.568	0.748
0.387	0.389	0.394	0.400	0.409	0.424	0.55	0.518	0.633	0.811
0.455	0.457	0.462	0.470	0.482	0.500	0.535	0.600	0.713	0.888
0.542	0.544	0.550	0.559	0.573	0.595	0.632	0.699	0.811	0.982

Figure 2.2-11

GLOBAL THIRD-ORDER POLYNOMIAL
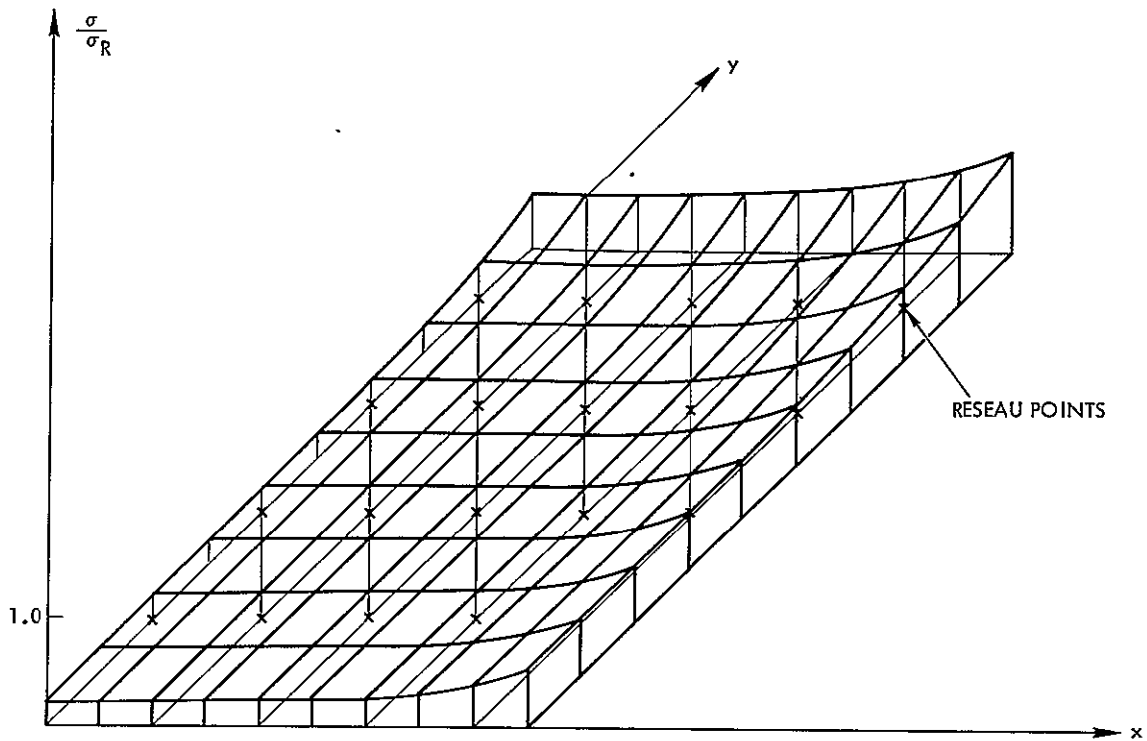
Figure 2.2-12

GLOBAL THIRD-ORDER POLYNOMIAL - STATISTICAL ERROR

Note that the function σ/σ_R is less than one over the whole range for the global third-order polynomial, but increases significantly for edge points. The biquadratic global polynomial statistical error is similar in behavior but is slightly smaller. For the bilinear and biquadratic interpolation approaches, σ/σ_R is one at the reseau points but decreases for internal points. However, σ/σ_R increases considerably above one at the edge points. This increase outside the reseau points is reasonable since extrapolated noise fluctuations can yield poor estimates. For the same noise configuration, a quadratic fit gives a larger error when extrapolated than a linear fit. Corrections at points near a reseau point are dragged along with the fluctuating reseau value and consequently, σ/σ_R is one at the reseau points.

As indicated previously, the total statistical uncertainty has the unavoidable term σ_N^2 of spatial noise present at the point being corrected. The presence of this term diminishes the importance of the considerable difference in σ/σ_R for the least-squares interpolative approaches. If the

spatial noise term is large compared to the reseau measurement error, it is clear that the average total statistical error in the interpolation approach can be about 1.4 times larger, at reseau points, than the same quantity in the least-squares approach. If the reseau measurement error is large compared to the spatial noise, the statistical uncertainty in the interpolation approach can be about three times as large, at reseau points, as the statistical uncertainty in the least-squares approach.

If the functional distortion is fairly constant over more than one frame, then an average of the coefficients obtained for past frames will lower the second term in the statistical uncertainty by the usual factor of n, the number of frames averaged. The total correction error becomes

$$\overline{\delta x^2} = \Delta F^2 + \sigma_N^2 + \frac{\sigma_N^2 + \sigma_m^2}{n} \; S(x, y)$$

where n is the number of frames in the average. If beam-pulling is an important factor in reseau position determination, coefficient averaging could greatly diminish this source of error. If the functional distortion is constant enough to allow many frames to be averaged in this way, then the statistical advantage of the global polynomial approach will be diminished or even effectively lost. For example, after nine frames, the interpolation approaches have a lower statistical error than a one-frame biquadratic global polynomial correction. After enough frames are averaged, the functional error will dominate the error expression for both approaches and will be the determining factor in accuracy comparisons.

To completely test the functional accuracy of various fitting techniques, one would need to know the exact expression for the functional distortion. Since there is no way of determining in advance the exact distortion magnitudes or even a complete list of unmodelled terms, one is forced to make tests using typical distortion terms whose magnitudes have been placed at the specification limits. This will be the procedure in the following examples. Such a procedure will reveal the fitting techniques that are inadequate for probable distortions. Because of symmetry in the pincushion and tangential terms and in the fitting functions, tests

using the $x(x^2 + y^2)$ and $x(x^2 + y^2)^2$ terms suffice to test all higher order terms in the image distortion.

The sensitivity of each algorithm to unmodelled distortion parameters was similarly evaluated via a digital computer program and the results are presented in Figures 2.2-13 through 2.2-21. The sensitivity of the bilinear interpolation algorithm functional error to unmodelled distortions is shown in Figure 2.2-13. The format of the grids in Figure 2.2-13 is the same as that in Figures 2.2-7 through 2.2-12. The entries in the first grid represents the sensitivity to the lower-order effects of pincushion type, second-order, distortions and those in the second grid the sensitivity to higher-order effects as discussed above. Thus, if one percent full scale first-order pincushion is present in the image, 6.58 percent of this distortion or 0.066 percent full scale will remain in the image corner. Similarly, 16.3 percent of second-order pincushion distortion will remain the same corner. These results are presented graphically in Figures 2.2-14 and 2.2-15. The same data is presented in Figures 2.2-16 and 2.2-17 for the biquadratic interpolation, Figures 2.2-18 and 2.2-19 for the global biquadratic, and Figures 2.2-20 and 2.2-21 for the global third-order algorithms, sensitivity of the global third-order algorithm to first-order pincushion is zero since that form of distortion is perfectly modelled by this algorithm. The results indicate that, for the distortions considered, the piecewise-biquadratic gives by far the lowest functional error. In order to become competitive with the piecewise-bilinear approach, the global polynomial approach must be at least third order for the distortion terms considered. With regard to smoothness, the global polynomial is best since it is continuous in all of its derivatives. The piecewise-biquadratic fit is much smoother than the piecewise-bilinear fit for two reasons. First, the biquadratic fit regions are larger so that there is less boundary at which the first derivative is discontinuous. Secondly, for well-behaved distortion curves, the jump in the first derivative at boundaries will be much smaller in the piecewise-biquadratic fit. The maximum errors are summarized in Table 2.2-2.

Modelling (First-Order Pincushion)

0 000	0.000	-0.000	-0.000	-0.000	-0.000	-0.000	-0.000	-0.000	-0.000
0.129	0.163	0.129	0 163	0.129	0.163	0.129	0.163	-0.129	0.026
0.206	0.274	0.206	0.274	0.206	0.274	0.206	0.274	0.206	-0.000
0.180	0.283	0.180	0.283	0.180	0.283	0.180	0.283	0.180	-0.129
-0.000	0.137	-0.000	0.137	-0.000	0.137	-0.000	0.137	-0.000	-0.412
0.437	0.609	0.437	0.609	0.437	0.609	0.437	0.609	0.437	-0.077
0.617	0.823	0.617	0.823	0.617	0.823	0.617	0.823	0 617	-0.000
0.489	0.729	0.489	0. 729	0 489	0.729	0.489	0.729	0.489	-0.231
-0.000	0.274	-0.000	0.274	-0.000	0.274	-0.000	0.274	-0.000	-0.823
0.746	1.055	0.746	1.055	0.746	1.055	0.746	1.055	0.746	-0.180
1.029	1.372	1.029	1.372	1.029	1.372	1.029	1.372	1.029	-0.000
0.797	1.175	0.797	1.175	0.797	1.175	0.797	1.175	0.797	-0.334
-0.000	0.412	-0.000	0.412	-0.000	0.412	-0.000	0.412	-0.000	-1.235
1.055	1.500	1.055	1.500	1.055	1 500	1.055	1.500	1.055	-0.283
1.440	1.920	1.440	1.920	1.440	1.920	1.440	1.920	1.440	-0 000
1.106	1 620	1.106	1.620	1.106	1.620	1.106	1.620	1.106	-0.437
-0.000	0.549	-0.000	0.549	-0 000	0.549	-0.000	0 549	-0.000	-1.646
-1.929	-1.346	-1.929	-1.346	-1.929	-1.346	-1.929	-1.346	-1.929	-3.678
-4.733	-4.115	-4.733	-4.115	-4.733	-4.115	-4.733	-4.115	-4 733	-6.584

Modelling (Second-Order Pincushion)

0 000	0 000	-0 000	-0 000	-0 000	-0 000	-0.000	-0 000	-0 000	-0 000
0 003	0 008	0 010	0 031	0 029	0 077	0 061	0 145	0.105	-0 099
0 006	0 015	0 017	0 056	0 047	0 137	0 098	0 259	0 169	-0.249
0 007	0.019	0 016	0 067	0 043	0 163	0 087	0 308	0 149	-0 505
-0 000	0 013	-0 000	0 53	-0 000	0 135	-0 000	0 257	-0 000	-0 922
0 077	0 109	0 099	0 203	0 164	0 391	0.272	0 673	0 423	-0 669
0 121	0 168	0.151	0 290	0 243	0 533	0 395	0 899	0 608	-0 706
0 106	0 165	0.130	0 284	0 203	0 523	0 323	0 881	0 492	-1 110
-0 000	0 066	-0 000	0.147	-0 000	0 310	-0 000	0 554	-0 000	-1 966
0 367	0 476	0 404	0 641	0 514	0.971	0 698	1 467	0 956	-1.175
0 540	0 686	0 591	0 889	0 743	1 296	0 997	1 905	1 353	-1 042
0 447	0 624	0 486	0 814	0 604	1 195	0 801	1 767	1.077	-1 688
-0 000	0 201	-0 000	0 323	-0 000	0.566	-0 000	0.932	-0 000	-3 254
1 025	1.303	1 077	1 539	1.233	2 012	1 494	2 720	1 858	-1.588
1 467	1 814	1 538	2 098	1 752	2 667	2 107	3 521	2 605	-1 174
1 181	1 588	1 236	1 849	1.399	2 373	1.673	3 158	2 055	-2 207
-0 000	0 457	-0.000	0 620	-0 000	0 945	-0 000	1 433	-0.000	-4 908
-2 267	-1 769	-2 362	-1 787	-2 648	-1 823	-3 124	-1 876	-3 791	-9 517
-5 836	-5 309	-6 070	-5 594	-6 771	-6.163	-7 940	-7.016	-9 576	-16 303

Figure 2.2-13

BILINEAR INTERPOLATION
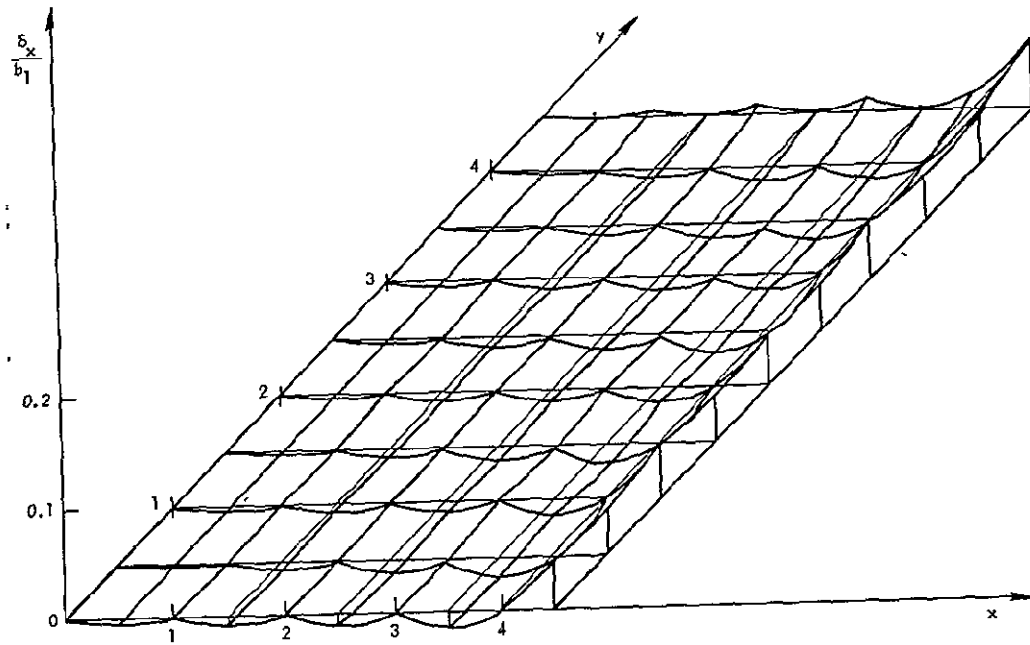
Figure 2.2-14

BILINEAR INTERPOLATION FUNCTIONAL SENSITIVITY to
first-order pincushion $b_1(x^2 + y^2)$
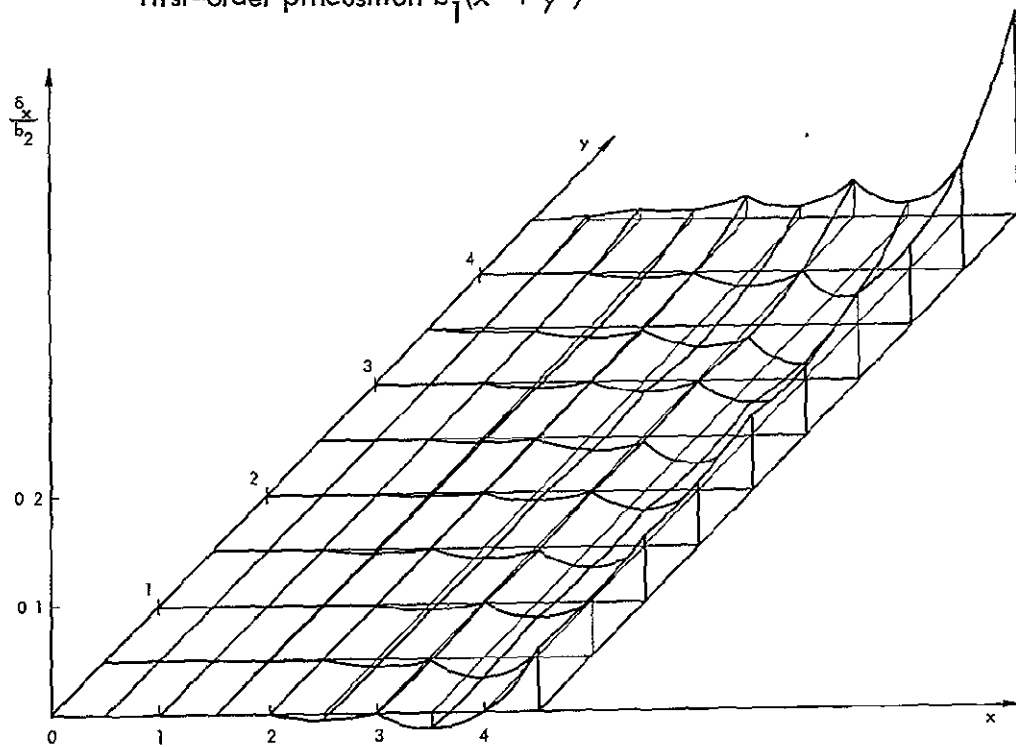
Figure 2.2-15

THE FUNCTIONAL ERROR FOR THE PIECEWISE-BILINEAR FIT to
the $x(x^2 + y^2)^2$ term (second-order pincushion)
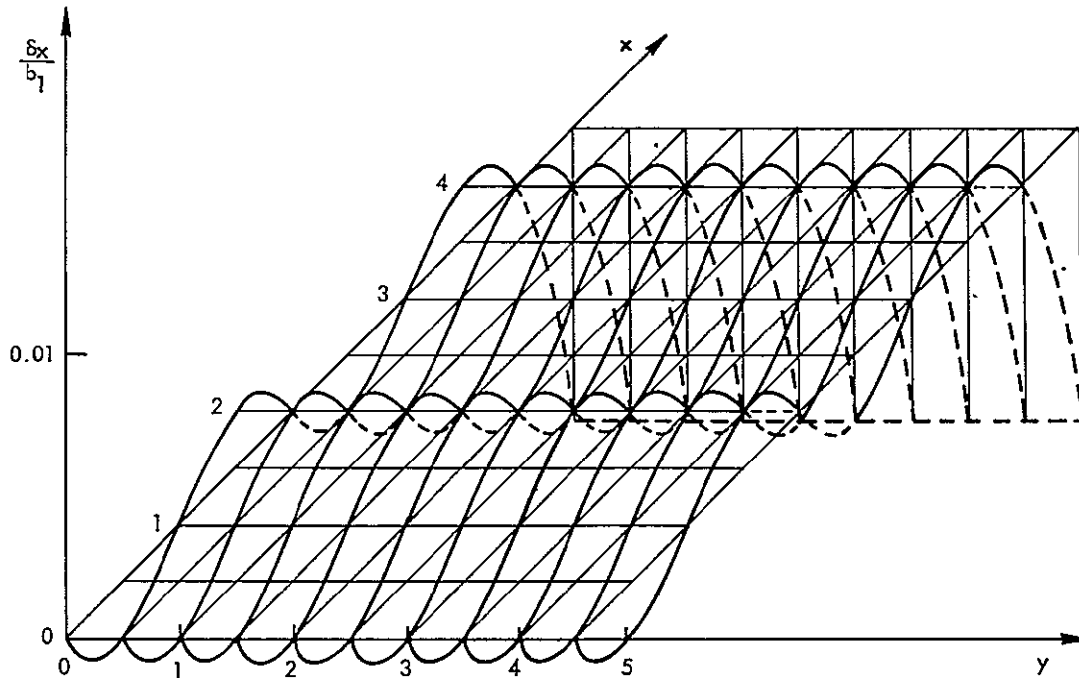
Figure 2.2-17

THE FUNCTIONAL ERROR FOR THE PIECEWISE-BIQUADRATIC FIT to the $x(x^2 + y^2)$ term (first-order pincushion)

It can be seen that errors are much greater in the image region outside the reseau pattern, indicating the advisability of extending the reseau pattern as close to the image edge as possible. Numbers are included in the table to indicate equivalent numbers of pixels.

Computer Requirements of Distortion-Processing Algorithms

Before the appropriate distortion-estimation algorithm can be selected, the computer processing time requirements for each must be evaluated. It can be shown that this will depend on the algorithm used for interpolation of intensity values at the 4200 x 4096 pixel output grid points in terms of the corrected input grid point values. The number of scan lines on the RBV is at most 4200; the 4096 pixels per line is consistent with resolution and convenient for computer analysis.

Modelling 2 (First-Order Pincushion)

0 000	-0 000	-0 000	-0. 000	-0 000	-0 000	-0 000	-0 000	-0 000	-0 000
-0 180	-0. 180	-0 180	-0 180	-0 180	-0 180	-0. 180	-0 180	-0 180	-0 180
-0 206	-0 206	-0 206	-0 206	-0 206	-0 206	-0 206	-0 206	-0. 206	-0 206
-0 129	-0 129	-0. 129	-0 129	-0 129	-0 129	-0 129	-0 129	-0 129	-0 129
-0 000	-0 000	-0.000	-0 000	-0.000	-0.000	-0 000	-0.000	-0.000	-0.000
0 129	0 129	0 129	0 129	0. 129	0 129	0 129	0 129	0` 129	0 129
0 206	0 206	0 206	0 206	0 206	0 206	0 206	0 206	0 206	0 206
0 180	0 180	0. 180	0 180	0 180	0 180	0 180	0 180	0 180	0 180
-0 000	-0 000	-0 000	-0 000	-0.002	-0 003	-0 003	-0 004	-0 005	-0 005
-0 180	-0 180	-0 180	-0 180	-0 183	-0 183	-0. 184	-0 184	-0 185	-0 186
-0 206	-0 206	-0 206	-0 206	-0 209	-0 209	-0. 210	-0 211	-0. 211	-0 212
-0. 129	-0 129	-0. 129	-0. 129	-0 132	-0 132	-0 133	-0 134	-0 135	-0 136
-0 000	-0 000	-0 000	-0 000	-0 003	-0 004	-0 005	-0 006	-0 007	-0 008
0 129	0 129	0 129	0 129	0 125	0 124	0 123	0 122	0 121	0 120
0 206	0 206	0 206	0 206	0 202	0 201	0 200	0 199	0 198	0 197
0 180	0 180	0 180	0 180	0 176	0 175	0 174	0 173	0 172	0 170
-0 000	-0 000	-0 000	-0 000	-0 004	-0 005	-0.007	-0 008	-0.009	-0 011
-0 386	-0 386	-0 386	-0 386	-0.391	-0 392	-0 393	-0 394	-0 396	-0 397
-1 029	-1 029	-1 029	-1 029	-1 034	-1 035	-1 036	-1 038	-1 039	-1 041

Modelling (Second-Order Pincushion)

0. 000	-0 000	-0. 000	-0. 000	-0. 000	-0 000	-0 000	-0 000	-0 000	-0 000
-0 035	-0 041	-0 044	-0 049	-0 070	-0 105	-0 115	-0 128	-0 177	-0 301
-0 044	-0 056	-0. 055	-0 056	-0 085	-0 137	-0 136	-0 137	-0 207	-0 422
-0 031	-0 046	-0 038	-0 028	-0 057	-0 115	-0 088	-0 061	-0 133	-0 417
-0 000	-0 018	-0 000	-0 023	-0 000	-0 058	-0 000	-0 '063	-0 000	-0 343
0 039	0 018	0 045	0 082	0 064	0 006	0 096	0 196	0 141	-0 261
0 070	0 046	0 080	0 127	0. 110	0 046	0 161	0 290	0 232	-0 239
0 068	0 039	0 077	0 128	0 104	0 021	0 148	0 288	0 210	-0 352
-0 000	-0 036	-0 000	0 046	-0 001	-0 119	-0 002	0 124	-0 003	-0 689
-0 357	-0 399	-0 366	-0 326	-0 394	-0 546	-0 439	-0 326	-0 503	-1 313
-0 425	-0 472	-0 436	-0 391	-0. 468	-0. 637	-0 520	-0 394	-0 592	-1 493
-0. 277	-0 328	-0 284	-0 229	-0. 305	-0 480	-0 337	-0 184	-0 383	-1 354
-0 000	-0 053	-0 000	0 069	-0 002	-0 178	-0 003	0 187	-0 004	-1 034
0 301	0 245	0 307	0 390	0 324	0 148	0 355	0 581	0 398	-0. 690
0 502	0 442	0 512	0 605	0 540	0 358	0 590	0 844	0 659	-0 499
0 457	0 393	0 466	0 563	0 490	0 290	0 533	0 799	0 594	-0 655
-0 000	-0 071	-0 000	0 091	-0 003	-0. 237	-0 004	0 249	-0 006	-1 379
-1 060	-1 141	-1 079	-1 006	-1 140	-1 431	-1 236	-1 029	-1 371	-2 911
-2 940	-3 033	-2 991	-2 952	-3 147	-3 525	-3 402	-3 283	-3 760	-5 520

Figure 2.2-16

BIQUADRATIC INTERPOLATION

Modelling Error 2: (First-Order Pincushion)

0 000	0 000	0 000	0 000	0 000	0 000	0 000	0. 000	0 000	0 000
1 610	1 610	1 610	1 610	1 610	1 610	1 610	1 610	1 610	1 610
3 169	3 169	3 169	3 169	3. 169	3 169	3 169	3 169	3 169	3 169
4 624	4 624	4 624	4 624	4 624	4 624	4 624	4 624	4 624	4 624
5 926	5 926	5 926	5 926	5 926	5 926	5 926	5 926	5 926	5 926
7 022	7 022	7 022	7 022	7 022	7 022	7 022	7 022	7 022	7 022
7 860	7 860	7 860	7 860	7. 860	7 860	7 860	7 860	7. 860	7 860
8 390	8 390	8 390	8 390	8 390	8 390	8 390	8 390	8 390	8 390
8 560	8 560	8 560	8 560	8 560	8 560	8 560	8 560	8 560	8 560
8 318	8 318	8 318	8 318	8 318	8 318	8 318	8 318	8 318	8 318
7 613	7 613	7 613	7 613	7 613	7 613	7 613	7 613	7 613	7 613
6 394	6 394	6 394	6 394	6 394	6 394	6 394	6 394	6 394	6 394
4 609	4 609	4 609	4 609	4 609	4 609	4 609	4 609	4 609	4 609
2 207	2 207	2 207	2 207	2 207	2 207	2 207	2 207	2 207	2 207
-0 864	-0. 864	-0 864	-0 864	-0 864	-0 864	-0 864	-0 864	-0 864	-0 864
-4 655	-4 655	-4 655	-4 655	-4 655	-4 655	-4 655	-4 655	-4 655	-4 655
-9 218	-9 218	-9 218	-9 218	-9. 218	-9 218	-9 218	-9 218	-9 218	-9 218
-14 604	-14 604	-14 604	-14 604	-14 604	-14 604	-14 604	-14 604	-14 604	-14 604
-20 864	-20 864	-20 864	-20 864	-20 864	-20 864	-20 864	-20 864	-20 864	-20 864

Modelling (Second-Order Pincushion)

|									
0 000	0. 000	0 000	0 000	0. 000	0 000	0 000	0 000	0 000	0 000
0 448	0 481	0. 579	0 735	0. 934	1. 160	1 390	1 595	1 743	1 796
0 895	0 961	1. 156	1 463	1 857	2 304	2 756	3 158	3 445	3 539
1 339	1 438	1 725	2 177	2 758	3 413	4 074	4. 697	5. 063	5 178
1 777	1 905	2 278	2 867	3 621	4 468	5 316	6 055	6 552	6 654
2 197	2 352	2 805	3 517	4 425	5 441	6 449	7 311	7. 861	7 908
2 583	2 762	3 284	4. 104	5. 145	6 301	7 435	8 378	8 932	8. 870
2 911	3 110	3 691	4. 599	5 747	7. 008	8. 225	9 200	9 702	9 466
3 147	3 362	3 988	4 963	6. 185	7. 513	8 763	9 712	10 096	9 610
3 247	3 473	4 128	5 144	6 405	7 753	8 982	9 839	10. 028	9 206
3 153	3 384	4 051	5 079	6 340	7 657	8 801	9 492	9. 400	8 145
2 792	3 022	3 683	4 691	5 908	7 136	8 125	8 568	8 100	6 303
2 079	2 300	2 933	3 887	5 010	6 087	6 844	6 947	5 999	3 543
0 906	1 111	1 694	2 556	3 531	4. 388	4. 831	4 495	2 952	-0 295
-0 850	-0 669	-0 161	0. 567	1 337	1 900	1 936	1 055	-1 207	-5 383
-3 333	-3 185	-2 779	-2 230	-1. 727	-1 538	-2 006	-3 549	-6 663	-11 920
-6 712	-6 607	-6 331	-6 008	-5. 839	-6 110	-7 186	-9 515	-13 624	-20 124
-11 177	-11 124	-11 010	-10 963	-11 199	-12 021	-13 818	-17 064	-22 321	-30 236
-16 944	-16 955	-17 033	-17 317	-18 034	-19 505	-22 141	-26 445	-33 011	-42 526

Figure 2.2-18

GLOBAL BIQUADRATIC
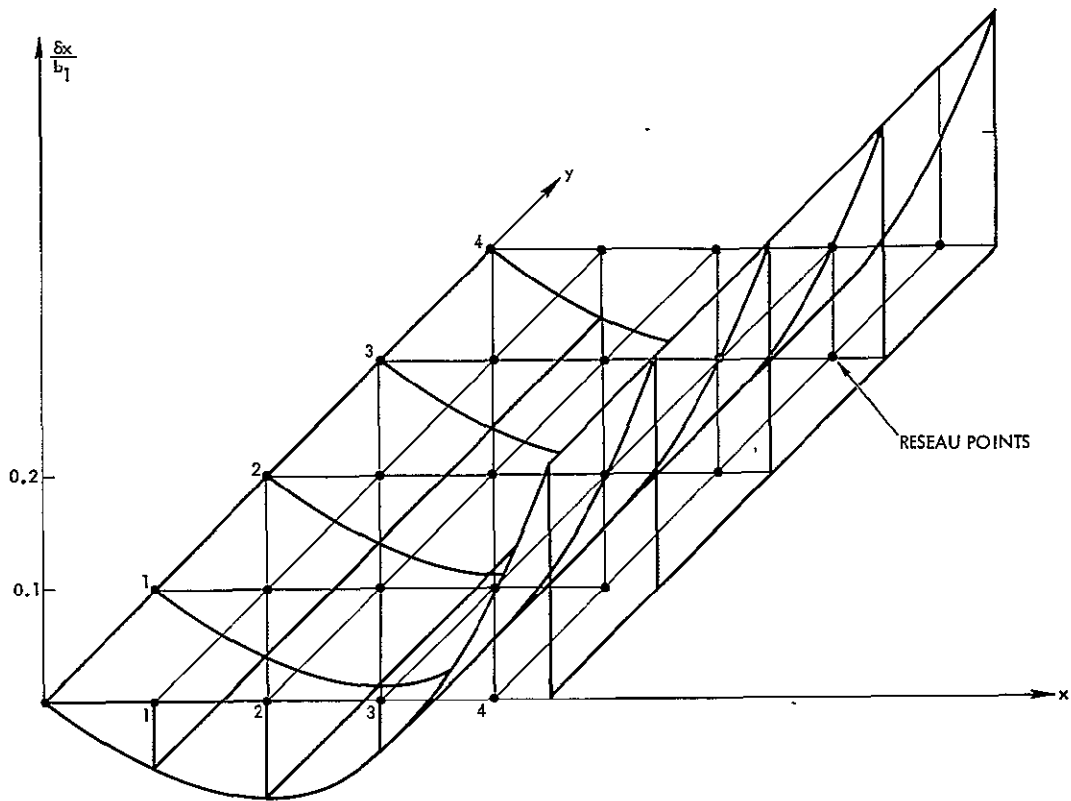
Figure 2.2-19

THE FUNCTIONAL ERROR FOR THE LEAST-SQUARES FIT of the
$x(x^2 + y^2)$ term by a biquadratic global polynomial (first-order pincushion)

Modellmg Error 2: (Second-Order Pincushion)

0 000	-1 757	-3 182	-3 994	-4 015	-3 218	-1 778	-0 127	1 001	0 515
0 000	-1 740	-3 150	-3 949	-3 961	-3. 160	-1 722	-0 081	1 028	0 513
0 000	-1 690	-3 054	-3 815	-3 800	-2 987	-1 557	0. 055	1 107	0 504
0 000	-1 608	-2 896	-3 595	-3 536	-2 704	-1 287	0 273	1 229	0 479
0 000	-1 496	-2. 680	-3 293	-3. 175	-2. 319	-0. 923	0 562	1. 382	0 425
0 000	-1 355	-2 410	-2 916	-2 726	-1. 844	-0 478	0 908	1 549	0 321
0 000	-1 189	-2 091	-2 473	-2 200	-1 291	0. 031	1 290	1. 706	0 141
0 000	-1 000	-1 731	-1 974	-1 612	-0. 680	0 583	1. 684	1. 825	-0 145
0 000	-0. 794	-1 338	-1. 432	-0 978	-0 030	1 153	2 060	1. 875	-0. 576
0 000	-0 575	-0. 921	-0 860	-0 316	0 634	1 713	2 386	1 815	-1 193
0 000	-0 348	-0 491	-0. 276	0. 350	1. 287	2 230	2 623	1 604	-2 046
0 000	-0 119	-0 060	0 304	0 998	1 896	2. 668	2 730	1 192	-3 189
0 000	0 104	0 358	0 858	1 600	2 430	2. 988	2. 660	0 527	-4 682
0 000	0 316	0 749	1 365	2 128	2 852	3. 144	2 361	-0. 449	-6 591
0 000	0 507	1 096	1 801	2 550	3 121	3 091	1 778	-1 801	-8 986
0 000	0 669	1 384	2 140	2 830	3 196	2 775	0 851	-3 597	-11 946
0 000	0 793	1 593	2 355	2 934	3 030	2 142	-0. 434	-5 911	-15 553
0 000	0 870	1 704	2. 417	2 820	2. 573	1 134	-2 297	-8 820	-19 895
0 000	0 888	1 696	2 293	2 447	1 774	-0 314	-4 660	-12 410	-25 067

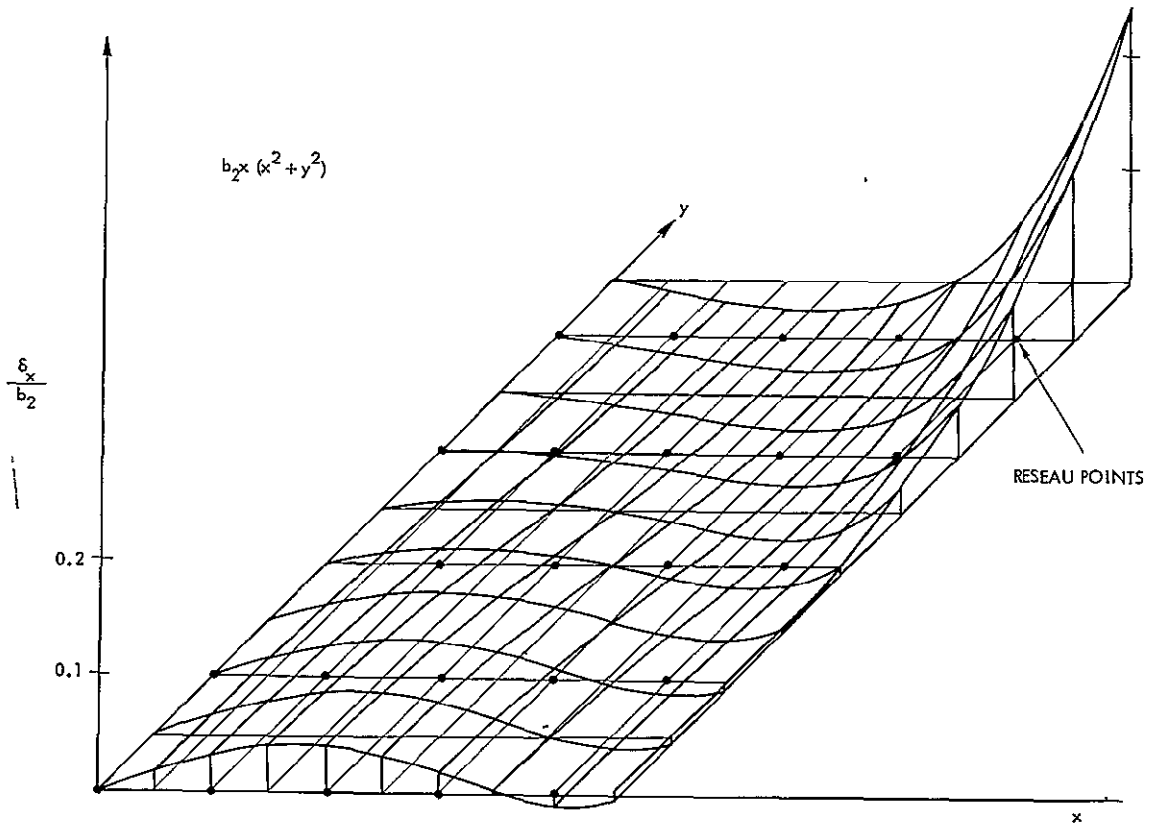Figure 2.2-20

GLOBAL THIRD-ORDER POLYNOMIAL

Figure 2.2-21

GLOBAL THIRD-ORDER POLYNOMIAL FUNCTIONAL SENSITIVITY
to second-order pincushion $b_2x(x^2 + y^2)$

Table 2.2-2.   Maximum Error Magnitudes for RBV Processing

Algorithm Error	Global Third-Order Polynomial	Global Biquadratic Polynomial	Piecewise Bilinear Interpolation	Piecewise Biquadratic Interpolation
(1) Total image				
Statistical (σ/σ_R)	0.982 (1.5)*	1.048 (1.5)	2.500 (3.8)	5.219 (7.8)
Sensitivity to first-order pincushion (percent)	0 (0)	21% (8)	6.61% (3)	1% (0.5)
Sensitivity to second-order pincushion (percent)	25% (2)	43% (4)	16% (1.3)	5.5% (0.5)
(2) Internal to reseau				
Statistical (σ/σ_R)	0.633 (1)	0.661 (1)	1.000 (1.5)	1.000 (1.5)
Sensitivity to first-order pincushion	0 (0)	9.2% (3.5)	1.9% (1)	0.2% (0.1)
Sensitivity to second-order pincushion	5.9% (0.5)	14% (1.3)	3.5% (0.5)	0.85% (0.1)

*Numbers in parentheses indicate equivalent pixels assuming 1 percent first-order pincushion, 0.2 percent second-order pincushion, and 0.5 pixel 1-sigma random distortion. Entries for statistical errors in parentheses are 3-sigma values.

Once a corrected position has been calculated for a given distorted point, the value of the intensity at that corrected point must be obtained from the input intensity array. Generally, the corrected point will fall within a rectangle of input array points as indicated in Figure 2.2-22. Three methods of estimating the intensity at x', y' will be described - nearest neighbor, three-point interpolation, and four-point interpolation.
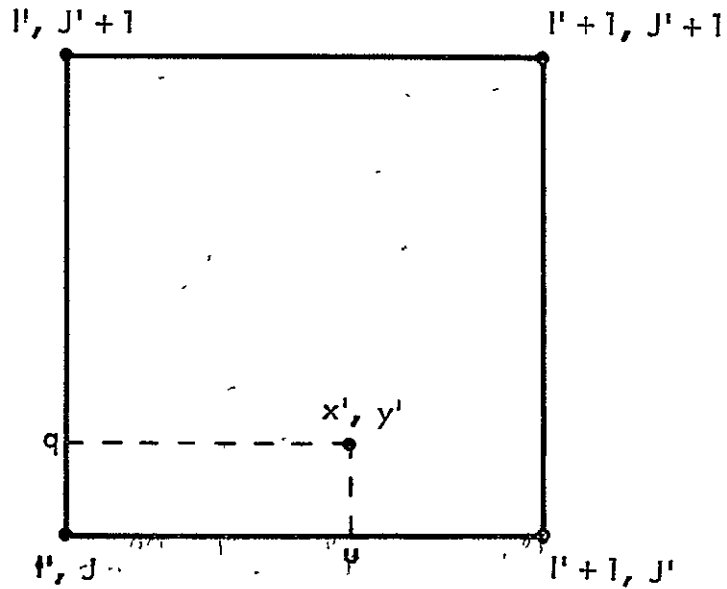

Figure 2.2-22

AN EXAMPLE OF THE INTENSITY CALCULATION GEOMETRY

In the nearest-neighbor approach one determines the closest of the surrounding points and assigns the intensity at that point to the point x', y'.

In three-point interpolation, one separates x' and y' into their integer and fractional parts and interpolates by expanding about the integer values as follows:

$$x' = I' + u \qquad y' = J' + q$$

$$R(x', y') = R(I', J') + u \left[R(I' + 1, J') - R(I', J') \right]$$

$$+ q \left[R(I', J' + 1) - R(I', J') \right]$$

This procedure is equivalent to passing a plane through the three points in use. An improvement in three point interpolation results if one first determines the nearest neighbor and then expands about that point.

In four-point interpolation, one uses all four adjacent points to interpolate the value of the intensity at x', y'. This procedure is another application of bilinear interpolation. The equations in this case are

$$R(I', y') = R(I', J') + q [R(I', J' + 1) - R(I', J')]$$

$$R(I' + 1, y') = R(I' + 1, J') + Q [R(I' + 1, J' + 1) - R(I' + 1, J')]$$

$$R(x', y') = R(I', y') + u [R(I', y') - R(I', y')]$$

The following estimates of computation time will be based on the number of equivalent arithmetic operations found in each technique. The word equivalent refers to the fact that one multiplication is equated to two adds. The ratio of equivalent arithmetic operations is assumed to be approximately equal to the ratio of computation times. However, estimates based on such ratios will be rough since "housekeeping" operations are not strictly proportional to arithmetic operations. In one case, the actual computation time for an existing machine language program is known and this value coupled with the operation ratios will yield an estimate of the computation times for the unprogrammed schemes. The policy behind this rather approximate approach is that, when one must compare unprogrammed schemes, a rough estimate of computation time is better than no estimate at all.

It is easily demonstrated that the number of operations required to determine the coefficients in the assumed polynomials is small compared to the number of operations required to apply these polynomials to all 10^7 points in the image and calculate an intensity for each point.

The computation time can be estimated in the following manner. In all cases considered, one would have to apply two polynomials of the form

$$\delta x = \sum_{mn} a_{mn} x^m y^n$$

to the points in the image, one for the x correction, one for the y.

With the global polynomial algorithms, there would be two such polynomials for the whole image, while in the interpolation procedures, there would be two polynomials for each region. By correcting the image row by row, one can cut down on computation time in the following way. Collect terms of the same power in x in the distortion equation which yields an expression of the form

$$z = g_1(y) + g_2(y)x + g_3(y)x^2 + \dots$$

where the g's polynomials in y. For a given row in a region, one can calculate the g-functions once at the beginning value of x. This calculation time is very small compared to what follows. Consider the bilinear case first. Since x increases in steps of one pixel, we can write

$$z_n = a_1 + a_2 n$$

and

$$z_{n+1} = a_1 + a_2(n+1) = z_n + a_2$$

Therefore, one addition for each coordinate is sufficient to calculate the correction at each point. For a given set of coefficients this addition is made 4200 times in the global polynomial case and about 500 times in the interpolation case.

Next consider the quadratic case for which

$$z_n = a_1 + a_2 n + a_3 n^2$$

Thus

$$z_{n+1} = a_1 + a_2(n+1) + a_3(n+1)^2$$

$$= z_n + A + B_n$$

where $B_n = B_{n-1} + 2a_3$ and $A = a_2 + a_3$

This procedure involves three additions/point for each coordinate. Therefore, six additions/point are necessary to calculate the correction in the quadratic case. Similarly, it can be shown that 12 additions/point are needed in the cubic case.

In summary, the computation time depends on the highest power of x in the correction polynomial. The number of equivalent arithmetic operations for the linear, quadratic, and cubic cases have been given.

Having calculated the geometric correction, one next calculates the intensity at the point in question using the input intensity array and one of the techniques outlined above. If one uses the nearest neighbor approach, about one equivalent operation per point is required. In three-point interpolation four adds and two multiplies are required for a total of eight equivalent operations ($1M = 2A$). In four-point interpolation six adds and three multiplies are required for a total of 12 equivalent operations.

The total equivalent arithmetic operations that result from combinations of geometric correction procedure and intensity calculation are summarized in Table 2.2-3.

Table 2.2-3. Equivalent Arithmetic Operations/Point
for Various Correction Schemes

Geometric Correction	Intensity Calculation		
	Nearest Neighbor	Three-Point Interpolation	Four-Point Interpolation
Piecewise-Bilinear	3	10	14
Piecewise Biquadratic	7	14	18
Global Polynomial (x^2)	7	14	18
Global Polynomial (x^3)	13	20	24

The computation time in seconds for an IBM 360/65 is presented in Table 2.2-4 for each of the schemes in Table 2.2-3. In constructing the table, it was assumed that the intensity array will consist of 4200 x 4096 values. The value marked with an asterisk was obtained by adding IBM 360/65 operation times for the machine language program prepared for TRW. All the other values are rough estimates based on arithmetic operation ratios relative to this reference program.

Table 2.2-4. Computation Times/Frame on an
IBM 360/65 in Seconds

Geometric Correction	Intensity Calculations		
	Nearest Neighbor	Three Point	Four Point
Piecewise Bilinear	250	800	1100 *
Piecewise-Biquadratic	550	1100	1400
Global Polynomial (x^2)	550	1100	1400
Global Polynomial (x^3)	1000	1600	1900

The computation time for the piecewise-bilinear, four-point interpolation program is 140 seconds on an IBM 360/85. Computation times on other computers were not estimated.

Conclusions

Distortion-removal procedures for RBV images involve a geometric correction and an intensity calculation. In this work, the accuracy of various geometric correction approaches has been investigated. The geometric correction error is a sum of two terms; a functional error and a statistical error. Each of these errors can be investigated separately. The functional error will depend on the actual form of the functional distortion found in the ERTS RBV. Since the actual

functional distortion cannot be predicted in advance, functional errors have been calculated for specific distortion terms that are not uncommon and are at the specification limit. The results for internal points may be summarized as follows, if one somewhat arbitrarily takes one pixel as a standard. The piecewise bilinear approach will give marginally adequate functional fits to pincushion and tangential terms such as $x(x^2 + y^2)$ and $x(x^2 + y^2)^2$ when these terms produce a 1 percent corner distortion. The piecewise biquadratic approach will give excellent fits to these terms. A biquadratic global polynomial will give poor functional fits to these terms, while a cubic global polynomial produces a functional error comparable to the piecewise bilinear approach. Even through the above evaluations are based on fits to specific distortion terms, the functional accuracy of the approaches should not change drastically for any distortion which exhibits about the same curvature and magnitude.

The statistical accuracy of the various approaches is independent of functional distortion and may be summarized as follows. The global polynomial approach yields a smaller statistical error than the interpolation procedures. If the reseau measurement error is large compared to spatial noise, the least-squares statistical error is a factor of three smaller than the interpolation statistical error in the cases considered. If the reseau measurement error is small compared to the spatial noise, the least-squares approach can lose its statistical advantage. If the functional distortion is constant over many frames for a given camera, then an average of correction polynomials of past frames will eventually bring the estimation statistical error below the functional error. In this case, the interpolation procedure would be superior to the global polynomial approach when both accuracy and speed are considered. Implicit in this result is the ability of coefficient averaging to reduce, and perhaps remove, the effect of beam-pulling errors in the reseau displacement measurement.

Based on the above accuracy results, timing requirements, and comments, a biquadratic interpolation algorithm is recommended. It is felt that the added accuracy over the bilinear interpolation is required as

a buffer against large unmodelled distortions. Also, a three- or four-point intensity interpolation algorithm is recommended as it is possible for the nearest-neighbor algorithm to generate undesirable cosmetic defects. Detailed timing estimates for the linear interpolation approach using the IBM 360/85 indicates less than a 3-minute processing time, which is commensurate with throughput requirements.

2.2.2.2 Image Motion Compensation - Smear Removal

The RBV camera is moving relative to the earth at such a rate that results in a 2 pixel smear due to the movement of the image across the vidicon surface during the effective aperture time of the shutter. The mathematical model for smearing is that adjacent elements are added to give a composite video value at that point. The problem is, therefore, to invert this operation and apply the result to the received video. Unfortunately, the required operator is an infinite series and requires infinite memory, or some unsmeared portion must be available.

A second, approximate, approach is to examine how many points in the input data stream must be examined for the correction function to give an output picture to given error. This problem is not fully out of the research and development stage as yet. Our conclusions are as follows:

Let the smear be n pixels long, let the resolution be 4200 pixel on each side of the image of dimension 1, say 1 inch. The smear dimension is then $n/4200''$. The continuous transform of the smear is

$$\frac{\sin\left(\frac{n}{4200}\right)\frac{\omega}{2}}{\frac{n}{4200} \cdot \frac{\omega}{2}}$$

This function has zeros at the zeros of $\sin (n/4200 \cdot \omega/2)$ i.e., at

$$\frac{n\omega}{2 \times 4200} = \pi,\ 2\pi,\ldots \text{etc.}$$

The first zero occurs at

$$\omega = 2\pi f = 2\pi \frac{4200}{n}$$

2-45

i. e. , at

$$f = \frac{4200}{n}.$$

The specification defines n = 2, i. e. , f = 2100 cycles. For a 4200 line sampled system the information content can only be 2100 cycles, band limited functions only, thus the first zero of the smear occurs at the highest signal sequal frequency obtainable. The inverse of this curve is required.

Suppose that the image has a flat spectrum, amplitude one on the ground, this is smeared on the vidicon face plate to give a (sin x/x) frequency response curve. Also, white noise of amplitude k is added (quantum effects). The filter necessary to compensate for smear thus must be (sin x/x)$^{-1}$ where x = (nω/8400). The inverse filter is shown schematically in Figure 2.2-23. This has not been drawn accurately but is intended to illustrate the argument only.
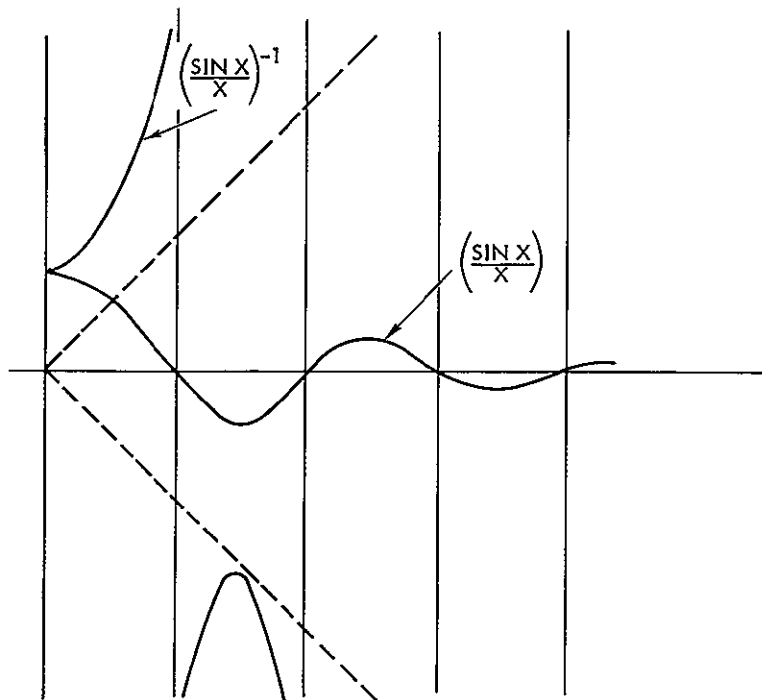

Figure 2.2-23

SIN X/X AND (SIN X/X)$^{-1}$

2-46

It is necessary to low pass filter the spectrum for sampling reasons, Figure 2.2-24, so that the sin x/x curve is defined only up to the first zero. This is an extremely fortunate occurrence since the smear is such that if the infinity seen in the spectrum falls in the passband, Figure 2.2-25, then a more complex phase reversal filter is required; we will return to this point.
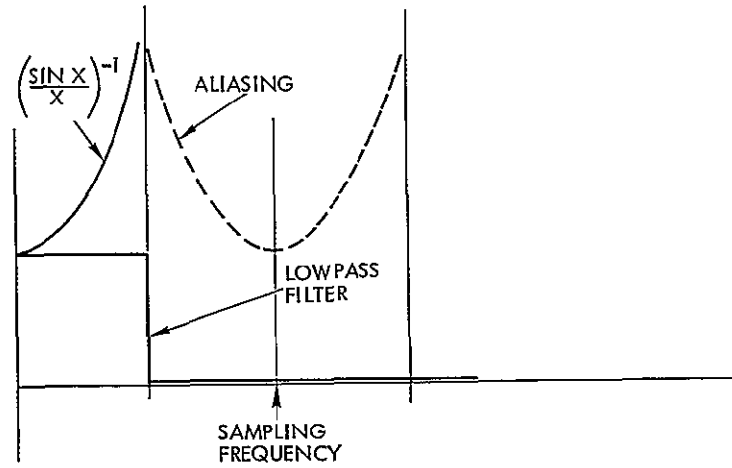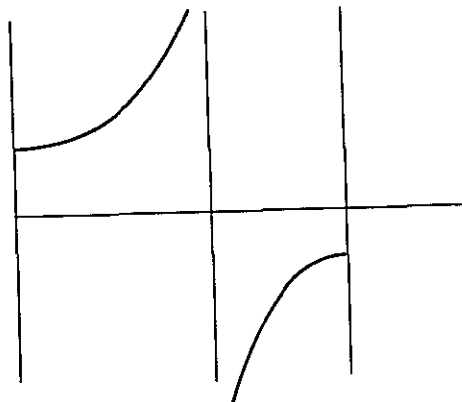

Figure 2.2-24

LOW PASS AND SAMPLED (SIN X/X)

Figure 2.2-25

SMEAR >2 AND A ZERO IN THE PASSBAND

Since the $\sin x/x$ signal was corrupted by white noise the compensated image will appear to have colored noise superimposed on it. We propose a Wiener filter, Figure 2.2-26, for its removal in a mean square optimal sense. Now the signal has unity spectrum, the noise spectrum is $(k\,x/\sin x)$ where k was the original amplitude: the optimum Wiener filter is now

$$W = \frac{S^2}{S^2 + n^2} = \frac{1}{1 + k^2 \left(\dfrac{x}{\sin x}\right)^2}$$
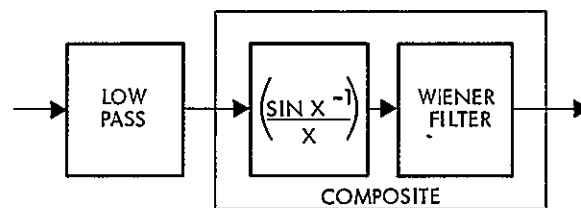

Figure 2.2-26

COMPOSITE FILTER

The composite filter is now

$$C = \frac{x}{\sin x}\left[\frac{1}{1 + k^2 \left(\dfrac{x}{\sin x}\right)^2}\right] = \frac{1}{\left(\dfrac{\sin x}{x}\right) + k^2 \left(\dfrac{x}{\sin x}\right)}$$

This is shown in Figure 2.2-27

If k = 0, we obtain
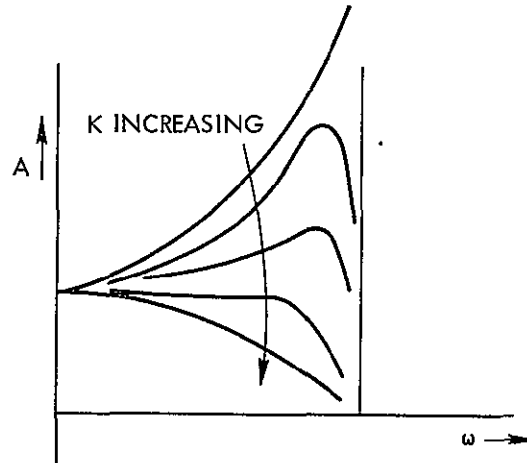
$$C = \frac{x}{\sin x}$$

2-48

Figure 2.2-27

NORMALIZED COMPOSITE FREQUENCY RESPONSES AS K, THE
additive noise, varies

If k is large we obtain

$$C = \frac{1}{k^2} \left(\frac{\sin x}{x} \right)$$

At the realistic 30 db signal to noise ratio, $k^2 = 1/1000$, the response is given in Figure 2.2-28. The inverse transform of this curve gives the time domain operator necessary.

If the smear is more than 2 pixels, it is necessary to use as a filter the inverse of a function which passes through zero inside the passband of the system. In this case the db and phase versus frequency curves can be approximated by a filter with a flat passband except at a notch at the first zero of the smear and with a phase characteristic which changes abruptly by 180° at the notch frequency, Figure 2.2-29.

In the case of the 2 pixel smear the amplitude characteristic of the compensating filter can be approximated by a sampled data filter or transversal filter either in the analog or digital domain with only a few terms since we only need to synthesize the rising portion of the compensation curve of Figure 2.2-28 because the falling portion is implicit in the ideal low pass filter necessary for digitization.
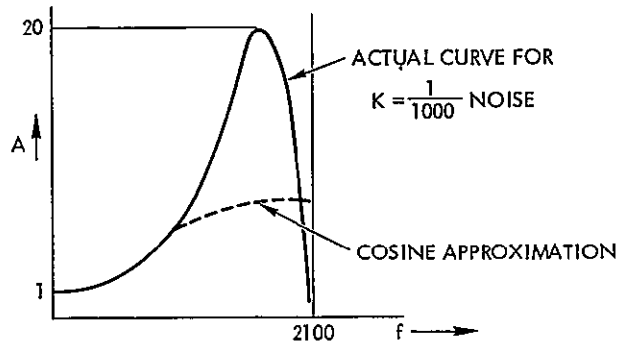
Figure 2.2-28

COSINE APPROXIMATION
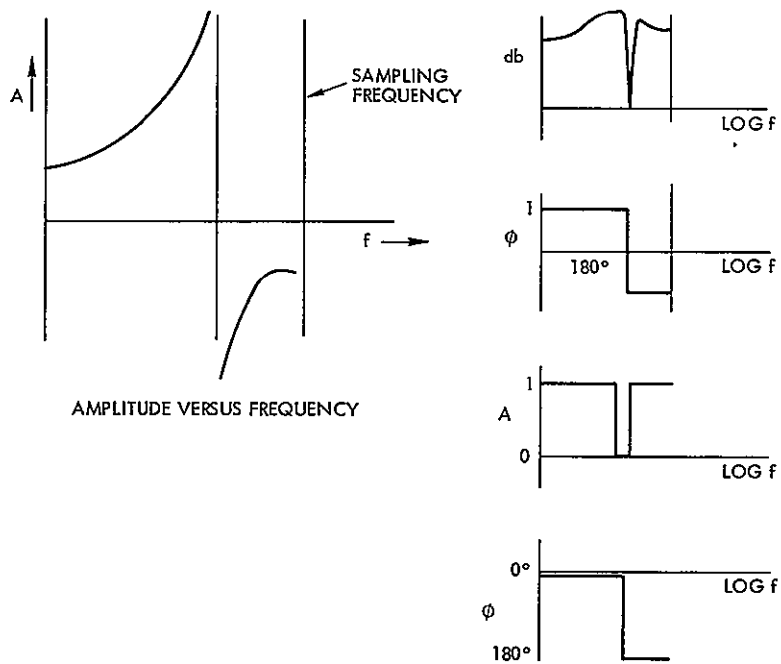
Figure 2.2-29

NOTCH FILTER DESIGN

The approximation will be improved by taking more terms.

The reasoning behind this statement of the necessity of only using few terms is as follows: consider a 3 point digital filter defined on a one dimensional lattice. Figure 2. 2-30.

Figure 2.2-30

THREE POINT ISOTROPIC FILTER

The z transform of this filter is

$$f(z) = a_1 z + a_0 + a_1 z^{-1} = a_0 + a_1 \left(z + \frac{1}{z}\right)$$

where

$$z = e^{ST}$$

and T = sampling period.

Let

$$s = j\omega$$

then,

$$f^*(j\omega) = a_0 + 2a_1 \cos \omega T \quad .$$

This frequency response is plotted in Figure 2. 2-31 schematically in the case where a_1 is negative. The desired function is shown in dotted lines.
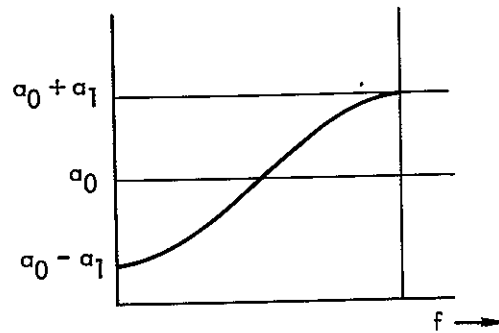
Figure 2.2-31

FREQUENCY RESPONSE OF 3 POINT FILTER
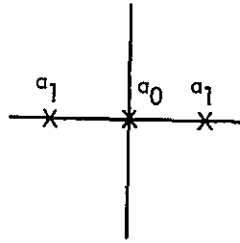
As f(z) includes more terms, i. e. , the operator expands, then the expressions become for a seven point filter,

$$f^*(j\omega) = a_0 + 2a_1 \cos \omega T + 2a_2 \cos 2\omega T + 2a_3 \cos 3\omega T$$

where a_0, a_1, a_2, and a_3 are free to be chosen by the designer.

In the case where smear involves more than 3 elements, the notch frequency must be entirely removed by the filter. Such a sharp cutoff is difficult to realize by means of filters with short impulse responses.

The application of Bernstein's theorem relating the maximum rate of change of a signal to the bandwidth would give a bound on the filter length; time has not thus far permitted this approach to be pursued.

The above equations apply equally to analog time domain, digital time domain, and digital Fourier domain operations. Efficiency and cost must decide on the removal means.

The one dimensional filter for smear removal will be combined with the other necessary operators and the preferred implementation deferred until these points have been discussed.

2.2.3 MSS Errors

The MSS has no problems with color registration, or with scan irregularities because of its basic construction.

a) Line scan skew errors arise from yaw offsets, from the earth's rotation, and from roll rate.

b) The MSS is subject to the same additive noise as the RBV. This is to a first approximation true, although it is conceivable that the data may be absolutely clean. A case in point is that the photo-sensing diode in the MSS may be coupled intimately with the analog to digital converter in such a manner that no ground loop problems can possibly occur. Additive noise from the communication channel at the spacecraft orbit altitude, under consideration in ERTS, presents no severe detection problems since adequate power is available in the transmitters.

c) The MSS errors arise from the attitude, roll, pitch and yaw, of the spacecraft, since it is stabilized in a bang bang fashion and therefore to a small extent fails to present a straight line in its sub-satellite point.

d) The MSS scan nonlinearity can be precalibrated, since it is not so sensitive to electrical interference.

It is demonstrated in this section that a second-order global polynomial correction technique can be used in the precision processing of MSS pictures with a modeling error less than the internal consistency of the picture reference points. This technique will greatly reduce the computing time required.

It is estimated that it would take an unacceptably large amount of time, several hours, to compute the precision ground point for each picture element, using attitude determination and satellite ephemeris data. In place of this, it is much more efficient to compute ground points, latitude and longitude, for a small number of reference points and "reseau" correct intermediate points as in the RBV. The computation of the pseudo-reseau points would require a negligible amount of time, and the reseau-correction (interpolation) time would be comparable to that for processing the RBV. It is demonstrated here that a 3 x 3 grid of points and a second order polynomial gives picture distortions less than the internal consistency of the reference points.

2.2.3.1 MSS Pseudo-Reseau Corrections

In the MSS bulk mode with no geometric corrections, the picture is represented in the scan angle (β_i) versus time (t_i) plane. The MSS pseudo reseau correction involves finding the mapping from the β versus t plane into the latitude (θ) versus longitude ($\emptyset$) plane by means of a knowledge of a small number of reference points. The problem can be summarized mathematically as follows:

Find the functions

$$\theta_i = \theta(\beta_i, t_i) \quad , \quad \emptyset_i = \emptyset(\beta_i, t_i) \tag{2-1}$$

given the locations of a grid of reference points θ_j, $\emptyset_j$. An obvious way to proceed with the solution of this problem is to expand θ_i and $\emptyset_i$ in a Taylor series about the reference points θ_j and $\emptyset_j$. For the latitude θ_i the second order Taylor series expansion is

$$\theta_i = \theta(\beta_j, t_j) + \frac{\partial \theta}{\partial \beta_j}(\beta_i - \beta_j) + \frac{\partial \theta}{\partial t_j}(t_i - t_j) + 1/2 \frac{\partial^2 \theta}{\partial \beta_j^2}(\beta_i - \beta_j)^2$$

$$+ 1/2 \frac{\partial^2 \theta}{\partial t_j^2}(t_i - t_j)^2 + 1/2 \left[\frac{\partial^2 \theta}{\partial \beta_j \partial t_j} \right.$$

$$\left. + \frac{\partial^2 \theta}{\partial t_j \partial \beta_j} \right] (\beta_i - \beta_j)(t_j - t_i) + (3^{\text{rd}} \text{ order terms}) \tag{2-2}$$

or

$$\theta_i = \theta(\beta_j, t_j) + \left[\beta_i - \beta_j, t_i - t_j, (\beta_i - \beta_j)(t_j - t_i), (\beta_i - \beta_j)^2 \quad , \quad (t_i - t_j)^2 \right] \begin{pmatrix} a_1 \\ a_2 \\ a_3 \\ a_4 \\ a_5 \end{pmatrix}$$

$$\theta_i = \theta(\beta_j, t_j) + M^{ij}\underline{a} \tag{2-3}$$

Where

$$a_1 = \frac{\partial \theta}{\partial \beta_j} \quad , \quad a_2 = \frac{\partial \theta}{\partial t_j} \quad , \quad a_3 = 1/2 \left[\frac{\partial^2 \theta}{\partial \beta_j \partial t_j} + \frac{\partial^2 \theta}{\partial t_j \partial \beta_j} \right]$$

$$a_4 = 1/2 \frac{\partial^2 \theta}{\partial \beta_j^2} \quad , \quad a_5 = 1/2 \frac{\partial^2 \theta}{\partial t_j^2} \quad \quad \quad (2-4)$$

Similarly for longitude $\emptyset_i$

$$\emptyset_i = \emptyset (\beta_j, t_j) + M^{ij} \underline{b} \quad \quad \quad (2-5)$$

The distortion vectors $\underline{a}$ and $\underline{b}$ can be identified with the geometric parameters as shown in Tables 2.2-3 and 2.2-4 respectively.

Table 2.2-3.   Cross Scan Distortion Parameters

Parameter	Term Name	Variable
$\theta (\beta_j, t_j)$	Picture centering	Pitch angle Ephemeris (tangential)
a_1	Skew	Yaw angle
a_2	Scale	Pitch rate Ephemeris (altitude)
a_3	Keystone	Yaw rate
a_5	Second order scaling	Pitch rate Ephemeris

Table 2.2-4. Along Scan Distortion Parameters

Parameter	Term Name	Variable
$\emptyset\,(\beta_j,\ t_j)$	Picture centering	Roll angle Ephemeris (normal)
b_1	Scale	Ephemeris (altitude)
b_2	Skew	Roll rate
b_4	Second order scaling	Ephemeris (altitude)

In order to solve for the distortion parameters it is only necessary to select as many reference values of θ_i and $\emptyset_i$ in equations (2-3) and (2-5) as there are distortion parameters. In the case of a second order polynomial this amounts to 5 + 1 reference points. These points must be chosen so that the sets of equations (2-3) and (2-5) can be inverted to solve for $\underline{a}$ and $\underline{b}$. An example of a non-singular set of such points is shown in Figure 2.2-32.

As can be seen from Table 2.2-5 the reference points are a subset (designated with circles) of a 3 x 3 grid of 9 points covering the full MSS picture. Thus reference points ①, ④, ⑦ are at the same scan angle but different times on the picture and point ⑨ is at the opposite corner of the picture from starting point ①. If Δt is the time of one scan line from $-\beta$ to $+\beta$, and the total picture takes $N\Delta t$ seconds to scan;
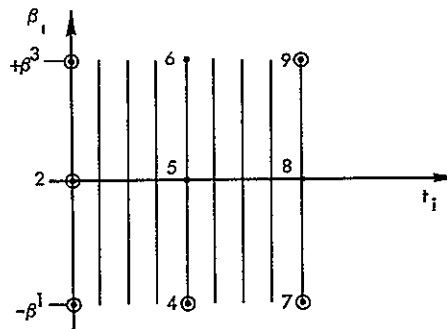

Figure 2.2-32

MSS PSEUDO RESEAU POINTS FOR SECOND ORDER
Taylor series

Table 2.2-5. Picture Points Used in Modeling Error Analysis for
No Attitude Limit Cycle Angles or Rates

Picture Point No.	Latitude	Longitude
1	45° 44' 56 0"	-99° 46' 35 0"
2	45° 41' 8. 4"	-100° 22' 35. 6"
3	45° 37' 11. 0"	-100° 58' 19. 0"
4	45° 33' 2. 4"	-101° 33' 58. 0"
5	45° 28' 41. 3"	-102° 9' 45. 5"
6	45° 19' 57. 5"	-99° 43' 22. 2"
7	45° 16' 11. 5"	-100° 19' 6. 9"
8	45° 12' 15 8"	-100° 54' 34. 7"
9	45° 8' 9. 1"	-101° 29' 58. 2"
10	45° 3' 49. 9"	-102° 5' 30. 2"
11	44° 54' 58. 8"	-99° 40' 13. 4"
12	44° 51' 14. 2"	-100° 15' 42. 6"
13	44° 47' 20 2"	-100° 50' 55. 0"
14	44° 43' 15 3"	-101° 26' 3. 3"
15	44° 38' 58. 1"	-102° 1' 20. 2"
16	44° 29' 59. 7"	-99° 37' 8 6"
17	44° 26' 16. 6"	-100° 12' 22 6"
18	44° 22' 24. 2"	-100° 47' 20. 0"
19	44° 18' 21. 1"	-101° 22' 13. 4"
20	44° 14' 5. 9"	-101° 57' 15. 4"
21	44° 5' 0. 3"	-99° 34' 7. 5"
22	44° 1' 18. 7"	-100° 9' 6. 6"
23	43° 57' 27. 8"	-100° 43' 49 3"
24	43° 53' 26. 5"	-101° 18' 28. 1"
25	43° 49' 13 2"	-101° 53' 15. 6"

then the distortion vector $\underline{a}$ is given in terms of the reference latitudes
$\theta_j = \theta \, (\beta_j, \ t_j)$.

$$a_2 = \frac{4 \, (\theta_4 - \theta_1) - (\theta_7 - \theta_1)}{N \Delta t}$$

$$a_5 = \frac{2 \, (\theta_7 - \theta_1) - 4 \, (\theta_4 - \theta_1)}{N^2 \Delta t^2}$$

$$a_3 = \frac{(\theta_9 - \theta_1) - (\theta_3 - \theta_1) - (N - 1)\Delta t a_2 - (N^2 - 1)\Delta t^2 a_5}{2\beta(N - 1)\Delta t}$$

$$a_4 = \frac{(\theta_3 - \theta_1) - 2(\theta_2 - \theta_1) - \Delta t^2/2 \, a_5 - \beta \Delta t \, a_3}{2\beta^2}$$

$$a_1 = \frac{(\theta_2 - \theta_1) - \Delta t/2 \, a_2 - \Delta t^2/4 \, a_5 - \beta \Delta t/2 \, a_3 - \beta^2 a_4}{\beta} \tag{2-6}$$

Similarly, the distortion vector $\underline{b}$ is

$$b_2 = \frac{4(\emptyset_4 - \emptyset_1) - (\emptyset_7 - \emptyset_1)}{N\Delta t}$$

$$b_5 = \frac{2(\emptyset_7 - \emptyset_1) - 4(\theta_4 - \theta_1)}{N^2 \Delta t^2}$$

$$b_3 = \frac{(\emptyset_9 - \emptyset_1) - (\emptyset_3 - \emptyset_1) - (N - 1)\Delta t b_2 - (N^2 - 1)\Delta t^2 b_5}{2\beta(N - 1)\Delta t}$$

$$b_4 = \frac{(\emptyset_3 - \emptyset_1) - 2(\emptyset_2 - \emptyset_1) - \Delta t^2/2 b_5 - \beta \Delta t b_3}{2\beta^2}$$

$$b_1 = \frac{(\emptyset_2 - \emptyset_1) - \Delta t/2 b_2 - \Delta t^2/4 b_5 - \beta \Delta t/2 b_3 - \beta^2 b_4}{\beta} \tag{2-7}$$

The procedure for interpolating to non-reseau points is then

- Compute $\underline{a}$ and $\underline{b}$ from the precision reference ground point (including attitude determination and ephemeris as well as earth rotation and oblateness).

- For non-reseau points compute θ_i and $\emptyset_i$ as

$$\theta_i = \theta_1 + M^{il}\underline{a}$$

$$\emptyset_i = \emptyset_1 + M^{il}\underline{b} \tag{2-8}$$

2-58

Actually interpolation could proceed from any other reference point (for example point ⑦) with the same results. Because of the way $\underline{a}$ and $\underline{b}$ are computed the interpolation (or modeling) error goes to zero in a neighborhood of a reseau point with the maximum modeling errors occurring midway between reseau points. Due to the geometric complexity of the modeling error, a timeshared computer program was developed that simulates the satellite motion and Earth rotation effects, as well as vehicle limit cycling. A set of pseudo reseau points was generated by the program as in Table 2.2-5. The distortion vectors $\underline{a}$ and $\underline{b}$ were then computed from equations (2-6) and (2-7) the scan angle β_j, t_j data was then transformed into latitude longitude for non-reseau points by means of the interpolation formulae. The modeling errors are then the difference between the interpolated values θ_i, ϕ_i and the exact values $\theta(\beta_i, t_i)$, $\phi(\beta_i, t_i)$

$$\varepsilon \theta i = \theta_i - \theta(\beta_i, t_i)$$

$$\varepsilon \phi i = \phi_i - \phi(\beta_i, t_i) \tag{2-9}$$

In the next section the ability of this method to remove MSS picture distortions is investigated for maximum (3σ) limit cycle conditions in both rate and angle.

2.2.3.2 Modeling Error for Second Order Polynomial

An error analysis of the second order global correction technique was conducted for the 25 MSS picture points given in Table 2.2-5. The pseudo-reseau points used were those indicated in Figure 2.2-32. Thus, in terms of Table 2.2-5 nomenclature, the reseau points are picture points 1, 3, 5, 11, 21, 25. Table 2.2-6 gives the latitude and longitude interpolation errors for the 25 picture points for zero limit cycle angles and rates. The errors, given in radian measure, in Table 2.2-6 go to zero at the six pseudo-reseau points, and reach a maximum latitude error of $7.74 \cdot 10^{-6}$ rad. at point number 22 and a maximum longitude error of $-3.936 \cdot 10^{-5}$ radian at point number 19. Translated into distance errors this is 162 ft north position error and 582 ft east position error.

Table 2. 2-6. Picture Distortions in Radians for No Attitude
Limit Cycle Angles or Rates

Point No.	Latitude Error	Longitude Error
o 1	0	0
2	3. 2525495E-06	3. 0984339E-05
o 3	2. 2482709E-09	1. 9819709E-08
4	-3. 569854E-06	-3. 0803167E-05
o 5	4. 9112714E-09	3. 9486622E-08
6	-1. 3842509E-08	-2. 7321221E-07
7	4. 120935E-06	2. 7293383E-05
8	1. 0164076E-06	-6. 0316961E-06
9	-3. 181729E-06	-3. 8573729E-05
10	-1. 0582989E-06	-9. 208823E-06
o 11	7. 2759576E-11	-1. 4551915E-11
12	5. 1795214E-06	2. 5707443E-05
13	2. 3929242E-06	-8. 4508938E-06
14	-2. 2486274E-06	-4. 1208084E-05
15	-1. 3825666E-06	-1. 1832875E-05
16	1. 3758836E-08	2. 6846101E-07
17	6. 3962725E-06	2. 5638037E-05
18	4. 0955238E-06	-7. 8625162E-06
19	-8. 1138205E-07	-3. 936619E-05
20	-1. 0134681E-06	-8. 5268985E-06
o 21	2. 910383E-11	-7. 2759576E-12
22	7. 7401237E-06	2. 6516791E-05
23	6. 0890052E-06	-4. 8700458E-06
24	1. 0904841E-06	-3. 3685566E-05
o 25	4. 813046E-09	3. 8366124E-08

Tables 2. 2-5, 2. 2-7, 2. 2-9, and 2. 2-11 are the picture points used in the modeling error analysis results given in Tables 2. 2-6, 2 2-8, 2. 2-10 and 2. 2-12 respectively.

Another modeling error run was made for the maximum roll, pitch and yaw limit cycle angles of

- roll = pitch = 0. 35°

- yaw = 0. 70°

- limit cycle rates = 0

2-60

Table 2.2-7. Picture Points Used in Modeling Error Analysis for
Maximum Roll, Pitch, and Yaw Angles

Picture Point No.	Latitude	Longitude
1	45° 41' 41.0"	-99° 41' 24.5"
2	45° 38' 13.5"	-100° 17' 30.6"
3	45° 34' 36.0"	-100° 53' 18.2"
4	45° 30' 47.6"	-101° 29' 0.1"
5	45° 26' 46.6"	-102° 4' 49.1"
6	45° 16' 42.4"	-99° 38' 14.3"
7	45° 13' 16.4"	-100° 14' 4.5"
8	45° 9' 40.6"	-100° 49' 36.4"
9	45° 5' 54.0"	-101° 25' 2.7"
10	45° 1' 55.1"	-102° 0' 36.3"
11	44° 51' 43.5"	-99° 35' 8.0"
12	44° 48' 19.0"	-100° 10' 42.7"
13	44° 44' 44.8"	-100° 45' 59.2"
14	44° 40' 60.0"	-101° 21' 10.3"
15	44° 37' 3.0"	-101° 56' 28.6"
16	44° 26' 44.3"	-99° 32' 5.6"
17	44° 23' 21.2"	-100° 7' 25.0"
18	44° 19' 48.7"	-100° 42' 26.5"
19	44° 16' 5.6"	-101° 17' 22.6"
20	44° 12' 10.5"	-101° 52' 26.1"
21	44° 1' 44.8"	-99° 29' 7.0"
22	43° 58' 23.1"	-100° 4' 11.5"
23	43° 54' 52.1"	-100° 38' 58.1"
24	43° 51' 10.8"	-101° 13' 39.7"
25	43° 47' 17.6"	-101° 48' 28.6"

Table 2.2-8.   Picture Distortion in Radians for Maximum
Roll, Pitch and Yaw Angles

Point No.	Latitude Error	Longitude Error
1	0	0
2	2.9057082E-06	3.1085321E-05
3	2.062734E-09	1.9856088E-08
4	-3.2217795E-06	-3.0864016E-05
5	4.5365596E-09	3.950845E-08
6	-1.3507815E-08	-2.6948692E-07
7	3.7734862E-06	2.7365772E-05
8	1.015389E-06	-6.0758393E-06
9	-2.8320137E-06	-3.8680002E-05
10	-1.0498225E-06	-9.2429182E-06
11	7.2759576E-11	-1.4551915E-11
12	4.8293805E-06	2.5750254E-05
13	2.3875727E-06	-8.5338324E-06
14	-1.9022191E-06	-4.1347921E-05
15	-1.3716817E-06	-1.188265E-05
16	1.3424142E-08	2.6479393E-07
17	6.0420607E-06	2.5657573E-05
18	4.0830637E-06	-7.9717574E-06
19	-4.724352E-07	-3.9520899E-05
20	-1.0057847E-06	-8.5674037E-06
21	2.910383E-11	-7.2759576E-12
22	7.3811425E-06	2.6526381E-05
23	6.0674029E-06	-4.9863083E-06
24	1.4185425E-06	-3.3829907E-05
25	4.4419721E-09	3.8380676E-08

Table 2.2-9. Picture Points Used in Modeling Error Analysis
for Maximum Sinusoidal Limit Cycle With
10 Second Period

Picture Point No.	Latitude	Longitude
1	45° 44' 48.3"	-99° 46' 21.6"
2	45° 41' 1.2"	-100° 22' 22.5"
3	45° 37' 4.3"	-100° 58' 5.9"
4	45° 32' 56.2"	-101° 33' 45.0"
5	45° 28' 35.5"	-102° 9' 32.5"
6	45° 19' 57.1"	-99° 43' 21.5"
7	45° 16' 11.0"	-100° 19' 6.1"
8.	45° 12' 15.3"	-100° 54' 33.7"
9	45° 8' 8.6"	-101° 29' 57.1"
10	45° 3' 49.4"	-102° 5' 29.0"
11	44° 55' 6.7"	-99° 40' 26.9"
12	44° 51' 21.7"	-100° 15' 56.1"
13	44° 47' 27.2"	-100° 51' 8.4"
14	44° 43' 21.8"	-101° 26' 16.7"
15	44° 39' 4.2"	-102° 1' 33.7"
16	44° 29' 55.2"	-99° 37' 1.0"
17	44° 26' 12.5"	-100° 12' 15.2"
18	44° 22' 20.4"	-100° 47' 12.8"
19	44° 18' 17.6"	-101° 22' 6.3"
20	44° 14' 2.7"	-101° 57' 8.4"
21	44° 4' 55.1"	-99° 33' 58.8"
22	44° 1' 13.7"	-100° 8' 57.9"
23	43° 57' 23.1"	-100° 43' 40.5"
24	43° 53' 22.1"	-101° 18' 19.3"
25	43° 49' 9.0"	-101° 53' 6.6"

Maximum rate = 0.01°/sec.

Frequency = 0.1 cps

Table 2.2-10. Picture Distortion in Radians for Maximum
Sinusoidal Limit Cycle With 10 Second Period

Point No.	Latitude Error	Longitude Error
1	0	0
2	3.243782E-06	3.0988187E-05
3	2.2446329E-09	1.9826984E-08
4	-3.561021E-06	-3.0805037E-05
5	4.9003575E-09	3.9486622E-08
6	1.9721741E-05	-3.3413206E-05
7	2.6201957E-05	-7.1776958E-06
8	2.5401074E-05	-4.1554202E-05
9	2.3463148E-05	-7.4877047E-05
10	2.7800903E-05	-4.6031761E-05
11	7.2759576E-11	-1.4551915E-11
12	9.191921E-06	2.4739675E-05
13	1.0443084E-05	-9.8041637E-06
14	9.8829296E-06	-4.2368447E-05
15	1.4893059E-05	-1.221773E-05
16	4.5294637E-05	-7.7008539E-05
17	5.1612777E-05	-5.0978182E-05
18	4.9291164E-05	-8.3704785E-05
19	4.4397333E-05	-1.1431007E-04
20	4.4233042E-05	-8.2441082E-05
21	2.910383E-11	-7.2759576E-12
22	7.8040939E-06	2.6371948E-05
23	6.1826322E-06	-5.0602321E-06
24	1.1671946E-06	-3.3824683E-05
25	4.809408E-09	3.8358849E-08

Table 2.2-11.   Picture Points Used in Modeling Error Analysis
for Maximum Sinusoidal Limit Cycle With
30 Second Period

Picture Point No.	Latitude	Longitude
1	45° 44' 49.5"	-99° 46' 23.7"
2	45° 41' 2.2"	-100° 22' 24.4"
3	45° 37' 5.1"	-100° 58' 7.6"
4	45° 32' 57.0"	-101° 33' 46.5"
5	45° 28' 36.1"	-102° 9' 33.8"
6	45° 19' 33.2"	-99° 42' 40.4"
7	45° 15' 48.7"	-100° 18' 25.6"
8	45° 11' 54.4"	-100° 53' 53.6"
9	45° 7' 49.3"	-101° 29' 17.2"
10	45° 3' 31.6"	-102° 4' 49.1"
11	44° 55' 0.3"	-99° 40' 16.1"
12	44° 51' 15.8"	-100° 15' 45.4"
13	44° 47' 21.7"	-100° 50' 57.9"
14	44° 43' 16.8"	-101° 26' 6.4"
15	44° 38' 59.5"	-102° 1' 23.4"
16	44° 30' 24.3"	-99° 37' 50.2"
17	44° 26' 39.8"	-100° 13' 3.8"
18	44° 22' 45.9"	-100° 48' 1.0"
19	44° 18' 41.3"	-101° 22' 54.3"
20	44° 14' 24.5"	-101° 57' 56.6"
21	44° 5' 3.8"	-99° 34' 13.3"
22	44° 1' 21.8"	-100° 9' 12.2"
23	43° 57' 30.7"	-100° 43' 54.7"
24	43° 53' 29.1"	-101° 18' 33.4"
25	43° 49' 15.5"	-101° 53' 20.8"

Maximum rate = 0.01°/sec

Frequency   = 0.0333 cps

Table 2.2-12. Picture Distortion in Radians for Maximum
Sinusoidal Limit Cycle With 30 Second Period

Point No.	Latitude Error	Longitude Error
1	0	0
2	3.244324E-06	3.0981602E-05
3	2.2446329E-09	1.9819709E-08
4	-3.5613157E-06	-3.0798685E-05
5	4.9039954E-09	3.9486622E-08
6	1.0846904E-04	-1.8671874E-04
7	1.062751E-04	-1.5677408E-04
8	9.6906035E-05	-1.8841257E-04
9	8.6449836E-05	-2.1993819E-04
10	8.2262446E-05	-1.9023074E-04
11	7.2759576E-11	-1.4551915E-11
12	5.3098302E-06	2.6487134E-05
13	2.7681344E-06	-6.5913482E-06
14	-1.5096048E-06	-3.7960395E-05
15	-1.5551268E-07	-6.8790177E-06
16	-1.0260715E-04	1.7342548E-04
17	-8.9804242E-05	1.9712332E-04
18	-8.5606127E-05	1.6313334E-04
19	-8.3877858E-05	1.3230419E-04
20	-7.7248835E-05	1.6498869E-04
21	2.910383E-11	-7.2759576E-12
22	7.7031327E-06	2.5948408E-05
23	6.0348502E-06	-5.6205899E-06
24	1.0463955E-06	-3.4243865E-05
25	4.8203219E-09	3.8358849E-08

The results are given in Table 2.2-8 and are little different from those in Table 2.2-6. This indicates, as expected, that a second order polynomial removes the picture centering and skewing distortions introduced by constant limit cycle angles.

Tables 2.2-10 and 2.2-10 give the modeling error results for sinusoidal limit cycle rates of 0.01°/sec maximum rate; Table 2.2-10 is for a 10 second period and Table 2.5.2-10 is for a 30 second period. The maximum error in Table 2.2-10 is 1690 ft. at picture point number 19, while Table 2.2-12 has an error of 3240 ft. at picture point number 9. The reason for the larger distortion error in Table 2.2-12 is due to the larger angle excursions associated with the 30 second period.

The modeling errors of 3240 ft are to be compared with the 2700 ft (3σ) internal consistency of the pseudo-reseau points themselves. It should be borne in mind, however, that the 3240 ft for the modeling error is more like a 6-sigma number since it is the maximum over the entire MSS picture of the distortions produced by a maximum sinusoidal limit cycle rate of 0.01°/sec.

Thus, it can be concluded that the MSS picture correction technique given here results in distortions less than or equal to the pseudo-reseau point accuracy. If it is desired to reduce the modeling error further piecewise corrections or higher order polynomials must be used.

2.2.4 Coherent Noise

Coherent noise is an extraneous signal which maintains its amplitude and phase over the time of taking a picture, e.g. a sum of harmonics of the power supply oscillator. This coherent signal may interfere with the picture in various fashions, depending on the ratio of line scan to noise frequency. The exact visual effect is largely impossible to predict unless special attempt is made to synchronize the interference and horizontal synch pulses.

A second class of noise which may, in an approximate sense, be included here is the out-of-focus shadow of the vidicon decelerating mesh which will be superimposed on the image. This interference is of low

amplitude, however, like grain in a photographic emulsion, will be visible in flat tonal areas of the image. The mesh superimposed on the image will be distorted by the electron lens geometric distortion, in that when the image is scanned in a raster fashion the mesh signal received will have the original mesh frequency as the carrier frequency with FM sidebands corresponding to a low index of modulation. The bandwidth therefore, is fractionally more than if no geometric distortions were present. The conclusion is then that the system, which removes structured noise, will also be able to remove mesh noise.

The above argument gives the impression that these errors are well defined and of great moment. This is somewhat of an exaggeration. The mesh and structured noise may be as high as 5 percent of the peak video signal. This figure is a pessimistic bound. It may not be visible in all the pictures.

If the noise must be removed, then two implementations are possible: analog and digital. Some of the details are common but the approach used is highly dependent on the particular noise structure.

Conceptually two approaches may be used

    a)   subtraction of an appropriate signal from the input

    b)   filtering of the input signal.

In the first case, the problem is to estimate the amplitude phase and frequency of the distortion, construct the signal artificially, and abstract it from the image. This should be done on a routine basis in the normal hands-off high throughput condition.

In the second approach we must estimate the interference and construct a filter to remove the offending frequencies.

In either case the implementation may be analog or digital.

If the noise is synchronized with the horizontal scan, then averaging all scan lines will give a constant term with a superimposed ripple which is the interference. This may then be subtracted. Approximately 2-1/2 images need to be added column wise to give a good estimate of the interference since the signal to noise ratio is 30db (approximately). The

additional noise, it was decided, should be at least 10db down on the video noise, i. e. , 40db below signal. This signal to noise ratio of 40db corresponds to 10^4:1 in power and thus 10^4 lines or 2. 5 images have to be averaged.

Ideal high pass filtering on this estimated signal will remove the dc term and shading and thus will give the correction in amplitude and phase.

It appears that the noise will be synchronized. This averaging and subtracting procedure is, therefore, the best approach. The approach is entirely digital and can be kept as a running average on all received images if required.

2. 2. 5 Computing the Spectrum

In the event that the noise is coherent in itself but not synchronized with the scans, then the spectrum must be computed in analog or digital. One may consider 2-D transforms as an option digitally, or 1-D transforms either analog or digitally.

Treating the signal as a one dimensional time domain signal we have the situation depicted in Figure 2. 2-33. It is important to know whether the noise exists in the signal during retrace, since this affects the spectrum. If the noise exists during retrace then the signal, but not
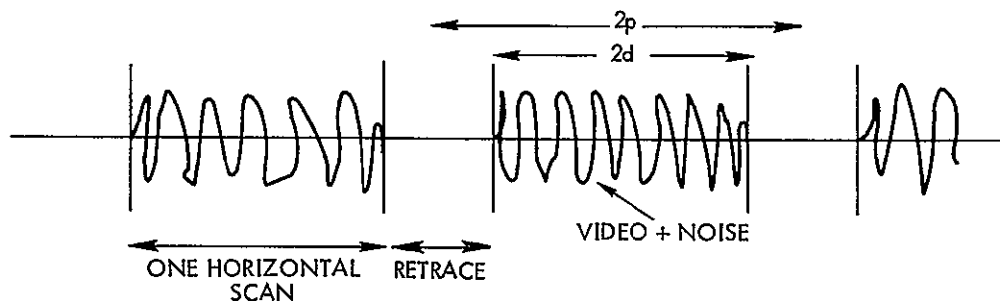

Figure 2.2-33

VIDEO FORMAT

the noise spectrum is convolved with the chopping window. If the noise is cut off, both signals are weighted by the window.

The estimate of the corrupting signal from the observed spectrum (Figure 2. 2-34) has the amplitude and phase given by the amplitude of the peak in the spectrum at f_1, the phase is given by the phase ϕ at f_1. The estimate based on the difference between the smooth spectrum and the peak cannot be used since the phase is completely unknown. The appropriate signal can be subtracted.

If filtering is to be used, then notch filters would be employed at frequencies f_1, f_2, f_3, etc. (Figure 2. 2-35).

In the case of omni-present noise then the simple notch filter will remove it. If the noise is chopped out during retrace then the notch filter will not completely remove the noise. The residue will be of an amplitude proportional to the percent time spent in retrace. A notch filter, which has a reduced but non-zero response at the notch frequency and furthermore has a phase inversion within the notch (Figure 2. 2-36), modifies the noise so that it disappears during active scan but is present during the retrace when it is not important.

The realization of the filter of Figure 2. 2-36 can be accomplished in either the analog or digital domain, but requires a non-minimum phase network in the analog domain, which may not be excessively hard to realize.

The computation of the spectrum, which dictates the implementation of removal, is complicated by the window effects of the retrace. In the case of synchronized noise, one line is sufficient for spectrum computation. In the case of nonsynchronized noise or noise of frequency relatively prime to the scanning frequency (the worst case), theoretically an infinite number of scan lines must be transformed as one record. In the latter case analog filtering is to be recommended since the spectrum analyzer art is well advanced and the alternative digital approach, whether by software or by special attachments, requires several lines, including retrace, to be transformed as a whole. If analog spectrum computation is used, then analog filtering is possible for commensurate errors. If digital spectrum estimation is used, then the digital filter becomes
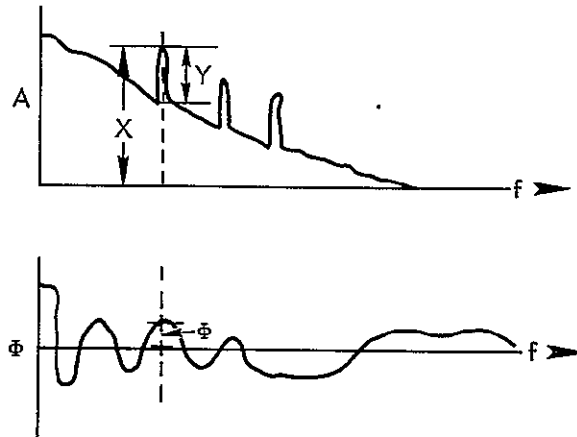
Figure 2.2-34

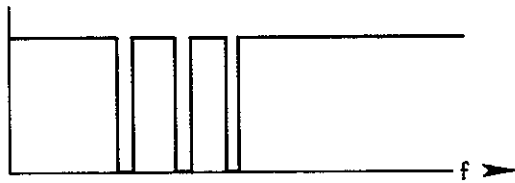COHERENT NOISE in
the frequency domain
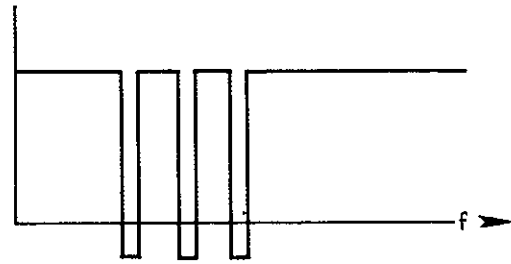

Figure 2.2-35

SIMPLE NOTCH

Figure 2.2-36

PHASE REVERSAL NOTCH

merely the multiplication of the appropriate notch frequencies by a coefficient, thus the filtering becomes trivial. The cost should also include an inverse transform, to recover the new image for geometric distortion.

The convolution approach to digital filtering appears impractical due to the length of the impulse response of the filter. Recursive techniques can be applied to reduce the number of multiplications per point. This requires further study, when the exact nature of the coherent interference becomes known.

2.2.6 Signal to Noise Ratio and Amplitude Quantization

The published data on the camera and tape recorder give a signal to noise ratio of 33db and 40db respectively. For the camera

S/N = 33db

noise power = 0. 0005

For the recorder

S/N = 40db

noise power = 0. 0001

We have in addition the noises due to

Communications   0. 0001

Recorder   0. 0001

$\therefore$ Sum of noise powers = 0. 0008

Combined signal to noise ratio = 31db, i. e. , a 2. 0db loss.

Quantization noise power = $q^2/12$ where q is the step width. The problem is to estimate the quantization word length q. The data passing through the quantizer is to be used in further processing steps. In the best corrected imagery this could be approximately a 29 point convolution operator (29 points obtained from gross timing estimates).

In the least corrected imagery (i. e. , point shifting to be discussed in the geometric correction section subsequently), the video is not used at all. Let us suppose that only one extra db is allowed in quantization, then in the highest quantization case, where an operation is a fixed point multiply, say 20 operations are to be performed, the signal to noise ratio is now (31-1) = 30db.

New noise power = 0. 001

Total extra noise power = 0. 001 - 0. 0008 = 0. 0002

Let the number of 8 bit byte operations be N

Power per operation = 0. 0002/N

Note that although we quantize to n bits we still do 8 bit byte arithmetic.

Let the quantizer have k steps then

$$q = 1/k$$

equating the quantization noise to the noise of a hypothesized operation. Hence

$$\frac{1}{k^2 12} = \frac{0.0002}{N}$$

Hence

$$k \doteq 20 \ \sqrt{N}$$

For 20 operations, k = 90 steps, or a 7 bit quantization

For k = 80, we may have 16 operations. If N = 1, then k = 20 steps, i.e., 5 bit quantization.

2.3 RESEAU EXTRACTION

As the error source analysis shows, the principle errors are geometric. The use of a 9 x 9 reseau provides adequate data to derive corrections; one is now left with determination of the best method to precisely locate the reseau.

Both the speed and accuracy of reseau detection are highly dependent on the particular algorithm used. The algorithm is in turn dependent on the signal to noise ratio of the video signal entering the processor, i.e., having gone through all signal conditioning including any required analog to digital conversion. In the good signal to noise case, where the reseau is significantly blacker than the rest of the picture, thresholding the video is sufficient. If the signal to noise ratio is poor, then correlation or matched filters are necessary. Amplitude selection is faster than matched filtering.

Given these considerations, several different algorithms have been developed and analyzed. These range from essentially manual methods through rather sophisticated digital techniques.

It should be noted that, depending on signal to noise and the overall processing environment, different algorithms are optimum.

2.3.1 Manual Measurement

The measurement of reseau marks on film is a standard photogrammetric procedure in which several types of accurate measuring stages or comparators are used. These manual techniques are quite slow, when a total of 81 points per picture must be measured. Computer-aided mensuration viewers can measure a frame in about 30 minutes. With standard comparators, the measurement time might be 1 to 2 hours per frame.

It might be noted, at this point, that the case A load is 45 RBV sets, or 135 images per day. At 30 minutes per frame, this leads to a need for nine computer aided measuration views, and nine analysts, to do the measurements manually. In case B, with 495 images per day, 31 viewers are needed. Manual measurement of every frame thus appears totally impractical.

For bulk mode II processing, it may be satisfactory to measure only two frames per pass and interpolate between the beginning and end conditions to establish distortion correction. Such a procedure would only be useful if a correlation method of correction is used, since registration errors would probably be more than could be tolerated.

An array of 9 x 9 reseau marks on the RBV faceplate will permit error correction to better than the 200-foot requirement, if biquadratic linear interpolation can be used to remove all errors. The reseau array format is shown in Figure 2.3-1.

The reseau array can be used to correct geometric errors introduced by the sensor and subsequent processing steps, which may be either electronic or photographic. To derive the greatest benefit from reseau calibration, the measurement should be carried out at the last stage of processing so that all distortion errors in the system can be corrected. Reseau measurement can be made on processes previous to the last, if the distortions caused by these processes are known, or if these errors are at least constant over one set of pictures, so that registration accuracy does not suffer.
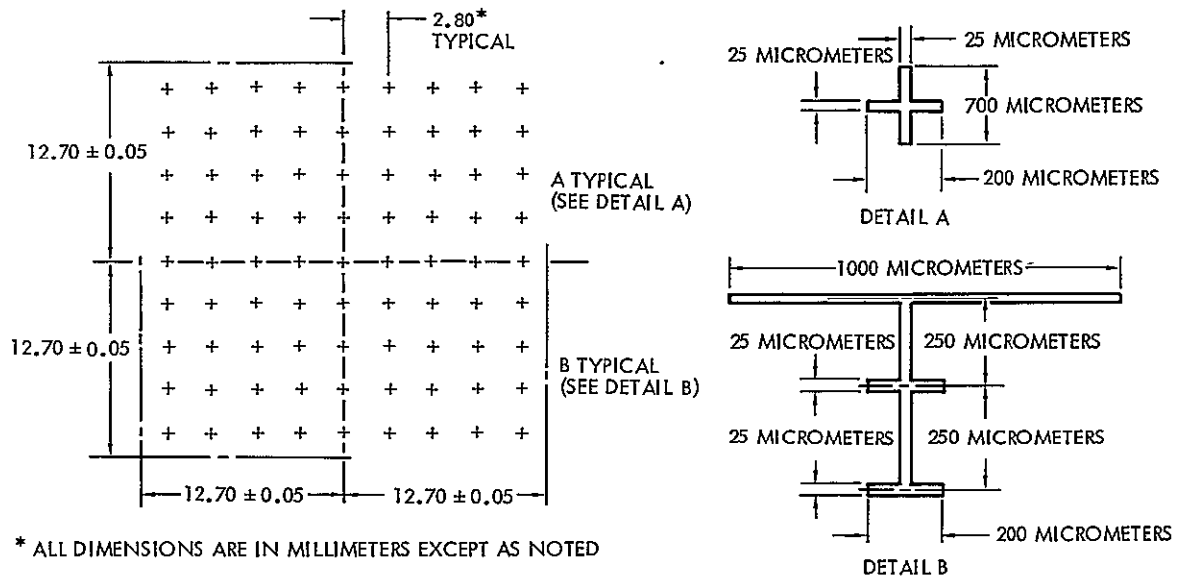
2.80*
TYPICAL

25 MICROMETERS | 25 MICROMETERS

12.70 ± 0.05

700 MICROMETERS

200 MICROMETERS

A TYPICAL
(SEE DETAIL A)

DETAIL A

1000 MICROMETERS

25 MICROMETERS | 250 MICROMETERS

12.70 ± 0.05

B TYPICAL
(SEE DETAIL B)

25 MICROMETERS | 250 MICROMETERS

200 MICROMETERS

12.70 ± 0.05 — 12.70 ± 0.05

DETAIL B

* ALL DIMENSIONS ARE IN MILLIMETERS EXCEPT AS NOTED

Figure 2.3-1

RESEAU ARRAY FORMAT

2. 3. 2 Shadow Casting

The technique of shadow casting can be used for estimating the reseau position. Shadow casting consists of forming the sum of all elements in a row and treating the row sums as points on a function as shown in Figure 2. 3-2. The process is identical for column sums. This technique lends itself to digital processing.

Assuming the worst case of prior knowledge of the reseau point position, the reseau will lie in an area of the picture of side of the order of one percent of the full image size or 40 pixels. The reseau size is 32 pixels giving an overall square of 112 pixels side dimension.

The minimum of each function detects the coordinate of the reseau. In the case of a skewed reseau, the ERTS specification, 10 percent maximum, allows at least one full length scan across the reseau and, therefore, does not affect the following argument.

For a scene of average brightness v and rms value e due to photon noise and a reseau with video value r and no additive noise (assumed
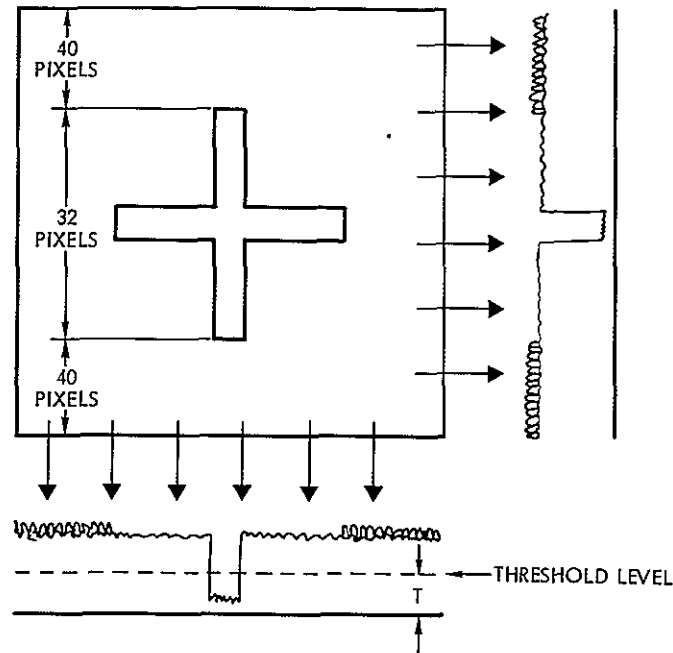
Figure 2.3-2

RESEAU DETECTION AVERAGE VIDEO V = 1/2 PEAK
opaque cross

clipped), then for the detection of a 32 column reseau in a field p square, and for the gaussian white noise assumption typical of photon noise:

The video sum value of the area not including a reseau is

$$pv \text{ with a variance of } pe^2$$

The area including a reseau has a video value of

$$(p-32) v + 32r \text{ with a variance of } (p-32) e^2$$

The optimum threshold is $[\mu_1 + \mu_2]/2$ if the gaussian distributions are identical. If the distributions are different as is the case here, the optimal threshold becomes biased towards the narrower distribution.

In Figure 2.3-3 we can define, p = square dimension

$$\sigma_1^2 = (p-32)e^2 \qquad\qquad \mu_1 = (p-32)v + 32r$$

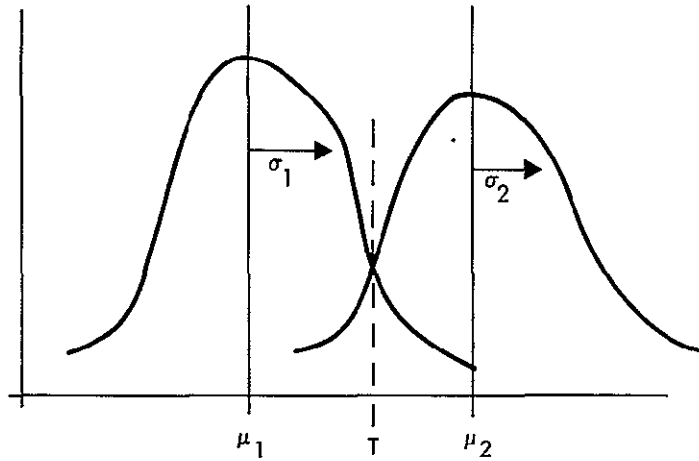$$\sigma_2^2 = pe^2 \qquad\qquad \mu_2 = pv$$

Figure 2.3-3

OPTIMUM THRESHOLD COMPUTATION

The optimal threshold depends on the criterion used. The criterion proposed is equal likelihood of error on higher and lower video, in this case let k be the multiplier of the relative σ's.

Then

$$\mu_1 + k\sigma_1 = \mu_2 - k\sigma_2$$

hence

$$k = \frac{\mu_2 - \mu_1}{\sigma_1 + \sigma_2}$$

and

$$T = \mu_1 + \frac{\mu_2 - \mu_1}{\sigma_1 + \sigma_2}\, \sigma_1$$

$$= \frac{\sigma_1 \mu_2 + \sigma_2 \mu_1}{\sigma_1 + \sigma_2}$$

The peak black = 0. 35 volts.

The peak white = 1. 5 volts, assume an average voltage of 0. 75.

The signal to noise ratio is 30db, say $e \simeq 0.032$

$$e^2 = 0.0001$$

Hence

$$\mu_1 = (p-32)\, 0.75 + 32 \times 0.35$$
$$= 0.75p - 12.8$$
$$\mu_2 = 0.75p$$
$$\sigma_1 = (p-32)\, 0.032$$
$$\sigma_2 = p \cdot 0.032$$

Hence k = number of sigmas and hence defining the probability of detection is

$$k = \frac{0.75p - (0.75p - 12.8)}{0.032(\sqrt{p} + \sqrt{p-32})} = \frac{12.8}{0.032(\sqrt{p} + \sqrt{p-32})}$$

p	32	64	128	256
k	71. 3	29. 4	18. 9	12. 9

We need p = 128 for geometric correction reasons assuming 1 percent of the image as the uncertainty in finding the reseau. This uncertainty may, in the worst possible case, go up to 3 percent (i. e. , 1 percent size, 1 percent centering, and 1 percent skew).

Shadow casting is, therefore, acceptable. At these sigmas the gaussian assumption is no longer good.

The signal to noise ratio, where the technique of shadow casting falls down, can be assumed to be the 2σ point on the probability curve, i. e. , a 97. 25 percent probability. Here for 128 x 128 square the required signal to noise ratio drops to 5. 74db. At this signal to noise ratio the picture would probably be unacceptable for other reasons.

Working backwards, we can compute the average video in a 128 x 128 square for a 3σ decision to be made.

$$k = 3 = \frac{32(v - 0.35)}{0.032[\sqrt{128} + \sqrt{96}]}$$

$$= \frac{32(v - 0.35)}{0.675}$$

Hence the extra signal above the black threshold need only be

$$(v - 0.35) = \text{excess} = \frac{3 \times 0.675}{32} = 63 \text{ millivolts}$$

The total signal range is $1.5 - 0.35 = 1.15$

$$\text{percent of range} = \frac{63}{1150} \times \frac{100}{1} = 5.5 \text{ percent of range.}$$

A local quadratic on the shadow function will locate the center of the reseau to less than one pixel.

2.3.2.1 Influence of Beam Bending

The ability to perform geometric correction on RBV imagery is due to a reseau, or set of fiducial marks, which has been etched on to the face of the tube. The positional accuracy of the reseau on a given camera can be determined accurately prior to launch, and the inflight distortions can, in principle, be corrected by inducing a rubber sheet distortion to force the reseau as found to match the calibration reseau.

The correction is possible only if a major proportion of the reseau points can be in fact detected. Several factors may conspire to reduce the detectability of the reseau points. Two cases, in general, are of interest: a. the case where a reseau point is not visible at all and b. the case where the signal to noise ratio is poor and where it is not a cost effective proposition to find all the points.

The purpose of this section is to examine these problems and evaluate the consequences.

The reseau mark in question has the dimensions given in Figure 2.3-4. The pattern is not especially suited to machine detection in shape or size. The two dimensional autocorrelation function is not especially sharp. The arms of the cross are 25μ or 4 resolution elements wide. It would be preferable to make the reseau at least the width of the 3 sigma points on the point spread function of the camera, i. e. , 6 scan elements wide assuming one sigma packing. This must be balanced against data loss using a wide reseau.
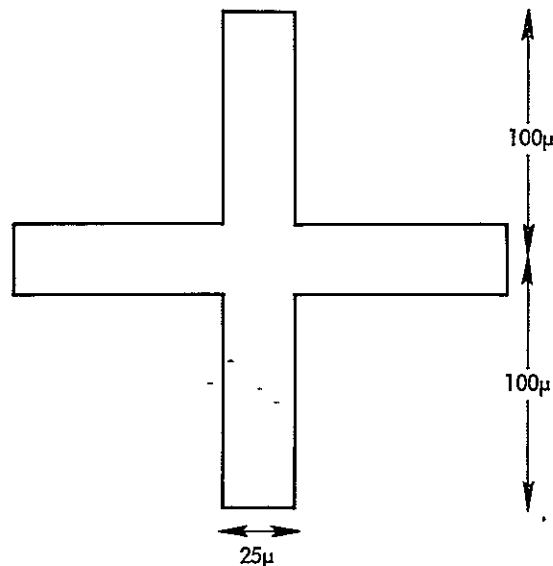

Figure 2.3-4

RESEAU MARK

A second point is that a lower or black clipping level exists in the camera electronics, which in adverse viewing conditions can clip the scene and the reseau making reseau detection impossible by any means, human or automatic.

A third point of interest is that the return beam vidicon is susceptible to beam pulling, in which the low energy beam is attracted to local high charge regions. If one considers a reseau point, opaque gold plated marking, over a uniform high flux portion of the scene, then the charge distribution in the vidicon will be as shown in Figure 2.3-5 schematically.
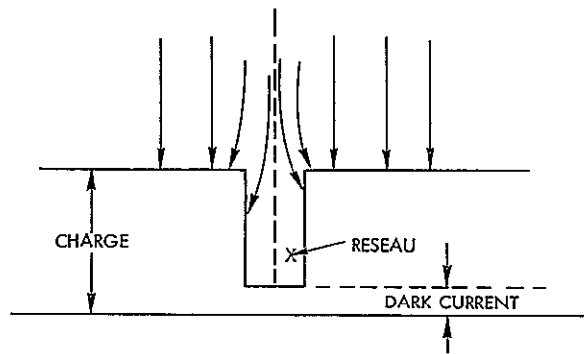
Figure 2.3-5
BEAM BENDING AT A RESEAU POINT

For independent beams, non-scanned, the beams (a) and (b) will be, for a high albedo, attracted to one side or the other of the reseau slot and, therefore, the reseau will at first glance not be visible in the video. The effects of scanning complicate this system from a trajectory point of view but increase observability.

Consider a step function in charge, (Figure 2.3-6) and left to right scanning. The video output will have the characteristic of Figure 2.3-6(b). The video will indicate the existence of bending with a rise time indicative of the magnitude of the pulling effect and on the beam voltage. Consider a unit step, Figure 2.3-6(c) with left to right scanning. In this case, as the beam scans, the charge is neutralized and the video fall time will indicate the beam dimension via the convolution effect.

The system is more complex for the case of a reseau point immersed in a high intensity portion of the image as shown in Figure 2.3-7. The mechanism is as in Figures 2.3-6(c) and (d) with the exception that there is an intermediate charge condition shown in Figure 2.3-7(b). The average charge should probably be considered here and thus both edges of the reseau will exhibit a finite rise time, however the positive and negative rise times will differ considerably.
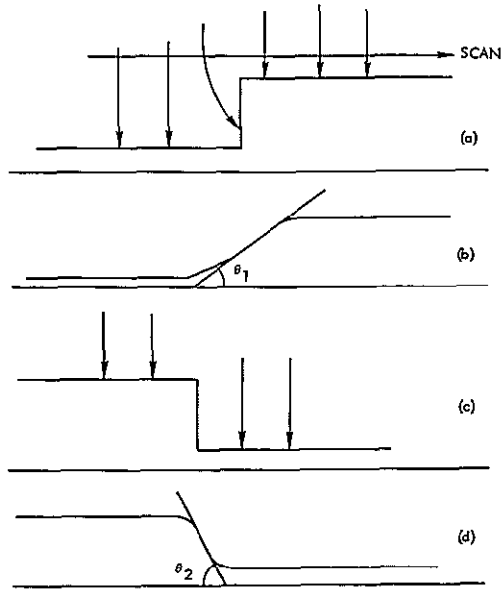
Figure 2.3-6
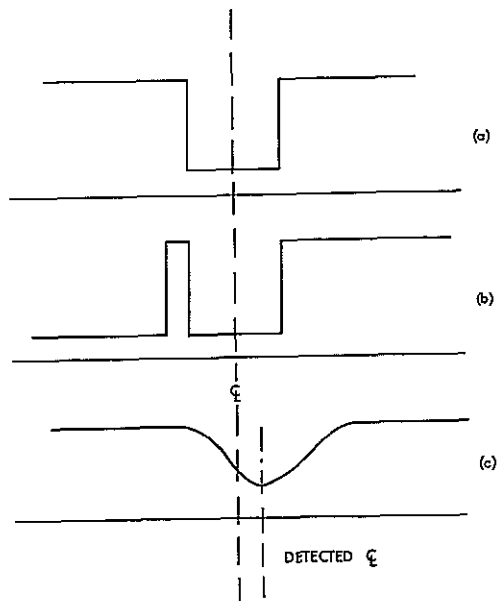
EFFECT OF UNIT STEP IN SCANNING

Figure 2.3-7

RESEÁU DETECTION

Simulation of the electron trajectories or experimentation on the actual tube would be necessary to give the exact shape but it would not appear that the reseau would disappear into the surrounding high albedo region due to beam pulling.

However, the asymmetric widening of the reseau mark influences the detection accuracy. The best indicator would appear to be the first occurrence of the reseau in the video rather than the midpoint of a thresholded videopulse.

The situation is more complex in two dimensions since the beam, although scanning in one dimension, neutralizes charge in two dimensions with an effect proportional to the volume under the integral

$$\int \int e^{-(x^2 + y^2)} \, dxdy$$

where the beam is assumed gaussian. Sharpening due to scanning will occur. The experimental approach is recommended due to intractability in the mathematics.

There will be considerable atmospheric scattering and some internal scattering contributing to some background radiation. The reseau is opaque and will be significantly lower than all other points in the picture. The Mariner experience confirms this, although considerably more variation in gray level is expected over the earth than is visible in say the moon or Mars, e. g. , oceans versus sand, large forest areas versus urban areas, etc.

If the signal to noise ratio is good, 30 db or so, then thresholding will suffice bearing in mind the systematic error described above.

If the signal to noise ratio is poor enough to cause difficulty, then the image will probably be too poor to be useful.

Beam pulling will not result in rendering the reseau invisible but will misplace the estimate of position if the usual methods of detection are assumed. Detection must consider the direction of scanning.

Firm numbers are not available on the effect measured in pixels as a unit of distance, however the above heuristic analysis should be enough to dispose of the problem as it affects the visibility of the reseau points in the video.

2.3.3 Analog Correlation

An investigation of possible analog means was undertaken. The concept investigated was to use analog correlation techniques to automatically locate and measure reseau marks on the laser beam recorder output film.

A maximum of 165 RBV sets per day is expected from ERTS B. A single reseau measuring station would have a maximum of 495 frames to process per day. Thus a rate of 20 to 30 frames per hour is indicated. The following requirements must be met:

a) Measurement rate, 2 to 4 seconds per point

b) Accuracy, 1 part in 6,000

c) Film format, 9 1/2-inches, roll

d) Film advance, automatic, binary code reader for frame number

e) Search, reseau point known to within ±0.10 inch in x and y.

The size of a reseau mark on the 9 1/2-inch format is a cross of 0.057 inch with 0.007-inch-wide marks. A scanning aperture of 0.003 inch would appear adequate, and with a 32 by 32 line raster, a raster size of 0.1 by 0.1 inch is indicated. The area to be searched is 0.2 by 0.2 inch. Pull-in, based on a signal from the mark, will be about ±0.005 inch, or ±5 percent of the raster width. Since searches may be carried out in increments of 0.010 inch, 400 maximum total raster scans will be required to search the 0.2-inch-square area.

Since a 32- by 32-line raster will require about 2 milliseconds, the maximum search time is 0.8 second.

Figure 2.3-8 shows a simplified block diagram of the approach. An image dissector is used for scanning the reseau. An x, y stage will

move the image tube over the film, which is held flat by a vacuum platen. The computer directs the scanner to a position where a reseau point is expected. A search is carried out on the scanner and, when correlation is obtained, error signals developed from the correlator will drive the x, y stage to a position of best registration. Readout of x, y encoders will designate the reseau position.

Figure 2.3-8
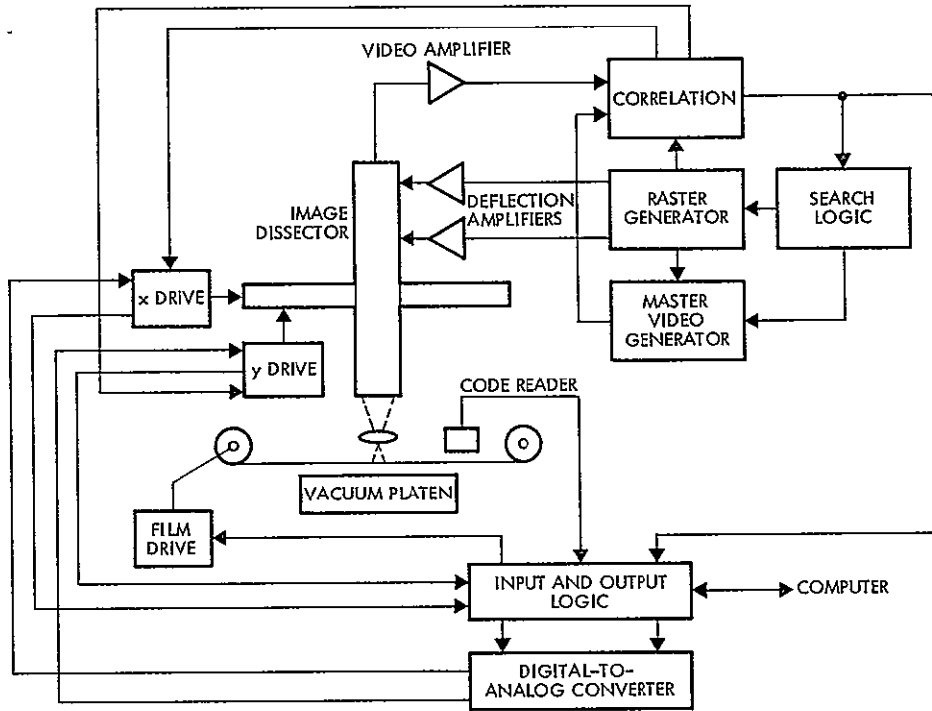BLOCK DIAGRAM OF AUTOMATIC RESEAU MEASURING DEVICE

The scanned image and an idealized video signal representing a reseau mark are correlated. Noise, in the form of image detail around the reseau, will be suppressed as long as detail does not correlate with the shape of the reseau. The frequency of false correlations is expected to be relatively low.

The predicted performance of this approach is given in Table 2.3-1.

Table 2.3-1. Predicted Performance of Correlation

Time Estimate		Accuracy	
Search time, seconds	0. 8, maximum 0. 4, average	Quantizing error, x, y stage, inches	0. 0004
Lockon and read, seconds	0 5	Correlation error, 0. 5 percent of W, inches	0 0005
		Servo error, inches	0. 0005
Slew to next point, seconds	1. 0	Scanner stability, 0 2 percent, inches	0 0006
Average time per frame	154 seconds 23 frames per hour	RSS	0. 0009 + 0 0004 inch 0. 0013 inch or 110 feet on ground

2.3.3.1 Interface Requirements

The automatic reseau measurement will transmit the frame code to the computer coordinates for each reseau mark received. After the reseau has been located, new x, y coordinates are transmitted to the computer.

2.3.4 Grid Pattern Reseau

Reseau points can be used to determine geometric distortions in photographs. For example, a least-squares fit of a two-dimensional polynomial can be made to the set of reseau points. If it is inappropriate to represent the distortion by a polynomial, the same technique can be applied with different functions.

However, each reseau point occupies some space on the photograph. The photographic information beneath the reseau points is lost, and can only be partly restored by interpolation. Also, the number of reseau points and their arrangement is fixed. An alternate procedure has been proposed. The alternate procedure will slightly degrade the picture everywhere, rather than completely erase it in places, and has greater flexibility.

The alternate procedure is to project a pattern onto the picture, such as a periodic pattern with a specified amplitude and frequency. The projected pattern will suffer the same geometric distortions as the picture. The result is a modified picture, i. e., the original picture plus the projected pattern, both distorted in the same way. The modified picture can then be cross-correlated with an undistorted copy of the pattern to estimate the linear distortions, i. e., translation, rotation, scale-factor variations, and skews.

The feasibility of the procedure depends on whether or not a pattern can be found which will not degrade the picture too much, but from which a good estimate of the distortion can be made.

For a periodic pattern, both the degradation of the picture and the accuracy of the estimate depend upon the amplitude of the pattern. Greater amplitudes will produce more accurate estimates but also poorer pictures. Consequently, the feasibility of the procedure depends on whether or not there is a range of amplitudes for which both the accuracy of the estimate of the distortion and the degradation of the picture are acceptable. This section examines the accuracy of the estimate as a function of the amplitude of the pattern. The degradation of the picture, however, is ignored.

The accuracy of the estimate also depends upon the size of the picture which is input to the cross-correlator. A smaller picture will, in general, produce a poorer estimate, since it represents a smaller sample. This effect would not pose a problem if the entire picture could be input to the cross-correlator. However, there is an opposite effect which makes this impractical. The geometric distortions are, in general, nonlinear, and the cross-correlator can only determine linear distortions. Moreover, the estimate of the linear distortions is affected by the nonlinear distortions. Consequently, the picture must be divided into segments, such that the nonlinearity of the distortion is small within segments, and each segment cross-correlated separately.

Since, for smaller segments the accuracy of the estimate will tend to be worse because of the smaller sample, but better because of the

reduced nonlinearity, there will be an optimum segment size, that is, a segment size which maximizes the accuracy of the estimate. The success of the procedure, therefore, depends on whether or not the maximum accuracy is good enough. This section examines the accuracy of the estimate as a function of the sample size. The effect of nonlinearity of the distortion is not studied.

Also, only translations have been examined to simplify the analysis. Nonlinearities can be inferred from translations. This can be done by treating the center of each picture segment as a reseau point. If the translation of the picture segment is known, the movement of the reseau point is also known, and it can be used as a conventional reseau point.

The remaining sections discuss the model, the analysis, and the results.

2.3.4.1 Model

The picture, or picture segment input to the cross-correlator, is assumed to be square with sides of length L, resolution Δ, N resolution elements along each horizontal and vertical line, and intensity I(x, y) at each point (x, y).

The analysis assumes that the intensity I(x, y) is a constant intensity I_o plus a random intensity W(x, y). The random intensity is assumed to be stationary, that is, to have the same statistical properties at every point on the picture. Also, it is assumed to have mean zero and an exponential autocorrelation function

$$R_{WW}(x, y) = \sigma^2 e^{-\sqrt{x^2+y^2}/\lambda}.$$

The parameter σ^2 can be interpreted as the variance of the random intensity at any point. The parameter λ can be interpreted as the separation at which the correlation coefficient between the random intensities at two points decays to $1/e$.

The pattern P(x, y) was chosen to be a two-dimensional sine wave, with amplitude A and period ℓ, which is the product of two one-dimensional

sine waves, that is, $P(x, y) = A \sin (2\pi x/\ell) \sin (2\pi y/\ell)$. This pattern was selected because its properties facilitate the analysis, and also because other two-dimensional periodic patterns can be approximated by a linear combination of such patterns.

Figure 2.3-9 shows one-dimensional representation of the picture $I(x, y)$, its constant component I_0 and random component $\overline{W}(x, y)$, the auto-correlation function $R_{WW}(x, y)$ of the random component, and the pattern $P(x, y)$.
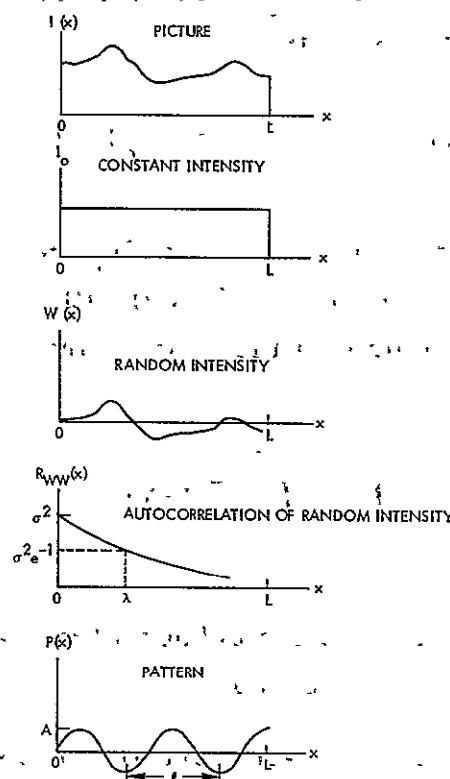

Figure 2.3-9

PICTURE FUNCTIONS

The next section discusses the analysis. It is not necessary to read the analysis section in order to read the results section. However, if the analysis section is skipped, several statements must be added at this point. The analysis makes several approximations and assumptions which are valid for large signal-to-noise ratios. Furthermore, the

ambiguity problem is ignored. An ambiguity problem exists if the period of the pattern is of the same order as the unknown translation being estimated, so that errors in the estimate of the unknown translation equal to integral multiples of the pattern period may occur.

2.3.4.2 Analysis

Basic Equations. The received picture (or picture segment) $Q(x, y)$ consists of the original picture plus the projected pattern, both distorted in the same way. It is assumed that the distortion consists of unknown translations a_0 and b_0 in the negative x and y directions. Then the received picture $Q(x, y)$ is

$$Q(x, y) = P(x - a_0, y - b_0) + I(x - a_0, y - b_0) \qquad (2.3-1)$$

The unknown translations a_0 and b_0 are estimated by cross-correlating the received picture $Q(x, y)$ with an undistorted copy $P(x, y)$ of the pattern. The output of the cross-correlator $Z(a, b)$ is

$$Z(a, b) = \int_0^L \int_0^L P(x, y) \, Q(x + a, y + b) \, dx \, dy \qquad (2.3-2)$$

The estimates $\hat{a}, \hat{b}$ of the unknown translations a_0, b_0 are the values of a and b which maximize $Z(a, b)$.

The output of the cross-correlator can also be expressed as, using Equation (2.3-1),

$$Z(a, b) = \int_0^L \int_0^L P(x, y) \, P(x - a_0 + a, y - b_0 + b) \, dx \, dy$$

$$+ \int_0^L \int_0^L P(x, y) \, I(x - a_0 + a, y - b_0 + b) \, dx \, dy \qquad (2.3-3)$$

The original picture $I(x, y)$ is a constant intensity I_O plus a random intensity $W(x, y)$, that is,

$$I(x, y) = I_O + W(x, y) \tag{2.3-4}$$

Consequently, if Equation (2.3-4) is substituted into Equation (2.3-3), we have

$$Z(a, b) = \int_0^L \int_0^L P(x, y) \, P(x - a_O + a, \, y - b_O + b) \, dx \, dy$$

$$+ \int_0^L \int_0^L P(x, y) \, I_O \, dx \, dy$$

$$+ \int_0^L \int_0^L P(x, y) \, W(x - a_O + a, \, y - b_O + b) \, dx \, dy \tag{2.3-5}$$

The second term is zero, since I_O is a constant, and the integral of the pattern over the picture is zero, for the pattern chosen. So the output of the cross-correlator is

$$Z(a, b) = \int_0^L \int_0^L P(x, y) \, P(x - a_O + a, \, y - b_O + b) \, dx \, dy$$

$$+ \int_0^L \int_0^L P(x, y) \, W(x - a_O + a, \, y - b_O + b) \, dx \, dy \tag{2.3-6}$$

or

$$Z(a, b) = F(a, b) + G(a, b) \tag{2.3-7}$$

where

$$F(a, b) = \int_0^L \int_0^L P(x, y) P(x - a_o + a, \ y - b_o + b) \ dx \ dy$$

$$G(a, b) = \int_0^L \int_0^L P(x, y) W(x - a_o + a, \ y - b_o + b) \ dx \ dy \quad (2.3-8)$$

Mean Square Estimation Error

If the output of the cross-correlator has a single peak, the peak can be identified by equating the first partial derivatives of $Z(a, b)$ to zero. Then the peak occurs where

$$\frac{\partial F}{\partial a} + \frac{\partial G}{\partial a} = 0$$

$$\frac{\partial F}{\partial b} + \frac{\partial G}{\partial b} = 0 \quad (2.3-9)$$

If the peak at $(\hat{a}, \hat{b})$ is sufficiently near to the unknown translation (a_o, b_o), the first partial derivatives of $F(a, b)$ can be linearized about (a_o, b_o) to give

$$\left(\frac{\partial F}{\partial a}\right)_o + \left(\frac{\partial^2 F}{\partial a^2}\right)_o (\hat{a} - a_o) + \left(\frac{\partial^2 F}{\partial a \ \partial b}\right)_o (\hat{b} - b_o) + \left(\frac{\partial G}{\partial a}\right) = 0$$

$$\left(\frac{\partial F}{\partial b}\right)_o + \left(\frac{\partial^2 F}{\partial a \ \partial b}\right)_o (\hat{a} - a_o) + \left(\frac{\partial^2 F}{\partial b^2}\right)_o (\hat{b} - b_o) + \left(\frac{\partial G}{\partial b}\right) = 0 \quad (2.3-10)$$

For the pattern chosen, the first partial derivatives and second mixed partial derivatives of $F(a, b)$ are zero at (a_o, b_o), so we have

2-92

$$\left(\frac{\partial^2 F}{\partial a^2}\right)_o \cdot (\hat{a} - a_o) + \left(\frac{\partial G}{\partial a}\right) = 0$$

$$\left(\frac{\partial^2 F}{\partial b^2}\right)_o (\hat{b} - b_o) + \left(\frac{\partial G}{\partial a}\right) = 0 \qquad (2.3\text{-}11)$$

Since $(\hat{a}, \hat{b})$ is the cross-correlator's estimate of the unknown translation (a_o, b_o), the estimation errors are

$$\hat{a} - a_o = \frac{-\left(\frac{\partial G}{\partial a}\right)}{\left(\frac{\partial^2 F}{\partial a^2}\right)_o}$$

$$\hat{b} - b_o = \frac{-\left(\frac{\partial G}{\partial b}\right)}{\left(\frac{\partial^2 F}{\partial b^2}\right)_o} \qquad (2.3\text{-}12)$$

The denominators are functions of the pattern $P(x, y)$ only, and, therefore, are not random variables. (See Equation (2.3-8).) The numerators, however, are functions of both the pattern $P(x, y)$ and the random component $W(x, y)$, and, therefore, are random variables. Consequently, the mean square estimation errors are

$$E(\hat{a} - a_o)^2 = \frac{E\left(\frac{\partial G}{\partial a}\right)^2}{\left(\frac{\partial^2 E}{\partial a}\right)_o^2}$$

$$E(\hat{b} - b_o)^2 = \frac{E\left(\frac{\partial G}{\partial b}\right)^2}{\left(\frac{\partial^2 E}{\partial b}\right)_o^2} \qquad (2.3\text{-}13)$$

Since the two expressions are identical in form, it is sufficient to consider the first one. To simplify the notation, we will denote partial differentiation with respect to a by primes, so that

$$E(\hat{a} - a_o)^2 = \frac{E(G')^2}{\left(F_o''\right)^2} \qquad (2.3-14)$$

where the subscript zero on the denominator indicates that F'' is evaluated at (a_o, b_o). The numerator $E(G')^2$ is the same at any point (a, b) since $G'(a, b)$ is stationary. The random function $G'(a, b)$ is stationary because the random function $G(a, b)$ is the output of a linear system with stationary input $W(x, y)$, by Equation (2.3-8).

The assumptions have been made that the output of the cross-correlator $Z(a, b)$ has a single peak, and that the location of the peak (a, b) is near the unknown translation (a_o, b_o). This is equivalent to assuming a large signal to noise ratio. Also, the ambiguity problem has been ignored.

Numerator Evaluation

We will now discuss how to evaluate the numerator and denominator in Equation (2.3-14) for the mean square estimation error, beginning with the numerator.

The auto-correlation function of $G'(a, b)$ is

$$R_{G'G'}(\alpha, \beta) = E \, G'(a, b) \, G'(a + \alpha, b + \beta) \qquad (2.3-15)$$

so that

$$R_{G'G'}(0, 0) = E \, G'(a, b) \, G'(a, b)$$

$$= E(G')^2 \qquad (2.3-16)$$

2-94

that is, the numerator $E(G')^2$ is the auto-correlation function of $G'(a, b)$ evaluated at the origin.

We can get the auto-correlation function of $G'(a, b)$ from the auto-correlation function of $G(a, b)$. If a stationary random function G has an auto-correlation function R_{GG}, then its first derivative G' has auto-correlation function $R_{G'G'} = -R''_{GG}$. Therefore, the numerator $E(G')^2$ of Equation (2.3-14) is given by

$$E(G')^2 = -R''_{GG}(0, 0) \qquad (2.3-17)$$

where the primes denote differentiation with respect to the first argument of R_{GG}.

We now need an expression for the auto-correlation function $R_{GG}(\alpha, \beta)$ of the random function $G(a, b)$. The expression for $G(a, b)$ is, by copying Equation (2.3-8),

$$G(a, b) = \int_0^L \int_0^L P(x, y) W(x - a_0 + a, \ y - b_0 + b) \ dx \ dy \qquad (2.3-18)$$

This represents a linear system with stationary input $W(x, y)$ and stationary output $G(a, b)$. Since the input is stationary, we can translate the input by any amount, and still have the same statistics for the output. Therefore, we can translate the input by (a_0, b_0) and compute the auto-correlation function $R_{GG}(\alpha, \beta)$ from

$$G(a, b) = \int_0^L \int_0^L P(x, y) W(x + a, \ y + b) \ dx \ dy \qquad (2.3-19)$$

If we multiply Equation (2.3-19) by $W(a + \alpha, \ b + \beta)$, and take the expected value, we have

$$R_{GW}(\alpha, \beta) = \int_0^L \int_0^L P(x, y) R_{WW}(x - \alpha, y - \beta) \, dx \, dy \quad (2.3\text{-}20)$$

where R_{WW} is the auto-correlation of W and R_{GW} is the cross-correlation of G and W.

Similarly, if we multiply Equation (2.3-19) by $G(a + \alpha, b + \beta)$, and take the expected value, we have

$$R_{GG}(a, \beta) = \int_0^L \int_0^L P(x, y) R_{GW}(x - \alpha, y - \beta) \, dx \, dy \quad (2.3\text{-}21)$$

Because of the finite resolution of the picture or, equivalently, the finite bandwidth of the analog function that represents the picture, the integrals of Equations (2.3-20) and (2.3-21) are actually the sums

$$R_{GW}(\alpha, \beta) = \sum_{m=0}^{N-1} \sum_{n=0}^{N-1} P(m\Delta, n\Delta) R_{WW}(m\Delta - \alpha, n\Delta - \beta)$$

$$R_{GG}(\alpha, \beta) = \sum_{m=0}^{N-1} \sum_{n=0}^{N-1} P(m\Delta, n\Delta) R_{GW}(m\Delta - \alpha, n\Delta - \beta) \quad (2.3\text{-}22)$$

where Δ is the distance between resolution elements, and N is the number of resolution elements in any horizontal or vertical line. We can suppress the dependence upon Δ by taking it to be one, and measuring other parameters in terms of Δ. Then the numerator $E(G')^2$ of Equation (2.3-14) for the mean square estimation error can be computed from

$$E(G')^2 = -R''_{GG}(0, 0) \quad (2.3\text{-}23)$$

where

$$R_{GG}(\alpha, \beta) = \sum_{m=0}^{N-1} \sum_{n=0}^{N-1} P(m, n) R_{GW}(m - \alpha, n - \beta)$$

$$R_{GW}(\alpha, \beta) = \sum_{m=0}^{N-1} \sum_{n=0}^{N-1} P(m, n) R_{WW}(m - \alpha, n - \beta)$$

For the picture model and pattern chosen, the Equations (2.3-23) are

$$E(G')^2 = -R_{GG}''(0, 0) \qquad\qquad (2.3-24)$$

where

$$R_{GG}(\alpha, \beta) = A \sum_{m=0}^{N-1} \sum_{n=0}^{N-1} \sin \omega m \cdot \sin \omega n \cdot R_{GW}(m - \alpha, n - \beta)$$

$$R_{GW}(\alpha, \beta) = A \sigma^2 \sum_{m=0}^{N-1} \sum_{n=0}^{N-1} \sin \omega m \cdot \sin \omega n \cdot e^{-\sqrt{(m-\alpha)^2 + (n-\beta)^2}/\lambda}$$

The frequency ω of the pattern is related to its period ℓ by $\omega = 2\pi/\ell$. Unfortunately, we do not have an analytic solution to Equations (2.3-24). We can, however, note that the numerator $E(G')^2$ is equal to $A^2 \sigma^2$ times a function of N, ℓ, and λ. The function can be computed from Equations (2.3-24) by letting A and σ equal one, and approximating R_{GG}'' by the second finite difference of R_{GG}.

We can derive an analytic solution if the random component $W(x, y)$ of the picture intensity $I(x, y)$ has no spatial correlation, which will be

valid for values of λ which are small compared to $\Delta = 1$. If $W(x, y)$ is spatially uncorrelated, its auto-correlation function $R_{WW}(\alpha, \beta)$ is

$$R_{WW}(\alpha, \beta) = \sigma^2 \qquad \text{for } \alpha, \beta = 0$$

$$= 0 \qquad \text{otherwise.} \qquad (2.3\text{-}25)$$

Then, using Equations (2.3-23), and the two-dimensional sine wave pattern with amplitude A and frequency ω, we have

$$R_{GW}(\alpha, \beta) = A\sigma^2 \sin \omega\alpha \cdot \sin \omega\beta$$

$$R_{GG}(\alpha, \beta) = A^2 \sigma^2 \sum_{m=0}^{N-1} \sum_{n=0}^{N-1} \sin \omega m \cdot \sin \omega n$$

$$\cdot \sin \omega(m - \alpha) \cdot \sin \omega(n - \beta) \qquad (2.3\text{-}26)$$

so that

$$E(G')^2 = -R_{GG}''(0, 0)$$

$$= \left(A^2 \sigma^2 \omega^2\right) \left(\sum_{m=0}^{N-1} \sin^2 \omega m \right)^2 \qquad (2.3\text{-}27)$$

Denominator Evaluation

We will now examine the denominator of the expression for the mean square error. The denominator is $(F_o'')^2$, the square of the second partial derivative of $F(a, b)$ with respect to a, evaluated at (a_o, b_o), where $F(a, b)$ is, by copying Equation (2.3-8),

$$F(a, b) = \int_0^L \int_0^L P(x, y) P(x - a_o + a, y - b_o + b) \, dx \, dy \qquad (2.3\text{-}28)$$

Since the translation (a_o, b_o) is unknown, we will assume it to be zero. Noting that the integrals of Equation (2.3-28) are actually sums, and that Δ was chosen to be one, we have

$$F(a, b) = A^2 \sum_{m=0}^{N-1} \sum_{n=0}^{N-1} \sin \omega m \cdot \sin \omega n$$

$$\cdot \sin \omega(m + a) \cdot \sin \omega(n + b) \qquad \cdot \qquad (2.3-29)$$

so that

$$F''(0, 0) = -A^2 \omega^2 \left(\sum_{m=0}^{N-1} \sin^2 \omega m \right)^2 \qquad (2.3-30)$$

and

$$\left(F_o'' \right)^2 = A^4 \omega^4 \left(\sum_{m=0}^{N-1} \sin^2 \omega m \right)^4 \qquad (2.3-31)$$

We noted previously that the numerator $E(G')^2$ is equal to $A^2 \sigma^2$ times a function of N, ℓ, and λ. From Equation (2.3-31), we can see that the denominator $(F_o'')^2$ is equal to A^4 times a function of N and ℓ. Consequently, the mean square estimation error is equal to $(\sigma/A)^2$ times a function of N, ℓ, and λ. This function can be computed from Equations (2.3-14), (2.3-24), and (2.3-31), with A and σ equal to one.

Result for Pictures Without Spatial Correlation

If the random component of the picture intensity is spatially uncorrelated, we can divide Equation (2.3-27) by Equation (2.3-31) to arrive at

$$E(\hat{a} - a_o)^2 = \left(\frac{\sigma^2}{A^2\omega^2}\right)\left(\sum_{m=0}^{N-1} \sin^2 \omega m\right)^{-2} \qquad (2.3-32)$$

By making the trigonometric substitution $\sin^2 \omega m = 1/2 (1 - \cos 2\omega m)$, the series becomes

$$\sum_{m=0}^{N-1} \sin^2 \omega m = \frac{1}{2}\sum_{m=0}^{N-1} (1 - \cos 2\omega m)$$

$$= \frac{N}{2} - \frac{1}{2}\sum_{m=0}^{N-1} \cos 2\omega m \qquad (2.3-33)$$

The series

$$\sum_{m=0}^{N-1} \cos 2\omega m$$

can assume a range of values, the exact value depending on ω. The $1/\omega^2$ factor in Equation (2.3-32) indicates that large values of ω are desirable. However, the value of ω cannot be too large if the ambiguity problem is to be avoided. Therefore, we can assume that the value of $\omega = 2\pi/\ell$ is intermediate, intermediate in the sense that the pattern period ℓ is large compared to $\Delta = 1$, the distance between resolution elements, but small compared to $N - 1$, the picture length. Then the series

$$\sum_{m=0}^{N-1} \cos 2\omega m$$

is roughly the integral of a cosine wave over a large number of cycles, and therefore, approximately zero (exactly zero, if ℓ is an integral

multiple of $\Delta = 1$, and $N - 1$ is an integral multiple of ℓ). So we can replace the series in Equation (2.3-32) by $N/2$, to get

$$E(\hat{a} - a_o)^2 = \frac{4\sigma^2}{A^2 \omega^2 N^2} \tag{2.3-34}$$

2.3.4.3 Results

If there is no spatial correlation of the picture intensities, the mean square error in the estimate of either the horizontal or vertical translation is

$$MSE = \frac{\sigma^2 \ell^2}{\pi^2 A^2 N^2}$$

where σ^2 is the variance of the picture intensity, A is the pattern amplitude, ℓ is the period of the pattern in resolution elements, N is the number of resolution elements along a side of the picture segment, and MSE is the mean square estimation error in resolution elements squared.

If there is spatial correlation of the picture intensities, the mean square estimation error must be computed from Equations (2.3-14), (2.3-24), and (2.3-31). This was done for various values of ℓ, N, and λ. Typical results are given in Figures 2.3-10 and 2.3-11 for a σ/A ratio of 10. Since the mean square estimation error is proportional to $(\sigma/A)^2$, the MSE for other σ/A ratios can be inferred from the graphs. A σ/A ratio of 10 was chosen because it seems plausible that for a pattern amplitude of $1/10$ a typical variation in picture intensity will not corrupt the picture unduly.

Figure 2.3-11 shows the MSE as a function of the correlation parameter λ, for $\ell = 10$ and $N = 30$. The correlation parameter λ is the distance, measured in resolution elements, at which the correlation between two points on the picture decays to $1/e$. Figure 2.3-10 shows that the MSE has a peak at a value of $\lambda \approx 1.5$ which is small compared to the pattern period $\ell = 10$. For values of λ larger than seven or eight, the MSE is less than one. Consequently, the cross-correlation would
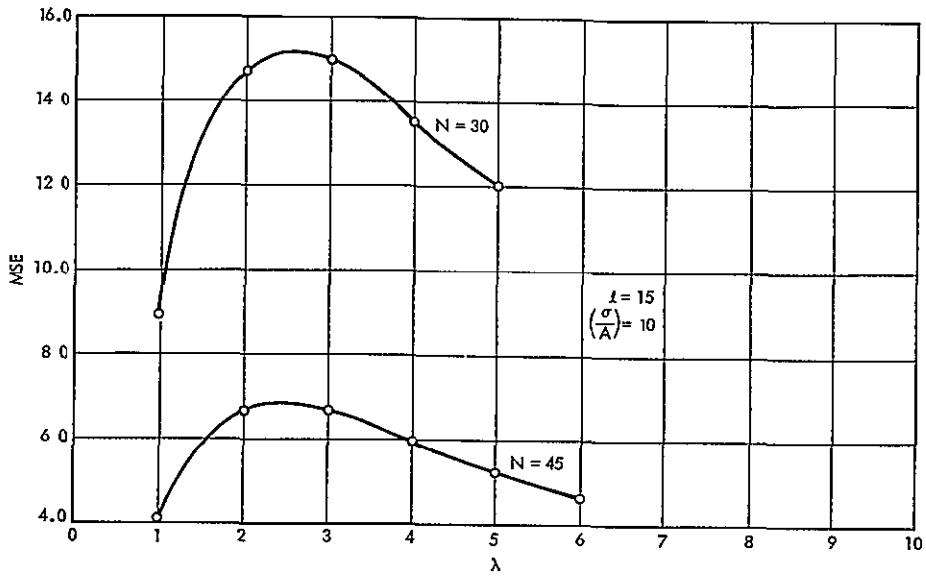
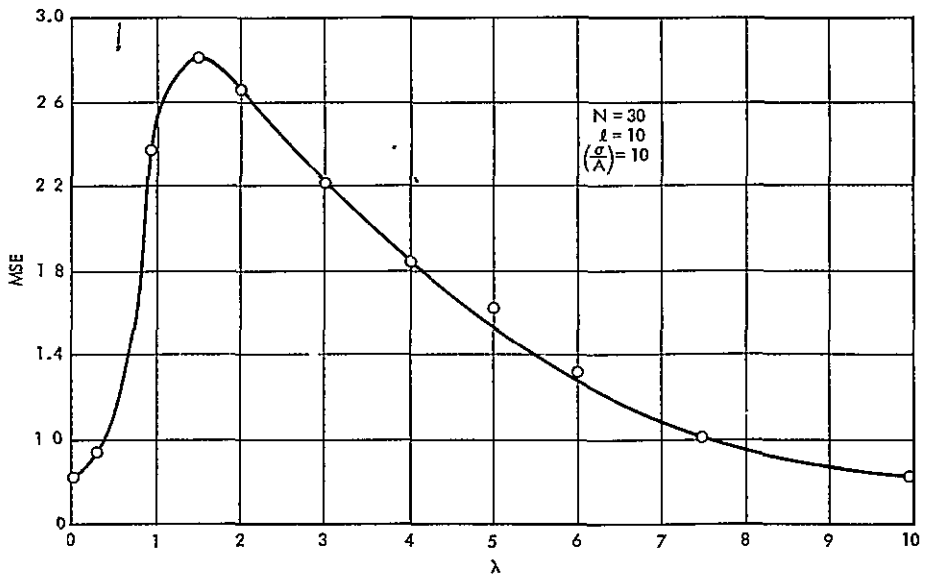Figure 2.3-10

VARIATION WITH CORRELATION PARAMTER, FIRST CASE

Figure 2.3-11

VARIATION WITH CORRELATION PARAMETER, SECOND CASE

seem to be very effective for large values of λ. For smaller values of λ, the MSE is as large as 2.7. If this is unacceptable, it can be reduced by using a larger N, that is, a larger picture segment.

Figure 2.3-11 shows similar graphs for $\ell = 15$ and $N = 30, 45$. The graphs confirm the nature of the MSE as a function of λ indicated by Figure 2.3-10, that is, a peak at a value of λ which is small compared to ℓ. The MSE's are rather large because of the large value of ℓ and the small values of N. Data points were not computed for larger values of N since the computer time required to evaluate a point is proportional to N^4. However, it is likely that the MSE is inversely proportional to N^2, as the formula for uncorrelated pictures indicates, so that MSE declines rapidly as N increases.

In summary, this study indicates that the use of patterns and cross-correlation is a possible way to determine geometric distortions. This conclusion, however, is based on several assumptions: (1) the picture has stationary intensities, (2) reasonably small values of ℓ, the pattern period, can be used without having ambiguity problems, and (3) reasonably large values of N, the size of the picture segment, can be used without introducing too much nonlinearity into the distortion.

2.3.5 Digital Correlation Detection of Reseau; Program Description

The reseau detection routine is based upon file search and object correlation techniques. The file is used to log the previous history of reseau locations and this history is used to speed the location of current reseau. The input picture is scanned in the vicinity of the previously found reseau location and all objects that are potential reseau are logged. A catalog is made of all potential reseau found in the vicinity of all previous reseau. This catalog is screened allowing only potential reseau with sizes comparable to those expected to remain in the catalog. The remaining points in the catalog may be substantial, primarily because of the size of the reseau as they appear on the vidicon and also because of potentially adverse noise levels in the image. To screen this catalog, clustering techniques are used to scan in the line direction and the sample direction to find a set of reseau with the following properties: a) There must exist no more than one reseau in the vicinity of any of the previously

found reseaus; b) The chosen reseau must exhibit smoothly varying line and sample coordinates in the two directions (geometric distortions typically exhibit bandwidths on the order of a half a cycle per picture dimension). Where ambiguities arise the reseau that are closest to the previously found location is chosen. In cases where the reseau could not be located, positions are estimated by using interpolation and extrapolation within the matrix of those found. The reseau locations for the current picture are used to update the history file and the reseaus then can be removed from the current picture. Reseau removal is achieved using two-dimensional linear interpolation within the data in the pictures surrounding each of the reseaus.

The program consists of several routines and phases. The first phase is called RIZEAU which is a routine to detect potential reseau locations. The next phase is called DETECT which screens the matrix of potential locations, thus determining the actual locations. The final phase is called RIZSAR and is used to remove the reseaus from the input picture. This phase consists of two subroutines, the first called RIZEAU and the second called CORRIZ. The routine RIZEAU first opens the data sets which are required. The routine next reads the reseau locations which were found previously. This is the reseau location history. The routine next converts these numbers and prints them on the line printer as an output. The remainder of the routine is a large loop which performs the detection process on the input picture. For each row of reseau this loop reads 80 lines beginning 40 lines above and ending 40 lines below the previously detected reseau for that row. The code guarantees that this 80 line block will not extend beyond the input picture, i.e., if necessary, fewer than 80 lines are considered. Because of the desire to restrict core, the lines are read six at a time and cycled through core. The detection process is made by calls to the routine CORRIZ which actually detects potential reseau. After finishing this loop, the subroutine RIZEAU then loads in the next phase called DETECT. The subroutine CORRIZ used in the phase RIZEAU is written in the assembler language because it does most of the computational work of detecting potential reseau. The routine CORRIZ basically operates by correlating an object resembling the reseau in the vicinity

of each point of the 80 line block of data which is being read through each row of the previously found reseau. At each point the average intensity value over the test object is compared with the average intensity value over the region located at the point at the point of interest and the following test is made:

If the average intensity value over the surrounding region is less than a threshold which is specified by the operator, the test proceeds no further since that area of the picture is so dark that the detection of the reseau is not reliable. If the value is sufficiently high the average over the central region is then examined. If this value is greater than the previously value the point is again ignored since the reseaus must be black. If the average value is less than the average, it must be lower by a percentage which is again specified by the operator. If this is not the case, the point is again ignored and the search moves on to the next point. If this is the case, the percentage expressed as an integer between 0 and 100 is output into a buffer, and represents a point which is part of a potential reseau. This test is repeated for every point along each of the 80 lines in the input block of data. Once the phase RIZEAU has performed this operation for each of the five rows of input, reseau control is transferred to the phase DETECT, which performs one sub-routine. Data is transferred to the routine DETECT through the common block name. The function of the first major loop is to scan the correlogram which was produced by the phase RIZEAU and to catalog objects which satisfied two conditions: a) The correlation peak must be circumscribable by a sample box. This is to eliminate any correlation object which might arise from edges or other elongated objects in the input image; b) All objects are eliminated which are not within a predetermined picture element radius of the previously found reseau. All potential reseau satisfying these two criteria are logged in a working buffer. If no potential reseau were located, this is noted on a line printer and a branch is made at which point the previous reseau locations are used. If fewer than the expected reseau are found, this is noted on the line printer and the search continues. By the nature of the search, to this point, the potential reseau are organized by increasing line count in the buffer. The next major loop scans each of the five blocks of potential

reseau and screens them by sequentially increasing the size of a window through which the absolute difference in line count of successive potential reseaus in the block must pass. The search continues until five blocks are found each containing at least 9 reseaus corresponding to the number possible along each line or until the total number of potential reseaus for a block is included if fewer than 9 were found for a block corresponding to some black space. If this search is unsuccessful, the same branch is taken as previously and the previous reseau locations are used. If this search is successful, the resulting potential reseau are reorganized based upon sample locations. A scan is made of the blocks of the potential reseaus. For those blocks with nine detected reseaus the average displacement in line and sample from the previous reseau location is computed. In this way an average translation for the picture reseau is determined and the remaining matrix of potential reseau is scanned and the potential reseau closest to the location determined by adding the average line and sample translation to the previous reseau position corresponding to that reseau is selected. If no potential reseau is found within 20 picture elements of these estimated locations, the estimated reseau position is used. The reseau buffer now contains the best estimate of the locations of the reseaus in the body of the picture. The program at this point has isolated 81 reseaus consisting of a 9 x 9 array in the body of the picture. These are logged on the line printer and used to update the reseau location history. The updating is performed by averaging the currently located reseau positions with the previous reseau location history and writing results back out on the history data set. At this point, the third phase called RIZSAR is initiated, if desired, and control is transferred to it. RIZSAR has received information from the previous phases through the common block. The function of RIZSAR is to process the input picture by removing the reseau as detected in the previous phases and in addition, to punch a set of cards containing the reseau location positions. This deck of punch cards can be used for subsequent geometric correction programs. The reseau removal is attempted only for the 81 reseau in the body of the picture.

2.4 OPTICAL IMAGE PROCESSING

Optical methods for correcting errors in imagery have many characteristics in common with digital methods; there are also a number of fundamental differences. Any attempt to adduce general advantages or disadvantages of one approach to image processing with respect to the other tends to be inconclusive, since the requirements and constraints of specific image processing problems vary widely. In fact, the studies of ERTS image data processing problems conducted by TRW, with the assistance of Itek and IBM, have shown that even in a relatively restricted application such as this, both methods have special characteristics which can be exploited in different parts of the system to give an optimum configuration to the overall design. The following sections provide an exposition of the optical methods proposed to give the basis on which the applicability of each to the image processing subsystem was determined.

2.4.1 Inherent Characteristics of Optical Methods

It is a fundamental property of optical manipulations of imagery that they operate on an entire field of view at once. This means that many of resolution elements can be processed in parallel, with enormous savings in time over point-by-point methods; by the same token, individual treatment of the points is precluded. Another limitation on strictly optical processing methods is that degraded resolution, whether it is incurred by diffraction effects, prior optical aberrations, film grain, or any other cause, can never be restored after the image has been recorded. This, however, is equally true of digital methods, unless information not contained in the imagery itself can be invoked. Some remarkable demonstrations of noise removal and image sharpening have been produced by spatial filtering in the Fourier domain, which can be implemented either quasi-optically or digitally. They depend, however, either on prior knowledge of what the shape of the image ought to be or on the assumption or actual knowledge that certain spatial frequency components constitute noise and not image information. There are situations in which such knowledge is available or such assumptions are valid, and in these situations Fourier domain processing can be useful, but it should be noted that noise removal and allied image manipulations always carry with them the likelihood that some image information will be removed along

with the noise. Two effects which may arise in ERTS imagery are amenable to this type of processing; they are structured noise resulting from electromagnetic interference effects, and uncompensated vehicle motion smear. From the nature of these effects and the information available, they can best be treated digitally, therefore, the discussion which follows does not include optical processing in the Fourier plane.

Optical processing of the type under consideration can inherently produce only zero- and first order geometric corrections. As will be seen later, this limitation can effectively be circumvented by sequential treatment of small segments of the image, but it remains true for the instantaneous field of view. The coordinate transformations for correcting image distortions, which are possible to effect by optical processing are shown in Figure 2.4-1. There are two zero order transformations: simple translations in x and y, respectively. The four first
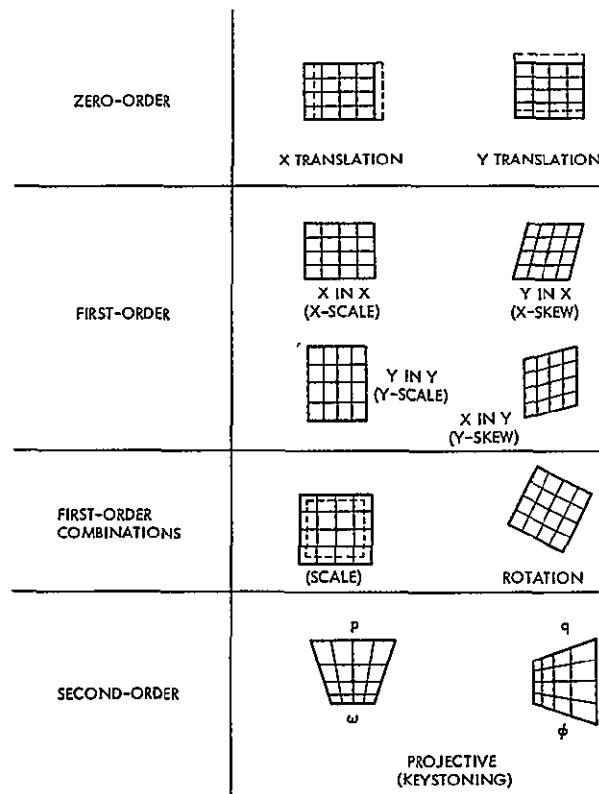

Figure 2.4-1

OPTICAL COORDINATE TRANSFORMATIONS

order transformations are differential x-scale (x in x), differential y-scale (y in y), x-skew (y in x), and y-skew (x in y). Two important combinations of these transformations result: 1), from equal departure of x-scale and y-scale from nominal, i. e., ordinary overall scale change, and 2), from equal x-skew and y-skew, i. e., overall rotation. One particular second order transformation, the projective transformation, or keystoning, is amenable to optical correction, and conventional optical rectifiers based on the Schiempflug principle are commonly used by photogrammetrists to correct this type of distortion. Keystoning will in fact produce a small but observable distortion in ERTS imagery due to satellite motions within the ACS limit cycle. The processing methods proposed, both optical and digital, are fully capable of removing this distortion without the introduction of an additional optical step.

2.4.2 Implementation of Optical Transformations

A generalized optical processing device, of the type being discussed, is shown schematically in Figure 2.4-2. It consists of an illumination source, a shutter or other means of controlling exposure, an input optical stage on which the image to be corrected is placed, an optical chain containing the elements necessary to make the optical transformations, control and driving provisions to set the various elements into the configuration necessary for the desired corrections, and an output optical stage on which unexposed film is placed. In operation of the device the optical-mechanical adjustments are made, then the output film exposed; thus, in effect, an optical printing has been made in which the output copy has received the desired corrections.

The two zero order transformations, x- and y translations are readily accomplished by corresponding translations of either the input or output stage. Alternatively, if the required translations are small, the translations can be effected by using a pair of wedges in the optical train to bend the optical path. The relative angle between the wedges determines the amount of translation, and the orientation of the pair determines the direction of translation.
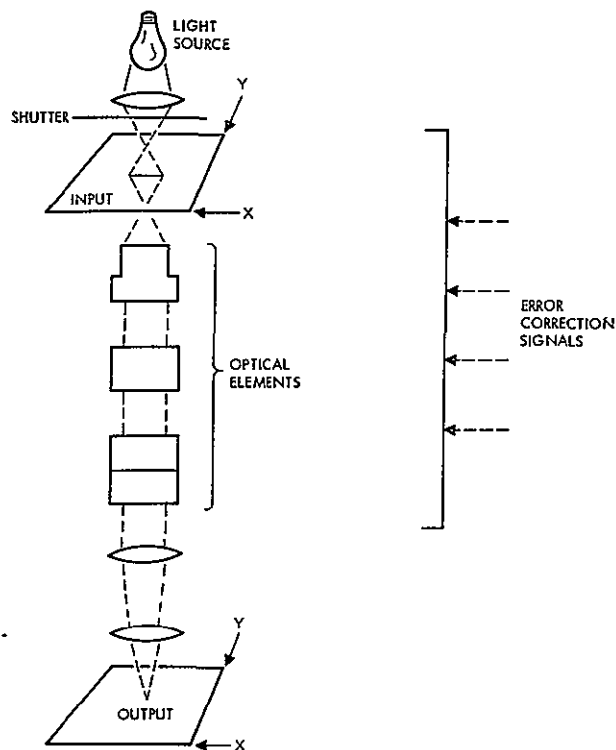
Figure 2.4-2

GENERALIZED OPTICAL PROCESSING DEVICE

The four first order transformations can be made by any of a number of combinations of elements providing four independent adjustments. One practical combination arises from treating the four transformations as magnification, rotation, differential scale, and skew, as illustrated in the first row of Figure 2.4-3. While these transformations are not independent of one another, their proper combination does encompass all first-order corrections, and they can be implemented by specific optical components. The second row, in Figure 2.4-3, shows the image displacements associated with each transformation, while the third row shows the appropriate optical components. The operation of the zoom lens and K rotator are quite straightforward; it is evident, however, that fixed power anamorphs do not independently correct differential scale and skew. Actually, the two anamorphs together achieve the differential scale and skew corrections with attendant magnification and rotation residuals, which are compensated in the zoom lens and K rotator.
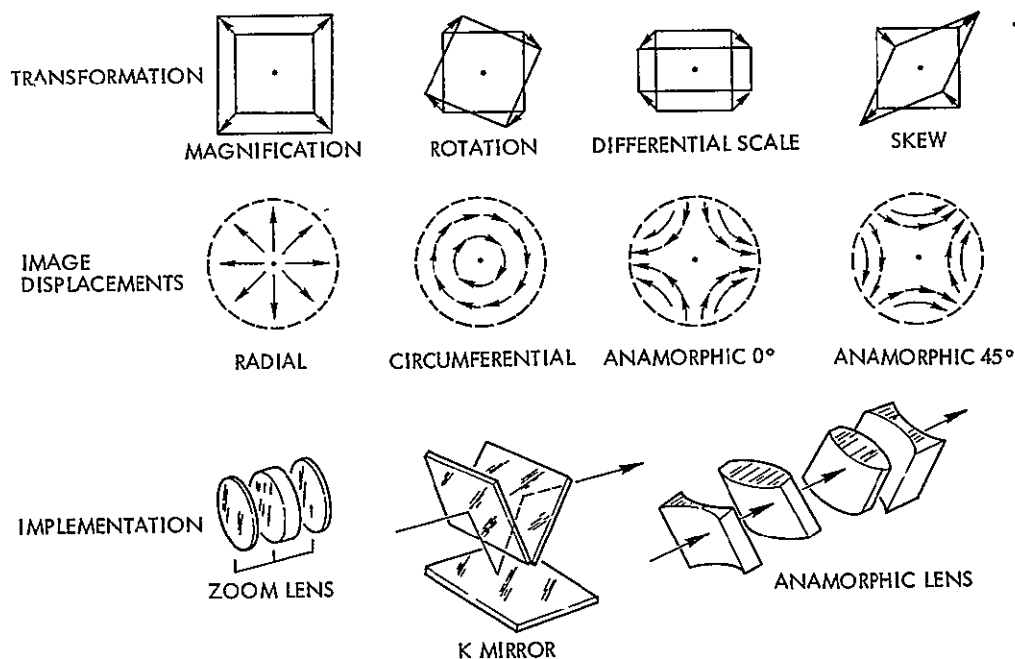
Figure 2.4-3

OPTICAL IMAGE TRANSFORMATION

When the transformations required are small, the optical elements can be considerably simplified while still achieving correction accuracies consistent with the input information, while actually increasing the modulation transfer function of the system. For example, if the range of scale changes required amounts to only a few percent, a fully optically compensated zoom lens can be replaced by a moveable fixed focus lens and the changes accommodated within the depth of focus of the system. Similarly, for small variations of x- and y- differential scales and skews, and with a narrow instantaneous printing slit, the anamorphic lenses can be removed entirely. These approaches are completely satisfactory for ERTS image processing, and are used in the design of the optical processing equipment, the precision photo restitutor, which is described later.

The physical means by which the correcting elements of the optical processing device are adjusted to give the desired results are implied by the foregoing. They consist of translations of stages and lens elements and rotations of prisms and anamorphic lenses by suitable servomechanisms.

2-111

The error signals which drive the servos must have been derived from some source of error information. In the past, area correlation with another image of the same scene has frequently been used as this source, as in examples where correlation of two images of a stereo pair has been used for data from which to produce an orthophotographic output. In ERTS image processing correlation techniques have an important place, but they are not the principal source of error information. The essential problem is to provide a coordinate transformation from the distorted imagery geometry to that providing an undistorted representation of the original scene, presented in terms of the required device adjustments. For RBV image data, the coordinate transformation is derived principally from reseau information, while for MSS image data spacecraft attitude and attitude rate values are the principal sources of information.

An instrument called the electronic registration optical stereoscope (EROS) embodying the foregoing optical correction principles has been developed by Itek. The EROS used correlation techniques to derive the error signals. It achieved zero-order transformations using a conventional x-y stage and first-order transformations using optical systems consisting of a zoom lens, a K rotator, and two anamorphic lenses. The outputs were presented visually to permit high resolution viewing of originally badly distorted stereo imagery. Direct application of EROS to ERTS image processing problems, even with the substitution of printing stages for the visual output, is limited both by its restriction to zero- and first-order corrections and by the optical problems attendant upon the very large object and image sizes required in ERTS.

Both these limitations can be removed by correcting the image a small segment at a time. Simpler optical elements can be used having well-corrected performance over a small field of view. Moreover, the overall correction of input imagery distortion can be a piece-wise linear approximation to a considerably higher order correction function. This kind of approximation can be made to be as accurate as the uncertainties in the basic error data justify. The discrete nature of the error information sources available for ERTS image data, such as the reseau points in the RBV imagery, is consistent with this approach.

2.4.3 Comparison of Optical and Digital Processing Methods

While a simple tabulation of advantages and disadvantages for optical and digital processing methods is not very satisfactory, since the differences are much more than quantitative, a number of useful comparisons can be made. Optical methods operate on a large number of points in parallel; digital methods must treat the image point by point. This suggests a tremendous speed advantage for the optical methods; occasionally this potential is realized, but more often a great deal of it is lost in a specific application. It has been seen that the optical correction values are established by mechanical adjustments of optical components; these relatively slow mechanical motions contribute significantly to the overall processing time. This is especially true when image segmentation is employed to achieve higher order corrections. Digital methods have been devised which perform the major transformation computations for moderately large blocks of points at once, but the constant block corrections must be applied to each point in turn. Thus, arithmetic computation time can be materially reduced but the manipulation of each point remains. The net result is some gain in speed, but at some expense in accuracy. Moreover, experience has shown that this type of approach is prone to disturbing cosmetic defects in that the block edges are often observable in a hard copy presentation of the output. The necessary hard copy presentation is itself an analog process which cannot be dismissed from consideration of digital methods. It tends both to increase the overall processing time of a digital system and to some extent to degrade the accuracy of the final man-interpretable product. Thus the processing times required for either optical or digital methods turn out to be roughly comparable, depending on the exact requirements and mechanization of the method, and one or the other approach can prove to be faster in a specific application.

The geometrical corrections effected by the optical processing methods discussed are mathematically equivalent to digital bilinear point interpolation algorithms over the area of the instantaneous printing segment. They are intrinsically better than digital block shifting, and not as good as more elaborate, but often time-consuming algorithms, such as biquadratic interpolation. These comparisons, while mathematically

2-113

correct, are also tempered by corollary considerations. The optical transformations are of themselves very accurate, but the mechanical adjustments which establish their values are subject to small but inevitable errors. Similarly, the residual errors of the digital approximations will be somewhat increased in any recording in pictorial form.

Photometrically the optical methods are intrinsically superior to digital methods, in that each point is moved optically to its proper location, while the digital approach determines an average density value for a specified grid point, with a resultant loss of resolution and/or contrast. Digital processing is capable by this procedure, of generating data suitable for output on a computer-readable tape referenced to a regularly spaced raster grid, while the optical methods are not. Finally, digital methods afford the opportunity of point-by-point photometric corrections; these are difficult or impossible using strictly optical techniques.

2.4.4 Precision Photo Restitutor (PPR)

Optical processing in the telemetry and image data processing will be performed with the precision photo restitutor (PPR). The PPR incorporates analog image correlation and a simplified optical transformation system to give zero- and first-order transformation to the images in a linear piecewise approximation to the error model, developed from the reseau measurement, spacecraft data, and ground truth, if necessary.

A simplified block diagram of the PPR is shown in Figure 2.4-4. A scanning table driven in x and y carries the input, control, and output film rolls. The output film is exposed by an image that is transformed from the input image by optical elements capable of introducing magnification, rotation, Δx, and Δy corrections.

These corrections are either programmed from computer generated data, or they are developed by the correlation system that detects relative distortion between the control image and the input image. Registration is ensured up to the limits of the linear approximation to the distortions within the printing slit. A printing slit of 0.811 by 0.05 inch has been selected for bulk processing. Thus, nine printing segments will be exposed over the image format.
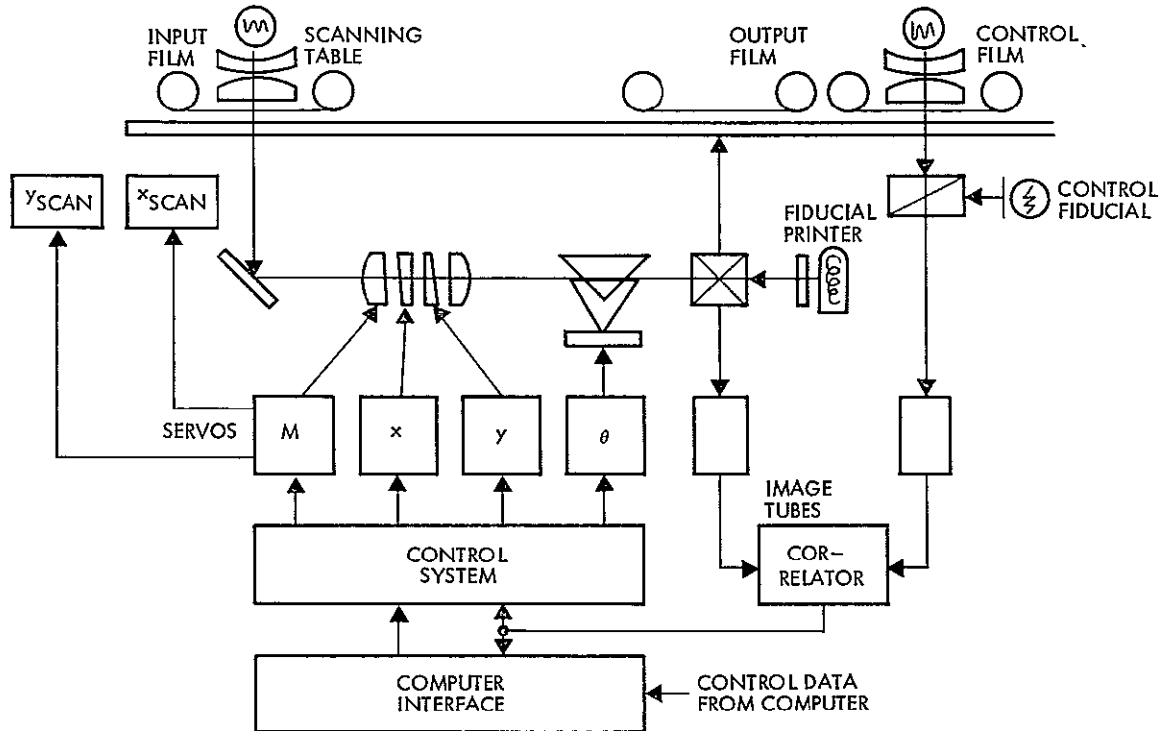
Figure 2.4-4
SIMPLIFIED BLOCK DIAGRAM OF PPR

Figure 2.4-5 indicates the scan process for film exposure in the PPR. In a computer controlled mode, the scanning table is positioned to enable strip number 1 to be printed. The exposure slit allows the film to be exposed, in a continuous fashion, as the table moves at a constant rate. During printing, the optical system is continuously controlled by computer generated data in order to shift the elements of the image within the slit in such a fashion to correct distortion. After each strip is printed, the scanning table is stepped to the next strip and the process is repeated.

The following major functional elements are included in the PPR system:

a) Optical system.

b) Correlation system.

c) Computer interface.
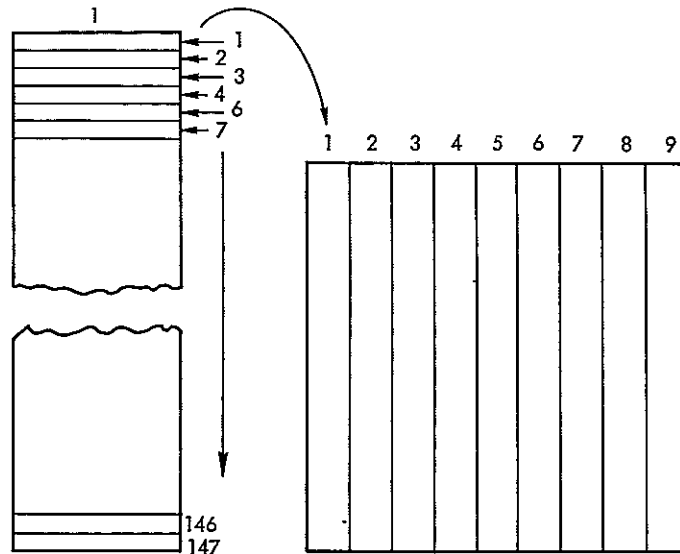
Figure 2.4-5

PPR SCAN PROCESS FOR FILM EXPOSURE

2.4.4.1 PPR Optical System

The two major objectives in the design of the PPR optical system are:

- To provide an optical system for duplicating of input imagery which will ensure high definition and flawless reproduction of input imagery

- To provide optical differential image correcting elements which are capable of following the positional commands, issued by the control computer or correlation system, with sufficient precision to correct input image geometry, with errors considerably smaller than the limit of input image resolution.

In carrying out the design objectives, the first consideration was to make the PPR printing and correction systems as simple as possible, consistent with the requirements, in order to maintain highest positional accuracy. Since film positioning tolerances were especially critical, it was decided that differential displacements of input would be accomplished in the optical system to avoid complicated film drive mechanisms.

Another consideration was the method used to obtain the required ±5 percent change in magnification from unity image reproduction. The

2-116

simplest approach was to move a single relay lens between the fixed input
and output planes and allow the image to defocus. The image quality
expected from this process was initially satisfactory, however, after the
effects of other degrading elements in the optical system were considered,
it became apparent that a focus correction would be necessary to provide
the required overall image quality. Rather than move the film and trans-
port assembly to provide focus, it seemed more convenient to make the
printing relay a symmetric pair of lenses and move the lenses separately,
so as to accomplish the required change in magnification and still main-
tain focus in the image.

The variable magnification relay stage consists of two identical
photographic triplet objectives with focal lengths of 360 millimeters which
form a symmetrical relay pair. In the 1:1 magnification position the two
lenses are separated far enough so that prism parallax correctors can be
mounted in the collimated beam between them. The relay pair is approxi-
mately centered between the input and output film planes. A ±5 percent
change in magnification is achieved by displacing the lens nearest the
input plane in a linear fashion to change the object conjugate. The other
lens is then driven to correct for defocusing.

The relay pair is operated at an effective aperture of f/20. At this
aperture ratio the triplet pair is expected to be nearly diffraction-limited
with approximately 75 percent modulation transfer at 10 line pairs per
millimeter for 1:1 magnification.

Image rotation of ±2 degrees is accomplished with a K-mirror
image rotator. Three reflections of the image within the K are required
for inversion and subsequent rotation about the optical axis. A rotation
of ±1 degree of the K assembly yields the desired ±2 degree image rota-
tion. The K configuration may consist of three adjustable plane first
surface mirrors, or one plane mirror and a silvered reflecting prism.
The prism arrangement is easier to align than the three independent
mirrors, if stringent manufacturing tolerances are maintained. The
significantly higher cost of the prism reflector is offset by the higher
cost of aligning and maintaining two separate mirrors of equal surface
quality. Surface tolerances on flatness and regularity must be held to
1/20 wave rms over the clear aperture of all three reflective surfaces.

A beamsplitter is included in the K assembly to fold the printing relay optical axis 90 degrees to the output film plane and to provide simultaneously an image for the input correlator. Space limitations dictate the placing of the fold inside the K housing. The beamsplitting optical device has a neutral spectral transmission and reflection. A solid glass cube beamsplitter has been indicated in the optical system schematic, Figure 2.4-6. Suitable compensation for the aberrations, introduced by the glass cube in the relay optical path, may be applied in the form of corrective optical elements. In the event that the relay lenses are special designs, compensation for the beamsplitter can be designed into the lenses. An alternative solution is to replace the cube with a thin membrane beamsplitter (pellicle).
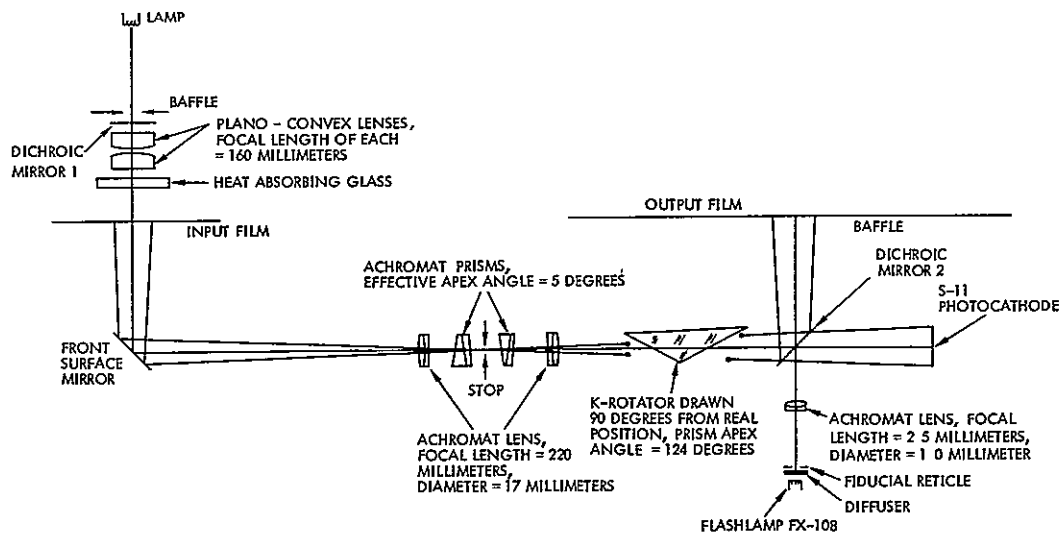
Figure 2.4-6
FIRST ORDER OPTICAL DESIGN FOR PPR DISTORTION CORRECTION

Differential displacement corrections between input and control photographs are introduced by deflecting the printing relay optical axis, rather than by direct differential translation of the input photograph, with respect to the control photograph. The optical deflection is accomplished with rotating prisms located between the relay lenses in the optical printing path of the PPR. The prisms consist of right circular cylindrical wedges, each of which introduces a small fixed angular deflection into the optical path. When used in pairs, the wedge deflections compensate each other so that, by rotating wedges with respect to one another, their net angular deflection is varied from zero to twice that of a single wedge.

Four separate achromatic wedge prisms are used to provide deflection along Cartesian X-Y axes. Each pair of wedges provides deflection only along one axis. For example, the deflection along the X-axis is

$$X = 2(n - 1)\theta s \cos\beta$$

where

θ = prism wedge angle

n = prism index of refraction

s = object distance of the relay

β = rotation angle of each of the two wedges of the X pair from the X axis

One major problem of the deflecting prisms is the chromatic dispersion introduced in deflecting the light beam by refraction. The dispersion can be corrected by making each wedge from a cemented pair of separate wedges of glasses, having different chromatic dispersions, such that the dispersion of one of the components compensates that of the other and no net dispersion results during deflection. This is called an achromatic prism. The wedge angle of each prism, for deflection of ±11 millimeters in the input film plane, is approximately 1.5 degrees depending on the refractive indices of the glasses used to make up the prisms. Deflection produced by each prism pair in the PPR is a function of both the mutual

rotation angle, β, and the distances from the input film plane of the relay lens, which is between the input film and the prisms. The servosystem driving the prisms must then receive inputs of both the amount of deflection required (Δx) and the position of the relay lens (Δs).

The prisms are made in the form of right circular cylinders, with clear apertures of approximately 1.6 inches, and are mounted concentrically within their respective drive motors.

2.4.4.2 Illumination Considerations

A radiometric analysis of the PPR printing, input/output, loop indicates that a 500-watt tungsten iodine projection lamp, similar to the Sylvania FCS lamp, will have appropriate power output and spectral radiance to adequately accommodate all expected modes of operation. From the following analysis it is shown that the radiance of the lamp in the spectral regions of interest is sufficient to permit black and white printing on EK film tape 2430, with the appropriate filters, the printing of false two and three color prints on color reversal film type 2448 (SO-151), visual alignment and testing, and light for proper operation of both the control and input/output vidissectors.

The condenser system that is used to project the source, filament, is of conventional condenser design. The condenser optics also provide the capability of eliminating unwanted radiation at long wavelengths, greater than $0.7\,\mu$, by means of a dichroic mirror positioned in the system so that this radiation is directed at an angle of 90 degrees away from the light path. This radiation, $\sim 0.7 - 0.9\mu$, will be sensed by a silicon photodiode to monitor the output of the lamp.

The radiometric analysis is summarized below.

Vidissector Requirements

It is assumed that for normal operation the photocathode (S-11) must generate $0.8\,\mu a/cm^2$. The response of the S-11 is such that the peak response at 0.45μ is 50 ma/w. This degenerates to about 20 ma/w at 0.35 and 0.57μ. Although the mean response of the S-11 is approximately 30 ma/w, the average response over the usable spectral band of 20 ma/w has been assumed for these calculations.

The system transmission varies with the film density in the input gate. Three values of system transmission have been determined based upon the following values for individual element transmission.

a) Condenser and dichroic beamsplitter $\cong 0.5$

b) Prisms (4) and fold mirror (coated $\cong 0.8$)

c) Relay (6 coated elements) $\simeq 0.9$

d) Beamsplitter $\cong 0.3$

e) Focal reference plate and clamp $\cong 0.95$

The irradiance produced in the plane of the image is defined by:

$$H = T \pi N \sin^2 \theta \ (w/cm^2) = \alpha N$$

where:

θ = half angle subtended at the image by the exit pupil

T = system transmission

N = object radiance

For an optical density D at the input of 0.2

$$\alpha_1 \simeq 1.5 \times 10^{-4}$$

for $D = 1.0$

$$\alpha_2 \simeq 3 \times 10^{-5}$$

for $D = 2.0$

$$\alpha_3 \simeq 3 \times 10^{-6}$$

The radiance of the light source must be

$$N = \frac{H}{\alpha_i}$$

The assumption has been made that the vidissector must have the stated power density with no photographic density at the input The required lamp radiance is

$$N = \frac{4 \times 10^{-5}}{1.5 \times 10^{-4}} \frac{W_2}{cm^2 - st} = \frac{0.3 \, W_2}{cm^2 - st}$$

It can be seen that the spectral radiance over the spectral response region of the S-11 is approximately 5 $W(cm^2 \, st)$. The appropriate neutral filtering will be inserted at the illuminator to produce the desired power density level at the photocathode.

Black and White Film Processing (Film Type 2430)

Calculations were made to determine the power densities required to produce densities of 0.1, 1.0 and 2.0 on the output film. The data used to determine the necessary exposures for the film is data produced at Itek, as was the data taken on the spectral radiance of typical tungsten-iodine projection lamps such as the BVA and FCS lamps. Corresponding densities of 2.0, 1.0 and 0.2 were assumed at the input film. For

D = 1.0 on 2430 film under normal processing
conditions

log exposure ≅ 0.5 mcs

t ≅ 0.05 second

$H \cong 1.5 \times 10^{-4} \, w/cm^2$

Required lamp radiance is

$$N = \frac{H}{\alpha_2} \cong 5 \, \frac{W}{cm^2 \, st}$$

The spectral radiance of a typical lamp in the region of interest is approximately

$$\frac{6W}{cm^2 \, st}$$

Color Film Processing

The color material to be used in the precision photo restitutor is film type EK-2448, formerly SO-151. This is a color reversal material. The following calculations are based on data determined from work performed at Itek.

The irradiance required to expose the film is

$$H \begin{vmatrix} \text{yellow} \\ \text{magenta} \\ \text{cyan} \end{vmatrix} \cong 6.5 \times 10^{-5} \text{ W/cm}^2$$

The corresponding lamp radiance required is

$$N \cong 0.5 \text{ W/cm}^2 \text{ st}$$

for a worst case condition which includes an additional transmission decrease factor of 0.5 due to the color separation filters. The minimum amount of available energy is for the yellow dye layer. At the present time, it has been assumed that the spectral response region of the film will be divided into five spectral bands, in order to produce the required color separation. The relative response of the dye layers is approximately equal over the spectral region of interest; therefore, the minimum spectral radiance available will be:

$$N \cong 0.9 \text{ W/cm}^2 \text{ st}$$

Photometric Requirements for Visual Observation at the Output Gate

In order for the eye to resolve a critical visual angle of a fraction of a minute of arc the background luminance must be on the order of 10^2 to 10^3 candles/m^2.[*] The equivalent irradiance is

$$H \cong 10^{-3} \text{ W/cm}^2$$

---

[*]Electro-Optics Handbook, RCA, Burlington, Massachusetts, 1968.

For the open gate, minimum density, condition at the input plane the
required lamp radiance N is

$$8W/(cm^2 st) \leq N \leq (80 W/cm^2 st)$$

The lamp radiance in the spectral region of interest is about

$$11 W/(cm^2 st)$$

Color separation, for production of the false color prints, is
accomplished by selective filtering at the output. Spectral bandpass
filters are used to properly isolate the color bands. These filters are of
appropriate spectral characteristics and neutral density. They are
located as near to the output film plane as possible, on a rotating disk,
so that the different filters can be quickly and easily interchanged. There
are no additional optics or mechanism required for color printing. Filter
quality is consistent with the requirements of the optical system.

2.4.4.3 Optical Performance

In determining the modulation transfer function of the optical system
diffraction due to the aperture stop of the relay is the first degrading
factor. The MTF of a diffraction limited f/20 imaging cone is represented
by curve A in Figure 2.4-7. The surface irregularities of the five
mirrors also reduce the image quality. If the mirror surfaces are 1/10
wavelength peak to peak, then the modulation loss due to the five mirrors
is illustrated by curve B. Defocusing also results in modulation loss.
The effect of maximum defocusing is illustrated by curve C. Another
source of modulation loss is the duplicating film. The modulation trans-
fer function of type 2430 film is represented by curve D. The effect of
mirror vibration and other minor sources of aberrations are budgeted
into curve E. Curve F represents the product of curves A through E;
it therefore is the system modulation transfer function for fixed values
of magnification, rotation, and translation, under static conditions.

MODULATION TRANSFER (y-axis)
DIFFRACTION, LINES PER MILLIMETER (x-axis)

A = MTF OF DIFFRACTION – LIMITED RELAY
B = MTF RESULTING FROM SURFACE IRREGULARITIES
    ON MIRROR
C = MTF RESULTING FROM DEFOCUSING
D = MTF OF TYPE 2430 FILM
E = MTF RESULTING FROM VIBRATION, WEDGES, ETC
F = SYSTEM MTF, i.e., PRODUCT OF CURVES A THROUGH E
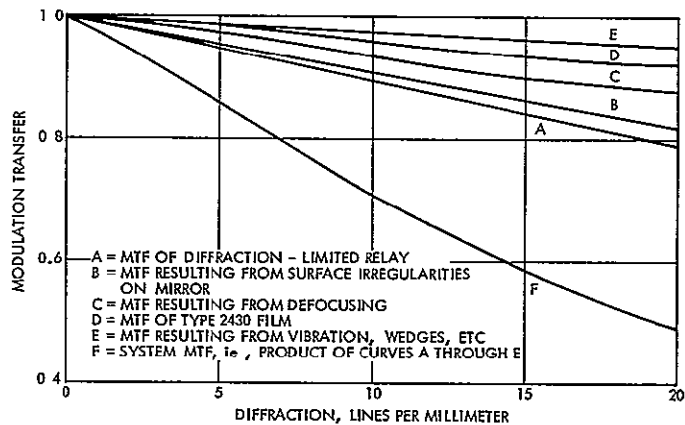
Figure 2.4-7

TRANSFER FUNCTIONS FOR PPR OPTICAL SYSTEM

Image smear produced by magnification changes, rotation changes, and translation changes that occur as the scanning slit moves one slit width have been estimated for worst case geometry corrections. Expected system MTF during dynamic correction are:

0.05 x 0.8 inch slit: 50 percent system response at 10 lp mm.

0.05 x 0.4 inch slit: 70 percent system response at 10 lp mm.

Correlation System

The precision photo restitutor can produce corrected imagery by computer-control, assuming that the data used to generate optical transformations is within the desired accuracy.

The use of correlation error signals directly to drive the transformation optical system is not considered as a basic production mode, because of uncertainty in the reliability of correlation of images in different spectral bands. However, correlation is used for initialization and to derive inputs to attitude determination. Moreover, it may find application in certain special processing situations.

The correlation system incorporated in the precision photo restitutor will be similar to the system employed with the Itek EC-5 correlator,

except that image dissector tubes are used in place of cathode ray tube scanners and photomultiplier detectors.

The scanning system consists of two image dissector tubes, vidissectors, that are integrated within the input film path and the control film path One of the vidissectors scans the input film image through an adjustable optical train which can introduce parallax, scale, and skew distortions to the image as seen by the vidissector. The other vidissector scans the control image. The film images are illuminated by back-lighting condensers and tungsten lamps so that the vidissectors receive light that is transmitted through the film image. By scanning the images with a special raster pattern, the vidissectors convert the density variations on the film, and hence transmission variations, to one dimensional analog electrical signals.

The two video signals from the vidissectors are fed into the electronics rack. Here the signals are correlated and analyzed into zero- and first-order error coefficients: X-Y parallax, X-Y scale, X-Y skew. Error signals are generated that are proportional to these correlation errors between the input image and the control image, and are used to drive servomotors attached to the optical correcting chain. Compensating amounts of parallax, skew and scale are introduced by the optics until the input image, as viewed through these optics, is correlated with the control image.

The vidissector tube consists of an electron imaging section and an electron multiplier stage. Photoelectrons are released from the vidissector photo cathode when the intensity transmittance variations of the electron cloud thus produced is preserved by a magnetic focusing field. The electron image is accelerated to an electric field where it impinges on a field stop containing a small aperture in the center Only electrons passing through the aperture can reach the electron multiplier dynode chain which follows. The image is scanned over the aperture in raster fashion by magnetic deflection coils. The size of the aperture, as well as its shape, determine the spatial resolution that can be achieved The electron optics limiting resolution is usually upwards of 80 to 100 lp/mm The image dissector selected for the system is the

ITT type F4011, which is a 1.5 inch-diameter, magnetically focused and deflected tube with a usable photocathode diameter of 28 millimeters Photo-cathodes of the S-1, S-11, and S-20 type can be provided, along with various aperture shapes and sizes.

For the image analysis system, both the S-11, and S-20 surfaces would be satisfactory. The S-20 surface is more efficient, but, the maximum permissible illumination with it is approximately 8 foot-candles, at which level phosphor loading becomes excessive. The S-11 surface, on the other hand, can withstand a maximum illumination of about 60 foot-candles, and it has therefore been selected for use in the image analysis system.

The aperture size is chosen to be consistent with the maximum required resolution, and signal to noise ratios

The resolution of the RBV image is expected to be about 4-5 cycles/mm. at 50 percent response. Thus, a scanning aperture in the image dissector of not less than 0.005 inches would appear to be indicated. The video signal noise ratio is a function of aperture size, bandwidth and illumination. An aperture of 0 005 inches will provide a signal to noise ratio of better than 10:1 with illumination levels available.

Scanning Pattern Stability

Any error in the position of the scanning patterns on the input and control images relative to the fiducial reference marks will be interpreted by the correlator as a parallax error. Several factors cause scanning pattern position errors.

External Magnetic Fields

In many environments strong magnetic fields are common. The electron image in the vidissector can be both distorted and displaced by ambient magnetic fields. To avoid this source of error, double magnetic shielding is employed around the vidissector tubes. Measurements show that these shields eliminate effects of all magnetic fields likely to be encountered in practice.

Internal Magnetic Fields

No amount of shielding will eliminate the effect of fields originating within the shielded space. In fact, the shield could easily worsen the situation To eliminate this problem, it is necessary to exclude all magnetic materials from within the shield. The deflection yolk cannot be excluded, and to keep a field from building up, a degaussing circuit is incorporated in the design. This circuit operates automatically each time the machine is turned on, and, if desired, can also be operated by pushbutton.

Deflection System Variations

The electrical circuits controlling positioning of the raster have been designed to give a stability of better than 0. 1 percent to prevent unwanted drift.

Correlation Accuracy

Past experience with other similar correlation systems indicate that x-y displacement error can be detected down to a level of about 0. 1 percent - 0. 3 percent of the width of the area scanned, provided that there is sufficient detail in the images to correlate. Thus a raster scan of 10-30 mm. is indicated for an accuracy of ±30 micrometers. The F 4011 image dissector can provide a raster scan of 25 millimeter maximum, however in areas of good image detail it is preferable to use a smaller raster so that measurements of distortion are more accurate. With electronic zoom, the size of the raster can be made to adapt to the amount of detail in the image to give optimum performance.

2 4.4.4 Image Correlation System Configuration

The image correlation system has three main subassemblies; the electronic chassis and the two vidisector packages. In Figure 2.4-4 each block refers to a functionally identifiable portion of the system. As optical inputs the image correlation system receives two similar images focused on the photocathode of the two vidissectors. As electrical inputs, the system receives standard 115V ±10 percent single phase 60 Hz power of 100 watts and a logic type control signal commanding the correlation

to be inhibited or enabled.   The electrical outputs of the system are a logic type signal indicating acceptable correlation quality and the error signals for X position, Y position, rotation, and magnification.

To provide error signals that are essentially independent of image quality, high speed adaptive correction loops are needed to apply scanning raster corrections such that the images appear to be registered to the electronic system.

Thus, the error signals are derived from the amount of correction applied to the rasters.

Referring again to Figure 2.4-8, we see that each image is scanned in a continuous fashion by means of triangular waveforms imposed on the image dissector deflection circuitry.   Video signals developed from the scanning process are amplified in the video amplifier.   To provide a relatively constant video signal output from wide variations in image density and contrast, dynode regulation is used on the photomultiplier section of the image dissector to normalize the dc component of the video output, and fast automatic gain control is applied to the video amplifier to normalize the high frequency signal obtained by scanning the image detail.

The two normalized video signals from the left and right images are multiplied in the video correlator circuitry contained in the electronics chassis.   To give both wide pull-in range for the system and high accuracy of registration, three parallel correlator bands are provided The correlator provides two outputs for further analysis.   One output, called the orthogonal correlation (OC) signal, is proportional to the instantaneous time displacement of the two video signals.   Thus, this output will be zero under conditions of perfect image registration.   The other output signal, called the normal correlation or cross correlation (CC) function, is proportional to the degree of total image registration, and thus will be maximum when the two images are in registration.

The two correlation signals from each correlator band are introduced to the channel selection logic and channel selector circuitry, which automatically selects the optimum correlator band output for further |processing.   The selection criteria used ensure that the low band information will be used for initial pull-in, after which the higher bands will be
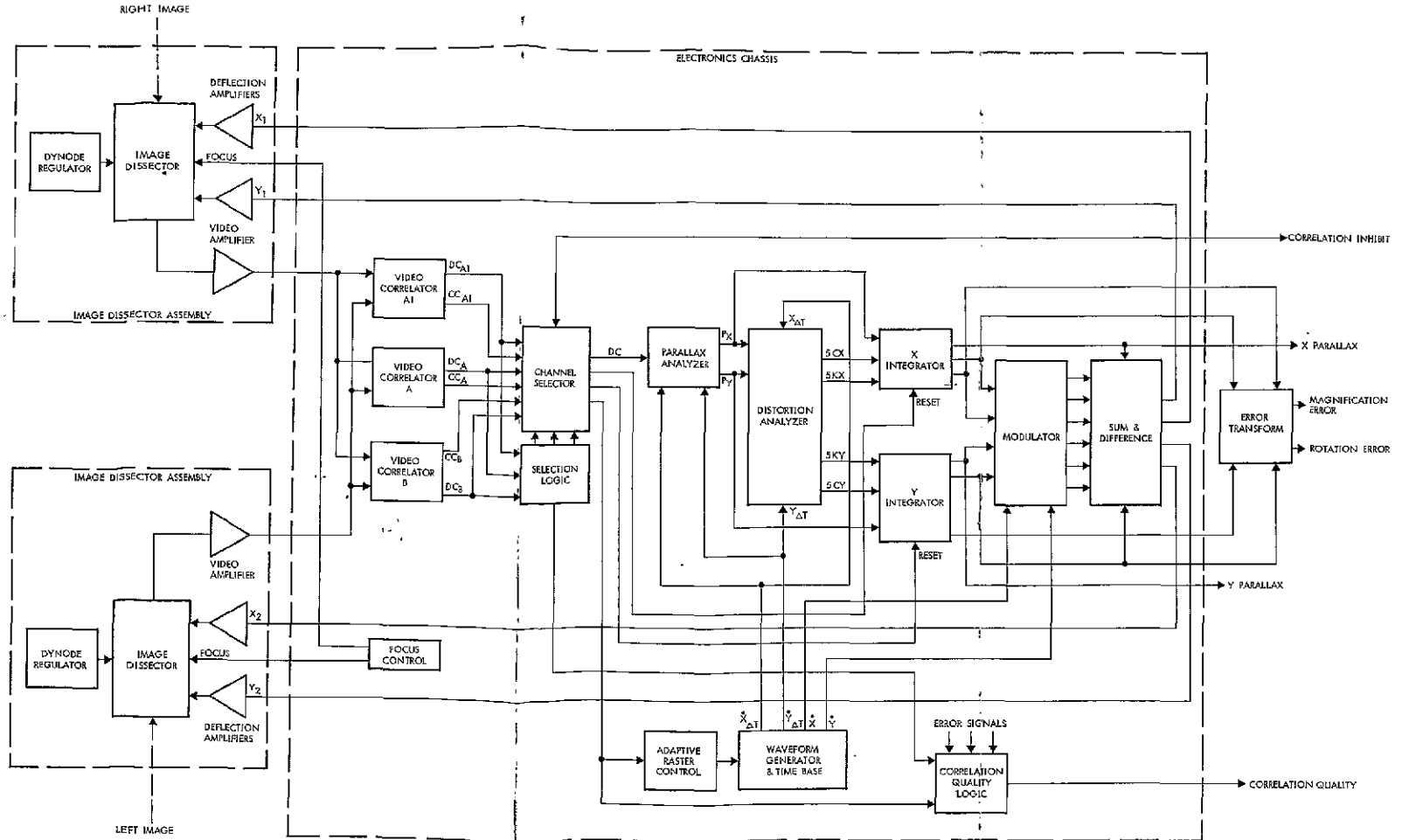
2-129

Figure 2.4-8
SYSTEM BLOCK DIAGRAM

2-131

progressively switched in for greater accuracy. Also, the low band information is switched out if sufficient information is available in the high band.

The channel selector and channel selector logic also contains additional circuitry that preprocesses the CC and OC signals for use in the adaptive raster control and the correlation quality logic.

The orthogonal correlation signals selected by the channel selector must be further processed to obtain the parallax, rotation and skew error signals. Parallax errors are developed by multiplying the OC error signal with the X and Y velocity scanning reference in the parallax analyzer to obtain the error signals, $P_x P_y$. These parallax error signals are further processed in the distortion analyzer circuit to obtain the scale and skew error signals, sc_x, sc_y, sk_x, and sk_y by multiplying with the X and Y position scan reference signal.

The X and Y parallax, scale and skew error signals are each fed to an integrator circuit that develops an output voltage proportional to the amount of correction applied to the rasters to obtain optimum correlation. If correlation quality is low or if the correlation system is not calling for automatic correction, initial conditions are established at the integrators by resetting. The error signals from the integrators are fed to the command and control system for distribution as required.

The integrator outputs are also used to provide correction to the scanning raster, in equal and opposite amounts, to achieve optimum correlation. The parallax error signals are fed to the vidissector deflection amplifier to cause appropriate X and Y position corrections. The X and Y rotation and magnification error signals are used to modulate the basic scan reference waveforms with the desired amounts of ΔX and ΔY signals to produce the desired raster distortion. The sum and difference circuit provides a composite deflection waveform, containing the desired component of distortion correction, which is the integrated to produce the triangular scanning waveform for the deflection amplifier.

The adaptive raster control utilizes the parallax errors, the orthogonal correlation signals, and the cross correlation signal to determine

an optimum raster size for good performance. The scan reference wave-forms from the time base are modulated by the raster size to maintain the error calibration constant with changes of raster size.

The time base provides appropriately synchronized square wave reference signals for system operation.

The correlation quality logic examines levels of the preprocessed CC and OC signals from the channel selector and channel selector logic as well as the X and Y position, rotation, and magnification signals to determine if the quality of the correlation is satisfactory.

As the photoprinting system does not handle X and Y rotation and magnification the X and Y signals are averaged in the sum board to provide singular rotation and magnification outputs to the command and control system.

The power supplies used for critical circuitry provide dual tracking outputs with good regulation to reduce the effects of supply variation on system accuracy. The high voltage supply and noncritical regulated supplies are powered from an unregulated +24 volt supply. Line filters are provided to reduce the effects of transients and high frequency interference on the power line.

Each of the vidissector subassemblies contain the vidissector tube, its focusing and deflection coils, a dynode regulator, a video amplifier, two deflection amplifiers, and magnetic shielding. The electronic chassis is a rack mounted slide out drawer containing the correlation system power supplies and electronic on plug in printed circuit cards.

Summary of Correlation System Performance

- Scanning System.

    F4011 Image Disector (ITT) with S11 photocathode

    Aperture: 0 005 inch

    Scanning raster: Dual-diagonal diamond with 31 line resolution

    Electronic Zoom: 4:1

    Frame rate: 560 Hz.

● Correlation Outputs:

Translation error: nominal pull-in range,   4 mm

Accuracy: 30 micrometers

Magnification error: Pull-in range,   5%

Accuracy,   .3%

Rotation error: Pull-in range,   2 degrees

Accuracy,   0.1 degree

Correlation Quality signal: Signal shall be high when the
correlator can pull-in and obtain useful error signals. A
low level will indicate correlation failure.

2.4 4 5 Computer Interface

The primary mode of operation for the precision photo restitutor is
one in which the optical elements are driven in an appropriate manner to
remove distortion from the imagery according to a pre-computed trans-
formation array which has been generated from reseau measurement
data, spacecraft attitude and calibration data. Before such transforma-
tions can be accurately applied to the input images in the PPR, it is
necessary to modify the frame of reference of these transformations to
the PPR machine reference. There, the position of each image must be
determined at the PPR, by measuring the location of the frame fiducial
marks, before optical transformation can be applied. Since the transfor-
mation array must be adjusted, a small amount of computing must be
done before each frame can be printed. This requirement means that
the PPR cannot be operated completely off-line unless a small computer
capability is added to the PPR system. The obvious advantages of a com-
pletely off-line PPR system must be weighed against the duplication of
computer power and the loss of flexibility which would be imposed in an
off-line situation. For these reasons, we have chosen to drive the PPR
machines on-line with the central computer

A second mode of operation for the PPR system requiring com-
puter interaction is one in which the correlator provides error signals

which are proportional to the relative distortion between an MSS input image and an RBV control image, as the scanning table is moved through the nine segments. During this mode, the optical elements are driven by the correlator to maximize the degree of correlation, and the position of these elements are read into the computer, as a function of scanning table position. Thus a map of zero and first order distortion is built up to give an accurate measure of the distortion errors. This error array may then be used to update the transformations required to correct all images of the MSS set, in the precision mode.

2.4.4.6 Computation and Control Requirements

In the computer controlled mode, the PPR first will read the position of three (or four) frame fiducial marks, enter the data into the central computer, and then print out the image under computer control.

The programs required for PPR operation are summarized below:

● Initialization

The computer receives the PPR frame fiducial positions, and transforms the nine 4 x 147 correction arrays to PPR coordinates by adjusting all x, y and θ values.

● Correction Array Calculation

Data from reseau measurement, spacecraft attitude, sensor calibration, ground truth and other sources are used in the computation of a set of nine 4 x 147 matrices which provide the PPR with optical element settings for correction of an entire image. In addition, instructions for control of scanning table position are provided at the beginning of each printing strip. The data rate for optical element settings of x, y, m, θ will be 800 bits/sec.

● Annotation Control

After an image has been printed, instructions will be provided to the PPR which will initiate tick mark and tick mark label printing, and data block printing. Instructions will include:

a) Y table position for tick mark exposure

b) X table position for tick mark exposure.

c) Tick mark label data.

d) Annotation table position.

e) Alphanumeric annotation data.

2.4.4.7 PPR Process Controller

The PPR process controller (PC) provides two functions necessary for PPR operation. The PC is the interface between the parallel data adapter (PDA) and the hardware of the PPR. It monitors signals from the PDA and controls lines to the PDA that determine when it is possible to pass data across the interface and when data is actually passed across the interface. The PC provides a decoding of the 48 bit data word from the input register into the various servo commands and process control commands arriving from the computer system. It also provides the routing of the servo position data and other data into a single 48 bit word to be read by the computer system.

Secondly, the PC controls the sequence and timing of all events that take place in the PPR. It demands and outputs data in the correct sequence at the proper time, and initiates and monitors all the detailed actions necessary to complete the general process requested by the main computer.

Process-Controller/Parallel-Data-Adapter

The parallel data adapter is the interface between the process controller and the computer system. It allows parallel transfer of a 48-bit data word across the interface in either direction. In addition to the input and output 48 line data buses, six lines will be used to control the flow of information across the interface (see Figure 2.4-9). The PDA has four lines which are read by the PC and the PC outputs two lines to the PDA.

DETAILED INFORMATION
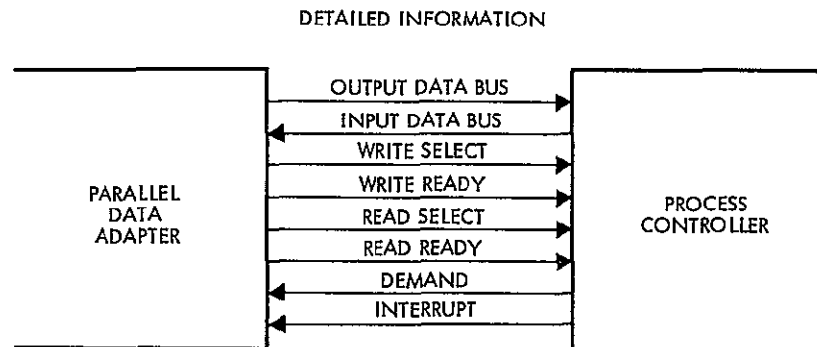
Figure 2.4-9
PPR/PC DATA FLOW

When data is read from the PC by the PDA, the PDA raises a read select line indicating to the PC that the PC output data bus will be read. When the PDA is ready to read the bus, it raises its ready line. When all the information is available in the PC output register, the PC raises the demand line to the PDA and the information is transferred. For a write operation the PDA raises the write select and write ready lines and the PC responds by raising the demand line. In addition, the PC outputs an interrupt line to the PDA to allow the PC to initiate action if necessary.

2.4.5 PPR System Performance Summary

The range of image geometry correction by the PPR is more than sufficient to match the distortion in the imagery of the various ERTS sensors caused by spacecraft attitude errors and sensor distortions.

In addition, the PPR has been designed as a high production rate processor for operation in a photographic laboratory environment, with minimum personnel attendance and maintenance requirements.

The specific performance features of the PPR are described in the following paragraphs.

2.4.5.1 Differential Correction of Input-Image Geometry

The capacity of the PPR for providing differential correction of input image geometry by correlation with a reference image, or absolute correction to ground truth meets or exceeds specified requirements. The precision with which corrections are made has been determined by an error analysis of the proposed PPR design. The individual contributors to the total error include:

- Setting accuracy in x-y position of both input and output relative to printing slit of 20μ RMS over 8-inch x 8-inch format.

- Differential image displacement in both x and y of up to ± 11mm with setting precision of 10μ rms.

- Differential magnification range of 0.95 to 1.05 ± 0.2 percent about nominal magnification of 1.0.

- Differential image rotation of ± 2 degrees with setting precision of ± 0.1 degree rms.

- RMS correlation accuracy at center of printing slit-bulk process mode: $\pm 60\mu$. Precision process mode: $\pm 30\mu$.

This error analysis leads to the following performance when used in a computer controlled mode, assuming no external errors.

Residual error, with 0.05 x 0.8 inch slit: ±182 ft

with 0.05 x 0.4 inch slit: ±130 ft

In a correlation mode, assuming no residual error in control image, the following performance is predicted:

Residual error, with 0.05 x 0.8 inch slit: ±260 ft

with 0.05 x 0.4 inch slit: ±145 ft

Correlation of input photo to reference photo can be continuous during the output printing process using a 0.050 inch by 0.8 inch slit in the bulk process mode and a 0.050 inch by 0.4 inch slit in the precision process mode.

2.4.5.2 Reproduction of Input Photographic-Image Quality

It is expected that the combined modulation transfer function (MTF) of ERTS sensors, telemetry, data processing, laser recorder and initial recording medium will limit intensity modulation of input photographic images to less than 1 percent relative response at 10 cycles/mm. The PPR is designed to preserve the modulation of input imagery at these spatial frequencies which are the highest in the imagery. Special attention has been given to the problem of preventing MTF reduction by scattered light in the printing optics.

Overall Image Quality

There will be no variation in specified image quality over the entire image format. The PPR will add no cumulative distortions or aberrations to the output image of magnitude greater than the precision limits of corrective elements and correlator as specified above.

Static Performance

Since the input photography is not likely to have modulation beyond 10 lp/mm the PPR system MTF will be measured and specified at 10 lp/mm. The PPR system MTF is expected to equal or exceed 75 percent relative response at 10 lp/mm.

Dynamic Performance

The PPR system MTF will be degraded from the specified static performance value during dynamic correction of input photo-geometric errors. The degree of degradation is approximately proportional to the degree of image correction required. Estimates have been made for system MTF during dynamic correction of worst case spacecraft attitude and sensor distortion mismatch as indicated in the study. Expected system MTF during worst case geometry corrections are:

Bulk Process Mode (0.05 x 0.8 inch slit):   50 percent system
                                              relative response
                                              at 10 lp/mm

Precision Process Mode (0.05 x 0.4 inch slit): 70 percent system
                                               relative response
                                               at 10 lp/mm

Photographic Uniformity

In addition to faithfully reproducing the input imagery the PPR will not add detectable beauty defects to the output film image due to variations in exposure (banding) multiple exposure (stripping) and distortion.

Banding - Periodic variations in image density along the direction of slit scan will have peak-to-peak amplitude of less than 0.02 in density.

Stripping - There will be no detectable stripping due to overlap or underlap of adjacent scan strips.

Processing Efficiency - The PPR will process input photography on continuous film rolls at the following rates depending on the process mode.

Bulk Process Mode - 2.5 minutes or less per output frame.

Precision Process Mode - Four minutes or less per output frame.

Additive Color - Three minutes or less per output frame per input color overlay.

The rates indicated above include time allowances for printing of all geographic tick marks, registration fiducials and data block with 5 second allowance for film frame advance.

Additive Color Printing

Provision is made in the PPR for additive color printing of multispectral inputs using EK color reversal film. Overlay registration accuracy of ±30 micrometers rms will be maintained. Up to five false color bands may be printed on a single color output frame.

2.4.6 Correlation Techniques

Correlation techniques can be used to detect the relative misregistration between two images containing approximately the same scene information. Thus, for example, a pair of photographs which are taken with a certain base separation, can yield height data when measured in suitable stereo photogrammetric equipment. If this equipment contains a correlation system, the height data can be obtained automatically, by correlating similar areas within the overlap region of the photographs.

In order to obtain accurate terrain height data, the correlation system is generally required to detect zero order (parallax) distortions, first order (scale, skew) distortions and possibly higher order distortions.

Correlation techniques can be applied advantageously to the detection of distortion errors in the RBV and MSS imagery. If, for example, a geometrically correct RBV image is produced, then correlation techniques will provide a measure of relative distortion between the master image and an image of the same area taken either from a second RBV sensor or from the MSS sensor. The outputs from the correlator can be used directly to drive optical correction elements, to remove distortion, or the errors may be analyzed by computer to arrive at an optimum transformation which then can be applied in the digital processing mode.

The ITEK EC-5 electronic correlator which is shown schematically in Figure 2.4-10 consists of two main sections:

- A flying spot scanning system mounted on the Planimat

- An electronics rack that can be located up to 15 feet from the Planimat

The scanning system comprises two cathode ray tubes which are integrated with the left and right viewing paths on the Planimat. The scanning patterns produced by these tubes are imaged on to the left and

VIDEO CORRELATOR
AND
DISTORTION ANALYZER

PHOTO
MULTIPLIER
TUBE

PHOTO
MULTIPLIER
TUBE

LEFT
DIAPOSITIVE

RIGHT
DIAPOSITIVE

X
PAR

Y
PAR

ADAPTIVE
CONTROL
CIRCUITS

Z
MOTOR

PHOTO
MULTIPLIER
TUBE

PHOTO
MULTIPLIER
TUBE

SCANNING
PATTERN
GENERATOR

CATHODE
RAY
TUBE

CATHODE
RAY
TUBE

Y
MOTOR

X AND Y
DEFLECTION

ANTI
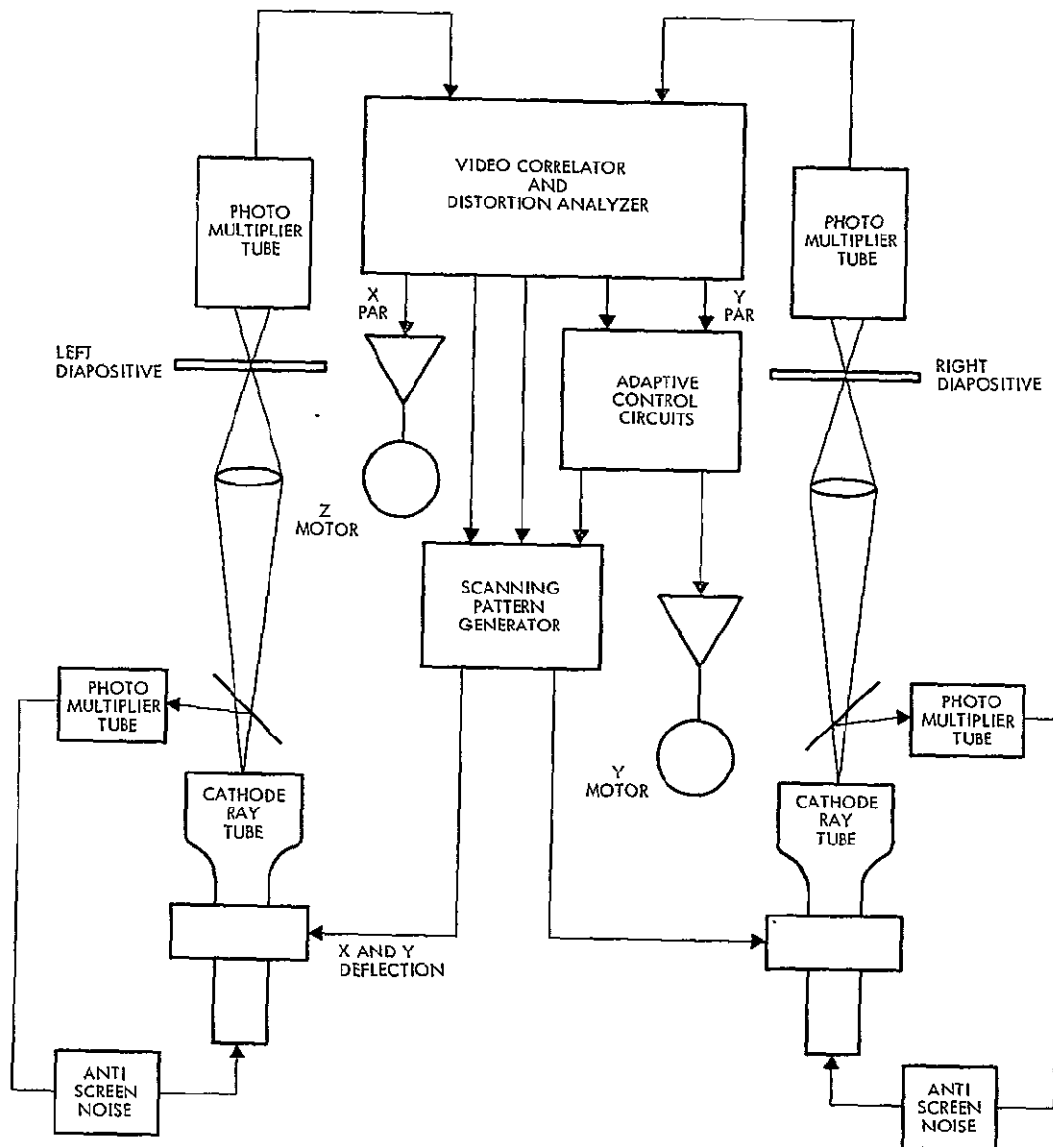SCREEN
NOISE

ANTI
SCREEN
NOISE

Figure 2.4-10

SCHEMATIC DIAGRAM of the ITEK electronic circuit

right diapositives, and the transmitted light, modulated by the images, is converted into electrical signals by two photomultiplier tubes. The two diapositives can be viewed continuously as a stereo pair through the eyepieces, using the normal Planimat optical system. Dichroic mirrors are used to separate the blue cathode ray tube scanning light from the yellow viewing light. The use of this system does not preclude the use of color material, although the blue end of the spectrum is lost. In order to maximize the stability of the system, an optical demagnification of 10 is provided between the CRT scanning pattern and the photographic plates. Alignment errors or disturbances in the scanning pattern are thereby reduced by a factor of 10.

The two video signals from the photomultiplier tubes are fed into the electronics rack. Here the signals are correlated and analyzed into the zero-order and first-order error coefficients: x-parallax, y-parallax, x-scale, y-scale, x-skew and y-skew.

The x-parallax signal, corresponding to the heighting error, is applied to a servo system which drives the motor controlling the height of the z-carriage in the Planimat, thereby correcting the x-parallax. The presence of terrain slopes causes x-scale and x-skew distortions to be present. These distortions must be removed to maintain good correlation between images, and are corrected in the present system by changing the shape of the scanning rasters by means of feedback to the scanning system. Figure 2.4-11 shows the scanning pattern and the method of correcting distortion.

2.4.6.1 Scanning Pattern

To provide uniform scanning over conjugate image areas, a Lissajous scanning pattern is used. This pattern is normally produced by two triangular waveforms for x- and y-deflection, which differ in frequency by the required frame frequency. It is necessary for the frame frequency to be substantially higher than the bandwidth of the correlation servo loop to enable frame frequency components to be filtered out. Furthermore, the number of scanning lines does not need to be large in order to detect zero and first-order distortion. In the present case, a scanning pattern with 31 lines across the diagonal is used, the frame frequency being 560 Hz.
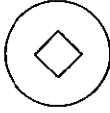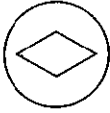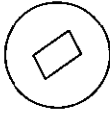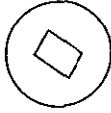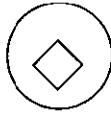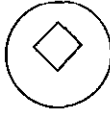
CONDITION	LEFT SCANNING TUBE	RIGHT SCANNING TUBE
NORMAL (NO DISTORTION)		
X-SCALE TRANSFORMATION CORRECTING DISTORTION DUE TO X-SLOPE		
X-SKEW TRANSFORMATION CORRECTING DISTORTION DUE TO Y-SLOPE		
Y-PARALLAX TRANSFORMATION CORRECTING MISALIGNMENT IN Y		

Figure 2.4-11

SCANNING PATTERN AND METHOD
of correcting image distortion

Some advantages can be gained by orientating the scanning pattern in the form of a diamond as shown in Figure 2.4-12. This pattern can be generated by merely rotating the deflection system through 45 degrees, or
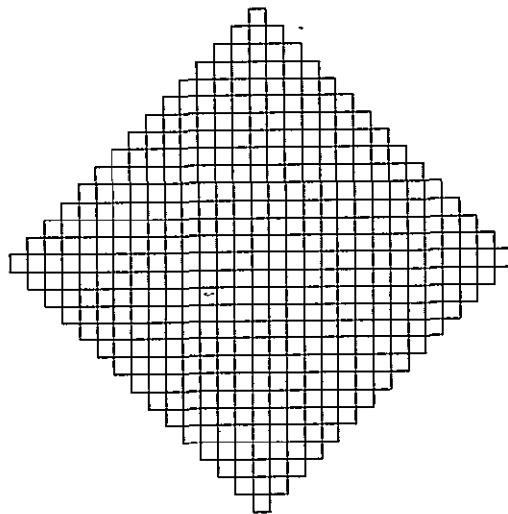
Figure 2.4-12

DIAMOND SCANNING PATTERN

by maintaining alignment of the deflection coils with the x- and y-axes and using a more complex scanning waveform. The diamond pattern has the advantage that the scanning spot always moves in either the x- or y-direction, enabling the quality of correlation in these directions to be evaluated separately. Separate monitoring of x- and y-correlation quality allows image areas of poor correlation to be covered with greater reliability.

2.4.6.2 Correlation

The video signals from the photomultipliers are fed through video amplifiers to the correlator where they are split into several frequency bands, the purpose of which is to allow the low spatial frequencies to be correlated first, progressing to higher frequencies as the accuracy of alignment is improved. The correlation process consists of multiplying the two inputs in a balanced, linear, four-quadrant multiplier. Two outputs are produced from the correlator as shown in Figure 2.4-13. One output consists of the normal correlation function which peaks at the point
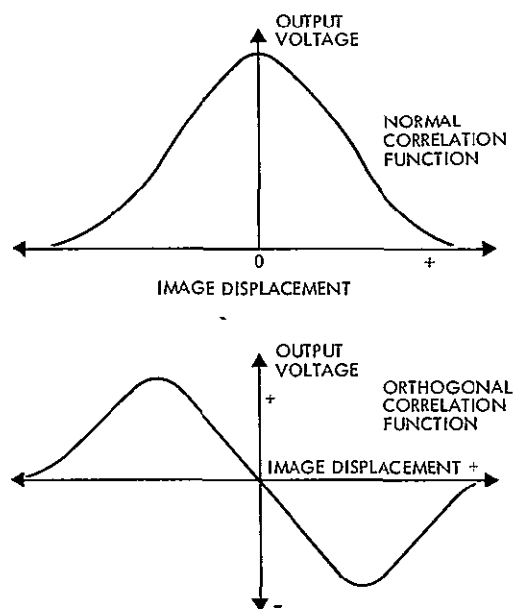
Figure 2.4-13
NORMAL AND ORTHOGONAL CORRELATION FUNCTIONS

of maximum correlation. This output is used as an indication of correlation quality. The second output is obtained by phase-shifting the signals before multiplication, resulting in the orthogonal correlation function which passes through zero with a change of polarity at the point of maximum correlation. This output contains the desired information on the magnitude and direction of image displacements between the scanned images.

The multiband correlator provides both wide-range pull-in and high accuracy; an electronic channel selector is used to select the optimum channel, depending on the degree of correlation between the two images. The correlator outputs are then analyzed to determine the magnitudes of each of the various distortion components. A schematic diagram of the correlator and analyzer is shown in Figure 2.4-14.
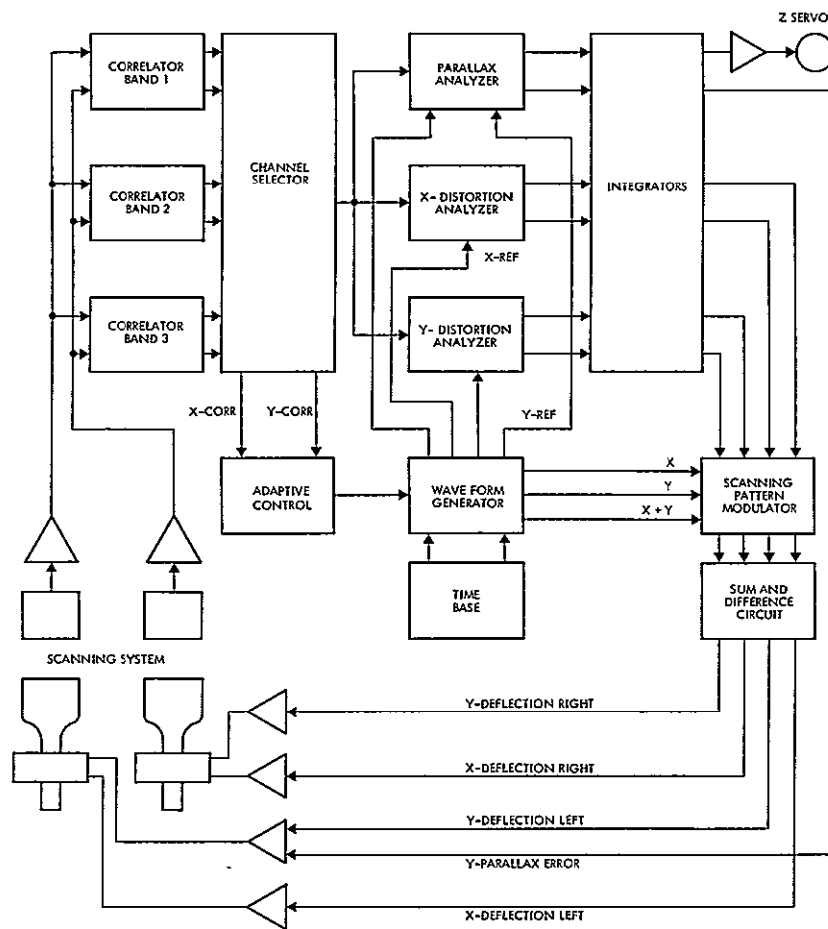
Figure 2.4-14

SCHEMATIC DIAGRAM of the multiband correlator and distortion analyzer

2.4.6.3 Distortion Analysis

The orthogonal correlator outputs are combined and multiplied by x- and y-reference waveforms whose instantaneous amplitudes specify the directions of the scanning spot at any instant. The integrated outputs of these multipliers represent the average x- and y-parallaxes between the two inputs.

The x-scale, x-skew, y-scale and y-skew distortion analyzers use multiplier circuits similar to the parallax analyzers. In this case, however, the reference signals are integrated x- and y-waveforms.

The two zero-order and the four first-order error signals are fed to x- and y-integrators, in order to provide sufficient gain for closed loop corrections. The integrators also incorporate a hold mode where error signals can be stored for a short time in the event a loss of either x- or y-information occurs.

The x-parallax error signal is applied to the z-servo on the stereo plotter. The y-parallax error signal, on the other hand, is applied directly to the y-deflection amplifier of one cathode ray tube to provide electronic correction of y-parallax.

The first-order error signals from the integrators are applied to the modulator to cause appropriate transformations to the scanning raster waveform. The modified scanning waveforms are added algebraically in the sum and difference circuit to provide equal but opposite transformations to the left and right rasters.

2.4.6.4 Adaptive Controls

The main adaptive controls are the channel selector, which controls the correlator frequency bands in use, the scanning pattern size control, the profiling speed or y-velocity, x-axis transformation loop gain, and the y-axis transformation loop gain.

Correlation is initially established using image detail of low spatial frequency to secure a good pull-in capability, progressing to higher spatial frequencies to obtain higher accuracy. The size of the scanning pattern is similarly reduced as correlation quality improves, and the profiling speed is increased.

A sudden drop in correlation quality produces a rapid shift to correlation of lower spatial frequencies, to a larger scanning pattern and to a lower scanning rate. In extreme cases the y-servo will cause the machine to stop profiling, or even to back up, while correlation is restored. A unique feature of the correlation system is that while the scanning pattern is completely amorphous in its ability to detect image displacements, the quality of correlation can be monitored separately in the x- and y-directions. Loss of correlation in either axis separately does not produce failure, but merely results in the relevant transformations being held at their existing values until correlation in that axis is reestablished.

Simultaneous loss of correlation on both axes, such as might be encountered when entering a body of water, results in conditional failure in which the size of the scanning patterns are maximized and the instrument is driven at a fixed rate until correlation is reestablished, or until a specified distance has been covered.

2.4.7 Correlation Techniques Analysis

As indicated in the preceding sections, correlation techniques play a central role in optical processing. The next sections outline the theory of the correlation methods, and describe a number of devices which operate on this theory.

2.4.7.1 Image Correlation Theory

The correlation process is the basic element in the automation of photogrammetric equipment. In broad terms, correlation means comparison. Many methods exist for comparing images by machine. These have been referred to as correlation methods, but only one technically correct method for correlation exists. This method is based on the mathematical relationship expressed by the cross correlation function. Expressed mathematically, the cross correlation function is

$$R(\tau) = \frac{1}{2T} \int_{-T}^{T} A(t)B(t + \tau)\, dt$$

where $A(t)$ and $B(t + \tau)$ are the two functions that represent the video

signals derived by scanning the two separate images, and τ is the relative displacement between the images. Therefore, $R(\tau)$ is a function of the displacement of the images. As the two images are brought into best agreement, $R(\tau)$ assumes a maximum value. The plot of $R(\tau)$ versus τ, as τ assumes values negative through zero to some positive value, results in a curve whose maximum occurs at the point of best agreement. At this point the rate of change of $R(\tau)$ with respect to τ becomes zero.

In practical correlators used to control and automate photogrammetric equipment, the derivative of the cross function is used to develop the control signals that are used to register the two images. A discriminator action is required that results in the output voltage passing through zero at registration, with positive voltages for positive errors and negative voltages for negative errors in image placement. Since the derivative $dR(\tau)/d\tau$ is related to the physical displacement between the images, it is difficult to obtain a signal that passes through zero at the point of best correlation over a large bandwidth as a function of τ. This problem may be solved in several ways. In one solution, delay lines are used to provide a fixed amount of electrical delay between the images, the algebraic difference between the delayed and the undelayed image becoming equal to zero at the point of best correlation. The maximum accuracy of the zero crossing occurs at the frequency whose delay is 90 degrees relative to the undelayed channel. In another method, the frequencies comprising the video signal are shifted by +45 degrees in one video channel and by -45 degrees in the other video channel to produce a 90-degree difference before they are multiplied and integrated. These, and other similar approaches, are band limited in frequency response because of the difficulty of maintaining the 90-degree difference in phase over wide bands of frequencies. This is overcome by using two or more band limited correlation channels in parallel, the midfrequency of each being centered in a different part of the video spectrum. The outputs of all correlation channels are added together, possibly through weighting networks, to produce error signals to control the automation.

The evaluation of the correlation is an automated photogrammetric machine is directed toward obtaining information about the accuracy of

lock-in or registration of the two images. This is the function of several parameters, including the bandwidth and the highest frequency passed by the correlation channel. The pull-in range of the correlator is defined as the greatest distance between the two images over which the electronic circuitry will detect correlation and automatically drive the images into registration. The pull-in range is largely dependent on the lowest frequencies in the passband of the correlator.

In devising a test plan for the analysis of the dynamic performance of the correlator, those factors that increase the pull-in range and the accuracy of lock-in or registration and those factors that cause the correlator to misbehave (lose lock, jitter, or hunt) must be considered. It must be determined whether performance is the result of the structure of the images, or if some anomaly exists in the correlator circuitry.

When a roll of test film is used with indicated points of reference and the cross correlation function that results from a single error such as x parallax is known, the action of an ideal correlator on this form of error can be predicted. The performance of the practical correlator can be compared to the predicted performance to arrive at a figure of merit for the predicted performance. In concept, the ideal correlator is a device that is not frequency band limited and produces a constant 90-degree phase difference for all frequencies in the two video signals over this unlimited bandwidth. The ideal correlator output is zero when the point of best registration is reached for all frequencies.

A real correlator, capable of controlling a servosystem, is not ideal. Since a correlator must necessarily be bandwidth limited within each channel to preserve a reasonable 90-degree phase difference and must be paralleled with responses in separate parts of the spectrum, there is a possibility of anomaly in the position of the zero crossing of the discriminator action for particular parts of the spectrum. Certain combinations of the spectral content of the images and the spectral characteristics of the correlation channel may also cause errors that result in poor system performance.

Correlator Performance

The main performance factors of the correlator and distortion analyzer are the pull-in range and the rms accuracy of alignment.

The pull-in range governs the accuracy with which the two images must be aligned before the automatic correlation system can take over and maintain alignment. A correlator with good pull-in range is also less likely to lose correlation. The pull-in range, p, is determined by the ratio of the line scan frequency, f_s, to the correlation center band frequency, f_c, and is given by

$$p = \frac{f_s}{2f_c}$$

In practice, a pull-in range of ±10 percent of the diameter of the viewed image is easily obtained, and ±20 percent has been achieved by suitable design. The lower the correlator center band frequency, the larger the pull-in range.

The rms accuracy of alignment, δ , depends on the pull-in range and on the peak signal to rms noise ratio of the correlator output signal, N. The rms alignment accuracy is given by

$$\delta = \frac{p}{N} = \frac{f_s}{2Nf_c}$$

For a given correlator signal to noise ratio, the accuracy decreases as the pull-in range increases. The requirements for good accuracy conflict with those for good pull-in range. The problem can be resolved by using several correlator frequency bands, starting at a low frequency to obtain good pull-in range and moving to higher frequencies as correlation accuracy increases. A three-band correlation system with automatic switching in which the center frequencies are in the ratio of 3.2:1 has recently been developed at Itek. If this technique is used, a pull-in range of ±10 percent and an rms accuracy of 0.1 percent of the correlated image diameter can be achieved with images containing sufficient detail.

The video signal to noise ratio expected from the image dissector output can be found from

$$i^2_{nk} = 2eI_k \Delta f$$

where

i_{nk} = rms noise current entering aperture

e = electronic charge = 1.6×10^{-19} coulomb

I_k = dc current entering aperture

Δf = bandwidth

The rms anode noise current is given by

$$i_{na} = \mu i_{nk} \left(\frac{\sigma}{\sigma - 1} \right)^{1/2}$$

where

μ = current amplification

σ = effective gain per stage of electron multiplier

Thus

$$i^2_{na} = \mu^2 i^2_{nk} \left(\frac{\sigma}{\sigma - 1} \right)$$

The dc anode current, I_a, is given by

$$I_a = \mu I_k$$

Therefore, substitution yields

$$i^2_{na} = 2e\mu I_a \Delta f \left(\frac{\sigma}{\sigma - 1} \right)$$

If dark current sources are neglected, the peak to peak signal current, I_s, is given by

$$I_s = 2MI_a$$

where M = modulation, given by

$$M = \frac{(c - 1)}{(c + 1)}$$

where c is the photographic contrast ratio.

Thus, the video signal to noise ratio is given by

$$S/N \frac{pp\ signal}{rms\ noise} = \frac{2MI_a}{\{2e\mu I_a \Delta f[\sigma/(\sigma - 1)]\}^{1/2}}$$

or

$$S/N = 2M\left[\frac{I_k}{2e\Delta f}\left(\frac{\sigma - 1}{\sigma}\right)\right]^{1/2}$$

For

$$I_k = J_k\left(\frac{a}{m}\right)$$

where

J_k = dc cathode current density, amperes per square centimeter

a = aperture area, square centimeters

m = linear magnification, cathode to defining aperture

we have

$$S/N = 2M\left[\frac{J_k a}{2e\Delta f m^2}\left(\frac{\sigma - 1}{\sigma}\right)\right]^{1/2}$$

If photograph density = 2, contrast ratio = 2:1 (density difference = 0.3), $M = 0.33$, aperture = 0.005 inch, $\Delta_f = 200$ khz, $\sigma = 2.6$, and $m = 1$, then J_k at a 20-foot-candle open gate is given, in amperes per square centimeter, by

$$J_k = \frac{I_s}{929} \left[\frac{20}{100}\left(\frac{50 \times 10^{-6}}{929}\right)\right] = 1.07 \times 10^{-8}$$

and

$$S/N = 0.66 \left(\frac{1 \times 10^{-8} \times 1.3 \times 10^{-3} \times 1.6}{2 \times 1.6 + 10^{-19} \times 5 \times 10^5 \times 2.6}\right)^{1/2} = 4.3$$

At a density of 3, with the same modulation, the signal to noise ratio will be reduced by $\sqrt{10}$ to a value of 1.5.

The error signal to noise ratio will be given approximately by

$$\frac{(S/N)_e}{(S/N)_v} = \left(\frac{\beta_v}{\beta_e}\right)^{1/2}$$

where β_v and β_e are the video bandwidth and error signal bandwidths. If the error signal bandwidth is equal to half the digital to analog sampling interval, then

$$\frac{(S/N)_e}{(S/N)_v} = \left(\frac{2 \times 10^5}{60}\right)^{1/2} = 55$$

This implies that a video signal to noise ratio of less than 1 will provide adequate error signal to noise ratios.

2.4.7.2 Existing Photogrammetric Instrumentation

It is a basic operation in present day map-making to produce photographs with no geometric distortions. Several instruments have been designed to produce orthophotographs, i.e., aerial photographs with the

parallax displacements produced by a central perspective point (the camera lens) removed, so that the photograph may be used in place of a map.

Restitution is the process of correcting the image displacements produced by variations in terrain height. There are two stages in the production of an orthophotograph: (1) determining the image displacements, on terrain height, at each point and (2) reprinting the original photograph with the appropriate corrections to the position of the imagery. In some instruments, the printing may be done simultaneously with height determination, on-line operation, whereas in other instruments two separate operations are involved.

In map compilation, height is determined by stereo plotting, which is the process of reconstructing the terrain height in the stereoscopic model from measurements made on stereoscopic pairs of aerial photographs. This operation is based on analog computation in which the camera system geometry is physically reproduced in the plotting instrument, or is reproduced by analytical plotting in which the reconstruction process is entirely mathematical.

Both types of plotting instruments may be automated by means of image correlation. Examples of this type of equipment are the B8-Stereomat (Autometrics Corporation), AS-11B/C (Bendix), Unamace (Bunker Ramo Corporation), and EC-5/Planimat (Itek Corporation). The image may be reprinted either electronically by means of a cathode-ray tube, or by optical projection, with appropriate corrections to the position of the image elements or graphs of elements. The quality of images produced by electronic printing is generally less than that which can be obtained by optical printing. Figures 2.4-15, 2.4-16 and 2.4-17 show orthophotographs produced by the Stereomat IV, the AS-11B/C, and the Unamace, respectively, which use electronic printing on a series of strips. Figure 2.4-18 shows an orthophotograph produced on the Zeiss GZ-1 from terrain height data produced by the EC-5 Planimat. The orthophotograph is printed in strips through a moving slit that uses an auxiliary lens system which satisfies the demand for truly sharp imagery
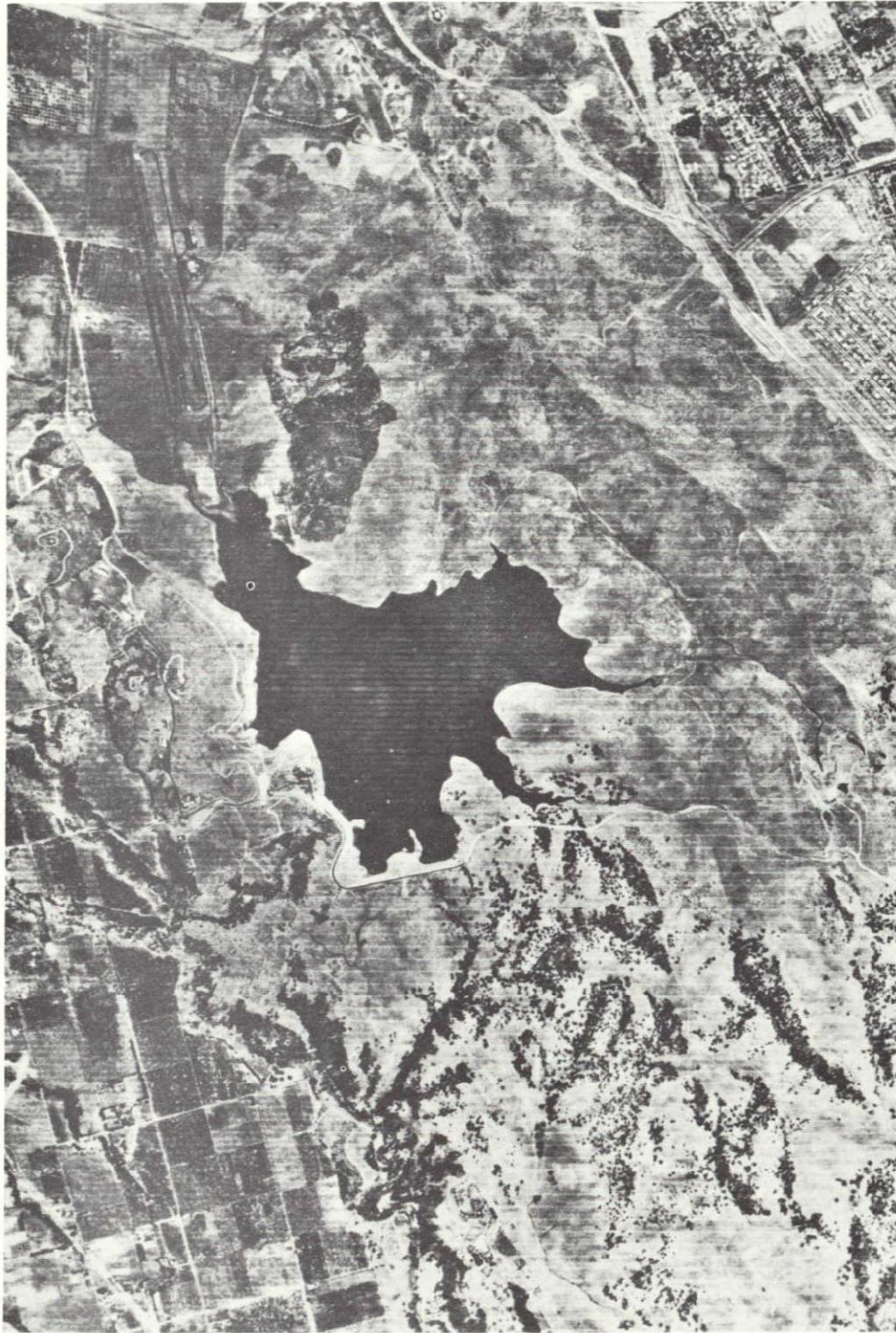
Figure 2.4-15

PORTION OF ORTHOPHOTOGRAPH OUTPUT FROM STEREOMAT IV;
source model is 6-inch frame photography (scale, 1:24,000) near
Pomona, California (See glossy print in envelope in back of volume)

Figure 2.4-16

SAMPLE ORTHOPHOTOGRAPH from AS-11C; source model is 6-inch
frame photography (scale, 1:48,000) near Fort Sill, Oklahoma
(See glossy print in envelope in back of volume)
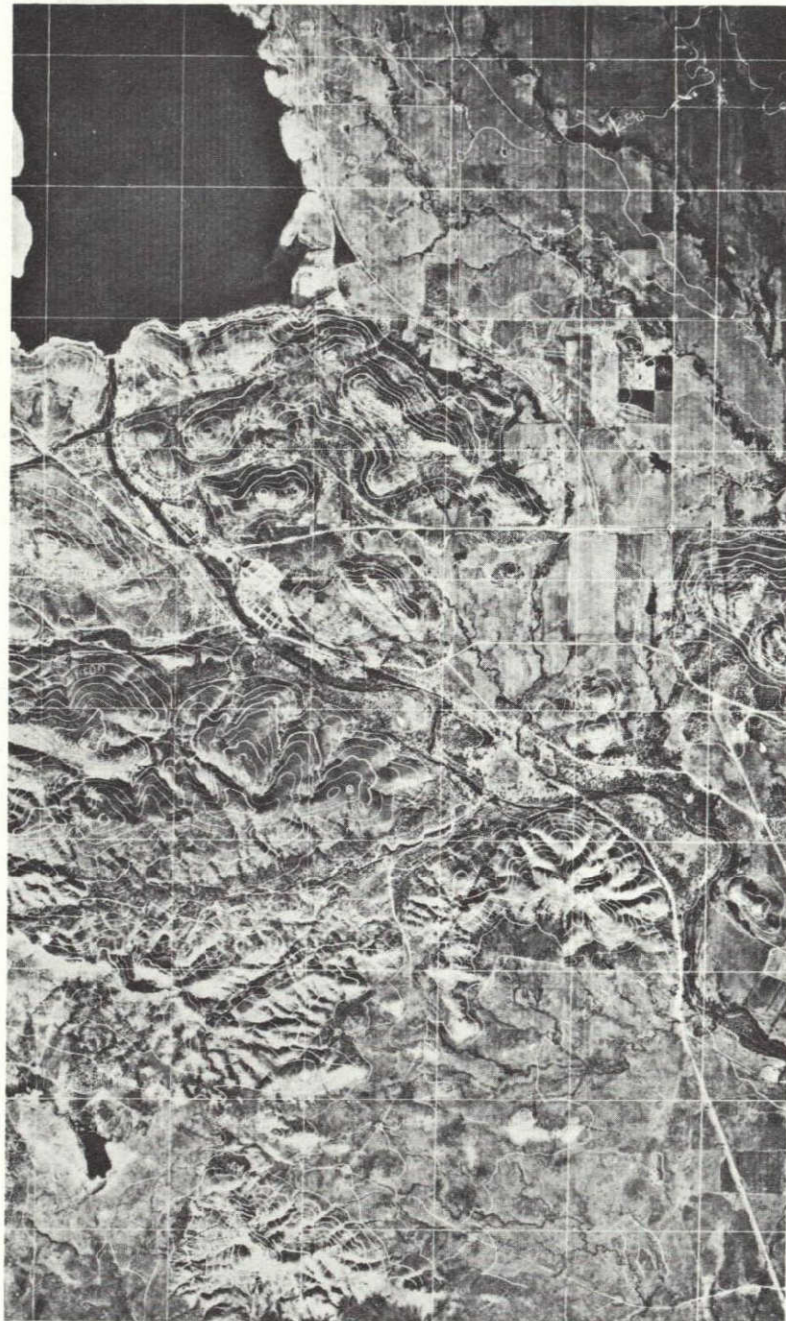
Figure 2.4-17

ORTHOPHOTOGRAPH with superimposed 40-foot contours of Fort Sill, Oklahoma, model; output scale is 1:50,000 (See glossy print in envelope in back of volume)

Figure 2.4-18

ORTHOPHOTOGRAPH PRODUCED BY ZEISS GZ-1 with profile data by
ITEK EC-5/Planimat (See glossy print in envelope in back of volume)

in the entire range of magnification over the whole photograph. Resolution in the range of 50 to 80 lines per millimeter, when referred to the original photography, is obtainable with the GZ-1. If optical projection is used for image distortion correction, color material is readily produced.

An analog stereo plotter, such as the Zeiss Planimat, is basically a mechanical analog computer designed to solve the triangulation equations from stereoscopic parallax in aerial photographs. Such instruments cannot be adapted to detect and quantify image displacements due to other causes without considerable, and uneconomic, modification.

Like the Zeiss Planimat, the GZ-1 orthoprojector, the only instrument of its type on the market, is specifically designed to correct stereoscopic x parallaxes and cannot be adapted for corrections of more general types of distortion. Because of these limitations, and also because of production requirements, existing photogrammetric instrumentation is not capable of providing the image processing required by the ERTS system. A special type of photographic restitutor, based on high resolution optical printing and capable of correcting the special distortions encountered in the RBV and MSS imagery, will be required.

2.4.7.3 Reconnaissance Photographic Restitutor (RPR)

Equipment to produce high resolution orthophotographs from reconnaissance photography has been designed and certain critical subsystems have been breadboarded and tested by simulation. The RPR was designed to accept cut film or glass plates up to 10 by 19 inches. The optical system provided a scale difference of 9x, a rotation of 360 degrees, and anamorphic correction to restitute a wide variety of input photographs to an orthophotograph.

As a candidate system for TIDP image processing, the RPR is over-designed as far as optical performance and correction capability is concerned. However, the production rates would not meet requirements.

The geometric error analysis indicates that a printing slit used for photographic restitution could be one-ninth the width of the image without significantly degrading performance. Also, an anamorphic correction capability is not required because we are dealing with an essentially flat

earth where differential scale and skew is negligible. Also, the antici-
pated corrections can be performed by linear rotation and magnification
over the relatively narrow slit dimension to a degree of accuracy consist-
ent with the requirements.

A new optical design will give increased production and acceptable
performance and will reduce the complexity of the photographic restitutor.
The new design will also incorporate roll film as input and output, and
will be capable of restituting from computer data in a computer controlled
mode.

2.4.7.4 Correlation of Multispectral Imagery

Previous correlation systems have been intended for use with
stereoscopic pairs of images. The differences between these images are
mostly geometrical, i.e., local x parallaxes depending on the distance of
the image point from the camera. In multispectral imagery, the differ-
ences between the various photographs are in reflectivity. The image
correlation systems developed at Itek can tolerate considerable differences
in average or local photographic density between the two images to be
correlated. However, when the difference is great enough to cause a
density reversal, the polarity of the electronic signals becomes inverted
and correlation may be degraded.

As an example of what can be done, Figure 2.4-19 shows some
multispectral photography from the Apollo SO-65 experiment. These
pictures were photographed directly off the viewing screen of Itek ARES
viewer, an electronic stereoscope with automatic image registration
based on image correlation. The input material was fourth generation
and was reproduced on a 500 line crossed-diagonal scan. In the ARES
viewer, the two images are normally viewed stereoscopically. For test
purposes, the left image can be subtracted electronically from the right
image to produce the difference images shown in Figure 2.4-19a.

With two images of identical density range, the subtracted image
will be a uniform gray provided that the images are perfectly registered.
If the images are of different densities because they were obtained in

VIEWED AREA
20 by 20 miles
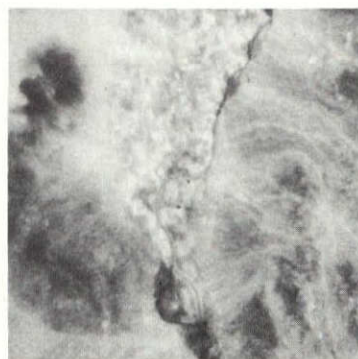
(a) CC
SO-246 + 89B
0.700 to 0.950 micron
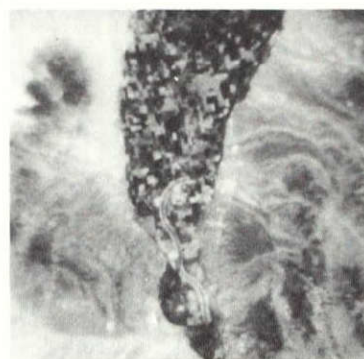
(b) DD
3400 + 25A
0.590 to 0.710 micron
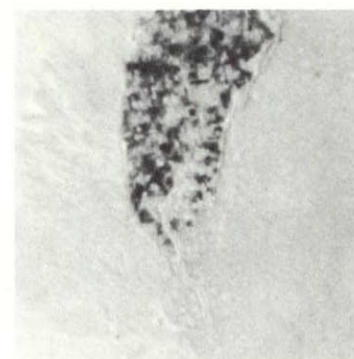
(c) DD - CC

Figure 2.4-19

SO-65 EXPERIMENT PHOTOGRAPHY correlated and registered by ARES

VIEWED AREA
17 by 17 miles
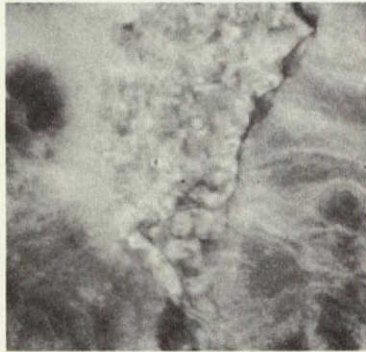
(d) CC
SO-246 + 89B
0.700 to 0.950 micron
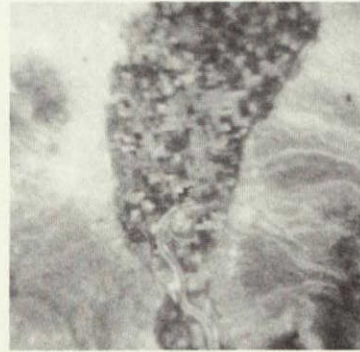
(e) BB
3400 + 58
0.500 to 0.570 micron
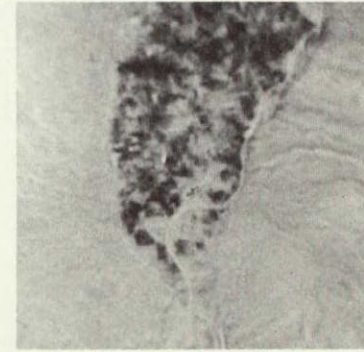
(f) BB - CC

Figure 2.4-19

SO-65 EXPERIMENT PHOTOGRAPHY correlated and registered by ARES (continued)

different spectral bands, some tonal variations may appear in the sub-tracted image. If misregistration is present, the misregistered images will be sharply outlined in black or white.

Figure 2-4-19a shows the results of correlating the red and infrared bands in photography covering an irrigated area of farmland surrounded by desert. The foliage in the farmland is reversed in density, and there are considerable density differences in the surrounding desert, presenting a potential problem to the correlator. The subtracted image in Figure 2.4-19c shows the density reversed area standing out strongly against the neutral gray of the nonreversed area. Correlation over the whole frame is good, as evidenced by the uniform gray tone of the non-reversed area. This indicates that a density reversal covering about 25 percent of the correlated area does not significantly degrade the performance of the correlator.

If the density reversal covers a larger area, as shown in Figure 2.4-19f, some degradation in registration becomes apparent.

The density differences produced by varying reflectivity in different spectral bands do not present a problem to the image correlator unless the difference is so great that a polarity inversion is produced. Even then, good operation is obtained if the reversed area does not exceed about 25 percent of the scanned area.

Areas will inevitably be present in which image correlation will be difficult or impossible. It must be pointed out that to obtain accurate registration of two or more complete photographs, it is not necessary to obtain correlation over 100 percent of the frame area. For example, if correlation can be obtained in the four corners of an image, sufficient information is thereby obtained to correct all zero- and first-order dis-tortions over the whole image area. Thus, even partial correlation of the images is an effective means of obtaining accurate image registration.

2.5 IMAGE PROCESSING SUMMARY TRADEOFF

2.5.1 Introduction

This section presents a summary tradeoff study which investigates the processing time requirements and expected residual errors for

various combinations of bulk and precision processing modes using the digital computer and the precision photo restitutor. The analysis from which the residual errors quoted below are obtained is contained in Volume 2 Section 5. This section is therefore concerned with a detail examination of the timing requirements for the various image processing configurations to be described subsequently.

2.5.2 Processing Modes

In the tradeoff study seven modes of RBV data processing and eight modes of MSS processing have been investigated. The different modes are designated by roman numerals and in both the RBV and MSS cases have been ranked in the order of increasing digital processing require-ments. The key features of each of these 15 modes of processing are tabulated on separate worksheets which are included at the end of this section. (See Figures 2.5-1 through 2.5-15). In each case the mechaniza-tion of the processing mode is described in words and with a diagram. Equations are given for the digital computer and precision photo restitutor processing time as well as the various residual errors in the picture and on the digital tape. Processing techniques requiring either image correlation or image block shifting have been noted under the heading special features.

Preceding the worksheets are two tables which summarize the timing and accuracy information which has been developed elsewhere in this document. These tables also list the symbols used in the analysis. Table 2.5-1 summarizes the processing times for both the precision photo restitutor and the digital computer for each function. In the latter instance the times are given for three different sizes of computers. Table 2.5-2 summarizes the various residual errors in the data as a function of the nature of the input or the mode of processing. These errors refer to the internal consistency of the image and are not to be interpreted as absolute error. This latter effect can be obtained by factoring-in the improvements expected from the use of ground truth.

The information presented in Tables 2.5-1 and 2.5-2 constitute the principal numerical parameters upon which the timing and accuracy

analysis of each mode is based. This data combined with the mode definitions described in the 15 worksheets provide the entire basis for the trade study described in the following sections.

2.5.3 Trade Study Formulation

Given the seven modes of RBV processing and eight modes of MSS processing, one can define a complete image processing system by specifying a combination of an RBV mode and an MSS mode for bulk processing and a combination of an RBV mode and an MSS mode for precision processing. For bulk processing this amounts to 56, (7 x 8), possible configurations.

The requirement, however, to generate a high-accuracy digital tape for precision processed pictures limits the number of precision mode possibilities to four, namely: RBV modes V and VII, and MSS modes VI and VIII. Only two possible combinations are logically consistent of the four precision mode possibilities. These are RBV mode VII and MSS mode VIII, or RBV mode V and MSS mode VI.

The study then has been confined to two cases for precision mode I of which the first case above has 56 (7 x 8) possible modes of bulk processing and the second case has 30 (5 x 6) modes since bulk modes of higher accuracy than the assumed precision mode have been discarded. Tables 2.5-3 and 2.5-4 summarize the equations for computing processing time of combined bulk and precision mode processing. The 1/20 factor in the precision column is the normalizing factor for 5 percent of the images being precision processed. Note that there are slight variations in the time of precision processing as a function of the mode of bulk processing. This variation is due to the fact that for some modes of bulk processing a portion of precision processing is done and need not be repeated. As an example, in RBV mode II one reseau is read as part of the bulk mode. The reseau information will normally be saved and if the same event is to be processed later in the precision mode only reseau data for the other two channels need be processed.

Table 2.5-3 lists the equations for estimating combined bulk and precision mode processing time for both the RBV and MSS sensors for

the case when precision mode I is defined to be RBV mode VII, MSS mode VIII. Table 2.5-4 lists the same information when precision mode I is defined to be RBV mode V, MSS mode VI.

A listing of the accuracy of the various modes of image processing is presented in Table 2.5-5. The information given in this table is collected from the various work sheets and presents results for RBV and MSS processing for both the output photographs and the digital reference tapes. In those instances where for the same event RBV or MSS channels are processed in different ways leading to different accuracies both are indicated. The resultant average accuracy for the set of pictures is then computed by root-sum-squaring the individual channel accuracies.

2.5.4 Analysis

In this section we will present the analysis used for determining the timing requirement. This is then followed by the presentation of the timing requirement for the 86 configurations. The expected residual errors are also presented.

Estimates of processing time are obtained by combining the data given in Table 2.5-1 with the equations listed in Tables 2.5-3 and 2.5-4. For the digital processing time, if T denotes the time to process totally one event then for case A the time to process all events acquired in one day, T' is obtained from the following equation

$$T' \left(\frac{hrs}{day} \right) = N \left(\frac{hrs}{day} \right) + T \left(\frac{min}{event} \right) \frac{63 \left(\frac{events}{day} \right)}{60 \left(\frac{min}{hr} \right)}$$

$$T' = N + 1.05\, T$$

The PPR time is calculated in an analogous manner.

Times for case B coverage for processing 5 days per week are obtained by multiplying by three.

The results of these calculations are summarized in Figure 2.5-16

which lists the times of processing both on the precision photo restitutor
and three sizes of digital computers for all 86 variations on bulk and
precision processing.

The size or number of computers is then estimated as follows. A
factor of safety of 1.30 is applied to each estimated digital processing
time (note that this is the only point in the analysis at which an arbitrary
factor is applied). The computers are then selected based on the infor-
mation supplied in Table 2.5-6.

The factors 3.0 and 4.5 in this table are based on the following
approximate scaling criteria

$$T_{65} \simeq 1.5 \ T_{75} \simeq 4.5 \ T_{85}$$

The number of PPR's is estimated in a similar manner except that
a factor of safety of 1.15 is used in estimating the time. Thus,

$$\text{Number of PPR's = greatest integer in} \left[\frac{1.15 \ T_{PPR}}{8.0} + 1 \right]$$

The results of these calculations are presented in Figure 2.5-17 in
which the regions of equal digital processor configuration are blocked out
with heavy lines. The RBV and MSS residual errors are also given for
each bulk mode. The digital tape accuracies for the two precision modes
are given in the mode number cell. The digital computer size for both
precision modes is given in the figure. If the required size is the
same only one computer is indicated. If by going to the precision mode
RBV mode V, MSS mode VI instead of RBV mode III, MSS mode VIII a
savings in computer size can be achieved, this is indicated by two com-
puter sizes connected with an arrow.

The recommended bulk I, bulk II, and precision I modes are
indicated. Precision II is treated as an add-on mode employing special
forms of digital processing and does not lend itself to this kind of tradeoff.
It is only necessary to assure enough margin or over capacity to do
whatever is required. The requirement for precision II processing has
not been imbedded in this analysis.

Case B deployment results are obtained by sealing all times by a factor of three. One cost saving tradeoff for case B is the possibility of reducing three-shift to second-shift operations. If the times listed in Figure 2.5-17 are such that

$$T < \frac{16.0}{(1.3)(3)} = 4.1$$

then the two-shift operation is possible. These occurrences are indicated in the matrix by the symbol 3→2.

2.5.5 Results - A Comparison of Alternatives

Figure 2.5-18 summarizes the candidate processing modes which offer the best possibilities for superior performance. The reasons for the mode selections are as follows:

$$\text{Bulk mode I} - \begin{Bmatrix} \text{RBV-I} \\ \text{MSS-I} \end{Bmatrix}$$

This was selected as the least cost mode since it uses the smallest computer plus the least number of PPR's. Approximately 40 percent of the pictures will have accuracies better than 0.5 nautical miles, less than 5 percent will exceed 2 miles.

$$\text{Bulk mode II} - \begin{Bmatrix} \text{RBV-IV} \\ \text{MSS-III} \end{Bmatrix}$$

This mode was selected because it provides high performance without depending upon either image correlation or digital block shifting to obtain the required throughput. If, however, either or both of these factors work as anticipated the bulk operating modes can be realigned to achieve even higher system performance. Table 2.5-7 summarizes the possibilities.

Note that six alternatives are possible all of which lead to some better system feature. If all modes work as anticipated, then $\begin{Bmatrix} \text{RBV-V} \\ \text{MSS-II} \end{Bmatrix}$

provides highest performance at moderate cost; whereas,
$\begin{Bmatrix} \text{RBV-III} \\ \text{MSS-II} \end{Bmatrix}$ provides an acceptable high level of performance at much
reduced cost.

Precision mode I - $\begin{Bmatrix} \text{RBV-VII} \\ \text{MSS-VIII} \end{Bmatrix}$

This mode was selected since it provides best correction of those
modes studies and also does not depend on the critical image correlation
and digital block shifting assumptions. If digital block shifting work as
anticipated then mode $\begin{Bmatrix} \text{RBV-V} \\ \text{MSS-VI} \end{Bmatrix}$ is possible.

Table 2.5-1. Processing Time for Precision Photo Restitutor

Operation	Symbol	Process Time
Precision photo restitutor, bulk mode	P	2 5 min/image
Precision photo restitutor, precision mode	2P	5 0 min/image
Precision photo restitutor, all other processing	22 x (2P)	1.9 hrs/day

Processing Time for Digital Operations

Computer Type		360/65	360/75	360/85
Operations	Symbol	Process Time		
Reseau/attitude correction of RBV	R	0 8 min/ image	0 5 min/ image	0 2 min/ image
MSS yaw determination	A	0	0	0
Precision photo restitutor open loop drive signals	S	0 8	0 5	0 2
RBV/MSS format for laser beam recorder	L	0	0	0
RBV image processing, point shifting	B_R	1 2	1 0	0 8
MSS image processing, point shifting	B_M	0 8	0 7	0 6
RBV image processing, linear interpolation	I_R	8 3	4 9	2 4
MSS image processing, linear interpolation	I_M	5 4	3 2	2 3
All other non-image processing NDPF, case A	N	3 4 hrs/ day	2 2 hrs/ day	0.8 hr/ day

Table 2.5-2. Image Processing Accuracy
(all errors are quoted for a
3σ confidence level)

Type	Symbol	RBV ft	MSS ft
Attitude (without correction)	$\sigma'_{A_{R,M}}$	960	9000
Attitude (with telemetry corrections)	$\sigma_{A_{R,M}}$	200	1900
Attitude (RBV/MSS correlation for yaw bias determination	σ'_{A_M}	-	1500
RBV Camera (without reseau correction)	σ'_R	12,000	-
RBV Camera (with reseau correction)	σ_R	230	-
Laser beam recorder distortion	σ_L	330	330
Precision photo restitutor open loop correction	σ_S	620	620
Precision photo restitutor closed loop correction	σ_P	620	620
Photoprocessing distortion	σ_R	540	540
Digital processing (point shifting)	$\sigma_{B_{R,M}}$	140	850
Digital processing (linear interpolation)	$\sigma_{I_{R,M}}$	100	600

2-171

Table 2.5-3. Image Processing Time

RBV Mode VII = Precision Mode I

RBV Mode	Bulk		Precision		Sum	
	Computer	PPR	Computer	PPR	Computer	PPR
I	$3L$	0	$1/20\,(3L + 3R + 3I_R)$	0	$3.15L + 0.15R + 0.15I_R$	0
II	$3L + R + S$	3P	$1/20\,(3L + 2R + 3I_R)$	0	$3.15L + 1.1R + S + 0.15I_R$	3P
III	$3L + R + B_R$	2P	$1/20\,(3L + 2R + 3I_R)$	0	$3.15L + 1.1R + B_R + 0.15I_R$	2P
IV	$3L + 3R + 3S$	3P	$1/20\,(3L + 3I_R)$	0	$3.15L + 3R + 3S + 0.15I_R$	3P
V	$3L + 3R + 3B_R$	0	$1/20\,(3L + 3I_R)$	0	$3.15L + 3R + 3B_R + 0\ 15I_R$	0
VI	$3L + R + I_R$	2P	$1/20\,(2L + 2R + 2I_R)$	0	$3.1L + 1.1R + 1.1I_R$	2P
VII	$3L + 3R + 3I_R$	0	0	0	$3L + 3R + 3I_R$	0

MSS Mode VIII = Precision Mode I

MSS Mode	Bulk		Precision		Sum	
	Computer	PPR	Computer	PPR	Computer	PPR
I	$4L$	o	$1/20\,(5L + A + 4I_M)$	0.1P	$4.25L + 0\ 05A + 0.2I_M$	0.1P
II	$4L$	4P	$1/20\,(5L + A + 4I_M)$	0.1P	$4.25L + 0\ 05A + 0\ 2I_M$	4.1P
III	$4L + S$	4P	$1/20\,(5L + A + 4I_M)$	0.1P	$4.25L + S + 0\ 05A + 0\ 2I_M$	4.1P
IV	$4L + B_M$	3P	$1/20\,(5L + A + 4I_M)$	0.1P	$4.25L + B_M + 0\ 05A + 0.2I_M$	3.1P
V	$4L + 4B_M$	0	$1/20\,(5L + A + 4I_M)$	0.1P	$4.25L + B_M + 0.05A + 0\ 2I_M$	0.1P
VI	$5L + A + 4B_M$	P	$1/20\,(4L + 4I_M)$	0	$5.2L + A + 4B_M + 0.2I_M$	P
VII	$4L + 4I_M$	0	$1/20\,(5L + A + 4I_M)$	0.1P	$4.25L + 0\ 05A + 4.2I_M$	0.1P
VIII	$5L + A + 4I_M$	P	0	0	$5L + A + 4I_M$	P

Table 2.5-4. Image Processing Time

RBV Mode V = Precision Mode I

RBV Mode	Bulk		Precision		Sum	
	COMPUTER	PPR	COMPUTER	PPR	COMPUTER	PPR
I	$3L$	0	$1/20\,(3L + 3R + 3B_R)$	0	$3\ 15L + 0\ 15R + 0.15\,B_R$	0
II	$3L + R + S$	3P	$1/20\,(3L + 2R + 3B_R)$	0	$3.15 + 1.1R + S + 0.15\,B_R$	3P
III	$3L + R + B_R$	2P	$1/20\,(2L + 2R + 2B_R)$	0	$3.1L + 1.1R + 1.1\,B_R$	2P
IV	$3L + 3R + 3S$	3P	$1/20\,(3L + 3B_R)$	0	$3.15L + 3R + 3S + 0\ 15\,B_R$	3P
V	$3L + 3R + 3B_R$	0	0	0	$3L + 3R + 3B_R$	0
VI	–		–		–	
VII	–		–		–	

MMS Mode VI = Precision Mode I

MSS Mode	Bulk		Precision		Sum	
	COMPUTER	PPR	COMPUTER	PPR	COMPUTER	PPR
I	$4L$	0	$1/20\,(5L + A + 4B_M)$	0.1P	$4.25L + 0\ 05A + 0\ 2B_M$	0 1P
II	$4L$	4P	$1/20\,(5L + A + 4B_M)$	0.1P	$4.25L + 0.05A + 0.2B_M$	4 1P
III	$4L + S$	4P	$1/20\,(5L + A + 4B_M)$	0 1P	$4\ 25L + S + 0.05A + 0.2B_M$	4.1P
IV	$4L + B_M$	3P	$1/20\,(5L + A + 4B_M)$	0.1P	$4.25L + 0.05A + 1.2B_M$	3.1P
V	$4L + 4B_M$	0	$1/20\,(5L + A + 4B_M)$	0.1P	$4.25L + 0\ 05A + 4\ 2B_M$	0 1P
VI	$5L + A + 4B_M$	P	0	0	$5L + A + 4B_M$	P
VII	–		–		–	
VIII	–		–		–	

Table 2.5-5. Image Processing Accuracy

RBV Accuracy (3σ)

RBV Mode	Photographs			Digital Tape	
	Reference Channel	Other Channel	Average Picture	Reference Channel	Other Channel
I	12,000 ft		12,000 ft	12,000 ft	
II	880	1,200	1,100	12,000	
III	720	1,090	980	340	12,000
IV	880		880	12,000	
V	720		720	340	
VI	710	1,090	980	320	12,000
VII	710		710	320	

MSS Accuracy (3σ)

MSS Mode	Photographs			Digital Tape	
	Reference Channel	Other Channel	Average Picture	Reference Channel	Other Channel
I	9,000 ft		9,000 ft	9,000 ft	
II	—		$\sqrt{1183000 + \sigma^2_{RBV}}$	9,000	
III	2,100		2,100	9,000	
IV	2,200	2,320	2,280	2,100	9,000
V	2,200		2,200	2,100	
VI	—		$\sqrt{3373000 + \sigma^2_{RBV}}$	1,870 ($\sigma_{RBV} = 720$)	
VII	2,100		2,100	1,900	
VIII	—		$\sqrt{3011000 + \sigma^2_{RBV}}$	1,760 ($\sigma_{RBV} = 710$)	

Table 2.5-6. Computer Selection Criteria

Condition	Selected Computers
$T_{65} < \dfrac{8.0}{1.3}$	65
$T_{65} > \dfrac{8.0}{1.3},\ T_{75} < \dfrac{8.0}{1.3}$	75
$T_{75} > \dfrac{8.0}{1.3};\ T_{85} < \dfrac{8.0}{1.3}$	85
$\dfrac{8.0}{1.3} < T_{85} < \dfrac{8.0}{1.3} + \dfrac{8.0}{(4.5)(1.3)}$	65, 85
$\dfrac{8.0}{1.3} + \dfrac{8.0}{(4.5)(1.3)} < T_{85} < \dfrac{8.0}{1.3} + \dfrac{8.0}{(3.0)(1.3)}$	75, 85
$\dfrac{8.0}{1.3} + \dfrac{8.0}{(3.0)(1.3)} < T_{85} < \dfrac{16.0}{1.3}$	85, 85
$\dfrac{16.0}{1.3} < T_{85} < \dfrac{16.0}{1.3} + \dfrac{8.0}{(4.5)(1.3)}$	65, 85, 85
$\dfrac{16.0}{1.3} + \dfrac{8.0}{(4.5)(1.3)} < T_{85} < \dfrac{16.0}{1.3} + \dfrac{8.0}{(3.0)(1.3)}$	75, 85, 85
$\dfrac{16.0}{1.3} + \dfrac{8.0}{(3.0)(1.3)} < T_{85} < \dfrac{24.0}{1.3}$	85, 85, 85

Table 2.5-7. Processing Alternatives

Condition	Alternative Mode	Potential Gain
If digital block shifting is feasible	RBV-V MSS-III	RBV error reduced
	RBV-IV MSS-VI	MSS error reduced
If both digital block shifting is feasible and computer times are overestimated	RBV-V MSS-VI	RBV and MSS errors reduced
If image correlation is feasible	RBV-IV MSS-II	MSS error much reduced
If both digital block shifting and image correlation are feasible	RBV-V MSS-II	RBV error reduced; MSS error much reduced
	RBV-III MSS-II	Processing requirement drastically reduced

2.5.5.1 RBV Mode I

Mechanization

Print on laser beam recorder without correction.
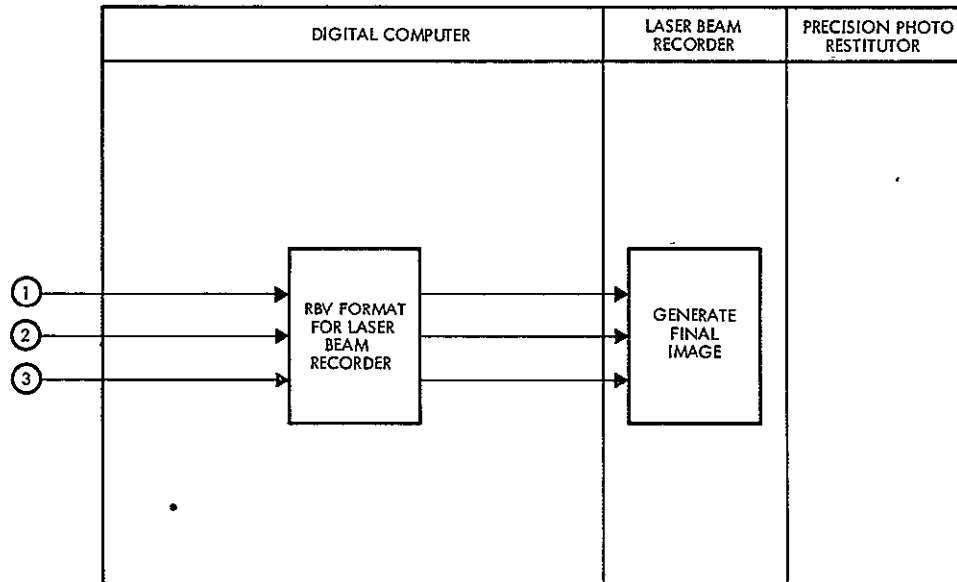
Figure 2.5-1

RBV MODE I

Throughput

Digital time = 3L	360/65	360/75	360/85
	0	0	0
Precision photo restitutor time = 0	0		

Accuracy

Picture	$\sigma = \sqrt{\left(\sigma_{A_R}{'}\right)^2 + (\sigma_R{'})^2 + \sigma_L{}^2 + \sigma_Q{}^2}$	12,000 ft
Digital Tape	$\sigma = \sqrt{\left(\sigma_{A_R}{'}\right)^2 + (\sigma_R{'})^2}$	12,000 ft

Special Features

None.

2.5.5.2 RBV Mode II

Mechanization

Attitude data input plus digital reseau detection to derive open-loop correction of one channel. Channels 2 and 3 corrected by image correlation on a precision photo restitutor.
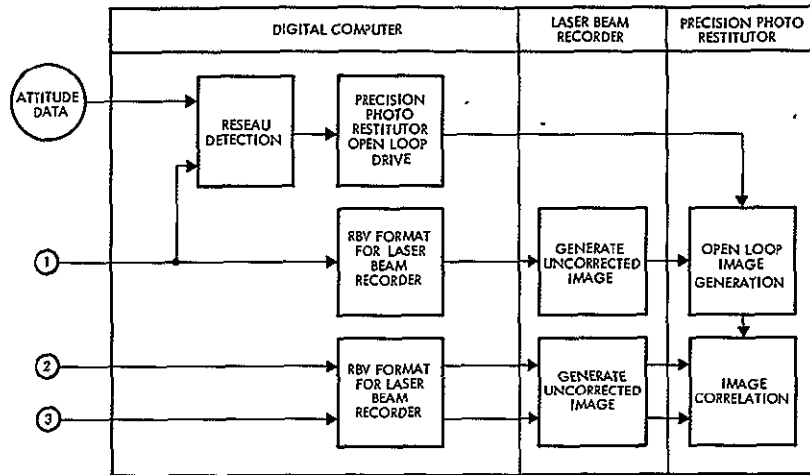
Figure 2.5-2

RBV MODE II

Throughput

	360/65	360/75	360/85
Digital time = 3L + R + S	1 6 min/ event	1 6 min/ event	0.4 min/ event
Precision photo restitutor time = 3P	7. 5 min/event		

Accuracy

Picture ①	$\sigma_{①} = \sqrt{\sigma_{A_R}{}^2 + \sigma_R{}^2 + \sigma_S{}^2 + \sigma_O{}^2}$	880 ft
Picture ②,③	$\sigma_{②,③} = \sqrt{\sigma_{①}{}^2 + \sigma_P{}^2 + \sigma_Q{}^2}$	1200 ft
Picture average	$\sigma_{avg} = \sqrt{\frac{1}{3}\left(\sigma_{①}{}^2 + \sigma_{②}{}^2 + \sigma_{③}{}^2\right)}$	1100 ft
Digital tape	$\sigma = \sqrt{\left(\sigma_{A_R}{}'\right)^2 + (\sigma_R{}'')^2}$	12, 000 ft

Special Features

Requires image correlation.

2.5.5.3 RBV Mode III

Mechanization

Attitude data input plus digital reseau detection, digital block shifting, and laser beam recorder print of final image for one channel. Channels 2 and 3 corrected by image correlation on a precision photo restitutor.
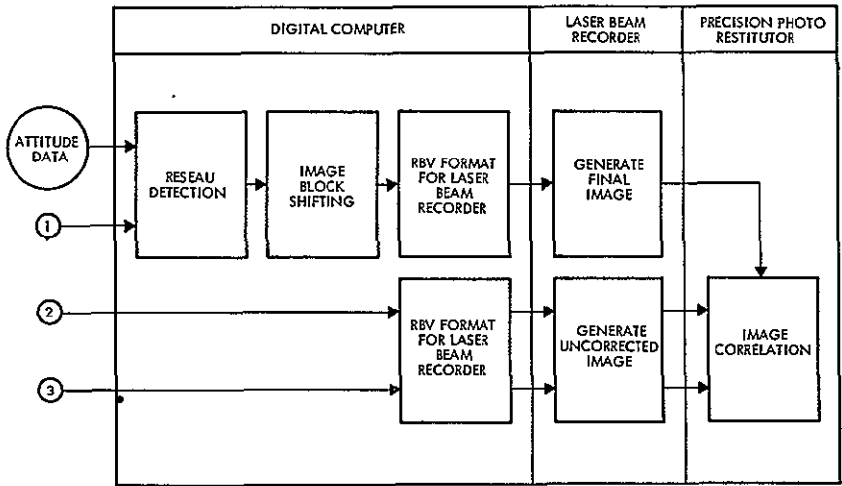
Figure 2.5-3

RBV MODE III

Throughput

Digital time = 3L + R + B$_R$	360/65	360/75	360/85
	2 0 min/ event	1 5 min/ event	1 0 min/ event
Precision photo restitutor time = 2P	5 0 min/event		

Accuracy

Picture ①	$\sigma_{①} = \sqrt{\sigma_{A_R}^2 + \sigma_R^2 + \sigma_{B_R}^2 + \sigma_L^2 + \sigma_Q^2}$	720 ft
Picture ②,③	$\sigma_{②,③} = \sqrt{\sigma_{①}^2 + \sigma_P^2 + \sigma_Q^2}$	1090 ft
Picture average	$\sigma_{avg} = \sqrt{\frac{1}{3}\left(\sigma_{①}^2 + \sigma_{②}^2 + \sigma_{③}^2\right)}$	980 ft
Digital tape	$\sigma_{①} = \sqrt{\sigma_{A_R}^2 + \sigma_R^2 + \sigma_{B_R}^2}$,	340 ft
	$\sigma_{②}\,_{③} = \sqrt{\left(\sigma_{A_R}{}'\right)^2 + \left(\sigma_R{}'\right)^2}$	12,000 ft

Special Features

Requires both image correlation and image block shifting.

2.5.5.4. RBV Mode IV

Mechanization

Attitude data input plus digital reseau detection to derive open loop correction of all these channels on a precision photo restitutor.
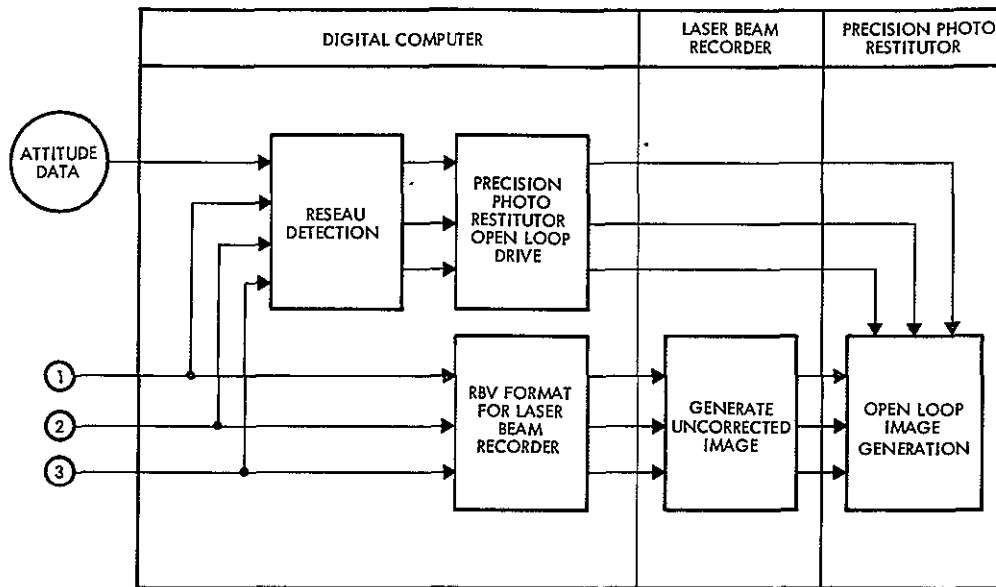
Figure 2.5-4

RBV MODE IV

Throughput

Digital time = 3L + 3R + 3S	360/65	360/75	360/85
	4.8 min/ event	3 0 min/ event	1.2 min/ event
Precision photo restitutor time = 3P	7. 5 min/event		

Accuracy

Picture	$\sigma = \sqrt{\sigma_{A_R}^{2} + \sigma_R^{2} + \sigma_S^{2} + \sigma_Q^{2}}$	880 ft
Digital tape	$\sigma = \sqrt{\left(\sigma_{A_R}'\right)^{2} + \left(\sigma_R'\right)^{2}}$	12, 000 ft

Special Features

None.

2.5.5.5 RBV Mode V

Mechanization

Attitude data input plus digital reseau detection, digital block shifting, and laser beam recorder print of final image for all three channels.
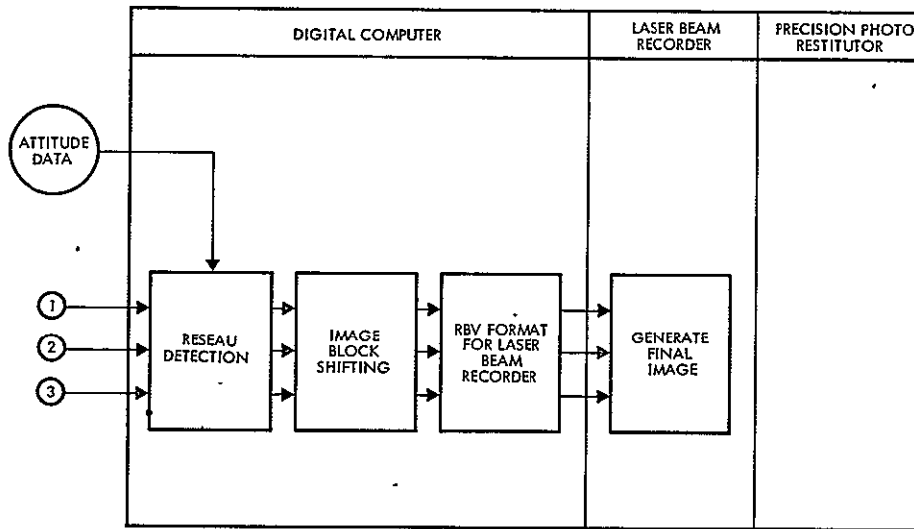
Figure 2.5-5

RBV MODE V

Throughput

Digital time = $3L + 3R + 3B_R$	360/65	360/75	360/85
	6 0 min/ event	4 5 min/ event	3 0 min/ event
Precision photo restitutor time = 0	0		

Accuracy

Picture	$\sigma = \sqrt{\sigma_{A_R}^2 + \sigma_R^2 + \sigma_{B_R}^2 + \sigma_L^2 + \sigma_Q^2}$	720 ft
Digital tape	$\sigma = \sqrt{\sigma_{A_R}^2 + \sigma_R^2 + \sigma_{B_R}^2}$	340 ft

Special Features

Requires image block shifting.

2.5.5.6. RBV Mode VI

Mechanization

Attitude data input plus digital reseau detection, image processing by point-by-point linear interpolation and laser beam recorder print of one channel. Channels 2 and 3 corrected by image correlation on a precision photo restitutor.
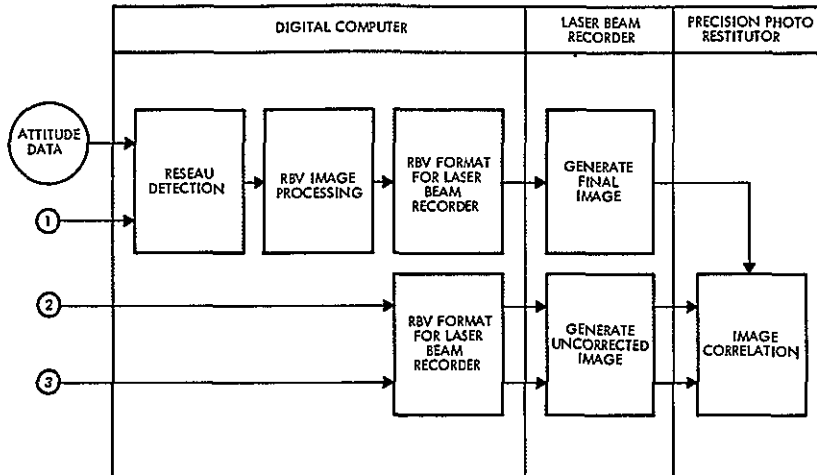
Figure 2.5-6

RBV MODE VI

Throughput

Digital time = $3L + R + I_R$	360/65	360/75	360/85
	9 1 min/ event	5 4 min/ event	2 6 min/ event
Precision photo restitutor time = 2P	5 0 min/event		

Accuracy

Picture ①	$\sigma_① = \sqrt{\sigma_{A_R}^2 + \sigma_R^2 + \sigma_{I_R}^2 + \sigma_L^2 + \sigma_Q^2}$	710 ft
Picture ②,③	$\sigma_②③ = \sqrt{\sigma_①^2 + \sigma_P^2 + \sigma_Q^2}$	1090 ft
Picture average	$\sigma_{avg} = \sqrt{\frac{1}{3}\left(\sigma_①^2 + \sigma_②^2 + \sigma_③^2\right)}$	980 ft
Digital tape	$\sigma_① = \sqrt{\sigma_{A_R}^2 + \sigma_R^2 + \sigma_{I_R}^2}$	320 ft
	$\sigma_②,③ = \sqrt{\left(\sigma_{A_R}'\right)^2 + \left(\sigma_R'\right)^2}$	12,000 ft

Special Features

Requires image correlation.

2.5.5.7 RBV Mode VII

Mechanization

Attitude input plus digital reseau detection, digital image processing by point-by-point linear interpolation and laser beam recorder print of all channels.
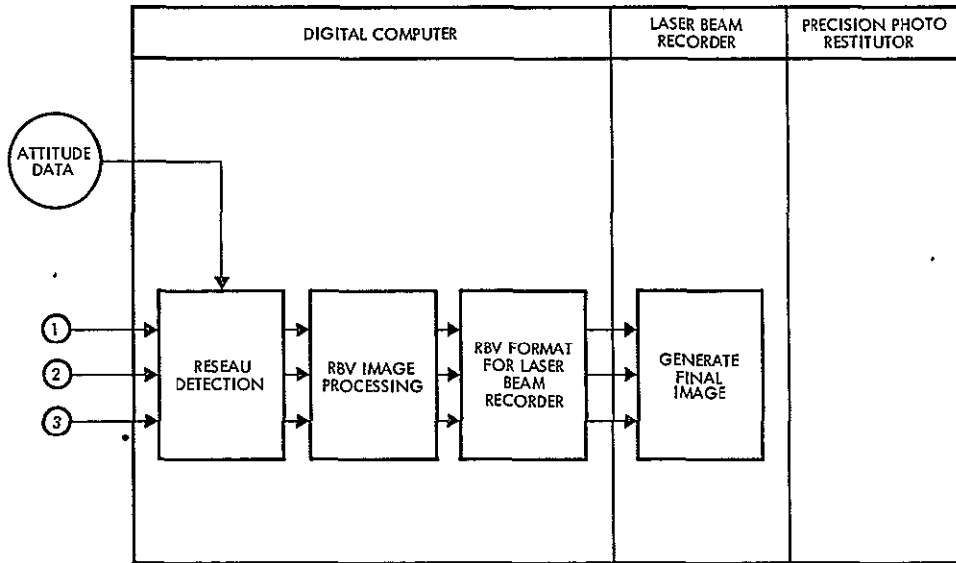
Figure 2.5-7

RBV MODE VII

Throughput

Digital time = 3L + 3R + 3I$_R$	360/65	360/75	360/85
	27.3 min/ event	16 2 min/ event	7 8 min/ event
Precision photo restitutor time = 0	0		

Accuracy

Picture	$\sigma = \sqrt{\sigma_{A_R}^2 + \sigma_R^2 + \sigma_{I_R}^2 + \sigma_L^2 + \sigma_Q^2}$	710 ft
Digital tape	$\sigma = \sqrt{\sigma_{A_R}^2 + \sigma_R^2 + \sigma_{I_R}^2}$	320 ft

Special Features

None.

2.5.5.8. MSS Mode I

Mechanization

Print on laser beam recorder without correction.

DIGITAL COMPUTER	LASER BEAM RECORDER	PRECISION PHOTO RESTITUTOR

(1)
(2) → MSS FORMAT FOR LASER BEAM RECORDER → GENERATE FINAL IMAGE
(3)
(4)
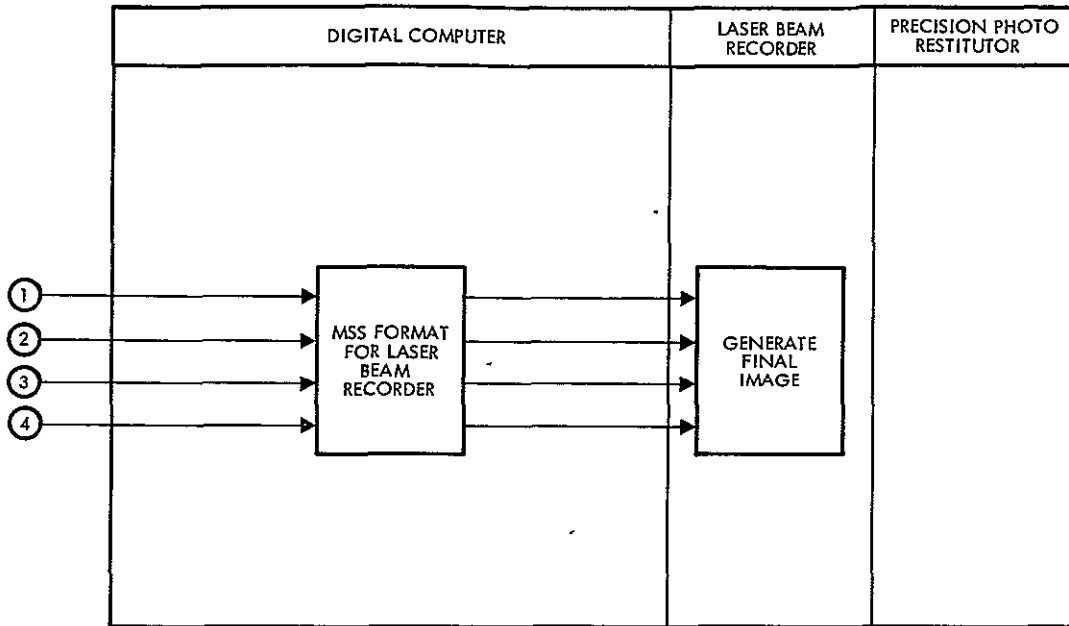
Figure 2.5-8

MSS MODE I

Throughput

Digital time = 4L	360/65	360/75	360/85
	0	0	0
Precision photo restitutor time = 0	0		

Accuracy

Picture	$\sigma = \sqrt{\left(\sigma_{A_M}'\right)^2 + \sigma_L^2 + \sigma_Q^2}$	9000 ft
Digital tape	$\sigma = \sigma_{A_M}'$	9000 ft

Special Features

None

2-182

2.5.5.9 MSS Mode II

Mechanization

Print one channel directly on a laser beam recorder. Correlate image with the nearest RBV channel to produce a corrected MSS image on a precision photo restitutor. Use the derived precision photo restitutor error signals to correct open loop on the other three MSS channels.
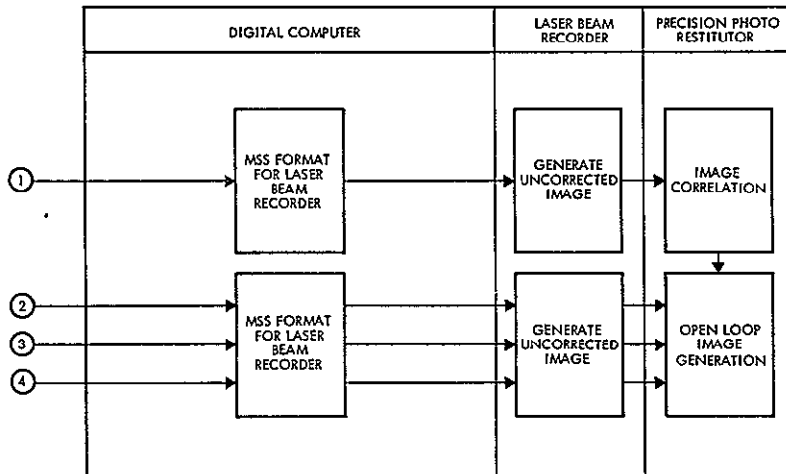
Figure 2.5-9
MSS MODE II

Throughput

Digital time = 4L	360/65	360/75	360/85
	0	0	0
Precision photo restitutor time = 4P	10 0 min/event		

Accuracy

Picture ①	$\sigma_① = \sqrt{\sigma_{RBV}^2 + \sigma_P^2 + \sigma_Q^2}$	—
Picture ②, ③, ④	$\sigma_{②, ③, ④} = \sqrt{\sigma_①^2 + \sigma_S^2 + \sigma_Q^2}$	—
Picture average	$\sigma_{avg} = \frac{1}{2}\sqrt{\sigma_①^2 + \sigma_②^2 + \sigma_③^2 + \sigma_④^2}$	—
Digital tape	$\sigma = \sigma'_{A_M}$	9000 ft

Special Feature

Requires image correlation.

2.5.5.10 MSS Mode III

Mechanization

Attitude data from telemetry is used to derive a common open loop correction for all channels on precision photo restitutor.
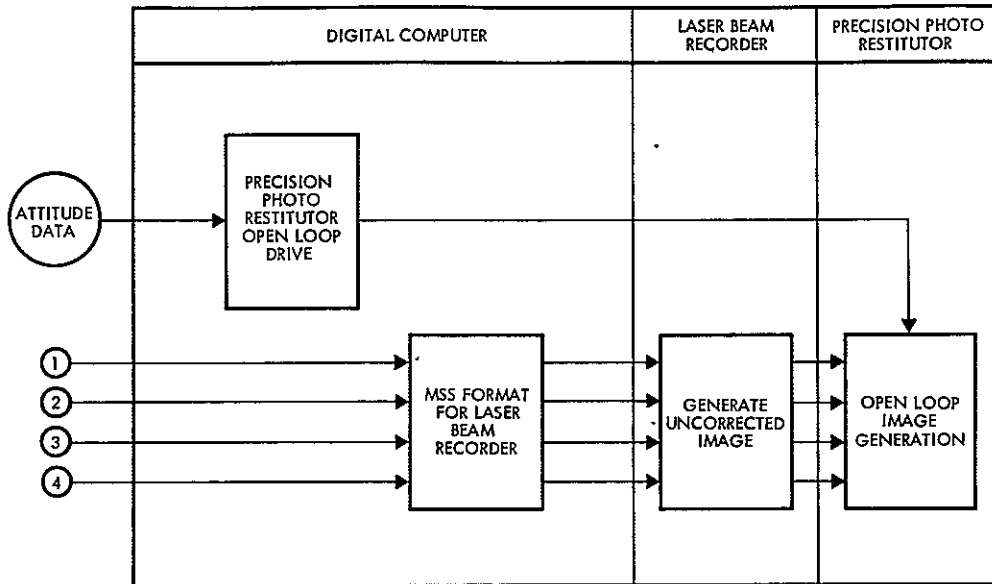
Figure 2.5-10

MSS MODE III

Throughput

		360/65	360/75	360/85
Digital time = 4L + S		0. 8 min/ event	0. 5 min/ event	0 2 min/ event
Precision photo restitutor time = 4P		10 0 min/event		

Accuracy

Picture	$\sigma = \sqrt{\sigma_{A_M}^2 + \sigma_S^2 + \sigma_Q^2}$	2100 ft
Digital tape	$\sigma = \sigma_{A_M}{}'$	9000 ft

Special Features

None

2.5.5.11 MSS Mode IV

Mechanization

Attitude data is used with digital image block shifting and the laser beam recorder to provide a corrected image for one channel. Image correlation on the precision photo restitutor is used to correct the other three channels.
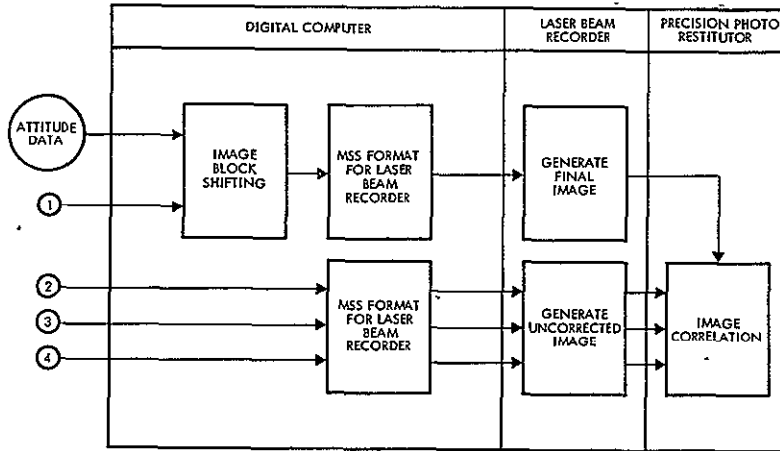
Figure 2.5-11

MSS MODE IV

Throughput

Digital time = $4L \div B_M$	360/65	360/75	360/85
	0 8 min/ event	0 7 min/ event	0 6 min/ event
Precision photo restitutor time = 3P	7 5 min/event		

Accuracy

Picture ①	$\sigma_{①} = \sqrt{\sigma_{A_M}^2 + \sigma_{B_M}^2 + \sigma_L^2 + \sigma_Q^2}$	2200 ft
Picture ②, ③, ④	$\sigma_{②, ③, ④} = \sqrt{\sigma_{①}^2 + \sigma_P^2 + \sigma_Q^2}$	2320 ft
Picture average	$\sigma_{avg} = \frac{1}{2}\sqrt{\sigma_{①}^2 + \sigma_{②}^2 + \sigma_{③}^2 + \sigma_{④}^2}$	2280 ft
Digital tape	$\sigma_{①} = \sqrt{\sigma_{A_M}^2 + \sigma_{B_M}^2}$,	2100 ft,
	$\sigma_{②, ③, ④} = \sigma_{A_M}$,	9000 ft

Special Features

Requires both image correlation and image block shifting.

2-185

2.5.5.12 MSS Mode V

Mechanization

Attitude data is used with digital image block shifting and the laser beam recorder to provide a corrected image for each channel.
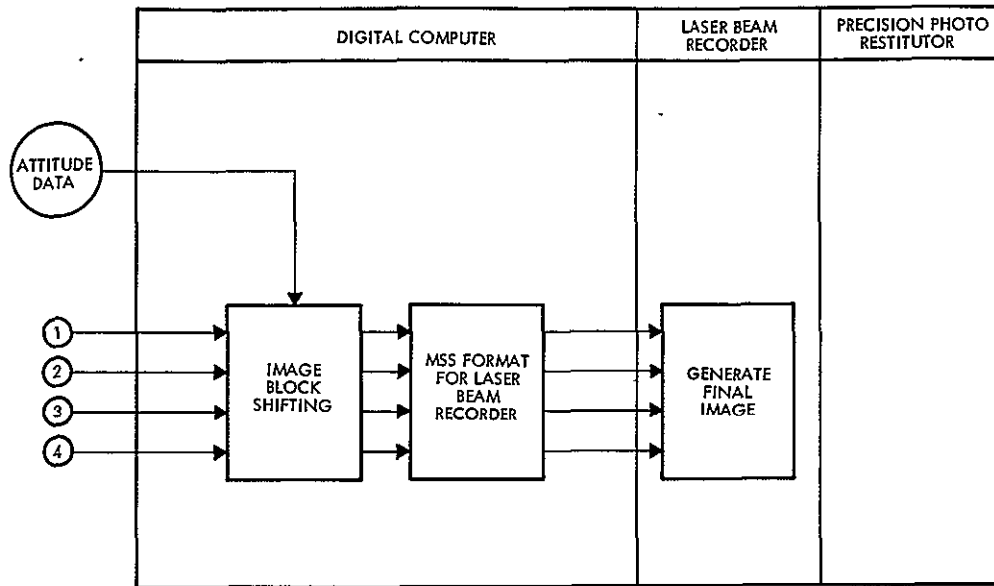
Figure 2.5-12

MSS MODE V

Throughput

Digital time = $4L + 4B_M$	360/65	360/75	360/85
	3 2 min/ event	2. 8 min/ event	2 4 min/ event
Precision photo restitutor time = 0	0		

Accuracy

Picture	$\sigma = \sqrt{\sigma_{A_M}^2 + \sigma_{B_M}^2 + \sigma_L^2 + \sigma_Q^2}$	2200 ft
Digital tape	$\sigma = \sqrt{\sigma_{A_M}^2 + \sigma_{B_M}^2}$	2100 ft

Special Features

Requires image block shifting.

2-186

2.5.5.13 MSS Mode VI

Mechanization

Print one channel directly on a laser beam recorder and correlate image with the nearest RBV channel. Use the derived error signals from the precision photo restitutor in combination with the input attitude data to determine attitude. Input results to digital block shifting on all four channels. Print corrected image on laser beam recorder.
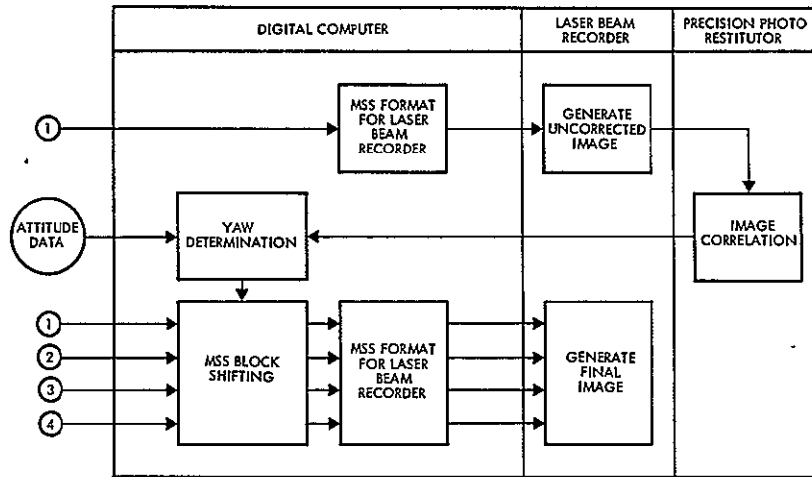
Figure 2.5-13
MSS MODE VI

Throughput

Digital time = 5L + A + 4B$_M$	360/65	360/75	360/85
	3. 2 min/ event	2. 8 min/ event	2 4 min/ event
Precision photo restitutor time = P	2 5 min/event		

Accuracy

Picture	$\sigma = \sqrt{\sigma_{RBV}^2 + \left(\sigma_{A_M}"\right)^2 + \sigma_{B_M}^2 + \sigma_L^2 + \sigma_Q^2}$	—
Digital tape	$\sigma = \sqrt{\sigma_{RBV}^2 + \left(\sigma_{A_M}"\right)^2 + \sigma_{B_M}^2}$	—

Special Features

Requires digital block shifting.

2-187

2.5.5.14 MSS Mode VII

Mechanization

Input attitude data and perform point-by-point linear interpolation on all four channels. Print directly using the laser beam recorder.

| DIGITAL COMPUTER | | LASER BEAM RECORDER | PRECISION PHOTO RESTITUTOR |

ATTITUDE DATA

① ② ③ ④

MSS IMAGE PROCESSING → MSS FORMAT FOR LASER BEAM RECORDER → GENERATE FINAL IMAGE
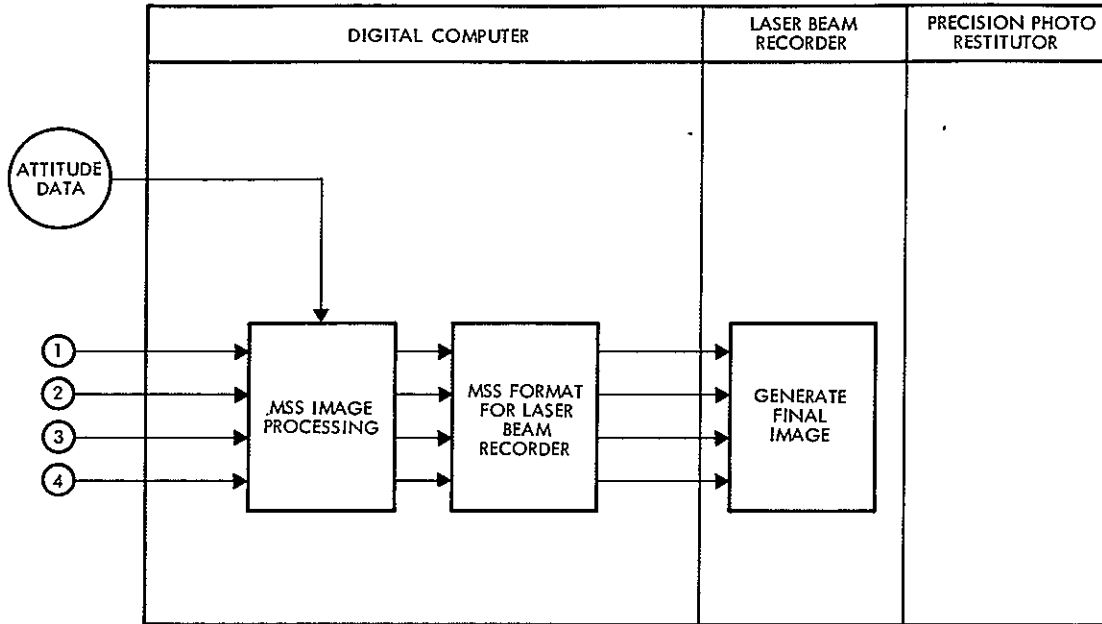
Figure 2.5-14

MSS MODE VII

Throughput

Digital time = $4L + 4I_M$	360/65	360/75	360/85
	21 6 min/ event	12 8 min/ event	9 2 min/ event
Precision photo restitutor time = 0	0		

Accuracy

Picture	$\sigma = \sqrt{\sigma_{A_M}^2 + \sigma_{I_M}^2 + \sigma_L^2 + \sigma_Q^2}$	2100 ft
Digital tape	$\sigma = \sqrt{\sigma_{A_M}^2 + \sigma_{I_M}^2}$	1900 ft

Special Features

None.

2.5.5.15 MSS Mode VIII

Mechanization

Print one channel directly on a laser beam recorder and correlate image with the nearest RBV channel. Use the derived error signal from the precision photo restitutor in correlation with the input attitude data to determine attitude. Input results to point-by-point linear interpolation for all four channels. Print corrected images on laser beam recorder.
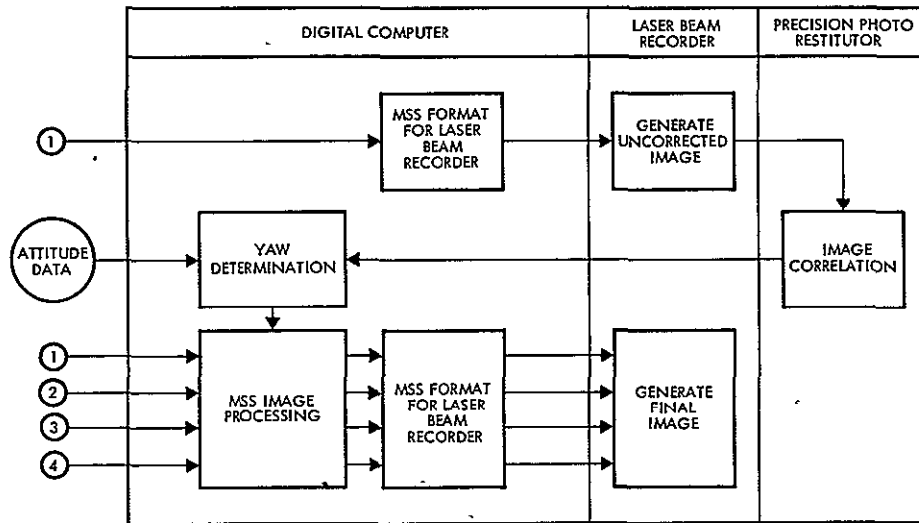
Figure 2.5-15
MSS MODE VIII

Throughput

Digital time = 5L + A + 4I$_M$	360/65	360/75	360/85
	21 6 min/ event	12 8 min/ event	9 2 min/ event
Precision photo restitutor time = P	2 5 min/event		

Accuracy

| Picture | $\sigma = \sqrt{\sigma_{RBV}^2 + \left(\sigma_{A_M}''\right)^2 + \sigma_{I_M}^2 + \sigma_L^2 + \sigma_Q^2}$ | — |
| Digital tape | $\sigma = \sqrt{\sigma_{RBV}^2 + \left(\sigma_{A_M}''\right)^2 + \sigma_{I_M}^2}$ | — |

Special Features

None.

2-189
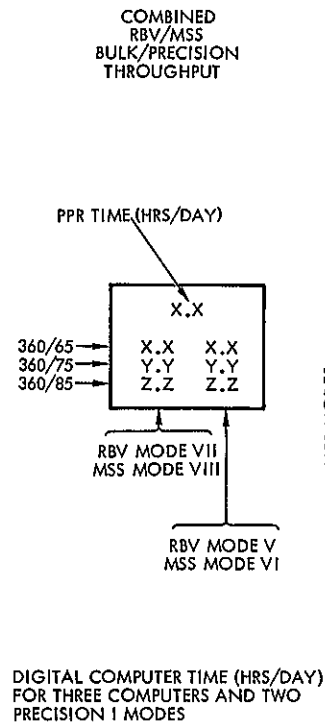
RBV MODES

MSS MODES	I	II	III	IV	V	VI	VII
I	2 2 6 0 3 9 3 8 2.6 1.7 1.1	10 1 7.6 5.6 4.8 37 2 1 1.6	7 5 8 0 5 9 5 3 4 1 2 8 2 1	10 1 10 9 8 8 6 8 5.7 3 0 2 4	2 2 12 2 9 9 8 4 7 1 4 9 4 1	7 5 15 0 9 1 4 3	2 2 33 2 19 9 9 5
II	12.7 6.0 3.9 3 8 2.6 1 7 1 1	20 6 7.6 5.6 4.8 37 2 1 1.6	18 0 8 0 5 9 5 3 4 1 2 8 2 1	20 6 10 9 8.8 6.8 5 7 3.0 2.4	12 7 12.2 9 9 8 4 7 1 4.9 4 1	18.0 15 0 9 1 4 3	12 7 33 2 19 9 9 5
III	12 7 6 9 4 8 4 3 3.2 1 9 1 3	20 6 8.5 6 4 5 3 4.2 2.4 1.7	18 0 8 9 6 4 5 8 4 6 3 0 2 3	20 6 11 6 9 7 7 4 6 1 3 2 2 6	12 7 13 0 10 8 8 9 7 6 5 1 4.3	18.0 15.9 9 7 4 5	12 7 34 1 20 4 9 8
IV	10 1 6.9 4 8 4.5 3.4 2.4 1 8	18 0 8.5 6 4 5 2 4.4 2 8 2 2	15 3 8 9 6 8 6 1 4 9 3 4 2 8	18 0 11 6 9 7 7 6 6 4 3 6 3 0	10 1 13 0 10 8 9 2 7 8 5 5 4 8	15 3 15.9 9 9 5 0	10 1 34 1 20 6 10 2
V	2 2 9 4 7.3 6 7 5.6 4.3 3.6	10 1 11.0 8 9 7.7 6 6 4.7 4.1	7 5 11 4 9 3 7.7 7 1 5 3 4 6	10 1 14 3 12 2 9 8 8 6 5 5 4 9	2 2 15 5 13 3 11 4 10 0 7 4 6 6	7 5 18 4 12 1 6 8.	2 2 36 6 22 8 12 1
VI	4.6 9.4 7 1 6 7 5.4 4.3 3 5	12.4 11.0 8 8 7.7 6.4 4.7 3.9	9 8 11 4 9 1 7 7 6 9 5 3 4 5	12 4 14 3 12 2 9 8 8 6 5 5 4 9	4.6 15 5 13 1 11 4 9 9 7 4 6 5	9 8 18 4 12.1 6 8	4 6 36 6 22 8 12.1
VII	2.2 29.0 17.1 11 4	10 1 30.3 18.2 11.7	7 5 30 7 18 7 12 4	10 1 33.6 20 2 12 6	2 2 34.6 21 7 14 5	7 5 37.7 22 5 14.0	2 2 55 9 33 3 19 2
VIII	4 6 27 6 16 5 10 9	12 4 29.1 17.5 11 3	9.8 29 6 18 1 12.0	12 4 32 4 19 5 12 2	4 6 · 33 6 20 1 14 0	· 9 8 36 6 21 9 13 5	4 6 54 7 32 7 18 7

Legend (left side):

COMBINED RBV/MSS BULK/PRECISION THROUGHPUT

PPR TIME (HRS/DAY)

	X.X
360/65 →	X.X X.X
360/75 →	Y.Y Y.Y
360/85 →	Z.Z Z.Z

RBV MODE VII
MSS MODE VIII

RBV MODE V
MSS MODE VI

DIGITAL COMPUTER TIME (HRS/DAY) FOR THREE COMPUTERS AND TWO PRECISION 1 MODES

Figure 2.5-16

RBV/MSS BULK/PRECISION THROUGHPUT

RBV MODES

		I		II		III		IV		V 340 FT		VI		VII 320 FT	
COMBINED RBV/MSS THROUGHPUT, ACCURACY TRADEOFF		NO CORRECTION, PRINT ON LBR		PPR DRIVES OPEN LOOP FOR ①, ②, ③ CORRELATION ON PPR		IMAGE BLOCK SHIFT FOR ① ② , ③ CORRELATION ON PPR		OPEN LOOP PPR CORRELATION FOR ALL THREE CHANNELS		IMAGE BLOCK SHIFT FOR ALL THREE CHANNELS		FULL IMAGE PROCESSING ON ①, ②, ③ CORRELATION ON PPR		FULL IMAGE PROCESSING ON ALL CHANNELS	
		NO PPR		IMAGE CORRELATION		IMAGE BLOCK SHIFT IMAGE CORRELATION				IMAGE BLOCK SHIFT NO PPR		IMAGE CORRELATION		NO PPR	

MSS MODES

I	NO CORRECTION, PRINT ON LBR / NO PPR	1	65	2	75→65	2	75→65	2	85→75	1	85	2	85	1	85 85
		12000 9000		1100 9000		980 9000		880 9000		920 9000		980 9000		710 9000	
					3→2		3→2		3→2		3→2				3→2
II	CORRELATE RBV ON ① ; USE SIGNALS TO DRIVE ②, ③ ④ / IMAGE CORRELATION	2	65	3	75→65	3	75→65	3	85→75	2	85	3	85	2	85, 85
		12000 12000		1100 1400		980 1300		880 1400		720 1300		980 1300		710 1300	
					3→2		3→2		3→2		3→2				3→2
III	PPR OPEN LOOP DRIVE FOR ALL FOUR CHANNELS	2	75→65	3	75	3	75	3	85→75	2	85	3	85	2	85, 85
		12000 2100		1100 2100		980 2100		880 2100		720 2100		980 2100		710 2100	
					3→2				3→2						
IV	IMAGE BLOCK SHIFT FOR ①, ②, ③ CORRELATION ON PPR / IMAGE BLOCK SHIFT IMAGE CORRELATION	2	75→65	3	75	3	75	3	85	2	85	3	85	2	85, 85
		12000 2280		1100 2280		980 2280		880 2280		720 2280		980 2280		710 2280	
									3→2						
V	IMAGE BLOCK SHIFT FOR ALL THREE CHANNELS / IMAGE BLOCK SHIFT NO PPR	1	85→75	2	85	2	85	2	85	1	65, 85	2	65, 85	1	85, 85
		12000 2200		1100 2200		980 2200		880 2200		720 2200		980 2200		710 2200	
		3→2		3→2											
VI (1870 FT)	CORRELATE WITH RBV FOR YAW, IMAGE BLOCK SHIFT FOR ALL CHANNELS / IMAGE BLOCK SHIFT	1	85→75	2	85	2	85	2	85	1	65, 85	2	65, 85	1	85, 85
		12000 12100		1100 2840		980 1910		880 2040		720		980 1970		710 1970	
		3→2		3→2											
VII	FULL IMAGE PROCESSING ON ALL CHANNELS / NO PPR	1	85, 85	2	85,85	2	85,85	2	85, 65	1	75, 85, 85	2	75, 85, 85	1	85 85, 85
		12000 2100		1100 2100		980 2100		880 2100		720 2100		980 2100		710 2100	
VIII (1760 FT)	CORRELATE WITH RBV FOR YAW FULL IMAGE PROCESSING FOR ALL CHANNELS	1	85, 85	2	85, 85	2	85, 85	2	85, 85	1	75, 85, 85	2	75, 85, 85	1	85, 85, 85
		12000 12100		1100 1950		980 1880		880 1950		720 1880		980 1880		710 1880	

BUY I

BUY II

ALTERNATE PRECISION I

PRECISION I

Legend key:

DIGITAL COMPUTER REQUIRED

POSSIBLE CHANGE IF BLOCK SHIFTING IS USED IN PRECISION MODE

NUMBER PRECISION PHOTO RESTITUTOR REQUIRED

X	XX → YY
	ZZZZ ZZZZ
	X → Y

RBV ERROR (FT)

MSS ERROR (FT)

DECREASED SHIFT POSSIBLE FOR CASE B

Figure 2.5-17

COMBINED RBV/MSS THROUGHPUT ACCURACY TRADEOFF

RBV MODES

	BEST PROCESSING MODES	I NO CORRECTION PRINT ON LBR NO PPR	II	III IMAGE BLOCK SHIFT FOR ① ; CORRELATION ON PPR FOR ②, ③, ④ IMAGE BLOCK SHIFT, IMAGE CORRELATION	IV OPEN LOOP PPR CORRELATION FOR ALL THREE CHANNELS	V IMAGE BLOCK SHIFT ON ALL CHANNELS IMAGE BLOCK SHIFT, NO PPR	VI	VII FULL IMAGE PROCESSING FOR ALL CHANNELS NO PPR
I	NO CORRECTION, PRINT ON LBR NO PPR	1 65 12000 9000						
II	CORRELATE RBV ON ① , USE SIGNALS TO DRIVE ②, ③, ④ IMAGE CORRELATION			3 75 → 65 980 1300	3 85 → 75 880 1400	2 85 720 1300		
III	PPR OPEN LOOP DRIVE FOR ALL FOUR CHANNELS			3 → 2	3 85 → 75 890 2820 3 → 2	2 85 720 2100		
IV								
V								
VI	CORRELATE WITH RBV FOR YAW, IMAGE BLOCK SHIFT FOR ALL CHANNELS IMAGE BLOCK SHIFT				2 85 880 2040	1 85, 85 720 2760		
VII								
VIII	CORRELATE WITH RBV FOR YAW, FULL IMAGE PROCESSING FOR ALL CHANNELS							1 85, 85, 85 2100 1880

MSS MODES

Legend:

DIGITAL COMPUTER REQUIRED

POSSIBLE CHANGE IF BLOCK SHIFTING IS USED IN PRECISION MODE

NUMBER OF PRECISION PHOTO RESTITUTOR REQUIRED

| X | XX | YY |
| ZZZZ | ZZZZ | |

RBV ERROR (FT)

MSS ERROR (FT)

X → Y

DECREASED SHIFT POSSIBLE FOR CASE B

BULK I

BULK II

ALTERNATE PRECISION II

PRECISION I

Figure 2.5-18

BEST PROCESSING MODES

2.6 GEODETIC CONTROL

· Precise geodetic control serves two functions in the NDPF

● To provide precise fixes of spacecraft attitude in selected frames thus permitting overall inprovement in location for all pictures

● To provide precise location data for selected images.

For both cases, the analysis must be performed only on a limited number of images.

Ground geodetic control will be obtained from suitable maps. Total United States map coverage is available at 1:250,000 and 40 percent coverage at 1:25,000. National map accuracy standards ensure that the points mapped will be within 0.02 inch of their correct position 90 percent of the time. This gives 90 percent accuracies of 420 feet and 42 feet for the scales previously mentioned.

The map and photographic ground control station will consist of a console unit to allow simultaneous viewing with the following translation and mensuration capabilities:

a) The RBV/MSS imagery on a 9-1/2 x 18 inch viewing stage

b) One 9-1/2 x 8 inch viewing stage where two different scales of maps on 70-millimeter film may be transported and viewed in conjunction with the RBV/MSS imagery.

The two sets of maps (at scales of 1:25,000 and 1:250,000) will be reduced 25x and recorded on 70-millimeter Itek RS^{TM} film in north-south strips covering the United States. The console will provide a viewing capability with variable magnification for both the RBV/MSS imagery and the map imagery so that measurements of necessary control points, center reseau intersection, and the center of the map(s) can be made to 12 micrometers or better.

The degree of correction will be predetermined, i.e., this will establish the number of control points necessary to meet the required accuracy of the mode used. If geodetic control is needed, the RBV imagery will be placed on the viewing stage. The geographic location of the imagery will be determined from the RBV image frame, lower left corner in direction of flight, and the roll(s) of map film containing the proper map coverage will be selected from the map file and placed on the viewer. The RBV

image to be measured will be clamped to the viewer stage by the glass pressure plate provided on each stage of the viewer. Three of the four registration marks, upper left, upper right, and lower left, will be pointed and x, y coordinates for each will be recorded. The necessary map coverage similar to the RBV coverage will be located and clamped in place on the viewer. To comparing the RBV and map images, control points visible on both the map(s) and the RBV imagery will be selected. The precise x, y coordinates, elevation, and scale will be recorded from the chosen control points on both the RBV imagery and the map (preferably the 1:25,000) and recorded. This data will be placed in the proper format on the punched tape, or other suitable input device, to be used in the PPR in conjunction with the ephemeris data, reseau measurements, and other data supplied with the RBV imagery. The data to be extracted at the map and photographic station consists of:

a) x, y coordinates of three of the four registration fiducials, upper left, upper right, and lower left in the direction of flight.

b) x, y coordinates for the center reseau point on the photograph.

c) x, y coordinates, elevation, and scale for the picture center coordinates on the map(s), to be used with appropriate scale programs.

d) x, y coordinates of each geodetic control point from the RBV imagery.

e) x, y coordinates, elevation, and scale of the identical geodetic control points on the map(s).

If ground geodetic control is used, maps in scales of 1:250,000, 1:62,500, and 1:25,000 from U.S. Geological Survey, or a similar Federal agency, will be required. The coverage is 100 percent for 1:250,000, or about 500 maps. United States coverage is about 60 percent complete for 1:62,500, or about 8,000 maps. Coverage is about 40 percent complete for 1:25,000, or about 24,000 charts.

Map geodetic control gives an accuracy that is a function of map scale (see Figures 2.6-1, 2.6-2, 2.6-3 and 2.6-4), since maps are constructed to National Map Accuracy Standards for allowable error. Thus, the need for the best possible map commensurate with the photographic
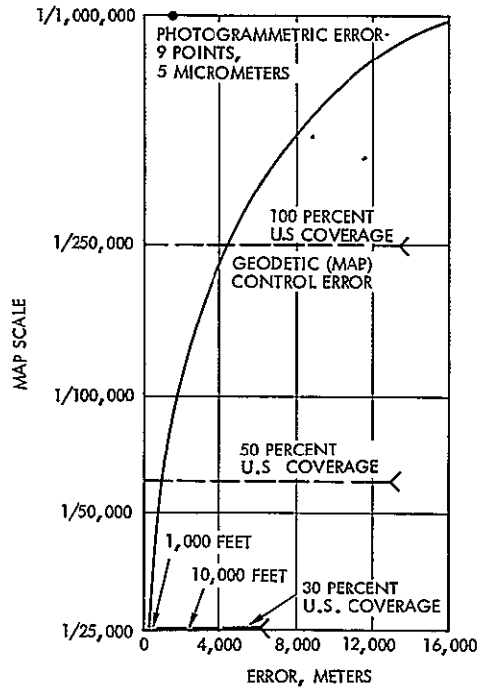
Figure 2.6-1

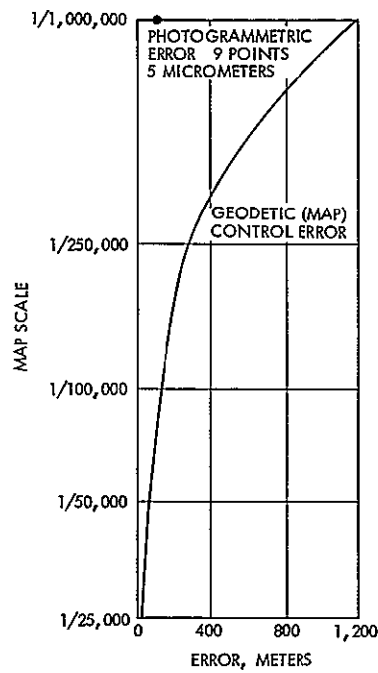ONE-SIGMA PLANEMETRIC ERROR using nine control points

Figure 2.6-2

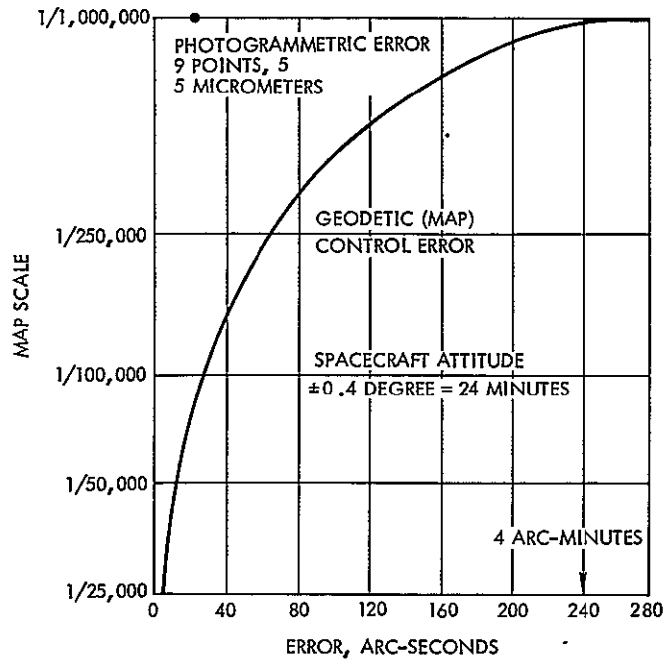ONE SIGMA VERTICAL ERROR using nine control points

Figure 2.6-3

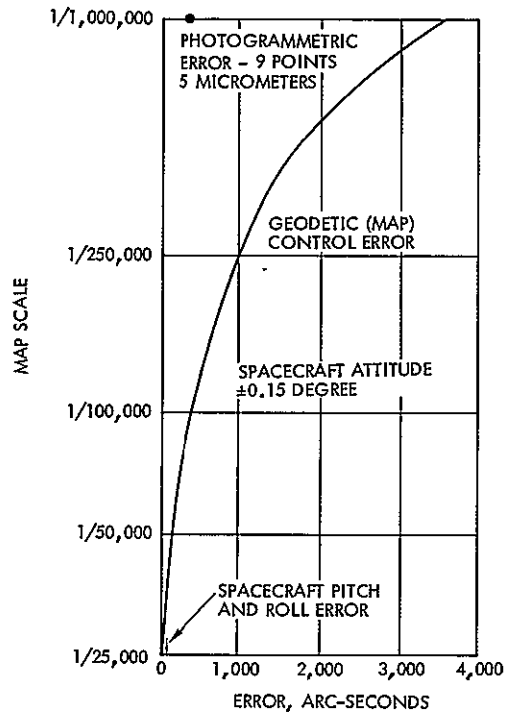ONE SIGMA AZIMUTH ERROR from nine control points

Figure 2.6-4

ONE SIGMA ROLL ERROR from nine control points

pointing accuracy capability is needed. A map scale of 1:25,000 should be used whenever possible. If nine map geodetic control points and pitch and roll from the satellite are used, it is expected that geodetic error will be ±980 feet or less.

It will be a contractor responsibility to set up the map console for the geodetic control technician. If standard practice is used for map and photographic point identification, the 1:250,000 map, the photograph, and any larger scale map must be viewed simultaneously. This would result in a three-viewer console design with a mensuration viewer similar to the Itek Mark II on left and right, and a film mensuration viewer similar to the Junior Reader in the center.

The center reseau point on the photograph and the picture center coordinates on the map (or maps) would be located and the data would be passed digitally to storage. Then nine points as near the edge as possible would be chosen on the photograph and map. Coordinates from the 1:25,000 or 1:62,500 could be entered manually on a typewriter keyboard if only one scale program was used, or they could be entered by locating crosshairs and pushing a button if three scale programs could be called.

The photographic map library would be in black and white, 25:1 reduction is now available, in microfiche or on 35-millimeter film or on 70-millimeter film if color is desirable. If an additional user viewer is desirable, it is probably best to use color, but a trained photointerpreter probably gains little over black and white. No accuracy degradation is involved in this reduction process.

From photogrammetric passpoint operations it is possible to accurately estimate the time needed to accomplish the procedure per photograph. An average of 1 hour per photograph, including coffee, eye rest, and lunch, is normal.

It should be noted that Figures 2.6-1 through 2.6-4 are errors in the accuracy of recovering the camera station position, altitude, and attitude from photogrammetric resection techniques. Although comparative accuracies on the photograph are closely related, they are not directly related. Photographic resection produces these numbers, but by biquadratic interpolation it should be possible to improve the planimetric errors.

2.7 ANNOTATION REQUIREMENTS

In order to be useful to anyone, the imagery from ERTS must be clearly identified; anyone who has examined the excellent but anonymous magazines of pictures taken from Gemini will appreciate the point.

The following sections describe the requirements defined. For the details of how the requirements are met, see Volume 14.

The basic requirements are:

- Provide clear identification of the sensor and channel providing the data.

- Provide geographic and geometric references

- Provide means to calibrate the recorder and film photometrically.

Detailed requirements are given below.

2.7.1 Geographic Tick Marks

Tick marks must be placed around the film image to correlate the picture data with the appropriate geodetic system.

2.7.2 Registration Fiducials

Fiducials must be provided to allow registration of the various images of a set.

2.7.3 Sensitometric Strips

Strips must be provided for inflight calibration, and for the recorder.

2.7.4 Identification Data

Identification must include, but is not limited to:

- Date

- Time

- Spectral channel

- Sensor

2.7.5 Annotation Text

The annotation must include, but is not limited to:

- Picture time
- Subsatellite point
- Altitude
- Sun angle
- Receiving station
- Orbit
- Orientation
- Grid center of picture
- Available DCS data
- Processing date
- Quality Assessment

2.8 IMAGE RECORDING TECHNIQUES

One important decision to be made is the selection of a device to record images on film. The precision, speed, and cost of the device have a major impact on the NDPF. This section presents a compilation and analysis of information and specifications currently available on candidate film recorders for the ERTS NDPF application. The requirements of the NDPF and characteristics of a typical recorder are presented. The results of these compilations are compared and a selection is made of the most suitable recorder designs.

Four types of recorders were considered:

- Cathode ray tube recorder (CRT)
- Electron beam recorder (EBR)
- Laser beam recorder (LBR)
- Incoherent light beam recorder (ILBR)

The first was eliminated early in the study (see Section 2.8.4).

2.8.1 Assumptions

This study is constrained by the following considerations:

- The recorder must be the best overall available to fit the ERTS NDPF applications.

- These applications include reproduction of both RBV and MSS sensed image data.

- A single recorder design is to be selected for use with both data sensor sources.

- The recorder applications include reproduction of sensor data in a bulk processing mode, and image data processed in a precision processing mode.

- The same recorder design will be used for both modes.

- The recorder selection is made on the basis of the latest information available.

- Current information as portrayed in the comparison charts is assumed accurate as presented.

- Where definitive details are lacking, the interpretation of parameters is made in accordance with the enclosed definitions.

2.8.2 Recorder Selection

The characteristics of recorders were reviewed and compared with the ERTS recorder requirements, Table 2.8-1. The most likely candidates for each technology type were selected on the basis of suitability for the ERTS program. Criteria for this selection included all the parameters shown in Tables 2.8-2, 2.8-3 and 2.8-4 with special consideration given to resolution, dynamic range, image distortions, operating speeds, and film sizes.

A summary comparison chart, Table 2.8-1, for these candidates was compiled to include the special consideration parameters and others which affect only the interfacing of equipment. On the basis of this summary and the ERTS application requirements qualified by the constraints of this study, both the RCA and CBS laser beam recorders were found to be the most suitable devices currently available in the field. This selection was based upon what is still considered to be incomplete data.

Table 2.8-1.　Summary Comparison Chart

	CBS EBR	RCA LBR	CBS Lab LBR	Litcom ILBR (CLR)
Image Quality Characteristics				
● Resolution				
Spatial	12,000 TVL	6,000 TVL at 80% 15,000 TVL (limiting)	5,000 TVL at 80% 20,000 TVL at 50%	15,600 x 7,300 TVL
Dynamic range	200 1	100 1	not known	not known
● Distortions				
Within image	Linearity 0 25%	Linearity 0 01%	<0 01%	1 in 14,600 (7 3 inch scan) (0 07%)
Image to image	Registration to 1 in 5,000	Repeatability to 0 02%	0 01%	Included in above
External Functional Characteristics				
● Inputs				
Data type	Analog video	Analog video	Analog video, scanner- recorder	Analog video
Data rate	1 to 2200 lines/sec	1000-1500 lines/sec		60 lines/sec
Control type	(not known)	(Sync required for	(Sync required for	(non-synchronous scanning)
Control rate	(not known)	control)	control)	(non-synchronous scanning)
Material	70 mm roll	9 inch roll	5 inch roll, can go to 9 inch	15 x 22 inch frame
● Outputs				
Field size	50 mm x 50 mm	Up to 9 inch wide*	Currently 5 inch film, can go to 9 inch	7 3 x 7 3 inch *ᶜ (4/frame)
Field record time	5 sec to 30 min/ image	3 5 to 5 sec per image	-	1 min/image ** 4 min/frame
Internal Functional Characteristics				
● Scan method				
Transverse (along scan)	Electronic beam deflection	Mechanical beam deflection	Mechanical beam deflection	Film motion (drum)
Longitudinal (normal to scan)	Film motion or beam deflection	Film motion	Film motion	Mechanical beam deflection

ᶜThe ERTS image size of 7 3 x 7 3 inch, plus surrounding annotation, can be accommodated within this field size

ᶜUsing stated image format, assuming data, multiplexing, line by line

Table 2.8-2. Image Recording Comparative Analysis Electron Beam Recorder

Manufacturer / Parameter	CBS	Ampex	GE	3M	IBM San Jose Capability
Type recording	EBR - image recording-analog input	EBR-2 devices 1) Image reader (w/record feasible) analog input 2) Analog signal recorder (w/read back capability)	EBR-image recorder Analog input	EBR-digital input computer control (printer, on film).	EBR-image recorder analog input
Resolution	CBS brochure states 100 lp/mm 12,000 TVL on 70 mm film	1) 100 lp/mm on 4-1/2 scan equivalent to 22,800 TVL 2) Scan separation 20 μm on 21 mm field size ≈ 2010 TVL	>130 lp/mm If 4-1/2 inch field assumed this is ≈29,460 TVL	Film resolution 1500 lp/mm ≡ 30,000 TVL when a 10 mm field is assumed Note that this is film resolution and does not necessarily represent character record rate, or capability	10,000 TVL "of information" 5 μm spot, 50 mm field) 22,000 TVL "of information" (5 μm spot 4-1/2 inch field) Contiguous element recording in both image coordinates
Spot size	Approximately 2 μm	--	5 - 8 μm	--	5 μm
Grey scale	>20 Shades of grey	--	--	--	32 equal density steps in density range of 0 05 to 3 0 range
Dynamic range	200 1 for a film density of 0 to 3	--	Contrast ratio 100 1	--	500 1 For a density range of 0 05 to 2 75
Gamma	Gamma correction in video amplifier	--	--	--	Gamma variable 1 to 1 5 full grey level gamma correction
Registration	Pin registration required to 1 in 5,000	--	--	--	Frame to frame 0 1% for 70 mm including film tolerance
Repeatability Linearity	Scan linearity of <±0 25%	1) -- 2) -27 DB from reference level	--	--	0 1%
Jitter	--	1) -- 2) Timing error 0 25 ns rms	Horizontal is 1 in 25,000	--	1 in 30,000 in both directions
Scan coordinate error	Scan raster size maintained to 1 in 1,000 Geometric distortion < 0 05% in frame scan mode	--	--	--	--
Longitudinal error	--	--	--	--	--

Table 2.8-2. Image Recording Comparative Analysis
Electron Beam Recorder (Continued)

Manufacturer Parameter	CBS	Ampex	GE	3M	IBM San Jose Capability
Film size	70 mm roll (assuming 50 mm field) Line or frame scan	1) 5 inch 2) 35 mm roll	5 inch	16 mm roll (dry silver, heat developed)	70 mm roll w/ 50 mm field 5 inch w/4-1/2 inch field line scan
Film rate	1 frame per μ5 sec 5o 30 min	1) 0 25 inch/sec 2) --	0 37 to 0 98 inch/sec	--	1 frame per 5 seconds
Writing speed	--	--	--	30,000 lines/ minute also given as 60,000 characters/ second	
Scan rate	Variable 1 to 2200 lines/ seconds	--	--	--	Range of 1500 to 8333 Hz in 5 steps
Bandwidth	Requirements suggest 4 - 6 MHz video circuit band- width to 10 MHz	1) 0-25 MHz at 3 db 2) 0 5 to 100 MHz	20 MHz goal	--	10 MHz, video bandwidth to 50 MHz
Annotation	Digital input capability suggests annotation possible but not directly	--	--	Yes, as machine is printer	Not directly feasible
Filament life	--	--	1000 hours is an expectation	--	With better vacuum and LaB_6, 1000 hours
Comments					Compact gun Design
Cost	--	--	--	--	--
Special features					Special gun design permits compact size to scan large (4-1/2 inch) field with mini- mal error

Table 2. 8-3.   Image Recording Comparative Analysis
Laser Beam Recorder

Manufacturer / Parameter	Ampex	CBS Commercial Model	CBS Laboratory Model	Dresser	General Precision	RCA Engineering Model	Synergistics
Type recording	LBR - analog input recorder	Image reader/ recorder - digital control LBR	Image reader/ recorder LBR analog input	LBR - plotter digital inputs	LBR - reader	LBR-image recorder analog input	LBR data recorder-analog or digital
Resolution	10 mm scan line ≡ 1670 contiguous spots along scan with 6 μm spot and 12 μm line spacing This is ≡ 83 5 lp/mm or 167 TVL/mm\n\nFor a 10 mm x 10 mm frame, this is ≡ 1670 TVL in the vertical direction	100 lp/mm ≡ 10, 000 TVL extra-polated to 50 mm field size	20, 000 elements at 50% response, 5000 elements at 80% response	Max resolution 8, 000 contiguous spots in 40 inch wide field This is equivalent to 8000 TVL\n\nWhen extrapolated to 9 inch wide field this is ≡ 450 TVL	228 lp/mm 10, 500 elements in X scan 7, 500 elements in Y scan\n\nAssuming these figures are for contiguous elements the resolutions are 10,500 TVL in X, 7, 500 TVL in Y	6000 TVL at 80% response ≈ 15 lp/mm 15, 000 TVL at limiting resolution	
Spot size	6 μm	5 μm or 10 μm	5 μ Adjustable spot, 6-12 μ in vertical dire direction	5 mil or 10 mil	--	0 8 mil, horizontal 1 5 mil, vertical independently adjustable	--
Grey scale	No indication possibly because it is an analog data recorder	--	13 √2 steps	16 levels	--	13 √2 steps	--
Dynamic range	100 1 (30 DB)	--	--	Believed to be 100 1	--	>100 1	
Gamma	Appears to be variable over a factor of 3 with 50% light inten-sity modulation Compensatory circuitry permits a factor of 4	--	--	Intensity of each shade of grey adjustable from 0 1 to 21	--	Gamma correction for sensor	--

Table 2.8-3. Image Recording Comparative Analysis
Laser Beam Recorder (Continued)

Manufacturer Paramater	Ampex	CBS Commercial Model	CBS Laboratory Model	Dresser	General Precision	RCA Engineering Model	Synergistics
Registration	Maximum transport position error 10 μm ≅ 0 1% or 1 in 1000 in a 10 mm field	--	--	--	1 part in 10,000	--	--
Repeatability						0 02%	
Linearity	Scan velocity error < 0 01% (See coordinate errors also)	--	< 0 01%	See other parameters	See jitter	Currently 0 01% linearity	--
Jitter	Could be 0 01% for line length	Rotation of drum controlled by low jitter servo drive	0 01% - 0 02% in longitudinal direction	--	X jitter 0 35 μm Y jitter 1 1 μm	0 01% of raster width maximum	--
Scan coordinate error	Line length motor hunting < 0 01% Line shift Optical error 0 005% Skew sequential error 1 0% Skew fixed error 4% (Due to 2 beams)	--	0 01%	0 05% in scan direction	--	0 02%	--
Longitudinal error	Polygon face error 5 8% Transport flutter error 0 25%	--	0 01%	0 05% in film step direction	--	0 05%	--
Film size	16 mm roll	70 mm × 100 mm chip - frame format	Currently 5 inch roll, can go to 9 inch as required	42 inch wide 40 inch wide field	Probably microfilm aperture card	9-1/2 inch wide roll up to 125 ft Frame format 9 inch wide	8 mm roll
Film rate	7 5 inch/sec	Scan produced by drum rotation	Scan produced by swept beam	Variable 5 mil steps		Continuously selectable up to 4 inch/sec	

Table 2. 8-3. Image Recording Comparative Analysis
Laser Beam Recorder (Continued)

Manufacturer / Parameter	Ampex	CBS Commerical Model	CBS Laboratory Model	Dresser	General Precision	RCA Engi- neering Model	Synergistics
Writing speed	--	--	See resolution	Sweep speeds in steps 14 6 to 2 15 ms/sweep	--	--	Bit density along track 180K bits/ inch
Scan rate	1600 lines/sec (from 2 beams)	--	1250 lines/sec or as required	See writing	--	1000-1500 lines/sec.	36 tracks on film 1 2 megabyte
Bandwidth	0 to 5 5 MHz	--	100 MHz	--	--	0-4 MHz ±1 DB	Packing density 7 M bits/inch^2
Annotation	--	Digital, direct annotation feasible via computer.	Possible with the signal beam	Digital direct annotation feasi- ble via computer	--	--	Digital, direct annotation feasi- ble via computer
Filament life	N/A	N/A Helium-neon laser	N/A	N/A	N/A	N/A Helium-neon laser	N/A
Comments	Initially designed for generation of analog data recordings	Both a reader and a recorder, digi- tally controlled from computer	Both a reader and a scanner This 5 inch LBR is a lab model -- very recent information	Steps film for each scan (not continuous motion) tied to 360.	--	4-sided mirror prism w/single beam used, analog video input, sync input to control speeds	--
Cost	--	--	--	From $88, 500	--	--	$65, 000
Special features							

Table 2.8-4. Image Recording Comparative Analysis
Incoherent Light Beam Recorder

Manufacturer / Parameters	Litcom Division Litton Industries	Muirhead Instruments Ltd (England)	IBM*- Kingston	IBM - Research
Type recording	Pressfax image photo recorder - (CLR), analog drum scanner	Pagefax (black/white) recorder (CLR), "binary" drum scanner	Drum scanner - line drawing reader - (black on white) into digital format	Grating controlled scanner - CRT, FSS film reader (also has write mode)
Resolution	Max transverse resolution ->2000 1/inch for 22 inch long scan (44,000 elements) (same as horizontal) Max long resol ≡ scan density = 1000 1/inch for 15 inch ≡ 15,000 elements Note Hughes proposes 2 x 2 (4) pictures/field for MSS use Picture size = 7 291 inch x 7 2 x 91 inch For these conditions, maximum resolution is 15,582 TVL (horizontal) by 7,291 TVL (vertical)	Capability of 1500 TVL/inch soon (presently 1000 TVL per inch)		Resolution computed for reading - 45 μm spot across 9 inch diameter face = 5,080 elements But this is diagonal measurement of a picture Assuming square format using maximum tube diameter resolution is 3,090 TVL (elements) Resolution for writing would be function of scan rate and ability to change rate as this is writing mode modulation method See special features This resolution should not exceed the read mode resolution
Spot size	0 0028 x 0 0014 inch -(70 μm x 35 μm)	0 001 inch square	-	Minimum 37 5 μm at center - using 45 μm across 9 inch face
Grey scale	Can be 16 √2 shades for transparencies	Black or white only, (newspaper text)		None - as reader constant intensity maintained to 2%
Dynamic range	-		-	*Assumed 10 1 as ratio of exposure times, (variability unknown), see writing speed
Gamma	Correction provided			
Registration	See special features		‵	
Repeatability				
Linearity	Scan linearity and repeatability - Peak deviation <0 0005 inch (1/14,600 for 7 3 inch scan)			
Jitter	0 007% included in linearity figure (due to drum motor "hunting")	Less than 0 001 inch on a scan line		
Scan coordinate error (traverse)				
Longitudinal error		Line spacing repeatable to 10% (Expect 5%)		
Film size	Film frame on drum Field Size - 22 x 15`4 inch (max) MSS proposed 7 291 x 7 291 inch per picture	Assume film frame (known rotating drum) field size unknown)		Up to 10 x 10 inch frame sizes planned Transport movable 2 coordinates Field size 30 mm diameter

Table 2.8-4. Image Recording Comparative Analysis
Incoherent Light Beam Recorder (Continued)

Manufacturer / Parameters	Litcom Division Litton Industries	Muirhead Instruments Ltd (England)	IBM - Kingston	IBM - Research
Film rate	N/A film frame on rotating drum	N/A film on rotating drum		
Writing speed				
Scan rate	60 lines/sec Drum RPM = 3600	60 lines/sec Drum RPM = 3600		
Bandwidth		Intensity (on-off) Modulation to 1 MHz		
Annotation	Analog control direct annotation not practical	Input unknown, but "newsprint text" would indicate capability.		
Filament life	Light source is crater lamp - (glow - modulator tube)	Present crater lamp current high to obtain intensity Life = 4 hrs		
Comments	Recording time 1 04 min/pic (average) but it takes 4X that for one film frame containing 4 pictures (plus film change time)	Mentioned in both Westinghouse & Hughes ERTS documents Mfr quoted as saying no plans for grey level modulation	Model delivered to Canada, 3 years ago	
Cost		Lamp cost $20 for 4 hrs		
Special features	Four quadrant recording system allows registration errors to be function of relative "head position" for the 4 pictures on any frame (This system proposed by Hughes for MSS use) (Evidently this is recorder being used by Hughes)			For writing, a constant intensity beam is changed in velocity to produce exposure Beam position monitor (grating sensor) sends feedback via A/D to IBM 1130 which is control source Permits addressing to 1/16 spot diameter which yields 48,000 addressable points

Radical changes in the data for available recorders or in the ERTS require-
ments may show another design to be a better match with requirements.
For this reason and because in general LBR technology is rapidly develop-
ing, it is appropriate to leave the selection and detailed specification of a
particular laser beam recorder design to phase D of the ERTS program.
However, manufacturers' responses to a recording RFP which was issued
as a result of the present phase B/C effort have led to a tentative selection
of an RCA device.

Four candidate film recorders were selected as follows:

a)   RCA engineering model LBR

b)   . CBS laboratory model LBR

c)   CBS EBR

d)   Litcom ILBR

The following describes the considerations given to each of the
candidate recorders in arriving at the LBR selections:

- Resolution - All four candidates have more than adequate resolu-
  tion, in television lines, for the ERTS application.

- Dynamic Range - CBS EBR and RCA LBR both have adequate
  dynamic range for ERTS. The dynamic range for the Litcom
  ILBR is not known but the technology indicates a possible
  problem.

- Distortions - Litcom has the best linearity, followed by CBS lab
  LBR, RCA LBR, and CBS EBR respectively. Image to image
  figures are not directly comparable.

- Operating Speeds - The time to record a complete raster field is
  seen to be similar for RCA LBR and CBS EBR, with Litcom
  significantly longer. Throughput capability will also be affected
  by the film type, reloading and calibration considerations. With
  these criteria added, the CBS EBR while using roll film will
  suffer from vacuum system and calibration considerations, and
  Litcom will require more time to reload film for each frame.
  The resulting analysis appears to show that the RCA LBR and the
  CBS lab LBR have the best throughput and duty cycle capability.

- Film Size - RCA, CBS and Litcom can produce a picture image of
  7.3 inch x 7.3 inch. CBS EBR picture image size must be com-
  patible with an overall raster size of 50 mm x 50 mm including
  picture and annotation. The larger image capability better
  matches ERTS requirements.

In summary, both the RCA engineering model LBR and the CBS laboratory model LBR designs can provide resolution, dynamic range, and linearity more than adequate to meet the requirements of the ERTS program. These units should have the best throughput for any given input data rate and produce the preferred large image format. A tentative choice based on proposals submitted in response to a recent RFP is the proposed RCA device. A test pattern produced on the RCA engineering model is shown in Figure 2.8-1. A glossy print of this figure is included in the envelope at the back of this volume.

2.8.3 Recorder Comparative Analysis

The charts summarize all the available recorder information into a comparable format. The format chosen uses a common selected grouping of parameters which cover most of the characteristics as presented by the various manufacturers. Error data for image distortion, in particular, is in overlapping categories to more accurately show original information.

The charts are grouped to present parameters of all equipment by manufacturer within a technology type classification. The technologies considered were - Electron beam recording (EBR), Laser beam recording (LBR), and Incoherent light beam recording (ILBR) which is a grouping covering all other technologies for high resolution film recording such as cathode ray tube and crater lamp recording.

2.8.4 Analysis of the Cathode Ray Tube

Early in the ERTS project, a cathode ray tube seemed to be a likely device to record the images either from the video, or as output from digital image processing.

There are five major characteristics of photorecorders which must be considered for MSS and RBV application. These are:

- Registration - which involves temporal and spatial repeatability or stability.

- Radiometric Efficiency - which affects the maximum rate of recording.

- Resolution - which deals with the spatial frequency response or transfer function.
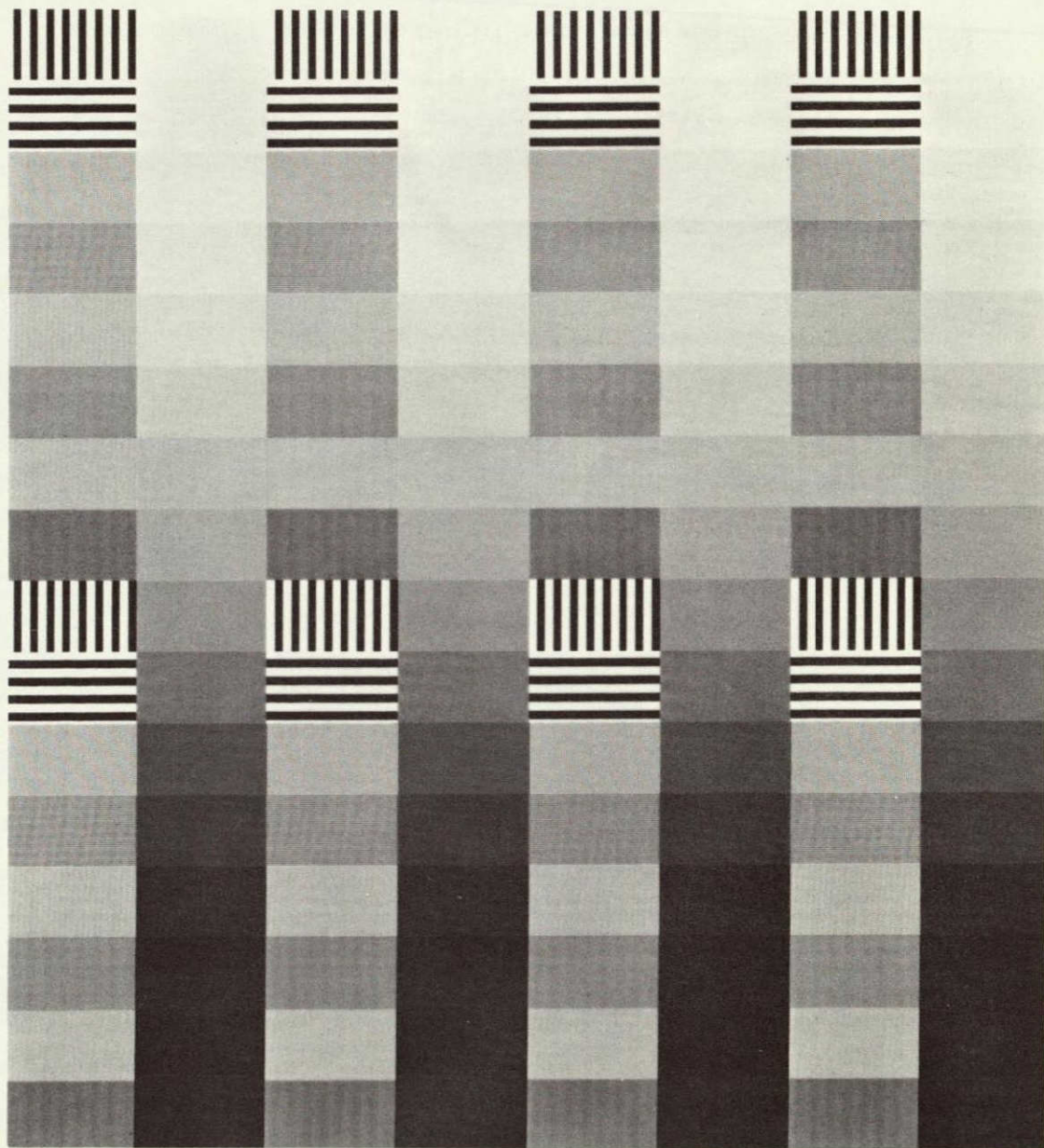
Figure 2.8-1

TEST PATTERN produced on RCA engineering model laser beam
recorder (See glossy print in envelope in back of volume)

- Dynamic Range - which deals with the photometric transfer function.

- Geometric Fidelity - which involves spatial geometric fidelity.

In summary, the cathode ray tube lacks the resolution and dynamic range of the electron beam recorder. It has the same sorts of stability problems. As a consequence, it was eliminated as the ERTS primary recorder. The recommendation for this came only after a careful examination of the best available cathode ray tube, from CBS, described in Section 2.8.4.3.

2.8.4.1 Registration Error

The first characteristic considered is that of registration. Despite some initial concern on this point, it appears that the registration characteristics of the CRT are adequate.

The question of acceptable registration must be examined first. Registration error is here defined as

$$E = \frac{\Delta d}{W}$$

where Δd is the scalar distance between two image points, one of which is taken to be at the theoretical or reference position for the other and W is the maximum frame dimension (length or width). Thus E is equally applicable as the defined registration error between two time-serial images obtained from the same recorder or concurrent images obtained from separate recorders.

In order to establish a criterion for registration acceptability, we will allow the angle included at the eye by Δd to be one minute of arc, which is the established normalized value for visual acuity. At a reading distance of 18 inches, Δd = 0.01 inch and W can be taken as 9 inches. This, then, establishes the registration error at

$$E = \frac{0.01}{9} = 0.0011$$

The reading distance and the value for W are consistent with normal practice with page size copy. Since the scale factors and intervening processes which would be necessary to consider for generation and/or viewing of different size frames, such as 70 mm, would be common to all forms of photorecording, the analysis being made herein applies to the unique properties of CRT systems although some similarity is clearly present with electron beam recorders.

Table 2.8-5 lists the most important registration error sources, e_j. These are assumed to be independent, random, and normally

Table 2.8-5. CRT Recorder Random Error Contributions

Error Source	e_j	e_j^2
Deflection yoke misalignment	2×10^{-4}	4×10^{-8}
Thermal variations in yoke	4×10^{-4}	16×10^{-8}
Orthogonality misalignment	4×10^{-4}	16×10^{-8}
Focus coil misalignment	2×10^{-4}	4×10^{-8}
Thermal variations in focus coil	2×10^{-4}	4×10^{-8}
Focus coil symmetry	4×10^{-4}	16×10^{-8}
Power supply drifts	5×10^{-4}	25×10^{-8}
CRT faceplate distortion	3×10^{-4}	9×10^{-8}
Magnetic memory*	(10×10^{-4})	(100×10^{-8})

$$\sum e_j^2 = 94 \times 10^{-8}$$

$$E = \sqrt{\sum e_j^2} = 9.7 \times 10^{-4}$$

*Magnetic memory may be neglected if the end-of-frame biasing current in the yoke is always the same, as can be assumed for raster-scan systems.

distributed.   Under these conditions it can be shown that for 99.87 percent
of all cases (standard score = 3), the combined registration error is
given by

$$E \cong \sqrt{\sum_{j=1}^{n} e_j^2}$$

which is sometimes called the RSS, or root sum square.   The computed
value for E in the table is 0.00097 which is smaller than the value
obtained as an acceptable error in the preceding paragraphs (0.0011).

It should be noted that some of the error sources listed (such as
CRT faceplate distortion) can be ignored when recording time-serially
from the same CRT, or can be considered systematic errors for any
given multi-channel installation.   Any systematic errors can be designed
or calibrated down to acceptably low values.   The most common of these
include deflection geometrical distortion (e.g., - pincushion), differential
optical magnification, and first order or Seidel aberrations.

2.8.4.2 Radiometric Efficiency

The radiometric efficiency of the CRT is a matter of soul concern,
particularly in competition with the EBR.   The CRT electron beam must
excite the phosphor which then exposes the film, whereas the EBR
electron beam directly exposes the film.   The result is that the EBR needs
a lower energy beam than the CRT, with attendant advantages.

Classically, exposure of light-sensitive emulsions has been stated
in photometric terms, with a few notable exceptions (e.g., x-ray plates).
Under ordinary conditions of daylight or artificial illumination, such
practice has been adequate.   When photographing spectrally restricted
sources such as CRT phosphor screens, we frequently find that a large
portion of the radiated energy lies outside the spectral limits defining
photometric units.   It is therefore necessary to employ a unified approach
which will accurately predict the energy transfer between source and
film.

We will confine our remarks to silver halide emulsions due to their considerably higher sensitivities compared with other more recently developed coatings. The basic spectral sensitivity of silver halides lies between 300 and 500 nm, being maximum at 400 nm. Such films are non-color sensitized or "color-blind". By selective dye sensitization, spectral sensitivity can be extended to near 600 nm in which case the material is called orthochromatic (ortho) or to 650 nm which is called panchromatic (pan) response.

There are four CRT phosphors which have the combined properties of relatively high efficiency, fine structure, low persistence, and suitable spectral response to be suitable for film recording. These are:

a) P5 - a medium short persistence blue phosphor lying between 350 and 600 nanometer with peak response at about 415 nanometer.

b) P11 - a medium short persistence blue phosphor lying between 400 and 580 nanometer with peak response at 460 nanometer.

c) P16 - a very short persistence bluish purple phosphor lying between 340 and 470 nanometer with peak response between 380 and 390 nanometer.

d) P24 - a short persistence green phosphor lying between 410 and 680 nanometer with a peak response at 510 nanometer.

The effective radiation magnitude from any phosphor depends upon the nature and energy of the exciting source, the quantum conversion efficiency of the phosphor material, and the nature of the screen deposition process. For electron beam excitation, Table 2.8-6 lists the radiant equivalents, or absolute efficiency (η), for the above phosphors. Table 2.8-7 lists the screen utilization factors (K) as a function of deposition process.

We will now define the phosphor-emulsion spectral transfer efficiency, α as follows: Let $A\lambda/A_{max}$ = relative phosphor radiation at wavelength λ, then

$$P_A = \int_{\lambda 1}^{\lambda 2} \frac{A\lambda}{A_{max}} d\lambda$$

where P_A is the relative radiance between the limits $\lambda 1$ and $\lambda 2$.

Table 2.8-6. Radiant Equivalents of Four Phosphors

Phosphor Type	Absolute Efficiency, η (Radiated watts per watt of excitation)
P5	0.025
P11	0.10
P16	0.049
P24	0.025

Table 2.8-7. Typical Phosphor Deposition Screen Utilization Factors

Screen Process	Utilization Factor, K
Coarse settled, aluminized	1.0
Fine-grain settled, aluminized	0.5
Vapor-reacted, unpolished	0.3
Vapor-reacted, polished	0.1

Similarly, let $B\lambda / B_{max}$ = relative emulsion sensitivity at wavelength λ, then

$$P_B = \int_{\lambda 1}^{\lambda 2} \frac{B\lambda}{B_{max}} d\lambda$$

where P_B is the relative emulsion response between the limits $\lambda 1$ and $\lambda 2$.

The spectral transfer efficiency may now be given as

$$\alpha = \frac{\int_{\lambda 1}^{\lambda 2} \dfrac{A_\lambda}{A_{max}} \dfrac{B_\lambda}{B_{max}} d\lambda}{\int_{\lambda 1}^{\lambda 2} \dfrac{A_\lambda}{A_{max}} d\lambda} \cdot$$

Table 2.8-8 lists values of α for the four previously mentioned phosphors combined with either orthochromatic or non-color sensitized emulsions.

The energy density available for recording can now be given as

$$E = \frac{\eta \alpha \beta K W \tau}{A} \times 10^7 \; ergs/cm^2$$

Table 2.8-8. Phosphor-Emulsion Spectral Transfer Efficiency

	P5	P11	P16	P24
α_1	0.68	0.50	0.95	0.15
α_2	0.87	0.87	0.93	0.81

α_1 = transfer efficiency with non-color sensitized emulsion

α_2 = transfer efficiency with orthochromatic emulsion

where

η = phosphor absolute efficiency (Table 2.8-6)

α = spectral transfer efficiency (Table 2.8-8)

β = optical efficiency

W = screen utilization factor (Table 2.8-7)

τ = time to scan area A, seconds

A = scanned area on phosphor, cm^2

The values chosen for τ and A in the above may apply to a single spot, a line, or a raster (providing that the lines are assumed to have negligible spacing). By substituting typical quantities in the expression for E and comparing the obtained energy with candidate film sensitivities, we can predict whether or not an acceptable film record can be obtained. Before doing so, we must define optical efficiency.

It can be shown that the energy radiated from an isotropic plane source is collected by an optical system proportionate to the fourth power of the cosine of the angular aperture. The resulting image irradiance is independent of the object distance because the inverse square law affects both the amount of radiation collected and the image size, thereby maintaining a constant ratio. The aperture of the optical system, or F-number, is the critical parameter affecting image irradiance. We can define the optical efficiency as follows:

$$\beta = \frac{f^2 HT}{4V^2 F^2} \cos^4 \theta$$

where

    f = focal length

    V = image distance

    F = aperture ratio (F-number)

    θ = angle of image point off axis

    H = transmission factor at points off axis due to lens barrel vignetting

    T = transmission factor due to reflection and absorption by glass

For modern lenses of six to eight glass-air surfaces, T = 0.7. We can allow θ = 15 degrees as a weighted average displacement for most important objects. Typically, we can assume H = 0.75. Finally, we can assign the following values assuming the condition of photorecording

from a 7.5 x 7.5 cm CRT area to a nominal 70 mm film base (approximately unity magnification):

$$V = 100 \text{ mm}$$

$$f = 50 \text{ mm}$$

$$F = 2.0$$

Under the above conditions the optical efficiency obtained is $\beta = 0.007$.

We are now ready to obtain E. Examining Tables 2.8-6 and 2.8-8 we find that the product $\alpha\eta$ is maximized by selecting the P11 phosphor and an orthochromatic emulsion. Assume the following values

$$\eta = 0.87$$

$$\alpha = 0.1$$

$$\beta = 0.007$$

$$K = 0.5$$

$$W = 0.2$$

$$\tau = 1$$

$$A = 45$$

from which it follows that $E = 13.5 \text{ ergs/cm}^2$. This compares favorably with medium speed emulsions requiring on the order of 0.1 erg/cm^2 at 430 nm to just obtain an image and 1 to 2 log E units to obtain full dynamic range. Resolution of such emulsions is on the order of 150 lines/mm. Under the conservatively assumed conditions, therefore, one RBV or MSPS frame can be recorded from CRT to film per second. It is not unreasonable to expect to achieve even faster recording times using CRT-film systems should this be necessary. Conversely, slower recording times may possibly be acceptable, thereby assuring beyond doubt that the maximum attainable image quality using CRT-film techniques could be expected.

2.8.4.3 CBS High Resolution CRT

The preceding theoretical analysis was sufficiently interesting to suggest that data should be acquired on an actual device.

A very high resolution (8000 TV lines) has been developed by CBS Laboratories. The tube has a very short persistance phosphor (P-24) and is used for photographing on film.

Complete display systems have been developed for commercial applications. The CRT has been used in the LINOTRON photocomposing system for the Government Printing Office (Electronics, April 3, 1967, pp 113-127). It is also used in a flying-spot scanning system for use in TV applications.

The dynamic range is ten $\sqrt{2}$ grey shades (32/1), and the precision of registration is 1/5000. A sophisticated electron optical system is used to eliminate raster distortion.

For the ERTS application, this component does not offer an advantage over the EBR from the standpoint of image quality, as the dynamic range of the CRT is far less than that of the EBR. No system development has been initiated for the ERTS application. Characteristics of the CRT are defined in Table 2.8-9.

Table 2. 8-9. CBS High Resolution Linotron Display Specifications

Item	Specification
Type No	CL 1242 P 24
Phosphor type	P-24 (fine-grain)
Tube diameter	7 in
Display	6 in
Tube length	26 in.
Magnetic components	Alignment coil
	Astigmatism coil
	Static focus coil
	Dynamic focus coil
	Major yoke (positioning)
	Minor yoke (writing)
	Pincushion correction pole pieces
Spot diameter	1 5 mil
Registration accuracy	0 02%
Stability-Long term	0 01%
Skew	0 05%
Deflection uniformity	0 10%
Pincushion distortion	1.0 mil in 5 in
Raster parallelism (opposite sides)	2 0 mils
Resolution	24 lpm at 20% response 8000 TVL limiting
Anode voltage	30 to 45 kv

The CBS CRT has been developed primarily for use in complete display systems. Development of a display system has not been initiated for the ERTS program. Although this CRT represents the state-of-the-art in recording CRT's, consideration of this component for the ERTS GDHS is not recommended as image quality will be inferior to that of the EBR, and funding of a complete display system development would be required.

2.8.4.4 Practical Considerations

There has been a long history in the broadcast industry, in the pre-video tape era, of trouble with using CRT's for precision recording. Some of the problems were, and are:

- Phosphor lifetime. When a CRT is used at the high beam currents required for peak performance, the phosphor luminescence drops with time. The effects vary widely and erratically across the tube face.

- Sensitivity and adjustments required by driving circuitry. The driving circuits require zero adjust and gain adjust; they tend to drift. To achieve precision beam placement requires both automatic compensation, and careful manual adjustments.

- Need for laboratory conditions. To achieve the system performance stated requires conditions hard to achieve in a practical working environment.

This latter point is quite significant. Consider the problem of achieving a spot precision of 1:8000 the resolution of the CBS tube. This requires that the noise voltage not exceed 1:16000, which corresponds to a power ratio of $(16,000)^2$, or 84 decibels signal to noise.

If one reduces this to an overall voltage accuracy of 1:4000, the signal to noise ratio drops to 72 decibels. This is still hard to achieve. If one precision CRT installation, sixty hertz noise could not be reduced to the necessary level. The sweep had to be synchronized with the power line so that the distortions would be uniform across the picture.

In the same case, a calibration run was made daily for both geometric and photometric behavior.

This set of practical considerations led to dropping the CRT as a recording device.

CONTENTS

3. PCM TELEMETRY AND DCS DATA PROCESSING REQUIREMENTS

3.1 SUMMARY OF REQUIREMENTS AND ENVIRONMENT

The basic telemetry, and the DCS data, arrive as a common stream. The video data arrives as a different stream handled in a different fashion. The basic requirements are thus:

a) Reformat and edit the telemetry stream into an appropriate form.

b) Pull out the necessary data, and generate annotation data.

c) Develop the necessary files for the DCS data.

Analysis of the problem has shown that this can be subdivided into six functional areas viz.:

- The digital tape generator accepts digitized data from the PCM data handling equipment and creates the digital PCM tapes, digital DCS tapes and the time reference tape.

- The PCM pre-processor verifies and/or corrects the Greenwich mean time assigned to the PCM data, extracts camera exposure times, merges orbital parameters and creates the initial space-craft reference tape.

- The attitude determination function determines the attitude of the spacecraft, creates the attitude history tape and merges the atti-tude data with the corrected time and orbital parameters, creating the final spacecraft reference tape.

- The image annotation function will generate the annotation data required by the bulk image processing function. An annotation tape will be created and the initial entries in the index/abstract file will be generated.

- The PCM data base generator will merge the spacecraft house-keeping parameters with the corrected time, orbit and attitude data. The housekeeping parameters will be quality flagged and converted to engineering units. This function will create the master digital data tape.

- The DCS data base generator will identify, verify and calibrate the DCS data. Time corrections will be made, when necessary, and the DCS tape will be created.

3.2 DIGITAL TAPE GENERATOR

In the design of the digital tape generator, consideration was given to the approach being used in the processing of OGO-F PCM telemetry

data. The concept of creating a separate magnetic tape containing only the Greenwich mean time and spacecraft clock readings, as the digital PCM tapes are created, will be expanded for ERTS to include the attitude data and camera exposure times. This approach allows the time correction, attitude determination and picture annotation functions to be performed with much less data manipulation, since the spacecraft housekeeping parameters which account for approximately 95 percent of the PCM telemetry are not processed until these functions are completed.

Since the processing required for the PCM and DCS telemetry will be similar in many aspects, full advantage of this commonality will be taken in designing the digital tape generator.

3.3 PCM PREPROCESSOR

In determining the method to be used to correct the Greenwich mean time assigned to the PCM telemetry data, the major consideration was the accuracy required by the attitude determination and picture annotation functions. The time correction techniques presently being used on the applications technology satellites (ATS), the interplanetary monitoring platforms (IMP) and the OGO satellites were studied with the following resultant conclusions. While the ATS technique provides the accuracy required, the amount of direct access storage required by this technique is prohibitive. The IMP technique is based on algorithms requiring more real time data than is anticipated from the ERTS spacecraft. The technique being used for OGO-6, while efficient and designed for comparable amounts of real time data, lacks the accuracy required for ERTS. Based on these findings, a technique for ERTS was decided upon which would be patterned after the OGO technique, but which would incorporate the algorithms of ATS to provide the required accuracy.

3.4 ATTITUDE DETERMINATION

The determination of satellite attitude is one of the more significant problems in ERTS. The largest single source of error in picture center is the attitude uncertainty. It is thus important to do the best possible job in using telemetry data to determine attitude.

The resolution accuracies specified for ERTS require two levels of spacecraft attitude determination. The first level, applicable to the coarse

resolution accuracy of 10 n. mi., is achieved by directly reading and
smoothing the appropriate data from ERTS telemetry tapes, viz., pitch,
roll, and yaw error signals. The second level of attitude determination
is applicable to the firm resolution accuracy of 2 n. mi. and is achieved
by optimally filtering all available telemetry data over wide time intervals
to update and improve spacecraft attitude estimates.

The method which accomplishes both required levels of attitude
determination is one of batch processing since this corresponds to the
manner in which the ERTS ground based system receives data, tape play-
back, etc. The program accepts processed telemetry data and, after
editing, proceeds to smooth the pitch, roll, and yaw data with a sliding
arc second degree polynominal. Outputs are obtained at the midpoint of
the smoothing interval and thus provide the first required level of attitude
determination.

The second level of attitude determination is based on a realistic
model of spacecraft attitude dynamics, coupled with a direct-search
optimal filtering function. The attitude dynamics program generates, by
numerical integration of the complete, nonlinear, coupled, attitude equa-
tions of motion, a set of ERTS pitch, roll, and yaw "trajectories" based
on an initial (To) attitude state and nominal values for several model
parameters whose exact values are not known. At each observation time,
computed values of observables are obtained from the results of the
numerical integration; a quadratic cost function is then formed and the
direct-search program (1) proceeds to systematically adjust the initial
attitude state and model parameters until this cost function is minimized.
The direct-search program is based upon Powell's direct search algorithm
for numerical optimization of a function of several variables and (2) uses
built-in logic to obtain the optimal estimation of attitude state.

To insure accurate and realistic data fits, all known disturbance
and error sources are to be included in the attitude dynamics model. Thus,
specified thermal deformation effects, sensor misalignments, and sensor
biases are to be incorporated, depending upon degree of uncertainty, with
an adjustable parameter.

The attitude state, angle and angle rates, required to initialize the
attitude dynamics model is obtained from the smoothing function, digital

filter, previously described. Additional data, e. g., wheel speeds, required to initialize the attitude dynamics model are received directly from the processed ERTS telemetry. Spacecraft orbit data, a solar ephemeris, and a model of the earth's magnetic field are also necessary to calculate all position-dependent disturbance torques.

The observables for the direct-search filtering consist of onboard-acquired (unsmoothed) pitch, roll, and yaw angles; wheel speeds; solar array shaft angles; onboard solar sensor data; and ground truth data. Coalescing all such attitude-dependent data into the direct-search procedure will yield the desired highly refined initial attitude and model parameter values necessary to obtain a definitive attitude history from the attitude equations of motion.

Although analytical filtering procedures (Kalman, differential correction, etc.) are applicable for the required second level of ERTS attitude determination, the direct-search batch process is preferred for the following reasons:

The first, and perhaps most important, is the ease of implementation and modification. Because the cost function* is systematically, not analytically, minimized by logical operations, there is no requirement to compute partial derivatives; since many analytical particles associated with the ERTS dynamic environment, e. g., magnetic field torques, are difficult to obtain, this direct-search feature is particularly significant with respect to reducing programming costs.

The second is that batch processing over a time span equal to the data gathering interval, station pass, tape playback, etc., more logically fits ERTS system requirements.

The third reason is the elimination of high-order matrix inversion associated with a state vector augmented for multiple parameter estimation. In addition, the initialization and possible divergence problems associated with the Kalman filtering are non-existent.

---

*The proposed direct-search optimization program is not restricted to minimizing the quadratic form; it is also capable of minimizing the sum of the absolute values of the residuals.

The fourth and final reason is that the proposed direct-search optimal filtering procedure has been successfully employed in attitude prediction/parameter estimation systems developed for the currently operational RAE-A(3) and GRS-A(4) spacecraft.

3.5 ANNOTATION

Two methods were studied for computing the annotation parameters required for the bulk image processing and indexing. The intersection of the camera boresight and the earth can be computed by an analytic approach or an approach employing vector manipulation. Since both methods provided the required accuracy, the vector method was chosen because of its simplicity and speed.

3.6 PCM DATA BASE

It is in the PCM data base generator that the PCM housekeeping parameters are converted and merged with the skeletal data base created by the PCM preprocessor and attitude determination functions. Since additions and modifications to the calibration/conversion routines are normally encountered during the lifetime of a spacecraft, it was decided to maintain a separate file of calibration/conversion algorithms to allow for the simple and quick inclusion of these modifications. Although the normal mode of processing is assumed to be the generation of the archival master digital data tape, the PCM data base generator will be capable of producing the less precise and less complete quick-look tapes, along with the optional reports summarizing this data.

In the consideration of data compaction techniques which might be used to reduce the size of the PCM data base several techniques were found which provide for considerable compaction. However, the amount of compaction is a function of the requirements for reporting and/or recording changes in the various parameters. As the amount of change which can be tolerated increases, the amount of compaction increases. Since the parameters measured on ERTS number in the hundreds, sufficient time was not available to determine what the tolerances might be and thus evaluation of the various techniques was not possible during this study. When these requirements are defined, a compaction method can be chosen.

3.7 DCS DATA BASE

The major factors affecting the design of the DCS data base generator were the probability that platforms would be added to the system after launch, calibration of the platform sensors would occur periodically, sensors might be added to specific platforms and the planned use of this data is not clearly defined. In order to provide for the addition and/or modification of platforms in the data collection system a platform identification file will be created and maintained which will contain identification, location and sensor calibration data for each platform. The maintenance of this file would be a function of the information management programs and any changes to the platforms would have no effect on the DCS data base generator programs. Due to the uncertainty of the user requirements at this time, the DCS data will be recorded on a time sequential basis rather than one based on location, sensor type or individual platform.

CONTENTS

4. INFORMATION MANAGEMENT

4.1 GENERAL REQUIREMENTS AND APPROACH

One of the primary functions of ERTS is the collection of data of scientific interest. The original data and copies of processed data, must be archived; indexes must be prepared and maintained; and control must be exercised over the data flow through the NDPF.

The data which forms the basic input is shown in Tables 4-1 and 4-8. This data was analyzed; from the analysis, the data handling requirements were developed.

4.2 PHYSICAL STORAGE AND RETRIEVAL

The materials to be stored consist of:

- film

- magnetic tapes

The film will be stored, for a reasonable time, in the NDPF archives to facilitate the making of photocopies. As the demands on the data drop, it will be moved out of the NDPF to long term archival storage. Section 4.2.1 is an analysis of the physical storage and retrieval requirements for film.

For long term storage of source imagery, high density digital tape appears to be more attractive than the video tapes. Section 4.2.2 is a tradeoff study on various archival storage media.

4.2.1 Film Storage

The archival film storage media is the standard 9-inch wide film. There are two basic ways to store such film. This study defines the characteristics of each method, selects the optimum combination, and estimates the physical volume requirements. The two approaches are:

> Rolls: up to 200 feet of film in a plastic can 8 inches in diameter by 10-1/2 inches long.

> Sheets: single sheets, covered by an acetate envelope. The space occupied is approximately 10 x 10 in. 0.03 to 0.04 in. The range in thickness depends on how loosely the sheets are held.

Table 4-1. NDPF Data Base

Data Category	Data Item	Original Form	Media*	Volume		Period	Update Cycle	Keep	Data* Disposition	Remarks	Form	Media*	Recopy Cycle	Keep	Remarks	Comments
				\<Active Library\>							\<Archive Library\>					
Original data	S/C telemetry	Analog	MT	20 Tapes		Daily	None	6 months	Archives							Data in master digital data file
	Ephemeris	Digital	MT	1 Tape		Daily	None	6 months	Archives							Data in MDD and attitude history files
	DCS	Analog	MT	6 Tapes		Daily	None	6 months	Archives							Data in DCS file
	RBV imagery	Analog	VT	4 Tapes		Daily	None	3 months	Archives							
	MSS imagery	Analog	VT	4 Tapes		Daily	None	3 months	Archives							
Digital processed imagery	RBV	Digital	MT			Daily	None	1 year	Archives	100% Bulk	Digital	HD, HG MT	Based on test tape	Indef- inite		Case A-315 frames/ day, Case B-1315 frames/day
	MSS	Digital	MT			Daily	None	1 year	Archives	100% Bulk	Digital	HD, HG MT	Based on test tape	Indef- inite		
User requested data	Precision RBV	Digital	MT	A-9 frames		Daily	None	1 year	Destroy	5% Bulk						Case B, ERTS B 25 frames/day
	Precision MSS	Digital	MT	A-13 frames		Daily	None	1 year	Destroy	5% Bulk						Case B, ERTS B 41 frames/day
	Digitized RBV	Digital	MT	A-2 frames		Daily	None	1 year	Destroy	1% Bulk						Case B, ERTS B 5 frames/day
	Digitized MSS	Digital	MT	A-13 frames		Daily	None	1 year	Destroy	5% Bulk						Case B, ERTS B 41 frames/day
				ERTS A Case A	ERTS B Case B											
Imagery Bulk	RBV	BW Image	Film	189	495	Daily	None	1 year	See Comments	Frames/ Day						Destroy if all frames are bulk corrected
	MSS	BW Image	Film	252	825	Daily	None	1 year	See Comments	Frames/ Day						
Bulk corrected	RBV	BW Image	Film	189	495	Daily	None	5 years	Archives	Frames/ Day	BW Image	Film	200 years	Indef- inite		Master is second generation positive
	MSS	BW Image	Film	252	825	Daily	None	5 years	Archives	Frames/ Day	BW Image	Film	200 years	Indef- inite		Master is second generation positive
	RBV composite	Color Image	Film	13	33	Daily	None	5 years	Archives	Set/Day	Color Image	Film	100 years	Indef- inite		Master is second generation positive
	MSS composite	Color Image	Film	13	33	Daily	None	5 years	Archives	Set/Day	Color Image	Film	100 years	Indef- inite		Master is second generation positive
Analog precision	RBV	BW Image	Film	9	25	Daily	None	5 years	Archives	Frames/ Day	BW Image	Film	200 years	Indef- inite		Master is second generation positive
	MSS	BW Image	Film	12	41	Daily	None	5 years	Archives	Frames/ Day	BW Image	Film	200 years	Indef- inite		Master is second generation positive

Table 4-1. NDPF Data Base (Continued)

				Active Library							Archive Library					
Data Category	Data Item	Original Form	Media*	Volume (ERTS A Case A / ERTS B Case B)		Period	Update Cycle	Keep	Data* Disposition	Remarks	Form	Media*	Recopy Cycle	Keep	Remarks	Comments
				ERTS A Case A	ERTS B Case B											
Analog pre-cision (continued)	RBV composite	Color Image	Film	3	8	Daily	None	5 years	Archives	Set/Day	Color Image	Film	200 years	Indef-inite		Master is second generation positive
	MSS composite	Color Image	Film	3	8	Daily	None	5 years	Archives	Set/Day	Color Image	Film	200 years	Indef-inite		Master is second generation positive
Digital precision	RBV	BW Image	Film	9	25	Daily	None	5 years	Archives	Frames/Day	BW Image	Film	200 years	Indef-inite		Master is first generation positive
	MSS	BW Image	Film	12	41	Daily	None	5 years	Archives	Frames/Day	Bw Image	Film	200 years	Indef-inite		Master is first generation positive
	RBV composite	Color Image	Film	3	8	Daily	None	5 years	Archives	Set/Day	Color Image	Film	100 years	Indef-inite		Master third genera-tion negative
	MSS composite	Color Image	Film	3	8	Daily	None	5 years	Archives	Set/Day	Color Image	Film	100 years	Indef-inite		Master is third genera-tion negative
Data files	Index/abstract	Digital	Disk	31, 500 bytes		Daily	Daily	5 years	Archive	Case A	Digital	HD,HC MT	As needed	15-30 years	**	ERTS B, Case B, Vol=115,500 bytes/day
	DCS	Digital	MT	164, 000 bytes		Daily	Daily	5 years	Archive	Case A	Digital	HD,HC MT	As needed	15-30 years	**	ERTS B, Case B, Vol=820, 000 bytes/day
	Master digital data	Digital	MT	14 7 megabytes		Daily	Daily	1 year	Archive		Digital	HD,HC, MT	As needed	15-30 years	**	
	Attitude history	Digital	MT	13, 200 bytes		Daily	Daily	5 years	Archive		Digital	MT	As needed	15-30 years	**	Recopy cycle of archive tapes will be based on results of test tape checks
	Time history	Digital	Disk	200 bytes		Daily	Daily	5 years	Archive		Digital	MT	As needed	15-30 years	**	
	DCP	Digital	Disk	Small		as needed	as needed	Indef-initely	Purge	As required						
	Ground reference	Digital	Disk	40, 000 bytes		Weekly	Weekly	Indef-initely	Purge	As required						
	Map reference	Digital	Disk	Small		as needed	Monthly	Indef-initely	Purge	As required						
	Production control	Digital	Disk	6, 000 bytes		Daily	Daily	Indef-initely	Purge	As required						
	Library index	Digital	Disk	8, 000 bytes		Daily	Daily	Indef-initely	Purge	As required						
Hard copy	Montage catalog	Image Mosaic	Film	2 Sheets		18 days	None	5 years	Archive		Image	Film	200 years	Indef-initely		Bind into 1 volume yearly
	Abstract catalog	Alpha-merics	Paper	Variable		18 days	None	5 years	Destroy							
	Maps	Paper	Film	300		Monthly	Monthly	Indef-initely	Purge	As required						Maps will be on film

*LEGEND   VT - Video tape, MT - Magnetic tape, HD, HC, MT - High density, high capacity magnetic tape
Archives - GSFC

Note   Frame and set rates for table
ERTS A, Case A - 8 hour day, 5 day week
ERTS B, Case B - 8 hour day, 7 day week

If rolls are full, then 200 feet occupies approximately 704 in^3; the same amount of film (267 sheets) stored in the acetate envelopes will occupy between 800 and 1100 in^3, depending on the packing pressure. As will appear further on, the storage of entire rolls of 200 feet is difficult to achieve. The two forms are thus roughly equivalent from a volumetric point of view.

The basic problem with using rolls is that ERTS data does not come in 200 foot segments. Passes over the United States, for example, range from 3 to 20 frames; this is equivalent to 21 to 140 pictures, or 16 feet to 105 feet of film for either the raw or bulk processed film. Since the two sets of film are exposed at different times, one is the progenitor of the other, they are not together. We should keep the data together by orbital pass for convenience. Thus, to keep the film cans full, it is necessary to splice films from different orbits together.

Sheet film does not have this problem; it is very flexible with respect to filing. Unfortunately, it requires a great deal of handling, offers every chance for data to get out of order, and is troublesome to use for long term archiving.

Table 4-2 summarizes the characteristics of the two forms. The film size tradeoff study (Section 5.2) shows that rolling introduces no serious distortion, so that the rolls are not penalized on this account.

There are five types of film products to be archived; these are shown, together with the preferred storage form, in Table 4-3.

The data volume of sheets is simple to estimate:

Case A: 55 sheets/day; 20,075 sheets/year

Case B: 190 sheets/day; 69,350 sheets/year

The bulk roll volume is a bit more complicated, due to the problem of trying to fill the cans. There are several strategies.

The first is to put one orbital pass per can. The average number of frames (case A) per pass is 14; a set of data is thus 98 pictures of 9 inches each, or roughly 75 feet. This is clearly not a very good idea.

The second strategy is to splice both the raw and bulk processed film onto one spool. The longest pass (case A) is 21 frames. This gives

Table 4-2. Comparison of Roll Versus Sheet Storage

Property	Sheets	Rolls
File order flexibility	Excellent	No flexibility
Ease of locating one frame	Excellent	Nuisance
Ease of locating and copying a number of successive frames	Modest	Very good
Getting out of order	Very easy	Almost impossible
Volumetric efficiency versus data volume	Same for all volumes of data	Better for long strings of data: poor for small strings of data
Long term storage	Troublesome	Very good

Table 4-3. Archive Film Input Per Day Average

Units/Day (7-day week)	A	B	Storage Form
Sets	45	165	
Bulk records	315	1320	Roll
Bulk processed	315	1320	Roll
Color negatives	25	100	Sheet
Precision negatives	20	63	Sheet
Prot. color negatives	10	27	Sheet

rise to 147 negatives, or 111 feet for both the raw data and the bulk processed data; 222 feet will not go into the can.

This suggests the approach that if the pass is short enough (this turns out to be 19 frames or less), then both original and bulk processed are put in one can; if it is over this length, then they are put in separate cans.

An analysis was made of United States coverage, which involved 42 orbits. Table 4-4 presents the number of orbits versus the frames on that orbital pass. The number of cans required (one per pass for 19 or less frames; two for over 19 frames) is tabulated, along with the total feet

Table 4-4. Analysis of Can Storage Capacity

Frames	No Orbits	Cans	Total Feet
3	2	2	63
4	3	3	126
5	2	2	105
6	0	0	0
7	1	1	74
8	0	0	0
9	0	0	0
10	1	1	105
11	1	1	116
12	0	1	0
13	1	1	137
14	1	1	147
15	4	4	630
16	6	6	1008
17	8	8	1638
18	7	7	1323
19	0	0	0
20	3	6	630
21	2	4	441
Total		48	6543

of film (original, bulk process). This equates to 6543 feet of film in 48 cans, or an average of 136 feet per can.

If we elect to pool short passes (i. e., under 10 frames) which fill less than one-half of a can, we note that the eight shortest orbits, which now occupy eight cans, can actually fit in two cans. This leads to 42 cans for 6543 feet, or 155 feet per can.

This leads to the following average can count per day, as shown in Table 4-5.

To obtain the total space required for storage, we now derive the average storage volume per day in the archives. A sheet occupies a space 10 x 10 x 1/32 inches, or 3.125 in.^{3}. This leads to the storage volume estimate of Table 4-6.

Table 4-5. Estimate of Film Can Volume

	Case A	Case B
Average feet per day stored in cans	473	1733
Average cans/day; no pass pooling	3.48	12.76
Average cans/day; pool short passes	3.05	11.18
Cans/year; no pass pooling	1270	4657
Cans/year; pool short passes	1113	4081

Table 4-6. Cubic Feet of Film Storage Per Day of
Archival Storage

	Case A	Case B
Sheets/day	55	190
Cans/day	3.48	12.76
Sheets; $in.^3$/day	172	594
Cans; $in.^3$/day	2450	8983
Total: $in.^3$/day	2622	9577
Total: ft^3/day	1.523	5.542

4.2.2 Archival Tradeoff Study

4.2.2.1 Archiving Requirements

The ERTS satellite system will produce large amounts of image data covering the continental United States, at a steady rate, and of long term utility. Some of this data will be of great value many years after its original acquisition. This data, or at least the potentially useful portion of the data, must be retained or archived in a form which will permit recovery with a minimum of degradation, consistent with cost and operational factors. This section considers this problem including archival requirements, a survey of applicable technologies, a survey of current state of the art equipment applicable to the problem, a discussion of usage factors, and a recommended approach based on a tradeoff analysis of all applicable factors.

4.2.2.2 Archiveable Data Description

The principle source of the image data which must be archived, from the ERTS sensors are the RBV, and the MSS. These sensors are spatially and photometrically high resolution sensors and produce prodigious amounts of data. The RBV provides 4,200 x 4,096 resolution elements for each frame of imagery, with a potential of about 64 photometric levels. In digital terms this amounts to 103,219,200 bits per frame. The MSS provides 4096 x 2600 resolution elements per frame with six bit encoding. This corresponds to 63,897,600 bits in digital form. In the case of ERTS A there are three RBV and four MSS frames per data set. This corresponds to 309,657,600 bits of RBV data and 255,590,400 bits of MSS data per set. The total data volume is 565,248,000 bits for each image set.

There are two cases to be considered; for ERTS A 45 sets of image data will be received per day, and for ERTS B 165 sets of image data will be received per day. Table 4-7 delineates the total maximum data load which must be archived for each of these two cases as a function of days, weeks, and years.

Table 4-7. Total Maximum Data Load

Bits x 10^{10}	ERTS A	ERTS B
Per set	0.0565	0.0565
Per day	2.58	9.45
Per week	18.0	66.2
Per year	935.0	3440.0

This table represents only image data. In addition, up to 15 million bits of other data derived from telemetry must be archived.

A portion of this data will be unuseable due to cloud cover or other atmospheric or technical problems. The size of this unuseable portion is currently an unknown, however, even a factor of two would have little effect in the selection of the archiving methods.

4.2.2.3 Useful Life of Data

It is currently estimated that the principal useful life of the ERTS data will cover a span of 10 to 30 years; however, studies of changes involving earth resources may in the future require data to be preserved for much longer periods of time. Due to the cost involved in the original acquisition and potential future utility, it is essential that all useful data be preserved in some form of long life storage. This storage may be in the form of gray scale imagery, or in some other digital or analog form. The purpose of this analysis is to determine the most suitable form of long term storage and recovery consistant with the preservation of maximum utility, minimum storage volume and cost and other factors.

4.2.2.4 Image Data Archiving

Image data archiving differs somewhat from other forms of data archiving, in that an error rate well above that tolerable for numerical and alphameric data can be considered quite acceptable. This is due to the highly redundant nature of image information. Little information is obtained from a single resolution element but instead a number of closely correlated elements act as the information carrier. There is naturally a data loss when any error occurs, but there may be little or no actual useful information loss. This factor will permit the use of techniques employing higher storage density and a lower degree of environmental control than would be required for other forms of data stored digitally. Although the loss or acquisition of isolated error bits is not destructive to image information, clustering of these losses, or systematic errors are destructive and care should be taken to eliminate these types of bit error sources.

Although it is recognized that precise error-free recovery is not a requirement in an image archiving system, most of the work done in high density archival systems has not included this consideration. All commercially available units will therefore tend to provide very low bit error rates and from this point of view will be more than adequate for application to archiving in the ERTS system.

4.2.2.5 Archiving Technologies

There are two basic methods of storing information in compact form for later usage, analog, and coded. Analog storage involves the recording

of both spatial position information, and photometry in a form somewhat analogous to the original form. The data is not normally quantized but continuous in the amplitude domain. A typical analog image storage means is the grey scale photograph, or in another storage medium, video tape. Coded storage may involve a variety of coding schemes, however, the most common is digital. The principal difference between analog and digital storage is that analog storage uses the dynamic range of the medium for the purpose of information storage, while digital storage uses the dynamic range of the medium to provide a high degree of reliability so that errors in the recovery process are rare and the process highly repeatable. In general, analog storage systems hold a good approximation of the input information but cannot provide an exact or repeatable retrieval.

A wide range of media has been used for both types of storage. However, when ultra high densities are required, such as are needed for the ERTS archiving system, only optical and magnetic storage media offer significant promise. Both analog and digital storage methods on these media are discussed in the following subsections.

Optical Analog Storage Media

The principal means for analog storage of information on optical media is the use of photographic or other photosensitive coatings on a flexible transparent substrate. The most commonly used of these include silver halide films or plates, diazo or dye bleaching materials, and kalvar. Of these materials only silver halide materials provide adequate grey scale or dynamic range for possible ERTS application.

Silver halide films have a capability of preserving 35 to 40 gray levels. However, these levels are not precisely repeatable. The medium is, at least in regard to its macrocharacteristics, continuous in its gray level recording capability between the threshold of exposure and saturation level of exposure. Variation in grain size and in processing of the material will produce variations in density even with a precise exposure. Resolution is high however, and where the resolution capability is fully utilized it represents the most compact form of analog storage as well as the lowest cost for a permanent medium.

Recovery of information from silver films for use in digital image processing requires a precision scanner, with excellent signal-to-noise ratio, spatial accuracy, and photometric dynamic range. Cathode ray tube scanners have been developed at IBM and other sources capable of reliably separating up to 32 grey levels. These systems have also been demonstrated to be capable of providing spatial accuracies of up to one part in 4000 when properly aligned and calibrated. Absolute repeatability of the data over substantial periods of time is questionable unless careful calibration procedures are employed in the photometric measurement process.

The ERTS system will include an archive of all original bulk recordings, which provide the capability of such an archiving system at least as a backup at no additional media costs. It is not recommended, however, that the original analog images be used as the only archival storage for those images which are likely to require digital image processing.

Magnetic Analog Storage Media

Image data such as is derived from ERTS can also be stored in high density form by analog magnetic recording. The imagery will originate in FM/FM analog magnetic tape when acquired by the ground receiving stations. These tapes could conceivably be used as an archival storage medium. Two factors mitigate against their use for this purpose. The tapes are nonpermanent and will degrade somewhat with environmental changes, thus providing imprecise recovery of the information at a later time. This loss will not be localized but will be a general loss of fidelity in the image photometry. As a companion problem to this degradation with time, the reproduced data will be highly dependent on the state of health of the tape transducer system. The second major factor mitigating against the use of the analog tapes for archival storage is the bulk and cost of information stored in this fashion. Magnetically stored information is also subject to catastrophic loss due to stray magnetic fields or careless handling. The useful lifetime of ultrahigh density magnetically recorded data is an unknown, however, as the density increases the number of dipoles storing the photometric value decrease and the susceptability to influence by stray field or remaining bias fields increases.

Analog storage is therefore recommended only as short term storage in the magnetic form and as a backup storage in the photographic form.

Magnetic Digital Storage Media

The use of magnetic media to store digital information is well established in the data processing art. Magnetic tapes commonly record information on 2,400 foot reels at densities of 800 and 1600 bytes per inch. This corresponds to densities of 12,800 and 25,600 bits per square inch respectively. Recording at these densities is extremely reliable. However, the long wavelength and depth of the saturation recording raises the possibility of bit errors being injected due to the influence of magnetic areas, on surrounding areas when wound onto a reel for extended periods. The national archives has reported bit drop-out or insertion in tapes which are unused for extended periods of time. The extent of this problem is largely a function of the tape condition, recording conditions, and the data content as well as the storage environment.

Recent developments in ultrahigh density magnetic storage at IBM, General Dynamics, Ampex and several other industry sources have resulted in Magnetic storage at densities of up to 30,000 bits per linear inch and up to 100 tracks per inch. Storage densities for this generation of devices is about 1,000,000 bits per square inch. Higher linear densities usually result in lower track densities. The permanence of data stored magnetically at these densities is unknown, however, one manufacturer reports two year old tapes, when read having no read errors. In general, the short wavelengths should reduce or eliminate print through, but the small domains may increase bit dropout. The density of storage renders this storage medium reasonably practical from the standpoint of bulk and cost of media, and may prove very useful as a short term archiving means if not acceptable for long term storage. Digital magnetic data may be read and rewritten at any time without degradation, therefore this medium can be employed for archival storage in any event with the disadvantage that some as yet unassessable processing requirement will be to maintain an error free file.

Digital Optical Storage Media

The concept of storing digital information in compact form on optical media was introduced by the Bureau of Standards with a system for

photographing punched cards onto 35mm film. This system provided a significant reduction over the bulk of 80 column cards. More recent developments in this area have occurred over the past five to seven years with the development and continuing development of a number of new optical techniques. Among these techniques are recording of opaque and clear areas in binary code on photographic film using a precision cathode ray tube recorder, or electron beam recorder. Other media such as diazo films, photopolymers, photochromic films and kalvar have been used at least experimentally for this purpose either with cathode ray tube or electron beam recorders, or through combination systems involving reduction printing from a silver halide original. Many of these techniques are still viable and provide densities up to 5×10^6 bits per square inch. All of these media use a change in density or reflection to effect the storage and are directly viewable. Another optical medium was developed as a result of the Eidophor television display principle. This medium, thermoplastic recording uses electrostatic stresses produced by a modulated electron beam on a thermoplastic medium to distort the medium proportional to the stress pattern. No change in density occurs however, and the result is not directly viewable. The information is carried by the deviation of the optical rays passing through the medium by the distorted areas. This type of storage requires the use of Schlieren optics for decoding. This type of optics, in its simplest terms, involves passing light through the medium and aperturing out the undeviated rays leaving only the rays deviated by the pattern of distortion to be detected. Thermoplastic recording has the disadvantages of requiring a vacuum in the recording process and requiring the use of Schlieren optics in the readout. Schlieren optics not only produce the information from the deliberate distortions in the medium but also accentuate any scratches or other optically distorting defects in the material. No practical system for digital archiving has yet been constructed using this method.

The introduction of the laser has provided the means for increasing the storage density possible on optical media as well as extending the range of useful media. Some of the systems using lasers employ mirror deflection systems, others use birefringent KDP crystals for electro

optical deflection, while others use multiple parallel beams with multi-channel modulators and no optical deflection. Media used include photographic film, diazo films, and photochromic films, in the photosensitive category. One system which shows considerable promise uses an evaporated coating of a metal with a 50 percent reflectance on a polyester substrate. In this system the coating is either melted or evaporated away by a high power laser then checked at a decreased power. The reading process uses the same equipment, but decreased laser power. The process is self-limiting since the substrate does not absorb energy from the laser. This process is attractive since media costs are potentially low and high data densities are possible. Densities in excess of 20 million bits per square inch are currently being achieved in prototype equipment with 40 million bits projected in the future.

One of the systems using photographic film as the storage medium produces 36 tracks of data with up to 5,000 bits per linear inch. The medium employed is only 8mm in width thus up to 100 tracks could be accommodated in a one-inch wide medium. The effective density is 500,000 bits per square inch. This density can be increased to about 4 million bits per square inch by increasing the linear density and reducing the track width, at some compromise in error rate.

Optical ultra high density storage systems have been designed based on reels of media, strips of media, or chips and cartridges of media. These designs have been somewhat a function of the intended application. In most cases the unit of access and required access time were traded off with volume density and equipment complication. For the ERTS system the minimum unit of access effectively useable is one image or about 110 million bits. A more desirable unit of access is the image set, about 750 million bits, or some convenient multiple of sets. The tradeoff will be between ease of access for data recovery, cost of process, and storage volume and ease of recording.

Optical media as discussed in this document refer to media which are recorded and read by optical means and which are permanent in nature. Film, diazo, thermoplastics, and metalized coatings all have useful archival lifetimes of 50 to 150 years, if properly stored.

Digital Holographic Memory

Holography developed during the 1960 time period with the availability of coherent light from lasers shows promise of providing a very high capacity and compact optical memory suitable for archiving ERTS data. Several developments are known and published in this technology. IBM recently disclosed at the fall joint computer conference its work on a holographic storage. This system uses electro-optic light deflectors to select a segment of a holographic plate for illumination. The illuminated segment provides a holographic image registered with a matrix of photo-diode elements interconnected to provide a parallel readout of the stored data. A similar development at RCA has also been reported in the scientific press. The RCA developments indicate that flexible media such as conventional film bases may be used for digital holograms.

The principle advantage of a holographic storage is the ability to recover information satisfactorily from scratched and otherwise damaged optical storage media. This freedom from scratches and dirt permits easy storage and retrieval, and permits approaching the maximum densities of which photographic emulsions are capable. Densities in excess of 20 million bits per square inch are possible. This technique is still in the laboratory stage however, and practical equipment for such applications as ERTS archiving will not be possible within the 1972 time frame. Development of suitable holographic archival storage currently appears to be at least six to seven years away, and possibly longer. No further consideration will therefore be given to this method of archiving the ERTS data in the present archival study.

4.2.2.6 Archiving Equipment

A survey has been conducted to determine the availability of "off the shelf" equipment and techniques for use in the ERTS archival system. This survey has included both magnetic and optical recording systems with sufficient volume density to be considered for archival applications.

Computer Magnetic Tape

Conventional computer tape drives are readily available for recording information for archival storage. These units provide densities up to 1600 eight bit bytes per linear inch on 0.5-inch tape in 2400 foot reels. Each

tape holds approximately 3.5×10^8 digital bits. This corresponds to approximately two tapes per image set, or 90 tapes per day for ERTS A, and 330 tapes per day for ERTS B. This will in turn require a storage volume availability of 67 cubic feet per day for ERTS A, and 248 cubic feet per day for ERTS B. The cost of the tape would be approximately 1,440 dollars per day for ERTS A and 5,280 dollars per day for ERTS B. Annual tape costs for this form of ERTS archiving is over 0.5 million dollars for case A and over 1.9 million dollars for case B. Yearly tape storage requirements for ERTS B would be 91,000 cubic feet.

In view of these figures, coupled with the fact that periodic reprocessing to ensure permanence may be necessary, the use of conventional magnetic tape for the ERTS data archive is not recommended.

Ultra High Density Magnetic Tape

Recent advances in the art of magnetic recording have provided tape densities of up to 20,000 bits per linear inch, and 250 tracks per inch. Several tape systems which provide densities in excess of 500,000 bits per square inch are discussed in the following paragraphs.

Ampex 1900 and 1928 Units

Ampex Corporation has produced for several years, the 1900 tape unit. This tape unit provides 14 tracks of over 18,000 bits per inch density. This provides a density of 250,000 bits per square inch, with high reliability. In contrast to conventional tape the use of the 1900 would require only one tape per day for ERTS A and 3.33 tapes per day for ERTS B. The tape is 1 inch wide, and consists of 10,000 feet on a 14-inch reel. In volume this corresponds to 0.22 cubic feet per day for ERTS A and 0.7 cubic feet per day for ERTS B. In terms of annual cost for the worst case ERTS B, this form of archival storage will have a media cost of 120,000 dollars.

Ampex Corporation can also provide the 1928 tape unit with over 500,000 bit per square inch capacity. This unit is basically a 1900 with two 14 track heads to provide 28 tracks on the same one inch tape. This results in half the volume and half the media costs. A volume of less than 120 cubic feet per year is expected with a media cost of about 60,000 dollars per year.

The above figures on cost and storage volume are based on maximum utilization of the available tape surface. However, since these are reel to reel units without vacuum column buffering, the start and stop times and tape passed during these times are significant. An image will occupy about 20 inches of 28 track tape and 40 inches of 14 track tape. At 60 inches per second a stop time in the order of 2 seconds can cause the passage of up to 60 inches of tape between records assuming linear deceleration. In order to achieve sufficient effective density some system complexities such as backspacing prior to writing or reading the next record to accommodate the start/stop time may be necessary. At the worst, however, the cost and volume figures will increase by about a factor of three. This method of archiving is thus still a viable candidate.

Ampex-1932

The Ampex 1932 is an Ampex 1900 tape drive modified to use two 16 track heads thus providing 32 tracks across the one inch magnetic tape. A linear density of 20,000 bits per inch is maintained thus providing 0.64 million bits per square inch and 7.5×10^{10} bits per reel of tape. All other characteristics are similarly scaled to the performance of the 1928 tape unit.

General Dynamics - Unidar

Unidar is an ultra high density magnetic tape unit manufactured by General Dynamics. Recording density of this unit is approximately one million bits per square inch. The data is recorded on one inch tape in reels of 12,500 feet, using 32 parallel tracks of 30,000 bits per inch. Error rates of one unrecoverable error per 10^7 bits are reported by the manufacturer. Read in and read out rates of up to 921 megabits per second are specified. This system has a capacity of 1.44×10^{11} bits per reel of tape, although not all this density is useable due to the need for interrecord gaps and interblock gaps, headers, etc. It appears, however, that one tape per day will be adequate for the highest data rate. This tape is on a reel 16 inches in diameter, and about 1.5 inches in thickness. This size reel will require about 300 cubic inches for storage. Cost of the media is about 100 dollars per reel.

This tape unit is similar to the Ampex 1928 unit in that it employs reel to reel operation without vacuum buffering, and therefore has sub-

stantial start/stop times. The capacity and cost figures reported above are therefore the maximum that can be obtained and must be factored to determine the effective values. The factors which should be used are dependent on the ability to successfully eliminate blank tape gaps, and the cost of this process. The process seems to be similar to that required for the Ampex units.

The Unidar tape system will require between 350 and 700 tapes per year at a cost of 100 dollars per tape. The annual media cost is thus 35,000 to 70,000 dollars per year for the maximum storage case. The storage volume required per year is about 100 to 200 cubic feet.

The Unidar tape unit has been announced commercially, however, a 32 track unit has not been built or tested as yet. A 21 track version is to be delivered in the near future for use on the AUTEC range.

Other High Density Magnetic Tape Units

IBM and other manufacturers have either in development or available ultrahigh density tape units. IBM has demonstrated the capability of up to 30,000 bits per linear inch and up to 250 tracks across a one inch tape. Such a unit would provide a density of 7.5×10^6 bits per square inch. This unit, it must be emphasized, was a laboratory model, and a production version would probably not achieve this level of density. Densities in excess of two million bits per inch are expected to be achievable with reasonable development effort within the general time frame of the ERTS program. If a special development is conducted the addition of vacuum buffering would be advisable, since it would provide more realistic start and stop times compatible with data processing requirements.

Ampex Corporation has in development a helical track ultra high density (UHD) tape unit. This device called the terrabit memory will operate at 1,000 inches per second, at a density of over 1 million bits per square inch. It is expected to be available in 1972 using 14 inch tape reels and 2 inch tape. An error rate of less than 10^{-14} is expected.

Optical Media

Optical archiving equipment covered in the survey include the IBM photo digital trillion bit store delivered to several government agencies, Unicon developed by Precision Instrument Company, Synergistics PDR-5 and Foto Mem's FM 390 equipment.

IBM Photo Digital (1360)

The IBM photodigital trillion bit storage was designed for random access for relatively small units of information. This system is chip oriented using 1.38 x 2.75 inch chips located in cells containing 32 chips and measuring 3 x 5 x 1 inches. The system was designed to provide 3 second access time to any chip in the 2,250 cells in the system. A writing rate of 0.5 megabit/second and a reading rate of 1.8×10^6 bits per second. Data is recorded on the chips in 32 frames of 18,450 eight bit bytes each, for a total of 590,000 bytes per chip. The net density is 1.25×10^6 bits per square inch. In the recorded area a density closer to three million bits per square inch was achieved. At this density extreme data reliability including doubly redundant recording was obtained.

The IBM photodigital storage unit is not suitable for this application however, due to the relatively small number of bits per unit of storage. A typical ERTS image would require over 30 chips for storage, making the chip handling time the critical factor.

Unicon

Unicon is an archival storage unit developed by Precision Instrument Corp., Palo Alto, California. This unit uses the technique of evaporating a thin metallic film from a 50 percent reflective metal on a polyester substrate as the data storage medium. A strip technique is employed in Table 4-8. Strips 4.75 inches wide by 31.25 inches in length and 0.010 inches thickness are wrapped around a rapidly rotating precision drum. An Argon Ion laser is focused onto the surface with a spot diameter of under 4 microns. An electro-optical modulator switches the beam from high to low power. In the high power state the energy absorption is sufficient to cause removal of the metalized film struck by the laser beam. The exact mechanism is not well understood, and the material is either vaporized or melted and pulled into the surrounding film, by surface tension and preference for the lower energy state. In any event, the reflectivity drops from 50 percent to about 5 percent with the energy being passed through the substrate. An immediate read check can be made using lower laser beam power. An extremely high signal to noise ratio is obtained on reading and a density of 20 million bits per square inch of

Table 4-8. Summary of Archival Equipment Characteristics

Equipment Type	Medium	Bits/in^2 X10^6	Bits/in^3 X10^8	Medium Cost X10^{-7} ¢	Equipment Cost	Data Life	Data Rate	Access Unit	Storage Requirements	Relative Size$^+$	Development Status
Magnetic											
IBM-2401	tape	0 0256	0.0424	20	40K	limited	180K byte	$3\ 5x10^8$	A	1	P
Ampex-1900	tape	0.25	1 0	0.03	50K	unknown	15Mbit	$3.0x10^{10}$	A	1.1	P
Ampex-1928	tape	0.5	2.0	0.015	60K	unknown	30Mbit	$6.0x10^{10}$	A	1.1	MP
Ampex-1932	tape	0.64	2 56	0.013	60K	unknown	38Mbit	$7.5x10^{10}$	A	1 1	MP
G. D. -Unidar	tape	1.0	4.0	0.007	150K	unknown	115Mbit	$1\ 5x10^{11}$	A	1 2	AD
Optical											
IBM-1360	diazo chip	1.2	0.38	84.5	-	permanent	2Mbit	$3.2x10^5$	B	2.0	p****
P. I. C. -Unicon	metal strip	20	0 8	0 25	200K	permanent	4Mbit	$2\ 0x10^9$	B	2.2	p**
SYN. -PDR-5	silver	0 5	0.55	2.0	-	permanent	10Mbit	$1.0x10^9$	B	1.2	P
F. M. -390	film coated plastic card	0.42	0.084	0.25	-	permanent	0.8Mbit	$1.0x10^7$	B	2.3	AD

Key---- A   = Magnetic field free storage
      B   = Dust free storage
   Limited   = Estimated 5+ years
   Unknown   = Estimated 10 years or greater, no reason for loss with A storage
   ****   = No longer available
   **   = First unit sold but not delivered
   P   = Production equipment
   MP   = Modified production equipment
   AD   = Announced but in development
   +   = Normalized unit size to the IBM 2401 Tape Unit

medium is obtained with read out and recording rates of 4 megabits per second. The Unicon strip contains 1.9×10^9 bits of information, enough for more than two ERTS image sets. Error rates are comparable to conventional computer tape. The medium is currently expensive due to its low volume of manufacture but should be capable of being made at low cost in the future. Current costs are about 50 dollars per square foot. The medium is archivally as permanent as the base material, and is postable. It is not subject to environmental destruction.

The Unicon approach to the ERTS archival problem will require 82 strips per day. The strips themselves occupy a low volume, but when encased in the recommended protective cartridges measuring 1/4-inch in thickness the volume density becomes very poor. It is probable that with the higher allowable error rates for image data, a more compact storage arrangement can be provided.

If current cost and volumes remain unchanged the cost per day for ERTS B will run approximately $4,100, and the required volume for storage will be approximately 1.7 cubic feet per day. If the tapes can be stored with only a 10 mil separation, however, this volume requirement drops to 0.13 cubic feet per day or 48 cubic feet per year. This more compact storage seems feasible, but will require further analysis or experimentation to ensure that the data will not be damaged by closer packing of the strips. It is estimated that with sufficient production the media cost could be reduced to a cost compatible with magnetic tape cost.

The Unicon system is as yet untested in the field. A unit is scheduled for delivery to Pan American Oil Company midyear in 1970, and is expected to be operational during late 1970.

Foto Mem FM-390

This equipment is a card based system using a 4 x 6 inch plastic card coated with an opaque material. In the recording process this coating is burned away to form logical "1" bits. 10 million bits are recorded on each 4 x 6 Photo Data Card, or approximately 400,000 bits per square inch. The data is recorded in 300 tracks of approximately 33,000 bits per track. Access time to any track is 50 milliseconds.

This method of archiving will require up to 10 cards per image 80 cards per set, and 13,200 cards per day. No cost figures are available for the media, but the card handling problem as well as the low density, indicate that this approach is not well suited to the ERTS requirements.

Synergistics - PDR-5

This equipment is a laser recorder and reproducer which uses 2.5 mil mylar based 8mm film as its medium. It records in parallel 36 data tracks with up to 5,000 bits per inch per track. It is a reel oriented system, producing a permanent nonpostable record. The density of this system is lower than the others reported being only 500,000 bits per square inch. Its reel orientation and narrow width produces a poorer volume storage factor than the other media discussed. Read out rates of 10 megabits per second are provided for a storage capacity of 4×10^9 bits per 10-1/2 inch reel. This capacity will provide for 5 sets of ERTS image data. For ERTS B with 165 sets per day this corresponds to 33 reels per day or about 1.5 cubic feet per day of required storage volume. This amounts to over 500 cubic feet per year. Cost has not been fully assessed but including processing will be greater than the cost of high density magnetic tape systems. Due to the unfavorable match of cost and volume of storage, this approach is not recommended for the ERTS archival system.

Indexing and Labeling

The data put into the ERTS archival system must be capable of retrieval at a later date. The data will be stored in image sets and accessed by frame number. The access number, or frame number, will be included in a header for each image. This header will also include other pertinent identifying information such as reel number, satellite number, sensor type and identification, spectral region, calibration information, etc. The header must be capable of being read without error, therefore, if the error rate of the archival system is too high for this type of data it must be recorded redundantly. Triple redundancy is probably sufficient to ensure error free interpretation.

An index in machine searchable form is also a requirement of the archival system. The index should also be redundant, to avoid loss of

4-22

identifying and location information on the archived data. The exact form of the index is not known at this time, but it must include frame or access numbering, correlated with all other pertinent information which might be used to identify or locate the image data. It is anticipated that the index will be resident on either conventional computer tape or disc.

4.2.2.7 Summary and Conclusions

In summation the results of the archival tradeoff study indicate that ultra high density magnetic recording is the best method for archiving the ERTS image data, consistent with the requirement for 1972 implementation. The results of this study are summarized on Table 4-8. This method of archiving will provide lowest media costs, and acceptable storage density. The input of data into the archive is simplified by the use of large volume reels, however, this unit of access will make retrieval a slower process due to the necessity of passing tape to acquire the desired imagery set. This is considered the lesser of the two evils, however, since more data will go in than will come out.

The magnetic tape medium is not a permanent storage medium, in that it is subject to erasure or modification, by either improper storage conditions or improper handling. The short wavelengths of the recorded data due to the density and encoding techniques, and the presence of a large mass of neutral magnetization material due to the use of non-saturation recording will tend to increase the useful storage life. It is estimated that the minimum useful storage life will be greater than five years, and may be much longer. It is essential that test tapes be generated periodically, stored in the archive, and read out on a regular schedule. These tapes are recorded as worst case test tapes and in the periodic checks failure to obtain perfect read backs will signal a tape degradation problem in time to permit recovery of the archived data, and re-recording without data loss.

The magnetic tape medium should be stored in shielding containers, preferably in a magnetic field free room, and carefully handled to minimize the risk of data loss. Such storage equipment is readily available from several suppliers.

4.3 COMPUTER STORAGE AND RETRIEVAL

Data handling in a computer-based subsystem is done either by application programs, which handle each data file separately, or by generalized information programs which are designed to handle all files according to a set of predefined programs. With application programs, each data file is treated individually. Programs are developed which handle all data inputs to the file and all file maintenance, queries, retrievals, and outputs. Any changes to the initial file organization or methods of handling the data requires reprogramming to achieve the desired capability. Figure 4.3-1 indicates the basic flow of data to create, query, maintain, and output data using specialized programming techniques. Any changes to the established order or procedures for example, a different report format, requires a programmer to add another routine to the output program or alter an existing routine. This type of application program has great utility if data inputs, retrievals, and outputs remain relatively constant over an extended period.

Generalized information management programs are stand-alone information handling programs which allow users to specify their own file structures and do file maintenance, retrieval, and output in an easy to use English-like language. In general, these types of programs use tables to describe inputs, outputs and data files which allows programs to operate interpretively with the tables for doing the required processing. The user-oriented language allows him to specify his file structuring, maintenance, retrieval, and output procedures. Figure 4.3-2 illustrates the flow of data in generating and using a data file with a generalized information management program. The tables are described based on user specifications to generate the file, input table(s) describe the forms and content of the input data, and output tables describe the form and arrangement of reports. System user language allows him to specify maintenance, retrieval, and output procedures. Flexibility and ease of use are provided by generalized information management programs as non-programmers can create, maintain, query, revise, and output data as necessary.

To adequately assess which method is desirable for handling NDPF data, it is necessary to determine the functional requirements of the subsystem for data processing and the support and interface that are to be
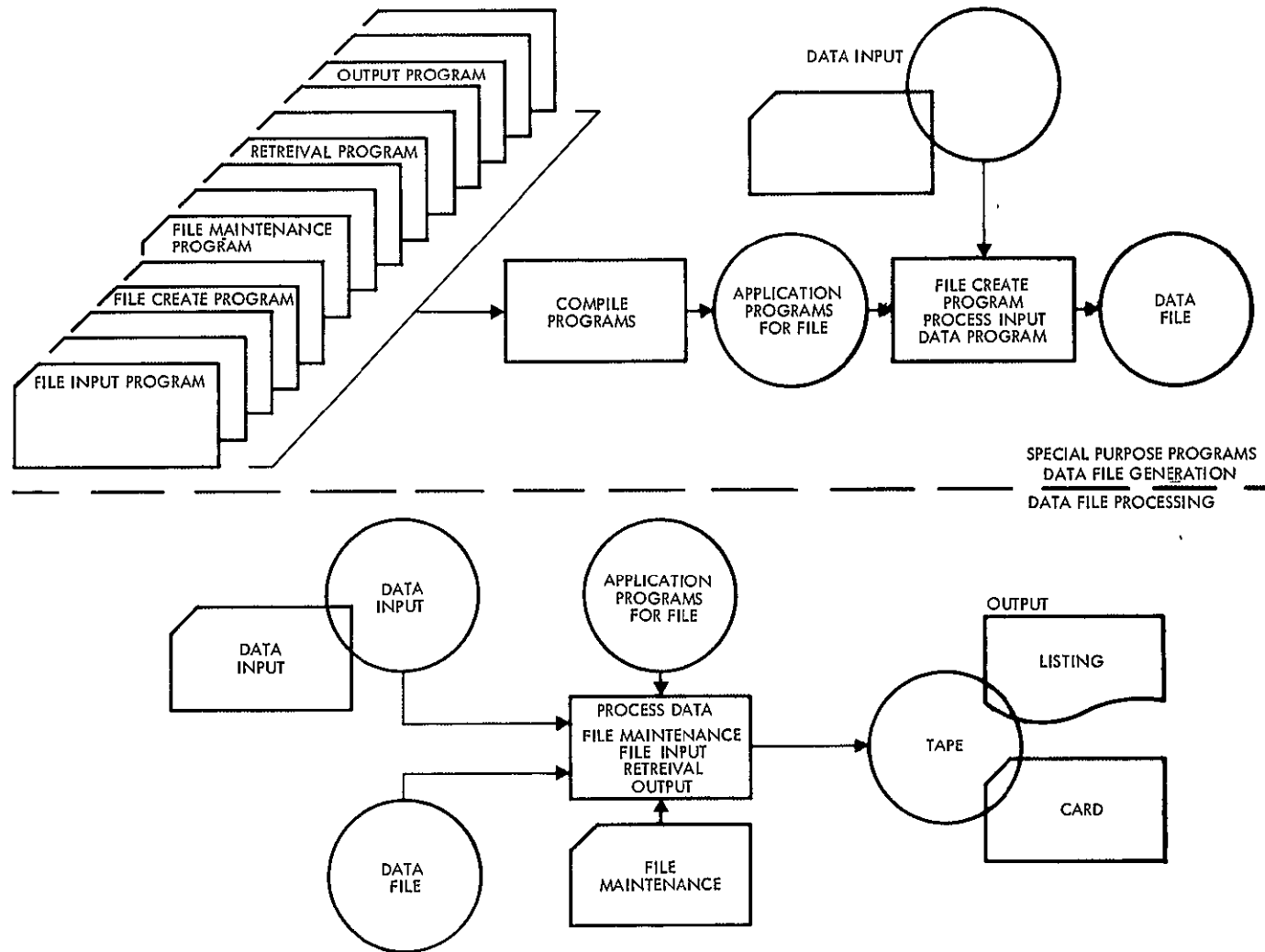
OUTPUT PROGRAM

RETREIVAL PROGRAM

FILE MAINTENANCE PROGRAM

FILE CREATE PROGRAM

FILE INPUT PROGRAM

DATA INPUT

COMPILE PROGRAMS

APPLICATION PROGRAMS FOR FILE

FILE CREATE PROGRAM PROCESS INPUT DATA PROGRAM

DATA FILE

SPECIAL PURPOSE PROGRAMS
DATA FILE GENERATION

DATA FILE PROCESSING

DATA INPUT

DATA INPUT

APPLICATION PROGRAMS FOR FILE

OUTPUT

LISTING

PROCESS DATA
FILE MAINTENANCE
FILE INPUT
RETREIVAL
OUTPUT

TAPE

CARD

DATA FILE

FILE MAINTENANCE

Figure 4.3-1

SPECIAL PURPOSE PROGRAMS - flow per data file

INFORMATION MANAGEMENT APPLICATION PROGRAM AND DATA FILE GENERATION

FILE DATA PROCESSING
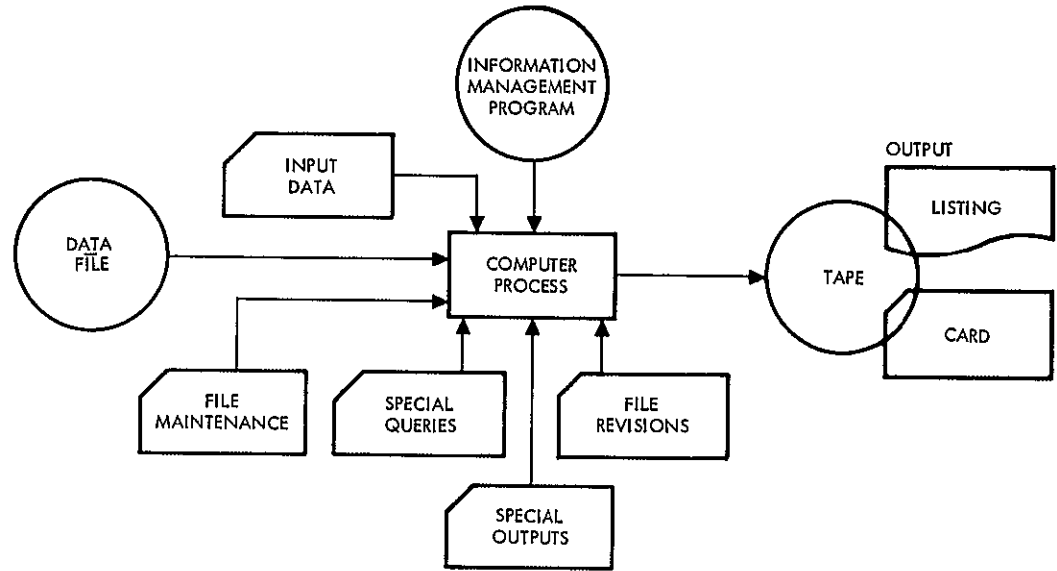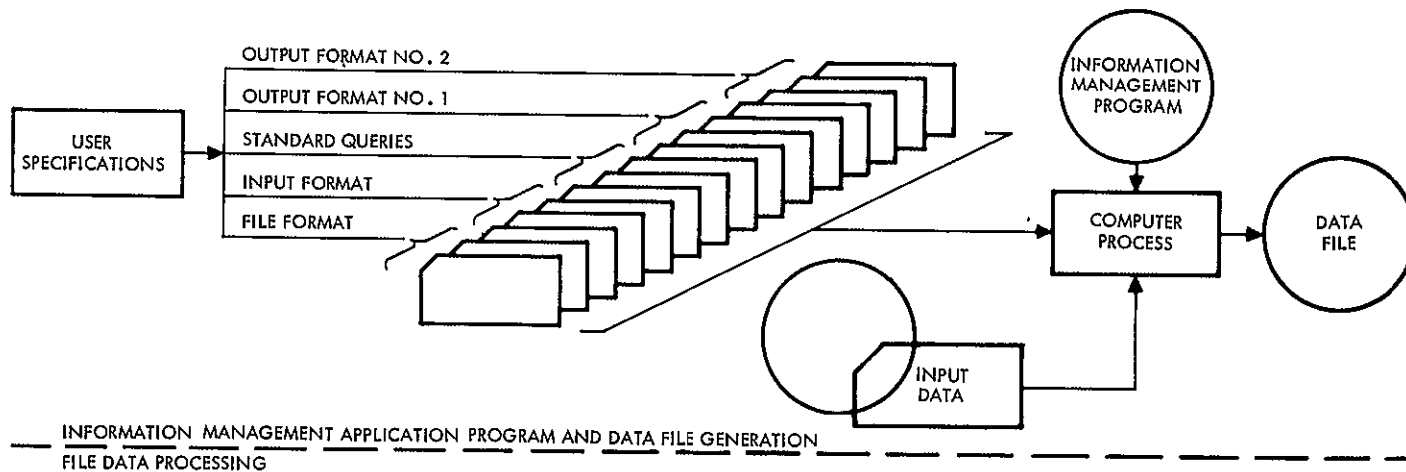
Figure 4.3-2

IMP APPLICATION PROGRAM – flow per data file

provided users. It is also necessary to determine what data is to be kept in files and how this data can be best structured and processed. Analysis of these requirements and the objective of the ERTS Program is necessary to determine how best to manage and process the NDPF data.

4.3.1 Information Management Requirements

The daily load of satellite and user data coming into the NDPF must be processed, converted, reduced, controlled, formatted, and disseminated to a large, diverse multi-disciplined user community. In the area of information handling, the NDPF must provide the following capabilities:

- Maintain a file of processed imagery

- Classify and abstract image data

- Maintain, in digital form, a master file of spacecraft performance data

- Annotate spacecraft data with time and quality

- Calibrate and correlate spacecraft data with orbit and attitude data

- Process DCS data

- Annotate DCS data as to source, time, and quality

- Annotate imagery

- Provide user with catalogs of image data and abstracted data

- Provide users with listings and plots of DCS data

- Provide spacecraft performance listings and plots upon request

- Provide production scheduling and data accounting capabilities

- Provide the interface to users for standard and requested data needs

There are additional data processing functions within the NDPF which do not fall into the area of information handling requirements, such as:

- Precision digital image processing

- Geometric transformations

Development of computer services to provide the information handling requirements of the NDPF imposes the following needs:

- An operating system to perform executive control of all transactions entering the system, to provide efficient use of the equipment and resources by controlling many aspects of the computer's operation, and to provide a system library for all NDPF application and utility programs.

- A series of information management programs for processing and handling data files.

- An appropriate set of data files organized to provide the desired capabilities and outputs.

The types and content of data files needed in the NDPF have a bearing on the type of information management program approach that must be taken. Therefore, a basic set of data files and their processing requirements must be developed in consonance with determining the needs for information management program applications.

4.3.2 Information Management Program (IMP)

In determining the requirements for processing formatted data files two tradeoff areas were considered. The first was concerned with choosing between a generalized information management capability, which could handle all files, and a special application capability, which would handle each file individually. A second tradeoff was concerned with the usage of the data files, i.e., whether or not the data should be stored on direct access devices, what the rates of data change would be, what types of queries would be run, how often the file structures would change, whether users would continually modify their needs, etc.

Initially the requirements for the NDPF data base were examined. As these requirements were developed they provided an insight to the specific application of an IMP to the creation and maintenance of NDPF data files and to the requisite retrievals and outputs engendered by user requests.

In conjunction with the examination of data base requirements, an analysis was done on the varied capabilities and capacities of IMP packages which are currently operating on third generation computers. The MITRE and CODASYL surveys were particularly used as a reference for this

study, though other sources (e. g. , articles in Datamation) were used as supplemental information. Particular attention was given to noting those capabilities which were important or necessary to the effective application in NDPF operations. In doing this, an IMP model was built up of those component parts which supported the applications under consideration.

In specifying NDPF requirements for IMP software, a certain amount of latitude existed as whether to include a given IMP capability as a component or not. For example, consideration was given to the need for an "automatic" multifile processing capability as judged against the adequacy of an ability to achieve multifile operations with non-multifile IMP capabilities. From the study of the aforementioned IMP surveys, it is clear that true multifile capability is more the exception than the rule, since development costs are high and application demands are not especially numerous. The need for true multifile capability is usually avoided in an operation either by virtue of its non-applicability or by means of careful file design. This latter solution appears most applicable to the NDPF operation.

Another feature, or capability, of IMP software that may be desirable is file indexing. This feature is particularly utilized with large data files against which queries or retrievals are run quite frequently to greatly reduce the time needed to locate specific data of interest. The question is· does the NDPF have such a file and will the demand for data be frequent enough to justify the possible expense of developing this capability? The answer is a qualified "yes" when one considers the increasing volume of image data which will be accumulated in the NDPF as case A transitions to case B and beyond. The qualification which must be raised concerns the user demands upon the ERTS data base. The assumption is that ERTS will remain a viable operation and that user demand will increase to reflect the increasing importance of the ERTS mission.

Consideration was also given to the need for remote terminal operations and the degree to which they would be employed. In the performance of the timeline analysis, it was noted that remote terminal operations would be employed at several points in the functional flow. There are in reality two major on-line functions that may be performed: (1) input data to a file and (2) retrieve and display data from a file. The

possible need for both of these functions are expressed in the timeline analyses. As the operational pace in the NDPF increases, the convenience of remote terminals becomes a necessity to provide a "short path" to computer data, especially for those inputs and requests whose delay is critical to the operation of the facility.

Final consideration was given to the inclusion of a graphic output capability. The primary concern for this capability was to provide plots of data such as image coverage, platform data, DCS data and scheduling, information. On the basis of IBM's experience with graphic program utilization in the Defense Intelligence Agency and other Department of Defense agencies, it was concluded that there would be a future need in the NDPF for coverage plots (plotted to map type and scale) and for graphic summaries particularly in the production control area. In view of these projected needs, a graphic output component was included in the IMP model.

In analyzing the various NDPF requirements for computational capability, it became quite clear that in certain areas of software application a generalized Information Management Program (IMP) would provide the most effective capability for the least cost. A generalized Information Management Program was selected for data handling purposes in the NDPF for the following reasons:

- The demonstrated capabilities of available IMP packages

- Applicability of IMP software to NDPF operations

- Versatility and growth capability of IMP

- Handles file changes easily and effectively

- Uses an English-like language

- Useable by non-programmers

- Reduces time to develop files which saves on programming effort, keypunching, test, and debug time

- Ease of restructuring files

- Ease with which reports may be generated

- Frees the user from device type, input/output processing and file organization

- Provides geographic area search capability

- Provides Boolean operators

4.3.2.1 General Information Management Program Description

The selected IMP permits non-programmers using English-like language, to specify data structures required to support a job function. It also performs extensive diagnostics and communicates to the user in meaningful terms. A high degree of independence from the physical storage of data is granted, although the user must be aware of the logical relationships between data elements. Terms used in this description of IMP are defined as follows:

- Data Base: A collection of data, available to the IMP, supporting the general mission or function of the installation. It is typically composed of many different logical sets of data (commonly called files).

- Data File: A logical set of data elements, grouped into associated arrays called records.

- Data File Records: That collection of data elements identifiable by a unique data value (a field or group of fields).

- Field· A single data element.

Data covering a broad spectrum of subjects will be received by the NDPF in varied forms and from many sources. This data is categorized by subject and added to a collection of similarly categorized data called a data file. To aid in placing each element of data into the file, and subsequently retrieving it, the files have a definite structure pattern called the file format. The file format is designed to group similar data. Each group is called a file record. Thus, a formatted file is an ordered collection of file records, each of which contains data arranged according to a previously established file format.

The field is the smallest-named entity that requires processing, however, it would be an advantage to refer to sub-elements of the field when logical or arithmetic operations require access to parts of the data within a field. The IMP also provides for grouping contiguous fields in the record and allows the resultant string to be named as part of the file format definition.

For some NDPF files, it is necessary to carry both repetitive and non-repetitive information in a file record. Repetitive data in a formatted file periodically reoccurs in a definable pattern. Such fields are therefore termed repetitive or periodic fields. Collections of field strings which are repeated as a group may be referred to as a periodic group or set. Each individual string or group in such a set may be called a subset. The collection of non-repetitive fields is defined as the master segment or fixed set.

The NDPF IMP provides structures composed of a master segment with at least one level of subordination that is, the periodic set or sets. It is also required that at least twenty-five periodic sets be definable in the file structure at that level of subordination. The format of each periodic set is independently defined and the repetition of one set need not be comparable with the repetitions of another. The capability to accommodate variable length data such as comments or descriptions within the file structure. These structures are shown in Figures 4.3-3 and 4.3-4.
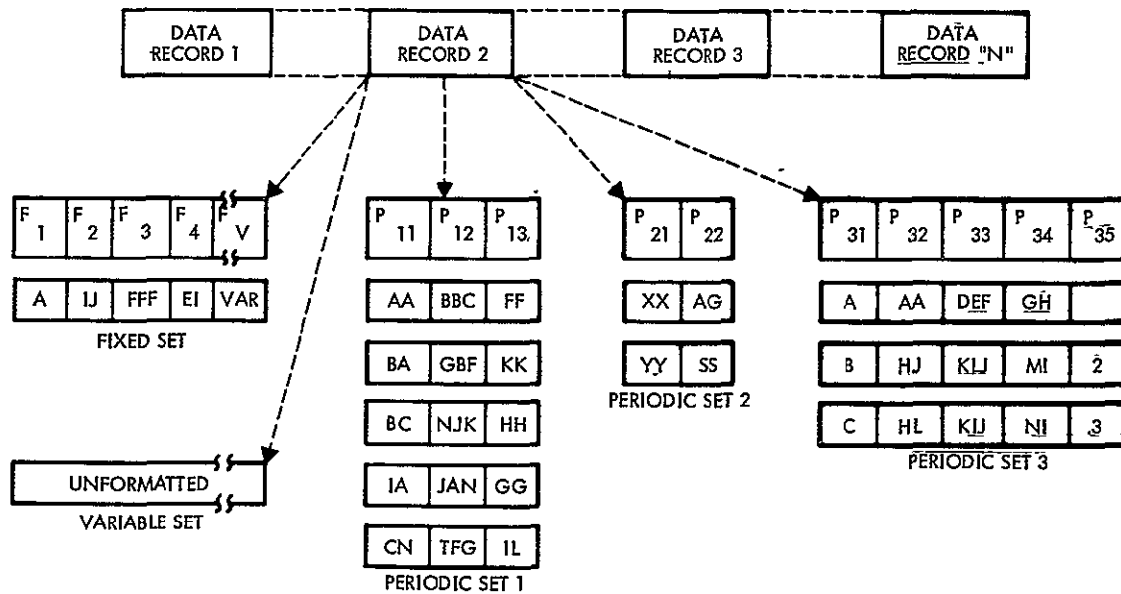
Figure 4.3-3

DATA RECORD ORGANIZATION

FIXED	FIELD	CONTROLS	SUBSET CONTROLS	SUBSET CONTROLS	VARIABLE CONTROLS

FIXED FIELDS	AIRLINE NAME	CITY OF DEPARTURE	TERMINAL	GROUND SERVICES	MANAGER

REPETITIVE SUBSET 1	FLIGHT NUMBER	A/C TYPE	PILOT	ETD

SUBSET 1, 1	FLIGHT LEG	ALTERNATE	AIRWAY

SUBSET 1, 1, 1	NAVAID	ETA
	NAVAID	ETA
	NAVAID	ETA

1, 1	FLIGHT LEG	ALTERNATE	AIRWAY

1, 1, 1

1, 1

1

SUBSET 2	NUMBER OF DAILY FLIGHTS	LOAD FACTOR	DATE

2

VARIABLE FIELD 1	LENGTH	FREIGHT DATA
2	LENGTH	CATERING DATA
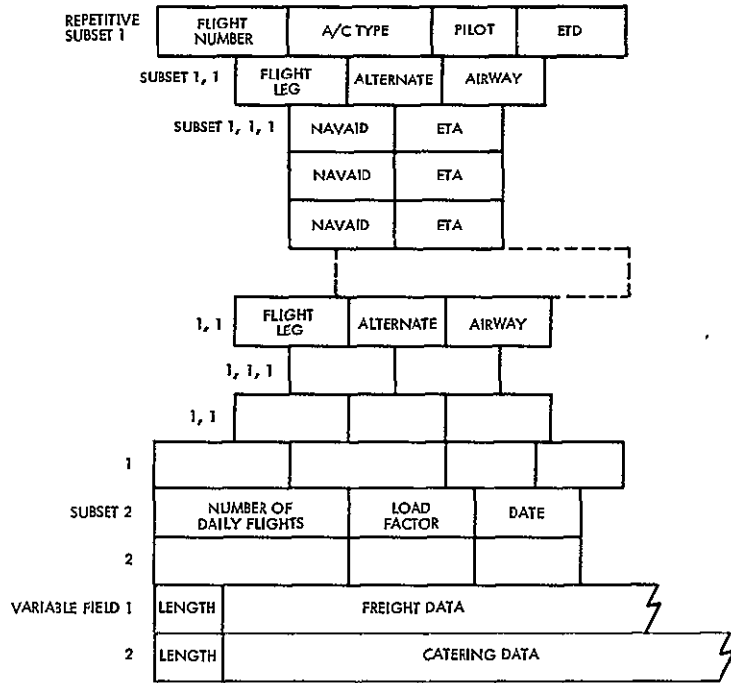
Figure 4.3-4

FORMATTED FILE

4.3.2.2 Information Management Program Description

The information management program comprises a group of
processing components or modules. Each component performs a general
task and they are associated with a general class of functions to be per-
formed. The relationship of these components within the IMP is presented
in Figure 4.3-5. These components are as follows:

- File creation

- Input processing

- File revision

- File maintenance

- Retrieval and sort

- Output generator

- Graphic output

- Remote terminal processing

- Utility
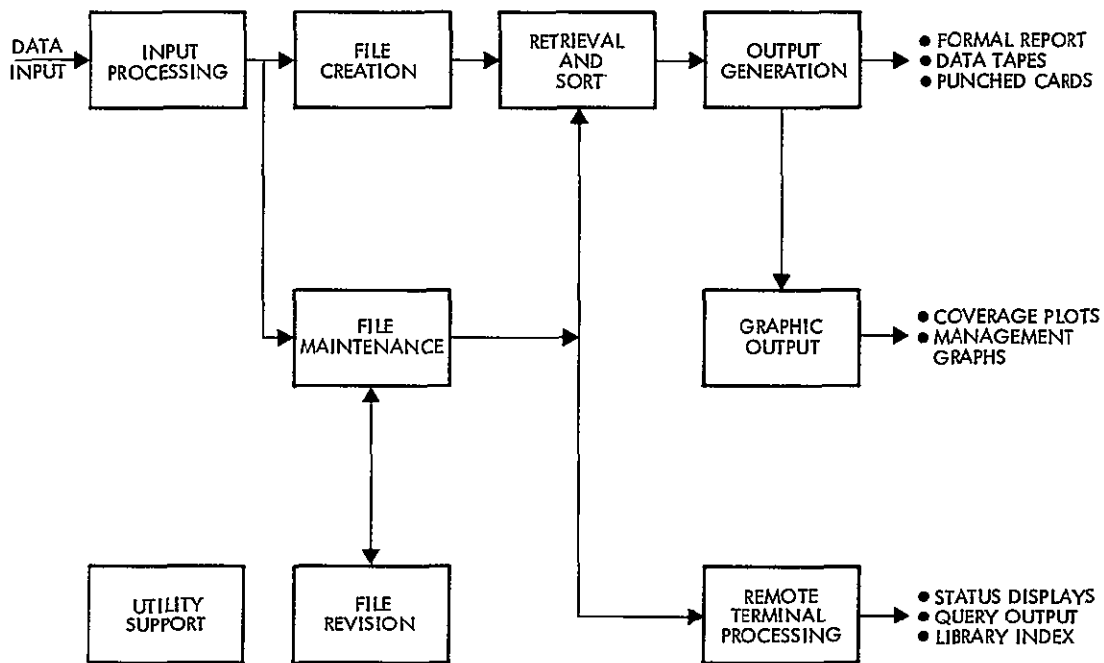
Figure 4.3-5

IMP COMPONENT CONFIGURATION

- File Creation:

  Creates the file structure
  Compiles file processing specifications
  Creates file processing instructions
  Generates the data file
  Provides for data file indexing

- <u>Input Processing</u>:

    Operates on input data prior to file entry
    Edits input data
    User specifies edit parameters
    Sorts input data as specified by user

- <u>File Maintenance</u>:

    Contains logical elements for file generation, file input
        processing, and data file indexing
    Add, modify, delete data file/index values, subsets,
        and records
    Audit input file contents
    Produce an audit trail of data input

- <u>File Revision</u>:

    Revise format of stored file data
    Copies selected data elements from current file to new
        file format
    Add, delete, and relocate fields
    Change field size and name

- <u>Retrieval and Sort</u>:

    Uses English-like condition/action language
    Retrieve specific records/data from files
    Uses comparison operators, e.g., "equal to," "less
        than," and "greater than."
    Provides a negative operator "not" to precede any
        comparison operator
    Uses Boolean connectors
    Provides geographic retrieval operators for irregular
        area searches

            Area to area (convex and concave shaped
                polygons)
            Point to point
            Point to area

    Provides for calling in subroutines for data value
        conversions
    Sorts fields in the master segment of the data file
        record
    Sorts fields in the periodic segments of retrieved
        data
    Contains extensive diagnostics

- Output Generator:

  Inserts headings and page numbers in pointed output
  Permits control over pagination and line spacing
  Produces tape, card, and printed output
  Performs logical and arithmetic operations
  Calls in subroutines and tables for file conversion
  Contains extensive diagnostics

- Graphic Output:

  Facilitates interface between IMP data files and graphic
      display equipment
  Accepts tape input   .
  Processes graphic display specifications of user such
      as map scale and type and symbol size and type
  Provides management graphs in the form of line, bar,
      and point plots

- Remote Terminal Processing:

  Provides for file querying and updating from remote
      terminals
  Enters data to a file
  Files protected against inadvertent modification or
      destruction
  Query language is similar to that used in the Retrieval
      and Sort
  Rapid response to queries

- Utility:

  Provides a data validation/conversion table generation
      capability

The IMP operates as one of many functions in the NDPF computer
complex.   It must therefore be compatible with, and achieve full per-
formance capability under the operating system installed with the selected
computer equipments.   IMP interfaces with the operating system are
designed and maintained to provide smooth operation.   Wherever pos-
sible and feasible, the IMP makes use of operating system services to
efficiently and effectively accomplish its purposes.   The IMP is called
as required in operations and its requisite software and applications
libraries and files are maintained at an appropriate level of readiness and
accessibility.   The facility with which the IMP components, the application
libraries and data files are joined in operation has been carefully con-
sidered in IMP system design.

4.3.3 Information Management Files

To provide the stated requirements for information handling of the data inputs within the NDPF, processing requirements, and outputs, an analysis was performed to identify and specify the files required for a flexible, useful and responsive information management capability. In the conduct of this analysis the following set of guidelines were established:

- Identify and determine all NDPF data handling functions

- Determine maximum NDPF requirements for data handling

- Determine present and projected future user requirements for information

- Determine user interface requirements

- Ensure flexibility of approach and operations

- Provide for minimum throughput time

- Ensure use of latest available techniques

- Determine the best means of maintaining and managing these files

- Identify and determine all NDPF input and output requirements

- Specify and develop those files necessary for NDPF operations

On the basis of this analysis, a set of data files have been identified to satisfy the requirements of the NDPF and provide the desired and necessary information handling capabilities. For each file specified, an analysis was made to determine its processing requirements, structure, use and capabilities within the NDPF. File characteristics covered were:

- Source and form of data

- Data elements

- Record size

- File size

- File utilization

- Maintenance requirements

- Query and retrieval requirements

- Output requirements

- Hardware requirements

Inputs to the NDPF files come from PCM telemetry and DCS processing, the production control system, and post processing of imagery within the NDPF. All inputs and outputs from these files are via the information management program except for some specialized files in the telemetry processing area. The total set of files maintained in the NDPF comprise the NDPF data base. The other part of the data base consists of all physical items containing data stored in the NDPF library. This library consists of an active library and archive library. NDPF files and data stored in the library and their daily volume inputs are summarized in Table 4-1.

The active library comprises the current data files; hardcopy RBV, MSS, and color composite imagery; and other data items which are maintained in active working storage. Depending on the volume of data and its use within the active library, a schedule for retiring data and physical entities to an archive library has been established. The best medium for storing the data in the archive library is covered in Section 4.2.2. Data retired to the archive library will be readily retrievable when required.

The set of files specified to meet NDPF requirements consist of those files that process user oriented information and, internal files which are needed in some data processing functions to develop desired system and user file capabilities. These files are:

- Index/abstract

- Master digital data

- DCS

- Production control status file

- Ground reference

- Map reference

- Library index

- Time history

- DCP

- Attitude history

4-38

The major features of these files is as follows:

4.3.3.1 Index/Abstract File

a) Description

The file provides an index to all RBV and MSS imagery processed and stored within the NDPF. This includes all corrected, precision processed, and color composite images generated in the NDPF. All content data, i.e., abstracts, about the imaged area that is developed within the NDPF is also contained in the file.

The index portion of this file contains the necessary annotation data for later processing of RBV and MSS imagery. Additional annotation data generated in this processing phase is also placed in the file.

The index/abstract file is structured to handle fixed data such as the index, and variable data such as the abstract data. The file is maintained on a disk for use in a direct access device. In operation, index information is generated in the PCM processing phase and passed on to the information management program. This program updates the file with new information. For example, after the imagery associated with the index is automatically processed, the photography will be screened for quality, cloud cover, and data content. Using an interactive display terminal, the operator calls in the index for that set of images, displays it on his screen, and updates the index by keying in the new data. In an alternate mode of operation, the new data is written on a form which is keypunched and placed in the file at a later time in a batch mode operation.

After a complete day's worth of imagery is added to the file, a retrieval is run against the file to output the index/abstract data and prepare a listing to be shipped to the users with the film. The users will also receive an abstract form which has been automatically prepared with image identifying information and room to add descriptive detail about the contents of the image. The abstract form will be structured to control the format of the data generated by the user. The user returns this form and the new abstract data is keypunched and added to the file.

Every 18 days the index/abstract data for that period is retrieved, printed and sent to all users with the Montage catalog sheets for the same period.

To produce the required 1000 copies of this catalog two options are available. In either case a single sharp catalog is made on computer printout paper. The catalog can be sent to the main GSFC print facility (or other government printing facility) for reproduction. If the 1000 copies are

to be generated within the NDPF, a reproducible master must be made. For the copies required, equipment such as the Itek platemaker is necessary to produce the master plate (mat) which is then run on a printing press such as the Multigraph 1250 offset press. The recommended approach is to do the reproduction outside of the NDPF.

The index/abstract file is queried on a daily basis to annotate imagery which has been revised or corrected within the NDPF. The file is also used to satisfy user requests for imagery over a geographic point, line or area and for abstract data based on keywords, descriptors, and attributes. Figure 4.3-6 illustrates some possible image coverage requests over geographic areas.

REQUESTS

(1) GOOD, CLOUD FREE, RBV, LATER THAN 1/73
(2) EXCELLENT, CLOUD FREE, MSS, ALL
(3) RBV AND MSS LATER THAN 1/3/73
(4) EXCELLENT RBV-1 JULY 74
(5) EXCELLENT, MSS COLOR 1,2,4 AND 2,3, AND 1,3,4 MAR-AUG 1973
(6) RBV, CLOUD FREE, NO SNOW, 1973
(7) RBV AND MSS IMAGERY FOR 1974
(8) MSS COLOR, 1,2,3 AND 2,3,4 EXCELLENT, CLOUD FREE, JUNE 1973
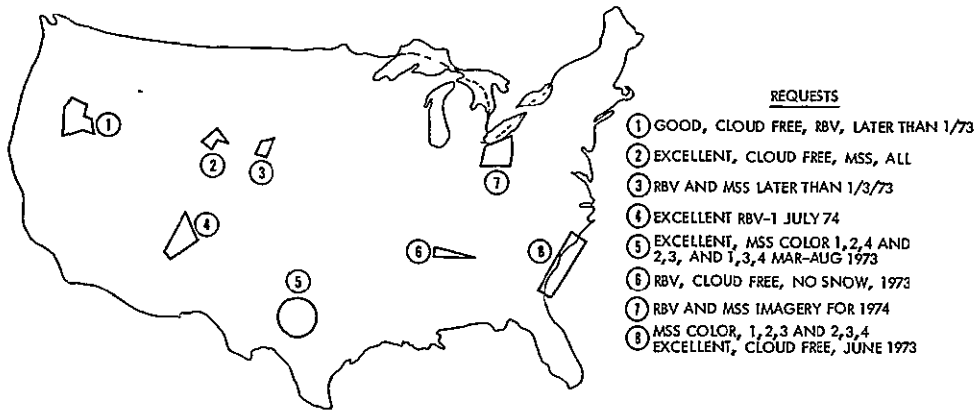
Figure 4.3-6

EIGHT POSSIBLE REQUESTS FOR IMAGERY COVERAGE

b) **File Structure**

One record is generated for a combined set of RBV and MSS imagery taken at the same time and imaging the same 100 x 100 nmi area. Data abstracted from only one or all individual frames within this combined set is also included within this record. This structure includes the capability to handle those times when imagery is obtained only one sensor and to index RBV calibration images. The data content of the index portion of the record is:

Orbit number   ⎫
                ⎬ Record control
Date   ⎪
                ⎪
Time of exposure ⎭

Calibration image

Center coordinate of image

Corner coordinate 1 of image

Corner coordinate 2 of image

Corner coordinate 3 of image

Corner coordinate 4 of image

Sensors

Spectral bands

Heading angle

Sun angle

Altitude

Roll

Pitch

Yaw

Cloud cover

Snow cover (optional)

Image quality

Special processing

    Bulk corrected - color composite

    Precision processed - color composite

    Color composite

Data content of annotation portion of the record is:

Coordinates of sub-orbital point

Acquisition site

Principle point-image UTM coordinates

Meridian divergence

Tick mark location 1 Label 1

Tick mark location 2 Label 2

Tick mark location 3 Label 3

Tick mark location 4 Label 4

Tick mark location 5 Label 5

Tick mark location n Label n

Identification code
Processing code and date

UTM zone

Reference mark 1

Reference mark 2

Data content of abstract portion of the record is:

Discipline

Sub discipline

Keywords - category

Attributes - type

Modifiers - descriptors

The size of each record will vary depending upon the amount of data abstracted for a combined image set. The average record size is considered to be 500 characters.

Using image acquisition rates of 45 sets per day for case A and 165 sets per day for case B the yearly amount of new data gathered for the index/abstract file based on a five day week and assuming a linear growth is:

Case A: 8.2×10^6 characters

Case B: 3.0×10^7 characters

c) Major File Characteristics

Some features and capabilities of this file, in conjunction with the information management program are:

Display and update at a terminal

Automatic indexing of new photography

Batch updating with user abstract data

Fixed records and sub-records and variable data

Geographic retrievals - point, circle, polygon

4-42

Retrievals using Boolean logic and English-like statements

Standard data catalog of all index/abstract data generated over an 18 day complete U. S. coverage period

Specialized output capabilities in response to user requests

4.3.3.2 Master Digital Data File

a) Description

This file provides a history of all PCM housekeeping telemetry that has been time corrected, merged and correlated with the time corresponding orbital and attitude data. The major use of this file is for analysis of the health of the ERTS spacecraft and its sensors.

Data for this file comes from different sources. PCM housekeeping telemetry is received at the tracking stations, where Greenwhich Mean Time data is attached to each telemetry data frame. This data is then sent to the OCC where it is verified and digitized. Orbital data comes from the STADAN/MSFN networks. The processing, merging and correlation of the data is done by a series of specialized programs in the Telemetry and DCS processing subsystem of the NDPF software.

b) File Structure

Data for this file consists of data in its original bit configuration and other data which has been calibrated into engineering units. There are 128 channels in each data frame telemetered. Two channels are subcommutated and can sample different sources throughout the 128 frame commutating cycle. One record is computed as 32 frames of a subcommutated sequence as attitude/orbit information is needed at this interval. The total daily input of data to this file is computed on the basis that, for every 4096 points (128 channels x 32 frames) of telemetry a record consists of:

7/8 of the 4096 points uncalibrated	=	3584 bytes
1/8 of the 4096 points calibrated	=	2048 bytes
8 hardware flags/frame	=	246 bytes
GMT	=	192 bytes
Orbit/attitude	=	200 bytes
Accounting	=	12 bytes
	Total	6282 bytes

There is one record for every 36.80 seconds of telemetry data. Therefore, the total is:

$$\frac{86,400 \text{ sec/day}}{36.80 \text{ sec/record}} = 2348 \text{ records/day}$$

2348 records/day x 6282 bytes/record = 14.7 megabytes/day

This large volume of daily input data and the specialized use of the file data dictates that this file be generated and maintained in the telemetry processing stream of the NDPF rather than handling and processing the data via the information management program.

4.3.3.3 Data Collection System

a) Description

The DCS file provides a history of all ground sensor data collected and transmitted via the data collection platforms. Ground sensors and data collection platforms, accurately sited on the ground, record data on the environment. Data is transmitted from the platforms to ERTS and relayed from the satellite to tracking stations which send the data to the OCC.

At the OCC the data is decommutated, time-tagged and written in digital form on magnetic tape. This data is then input to the NDPF. Here the DCS data is processed and changed into engineering units for input to the information management program for updating the DCS history file.

b) File Structure

The file is organized by collection platform and its sensors. When more definitive information becomes available about the specific sensors and users responsibilities for sensor data, the file may well be organized by user agency and the sensors collecting data for that agency. Data content of these records is as follows:

Platform number

Platform location

Sensor

Agency - Investigator

Acquisition site

Orbit - Revolution

4-44

Date

Time (Greenwich Mean Time)

Parameter 1

.

.

.

.

.

.

Parameter 8

Approximately 4100 DCS messages are received each day.
Each message contains eight sensor readouts which total
approximately 40 bytes of data. Therefore, each sensor is
sampled approximately 20 times a day for case A (4100
messages/day ÷ 200 platforms = 20.5 messages/day/platform).
The total daily input to the DCS File is 164,000 bytes.
Although each platform record is less than 80 bytes of data,
it will grow at a rate of 810 bytes a day (20.5 messages/day/
platform x 40 bytes/messages). For case B which contains
1000 platforms, the daily input to the DCS file is 820,000
bytes.

This file is maintained on tape due to the low volume of
input data. Standard user outputs will be developed to pro-
vide users information only on the ground sensors for which
they are responsible or on which they wish to receive
information.

c)   Major File Characteristics

Some features and capabilities of this file in conjunction with
the information management program are:

Automatic updating

Batch updating

Retrievals using Boolean Logic

Standard outputs

Special formatted reports

Output media - tape, cards, listings

4.3.3.4 Production Control Status File

a) Description

This file contains the current status and summary information on all jobs and work orders in the NDPF. The file is structured so that each process, controlled in the NDPF, comprises a sub-record tied to a fixed record identifier. Each process that is monitored by production control submits a transaction to the production control status file either on punched card or from a terminal device. Format of these transactions are standardized as much as possible to simplify the processing and maintenance of the file by the information management program.

The production control status file is updated daily with transactions recorded on cards and throughout the day with transactions from terminals. The file is also used to provide periodic summary reports and is capable of providing the current status on any job or work order.

b) File Structure

The production control file consists of a standardized set of records and sub-records for each process monitored in this functional area. The data content of these records is as follows:

ID record

    Job/work request number

    Date entered and recorded

    Orbit number

    Type ID

Function sub-record

    Function ID

    Date done

Storage sub-record

    Storage location

    Date stored

Quality sub-record

    Quality code

    Function

    Date

Record sizes will vary but should average 60 characters/ record. Assuming an average retention rate of 15 days from initial entry of a job or work order and a retention rate of 30 days after completion of these orders, the production control status file contains between 10,000 to 20,000 records during normal operation. This requires an on-line storage capability for approximately 1.2×10^6 characters.

c)   Major File Characteristics

Some of the features and capabilities of this file in conjunction with the information management program are:

    Automatic updating

    Display and terminal update

    Update multiple records

    Batch updating

    Retrievals using Boolean logic

    Audit of data prior to update

    Formatted reports for various levels of detail and summarization

    Special reports when required

4.3.3.5 Ground Reference File

a)   Description

The ground reference file is a repository of geographic coordinates for natural and cultural features resolvable on ERTS A/B imagery. Data in this file is used to improve the geometry/attitude and geo-location of the original imagery.

As the use of ground locations are required to improve and correct the geometry of the original imagery, the normal procedure is to find a feature on the image that can be located on a large-scale map, extract the coordinates for the feature from the map and put these values into a geometric

transformation program. To get complete coverage of the
U. S. with large-scale maps requires three map scales.
These are:

Map Scale	Coverage (%)	No. of Maps
1:250,000	100	500
1: 62,500	60	8,000
1: 24,000	40	24,000

A major program is now underway to develop complete
coverage of the United States with 1:24,000 scale maps. At
this scale, full coverage of the United States will amount to
approximately 60,000 maps.

Storing, locating and retrieving the large volume of maps in
their original form is slow, repetitive and very time con-
suming. Therefore, to provide geographic coordinate data
for geometric correction of images a scheme is required to
reduce map storage requirements, improve map retrieval
time and improve map and image correlation time. The
ground reference file is proposed as an alternative or sup-
plemental method to the use of maps.

In operation the ground reference file is maintained on a
direct access storage device. The operator doing the ground
reference correlation uses a display terminal. Based on the
image area, the operator retrieves and displays feature and
coordinate data from the file. He locates the same feature
on the image and using the terminal keyboard enters the dis-
played coordinate data into a transformation program.

b)   File Structure

Input to this file would have to be developed from a variety
of sources such as charts, maps, atlases, Board of Geo-
graphic Names, and other sources. Each feature is indexed
to an arbitrary north-south grid of 100 x 100 nmi squares.
The data content of the feature record is as follows:

Name of feature

Geographic coordinates of feature

Source of data

Grid designator

Near by feature

Direction

Distance

Name

Coordinates

The record is estimated to be 100 characters. Assuming
an average of 50 ground reference points per 100 x 100 nmi
grid, the file would contain approximately 18,000 records
and the ultimate size of the file would be 1.8×10^6 bytes.

The file is used daily in the post processing of images. If
a display terminal such as digital TV is used, the 1:250,000
maps could be video mixed in with the data on the face of the
CRT and the features could be keyed to the maps for more
rapid correlation with the image features.

c)   Major File Characteristics

Some features and capabilities of this file in conjunction with
the information management program are:

Direct access storage

Terminal retrieval and display

Update of fields and file

4.3.3.6 Map Reference File

a)   Description

The map reference file provides a rapid method for identifying
the maps which cover the area on each set of imagery. The
number of large scale maps that cover the United States is
very large (world coverage is significantly larger). If maps
are used in any form for ground location data, the time to
retrieve needed maps is significantly improved with this file.

Large scale maps for ground reference purposes will be in
film strip or chip form. The map reference file provides
either an automated or semi-automated method for retriev-
ing the necessary large scale maps which cover a set of
images. Small scale maps (1:250,000) will be indexed by
their area of coverage (map corner coordinates). When
telemetry data is processed and the four corner coordinates
of an image are determined, these coordinates form the basis
of a search query against the map reference file. The output
of this query is a list of maps (minimum 1 - maximum 4)
which cover the imaged area and is made available to the
mensuration operations.

In the semi-automated mode, the large scale maps would be indexed on these 1:250,000 maps. The maps would be manually retrieved and the location and accession number of the large scale maps would be read off directly from these index bases. In the automated mode, the map indexes would be in film chip form. They would be retrieved by the operator using the function keyboard on his display terminal. A film chip map would be automatically retrieved and displayed via closed circuit TV to the operator. The appropriate large scale map location and accession number would be read off the displayed index.

b)   File Structure

The data content of the map reference file record is as follows:

Accession number

Storage location - Original form

Storage location - Reduced form

Map number

Map date

Edition

Coordinates - Corner 1

Coordinates - Corner 2

Coordinates - Corner 3

Coordinates - Corner 4

A record consists of 100 characters. Based on complete coverage of the United States with maps at 1:250,000; there is approximately 500 records or approximately 50,000 bytes of data in the file.

c).   Major File Characteristics

Some major features and capabilities of this file in conjunction with the information management program are:

Logical updating with change data and new records

Terminal retrieval and display

Retrievals using Boolean logic

Geographic search capability

Sort and merge

Formatted output

Direct access storage

4.3.3.7 Library Index File

a) Description

The library index file provides a record and the location of all physical items stored in the active and archive portions of the library.

Items stored in the library are the final products of a process and, as necessary, the original input data. Based on an analysis of data that should be saved, the length of time it should be maintained and the form it should be stored, the NDPF library is comprised of an active and archive library (see Table 4-1). The archive storage area may be physically separate from the NDPF but a record of data stored there is maintained in the library index.

The file is updated daily with new acquisitions and is used in servicing requests for data in the library. For ease of updating and retrieval from a terminal, the file is maintained on a direct access device.

b) File Structure

The items maintained in the library consist of data files; processed imagery in roll film, cut film, and print form; catalogs; and digitized imagery. A record is made of each physical item. The data content of the records is as follows:

Accession number

Data content

Storage form

Storage location

Data of data

Date placed in library

Suspense date

Placed in archives

Office prime responsibility

4-51

Source of data

Archive sub-record

Storage form

Storage location

Data content

Each record is estimated to have 80 characters. The file
will be very small initially and will gradually increase in
size. The rate of growth depends on the number of separate
items stored and the retention period for these items (see
Table 4-1).

c) Major File Characteristics

Some features and capabilities of this file in conjunction with
the information management program are:

Display and update at a terminal

Batch updating

Standard formatted outputs of holdings

Special listings of holdings

4. 3. 3. 8 Time History File

a) Description

This file is a history of previously verified and corrected
GMT. The time history file is used to keep the time conti-
nuity of the PCM telemetry throughout the lifetime of each
ERT Satellite. This file provides the only source of data to
correctly time annotate the playback data if received sepa-
rately from the real-time data.

The time history file is used in the preprocessing phase of
the PCM data reduction stream. Data for input to this file
is generated by the time verification and correction section
of the preprocessor.

b) File Structure

The file is maintained on disk for use with a direct access
storage. It consists of several directory records and many
time line entries. The directory record is a quick index to

the location of the time reference desired. The time line entries give the time characteristics of a segment of time continuous data.

The daily input to this file is one entry of 42 bytes to the directory. The number of time line entries is variable but an average of two to three is expected. Each time line entry consists of 72 bytes. Based on an average growth rate of 200 bypes/day, the file will contain 73,000 bytes of data after one year of operation.

4.3.3.9 DCP File

a) Description

The DCP file contains data on each platform location and the calibration data on each sensor. This file is used in the DCS processing stream to change the DCS data into engineering units. The file is updated everytime a sensor is recalibrated and when new platforms and sensors are added or deleted.

b) File Structure

The file is maintained on disk for use with a direct access storage device. It is organized using the unique identification code of each platform. The data content of each record is as follows:

Platform ID

Location – geographic coordinates

Date

Sensor 1 calibration data

Sensor 1 calibration date

.

.

.

.

Sensor 8 calibration data

Sensor 8 calibration date

A record is approximately 100 characters. For class A with 200 platforms the file size is 20,000 bytes. For case B with 1000 platforms the file size is 100,000 bytes.

4. 3. 3. 10 Attitude History File

a) Description

The attitude history file provides a complete history of a spacecraft's orientation throughout its lifetime. Data for this file is developed from corrected GMT, orbital, and spacecraft data. Data for this file is generated during the processing of the PCM data.

A continuous attitude history is part of the data generated for the master digital data file. With this data available at all times, the need to maintain a separate and completely redundant attitude history is not warranted. Based on attitude data requirements, data for this file is extracted from the spacecraft, time, and orbit information every 140 seconds the spacecraft is not over the United States. When the satellite is over the United States, data is extracted every 18 seconds.

b) File Structure

The file will be organized by orbit and time. The data content of each record is as follows:

Orbit

Time (Greenwich Mean Time)

Roll

Pitch

Yaw

The sensor attitude data is in terms of a designated coordinate system. To provide a level of accuracy the data is extracted at intervals of 18 to 140 seconds as previously discussed. Using these sampling rates the following amount of data is generated daily:

3600 bytes of precision attitude/day

9600 bytes of non-precision attitude/day

The total daily input of 13, 200 bytes per day is considerably less than the approximately 600, 000 bytes a day to maintain a continuous, separate spacecraft attitude history. The file is maintained on tape. After one year of operation the file will contain 4.8×10^6 bytes of data.

A summary of the NDPF file sizes is given in Table 4. 3-1.

Table 4.3-1. NDPF — Data Base Size

File	ERTS A Case A*	ERTS B Case B*
Index/abstract	8.2×10^6	3.0×10^7
Master digital data	5.4×10^9	5.4×10^9
DCS	6.0×10^7	3.0×10^8
Production Control	1.2×10^6**	1.2×10^6**
Ground Reference	1.8×10^6**	1.8×10^6**
Map reference	5.0×10^4**	5.0×10^4**
Library index	2.0×10^6	3.0×10^6
Time history	7.3×10^4	7.3×10^4
DCP	2.0×10^4	1.0×10^5
Attitude history	4.8×10^6	4.8×10^6

*Bytes of data after one year of operation
**Maximum file size

4.3.3.11 Deleted Files

In the initial analysis of the data base file requirements of the NDPF, a set of files to perform the necessary functions within the NDPF were identified. Continued analysis of requirements, methods of utilizing identified files, and the benefits to be derived from these files resulted in the deletion of some files and the addition of a few small files. For example, to annotate the initial bulk imagery being processed, an annotation data tape is generated in the PCM processing function. Post-processing of imagery refines some of this annotation data and adds to it. However, a large portion of the original annotation data is still valid. A file of original annotation data would be nice to have; as it could be easily updated and data readily retrieved. In time, the annotation data file would become very large. Since the index record has almost all the data

elements required for annotation data, adding a few fields to handle specialized annotation data to the index record provides the same capability inherent in an annotation file. Consequently, a separate annotation file is not considered necessary for the NDPF data base.

A cross-index file was initially designated as being required to tie in associated records in the DCS; library index, and index/abstract files. Continued analysis of this requirement indicated a relatively high development cost to provide a cross-index capability in the information management program. Additionally, with respect to the DCS File, each ground sensor would be read out on the order of 360 times per 18 day cycle. In this period, there would be only one image set from the RBV and MSS sensors taken over the ground sensor and not necessarily at the same precise moment. As user needs for correlating ground sensor and image data are not well defined, and the volume of ground sensor data is large compared to image data, the value of providing the cross-indexing capability with only the index/abstract and library index files was not justified. Therefore, the need for a cross-index file at this time is not warranted and can be added later when system growth requires it.

Digital precision processing creates a large volume of data which has been processed by the computer. To obviate the need to repeat this processing effort, a file of digitized data was identified. Based on present concepts, the precision digitized data will be retained for only one year in the NDPF data base library as the original image data will be available in digitized form. Information on the images that have been precision digitized will be maintained in the index/abstract record until the precision digitized data is purged. Consequently, there is no need for a separate permanent digital image data file.

4.3.4 Interaction With Users

An examination has been made of interactions with users who wish to do their own searches, or who have other special needs.

4.3.4.1 User With Some Data Processing Capability

There are a number of different variables which might effect the extent of a user's in-house capability, but for the moment let us assume

the situation where the user has at minimum a data processing facility for handling data indexes and abstracts, but no precise image processing. It would be reasonable to expect then that NASA would do special image processing by request for that customer, and it would be logistically easier and operationally less expensive for NASA to distribute the index / abstract file in either magnetic tape or punched card form. The user would then have a direct machine-readable input to his system and he could process it in any manner desired. On the other hand, the two systems should be sufficiently comparable to allow a direct machine-readable flow back to NASA for incorporation of that customer's comments back into the central files.

A user with a large image processing capability would probably need raw video tapes or limited coverage digital image tapes. This type of situation would require a different interface, but is not likely in the early years of ERTS implementation because of reduced government spending.

The standard products to a user having some in-house capability would include RBV/MSS coverage indexes, probably in magnetic tape form, abstract catalogs in both machine readable and hard copy form, DCS magnetic tapes, hard copy montage catalogs, and hard copy imagery. Special products would include hard copy precision imagery and machine-readable information. Some bulk-mode machine-readable imagery (digitized tapes) and high precision digital imagery would be provided to the user having a large image-processing capability of his own.

4.3.4.2 User With No Data Processing Capability

Users with no data processing capability must rely on printed data and catalogs for the informational data, and hard-copy prints and montage catalogs for the imagery. Any precision imagery would by necessity be processed and reproduced in film form by NASA as the result of a user request, and the user would rely on NASA for timeliness and accuracy. Abstracting by this type of user would require completion of specially designed forms for input back to NASA or in some instances the user might have a keypunching capability sufficient to provide NASA a machine-compatible input.

Another variable would be the extent to which the user could search the index files to determine which frames of coverage he desired. Some could search their own internally-maintained indexes to verify their specific needs, while most would need the service performed by NASA. The latter case would most likely be more prevalent, and accordingly, a user liaison office and browse library is being provided in the NDPF facility.

In summary, the user interface must be interactive in the sense that NASA provides a data exchange and inquiry service to all users, whether the users have a data processing capability or not. This requires computer hardware appropriate to the evolving requirements of the user (but minimally supporting the NDPF requirements discussed earlier in this section) and software that allows a common exchange of data in two directions--initially for inquiry and index searching, and subsequently for maintenance of abstracts.

The information management programs will allow all users a common input mode to the data files, a common English-like language for retrieving data from all files in the system, and a flexible report generation and formatting capability consistent with all user's product needs.

Image classification (i.e. quality and cloud cover) is done in the NDPF and added to the index portion of the record. The abstract portion of the index/abstract file is generated by the users, returned to the NDPF, and merged into the file. Data content of the scene will not be abstracted in the NDPF due to the variety of information contained in the images, the numerous specialized disciplines involved, and for accuracy this effort can be very time consuming. Also, for the NDPF to do the abstracting, it would have to duplicate (but not on a one-to-one basis) the capabilities and personnel of the users. Therefore, the approach to obtain abstract data is to provide users a formatted user abstract form which is keyed to the imagery they receive.

The user abstract form will be automatically sent with the film and contain preprinted header information. This information will be basically the same data annotated on the image. Space will be provided for users

to report data they abstract. The completed form is returned to the NDPF and the abstracted data is keypunched and the file is updated with the information in a batch mode. The preprinted data does not need to be re-entered into the file. Only the record identification data (orbit, date, time) is required so that the abstract data is added to the correct record. The formatted user abstract form serves many functions such as:

1) Associates the form to the image

2) Provides a management tool which identifies:

    a) Users who receive the form

    b) Abstracts that have been returned

    c) Users who have not supplied an abstract within a specified suspense (cutoff) date

    d) Data for readily inserting the abstract data into the correct index/abstract record

3) It is structured to provide keywords, attributes, and descriptions to categorize textual data.

4) It allows for descriptive, free flowing, unformatted English text.

The user abstract form must be developed based on the users' ability to extract data from the imagery and his stated requirements for information. Important considerations are:

1) It must be developed in conjunction with the users.

2) It must provide for maximum user capability and flexibility.

3) It must not contain extraneous or unavailable data.

4) The variety and number of users that can provide an abstract and the many disciplines that can be included with the vast array of technical terminology they possess must be organized so that all needed discipline areas are reportable and retrievable.

The development of the user abstract form and the maintenance and retrieval of the abstract data are important considerations that will be done in phase D based on an analysis of users' requirements, capabilities, and data retrieval needs.

4.4 PRODUCTION CONTROL

4.4.1 Introduction

The design of the Production Control function has been influenced to a great extent by the recognition of the importance of this function in any system with more than one individual or resource. Too often this function is considered too late in the design process for practical implementation of effective control techniques.

It was first determined that the Production Control function would have the overall control and coordination responsibility for the NDPF. It is the basic tool for management personnel who are responsible for all basic operational decisions. It provides management with the basis for decisions and when these decisions have been made, it distributes the management decisions to the operating functions in the form of detailed work schedules and procedures.

The effective performance of these responsibilities can only be accomplished with a large amount of communication between the production control function and all the other functions. The design of the communication channels requires experience in related applications as well as data processing equipment and software for practical designs.

The production control operations and design developed thus far are based on those developed in similar installations of this type in the past. For example, large film processing installations and large scale computer operations were evaluated. From these evaluations the degree or extent of control proposed and its value to the NDPF operations were apparent.

Quality control, as a sub-function of the production control function, is included in the design proposed. It is included here because, based on present assessments, it does not appear to deserve its own separate functional level. If the production control function does grow in importance and the resultant organizational support grows, consideration should be made for making this a separate function.

The most important design consideration is that the production control function must be flexible. It is significantly affected by varying production schedules or loads and interfaces with all of the operations

personnel. But its most important external control is the management it is designed to service.

4.4.2 Production Control Requirements

The Production Control function is responsible for the overall coordination of the NDPF operation. In both the "bulk" and "request" modes, control is maintained and operations are monitored on a continuing basis.

To perform this broad responsibility, the production control capability must be in contact with all the functions of the NDPF. The communication will be in two directions, with general and detailed schedules, summaries, and work orders originating from production control, and detailed progress or status information returning to the production control system from the functions.

The basic functional requirements which production control must perform include:

Process control - Continuous audit of the major system operations to assure throughput success.

- Process identification - the development of standards and controls on the operations to be performed.

- Resource monitoring - the continuous checking of resource utilization and performance.

- Performance monitoring - the continuous auditing of the overall NDPF operations.

- Quality control - the review of the input and output of the operational functions.

Data control - Detail level monitoring of jobs, resources, inventories, tapes, products, etc.

- Status/progress data - the maintenance of current status of jobs, resources, and inventory at a detail level.

- Summary data - condensation of the detail data for more effective presentation to management.

- Historical data - data maintained in less accessible form for other than current or active jobs.

Job control - Interface with the user (both on input and output), and detail level scheduling and work order processing.

- Job identification - the development of standards identifying jobs and their required input and output.

- Job definition - defining the sequential functions to be performed for successful completion of a job.

- Job scheduling - the relating of the sequential function, jobs and resources in a chronological relation.

- Job monitoring - relating actual schedules to predicted schedules.

Management control - Continuous assessment of reports generated in each of the above areas to provide appropriate direction to the operating units.

- Workload analysis - presentations of data or the current and projected activity by resource or function.

- Performance analysis - a review of the scheduling and quality performance of a resource or function.

- Plans - organized input that forms the basis for production control direction to the operating functions.

- Schedules - the day to day direction to functions or resources.

Figure 4.4-1 is a general overview of the production control function. Input in the form of job progress, status information, schedules, and planning information is delivered to the computer in the form of transactions.

These transactions are audited and then used to update the production control status file stored in the computer. The updated file is in turn used to generate the detailed and summary reports. Figure 4.4-2 is a generalized diagram of the sequence in which these computer oriented operations are performed.

In order to design the production control capability, a detailed analysis of the operations was performed. This analysis identified all production control interactions and organized the operations into a standard set of job flows. It also generally described the production control status file as to size and content. Later, during phase D, this

INPUT FROM MANAGEMENT OR DESIGNER
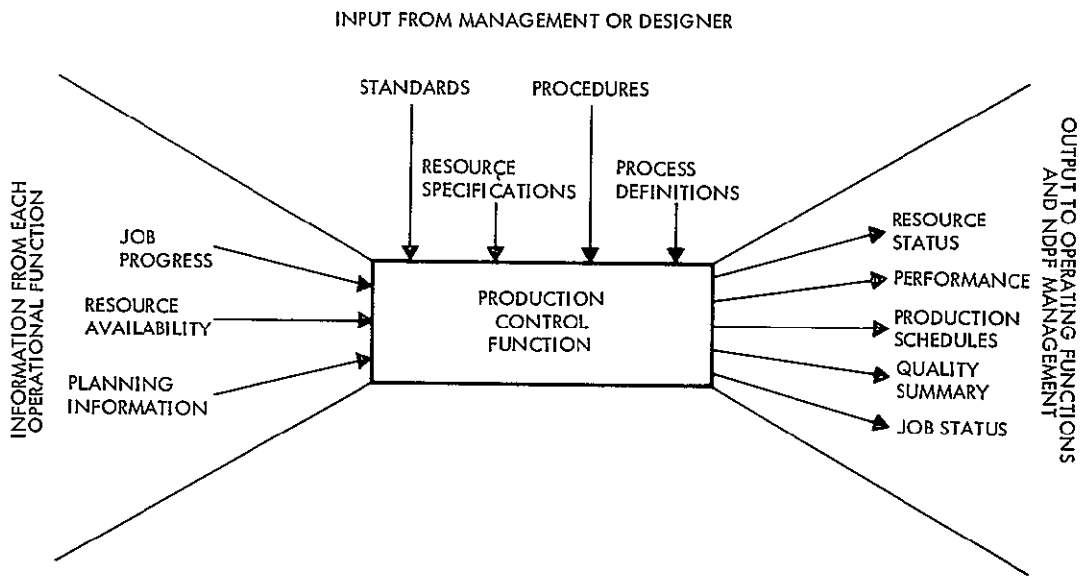
Figure 4.4-1

CONTROL FUNCTION DIAGRAM
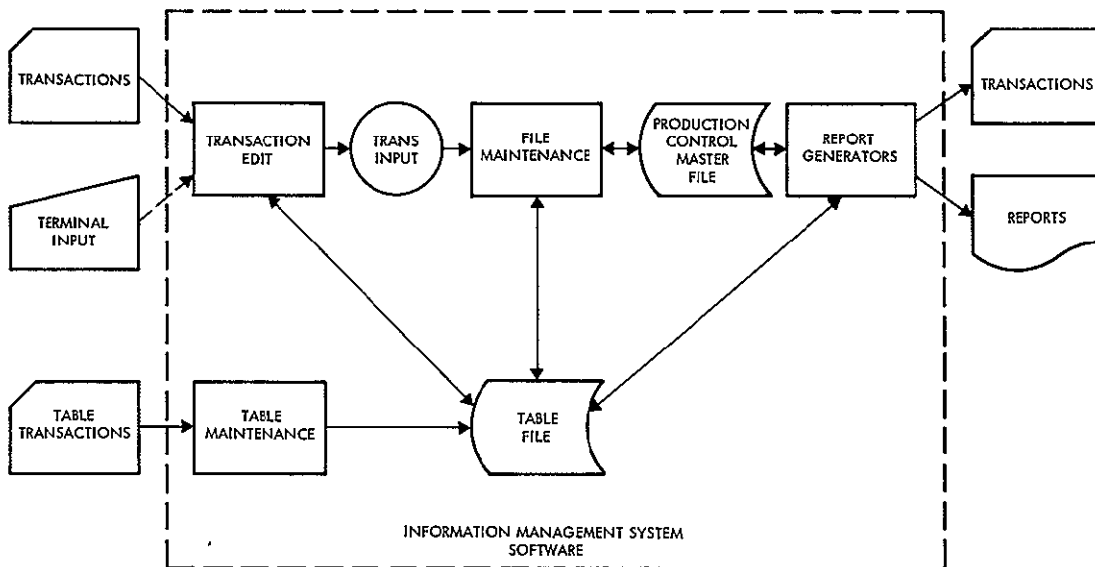
Figure 4.4-2

PRODUCTION CONTROL – COMPUTER PROCESSING

information will provide a basis for designing work order forms, the specific file contents, the required report formats, and the establishment of all standards and procedures. Although much of the specific production control design has been left for phase D, it was considered important during phase B/C to relate the functional flows with production control, and to identify the basic work flows and points of interaction.

The NDPF concept of production control revolves around the production control status file, which accepts machine-readable status inputs from the critical points in the job flows and assists management in scheduling, reporting status, and assuring uninterrupted flow of the many tapes, jobs, and products through the system. The system being proposed uses a series of keypunched cards, probably color-coded and pre-punched, which follow the jobs through the system and are entered as transactions at designated event points. Depending upon the frequency of reporting needs, the cards are collected and processed. This would occur at least once each working data, perhaps more frequently. Future production control workloads might require the use of remote terminals for transaction entries and receipt of scheduling priorities.

Briefly discussed below are the detailed steps required for phase D implementation of the production control capability. Five study areas are recommended:

- Validation of the specific production control interfaces
- File and report format design
- Forms design (work orders, transactions)
- Procedures
- Standards

The implementation requirements are discussed below, and a section follows identifying the critical points of production control interaction in the system, organized by functional area.

4.4.3 Implementation Requirements

To complete the design of the production control capability, the detailed information collected and summarized about each operational function must be reexamined and validated. Figure 4.4-3 suggests a

Function Name

No

Sequential Position - After function no. _____

Before function no. _____

Brief Description of Function

Major Logical Activity

Input Description

Source

Volume

Output Description

Destination

Volume

Resources Required for Function

Figure 4.4-3

PRODUCTION CONTROL ANALYSIS FORM

possible form which could be used to assemble the needed data. The completed forms would provide the data needed to identify each functional area. Another major requirement for production control design is information on the inputs and outputs for each of the functions. Figure 4.4-4 is a suggested form for collection of the information required. It becomes obvious from the above requirements that in the process of developing the input for the production control capability, the overall NDPF will be subjected to a critical design review, finally evolving into a specific design which when operational will include the production control capabilities as an integral part of each of the other functions.

In the performance of the production control function certain data must be accumulated and presented to management or the other functions in various forms. The design of the information management file is important to the efficient gathering, processing, and return of the data to the users.

Input/Output Name

Identification Code/Identifier

Where Used   Input to_____function.

                  Output from_____function.

General Description

                  `

Detail Description

Volume Information

Figure 4.4-4

INPUT/OUTPUT DEFINITION FORM

Several types of data must be stored in the production control file.
A partial list includes:

- Descriptions of each input or output tape, including inter-
  mediate tapes.

- Performance of each operation performed on each tape.

- Storage or location information on each tape.

- Summaries of various types.

- Quality control information on the various operations or
  tapes.

Separate files could be organized for each of the important types of
data required. This approach would offer simplicity in initial design and
would generally be the result of a piecemeal design effort. This type of
design, if followed through with improvements, eventually requires more
complex programming considerations to tie together these somewhat
unrelated files. In view of this and with adequate time for design devel-
opment during phase D, a single integrated file for all production control
information is recommended for this application. This one central pro-
duction control status file will have a basic key field, based on identifica-
tion by either a video tape or a work request. Associated with each

master record will be a variable number of detailed records relating to the master record.

4.4.3.1 Report Design

Efficient generation of well designed reports is also an important consideration. Control must be exercised to reduce the number of reports and consolidate or standardize where possible. This control must be exercised carefully to insure that reports that could serve useful purposes are not discouraged. The reports generated to support the production control capability might include the following types of information

Detailed Reports:	Summary Reports:
Job status by job ID	Job status summary
Job status by function	Function performance summary
Function performance	Resource performance summary
Resource performance	Quality control summary
Active work orders	Work request summary
Quality control detail	Daily and monthly production recaps
Work request status	Average elapsed time, shipped work orders

4.4.3.2 Forms Design

Much of the input to production control and several other functions will be provided from forms originated by users or requestors, production personnel, or others. Well designed forms for efficient origination and keypunching are important. Time spent on the design of documents such as the request or work order form and the transaction cards will be well spent in the long run. The forms design effort will include consideration of:

- The file copy needs of the permanent archives and all users of the form.

- Keypunch or other input to computer, and compatibility with production control status file.

- Minimal time on the part of the originators and others involved in the form processing.

4.4.3.3 Procedures and Standards

A major part of the design of the production control capability will be associated with the manual and/or clerical procedures. General broad based procedures are preferred to very detailed procedures that become obsolete almost immediately. This approach will result in secondary advantages in the form of optimum control and standards.

In the interest of reducing costs and confusion, existing procedures and standards should be reviewed in detail in all areas that will service ERTS as well as other scientific satellite projects. The confusion that is created when personnel involved in more than one project are forced to become familiar with several standards or forms can be very significant in operational cost. An example is the method used in assigning numbers to analog tapes recorded at the ground stations. It is suggested that the standards for all other scientific satellites apply to ERTS in this regard.

The production control function should be responsible for developing the unique standards necessary for control within the NDPF. Items such as identification schemes for individual frames, work orders, or tapes fall within this range of activity. Standards in reports is an important area of concern. Reports have a custom of becoming specialized to individuals or limited areas of concern. Controls on design of reports to generalize them can result in significant savings on the part of the maintenance and operational personnel.

4.4.4 Interaction with NDPF Operations

Operationally, production control will monitor the daily inputs to the NDPF. Queries will be run daily against the production control status file to identify those items available for processing. When all required elements of a processing line or chain are available in the NDPF, work orders and transactions are generated and sent to the appropriate functional areas concerned with processing and completing the job requirements. The transactions are structured so that each identified critical process and functional area have a ready and easy method to communicate back to production control when a process is finished or must be delayed due to problems. They are also the vehicle used to update the status file.

Work orders contain the necessary information to identify the job requestor, type of process and output desired and the identification and location of the data sources to be processed.

The built in notification system using transaction cards related to specific jobs and work orders provides the necessary information to production control for keeping track of a job, process, and work order. It also provides the basic data for daily status reports of work in progress and work completed. Transactions also provide the means' of alerting production control to malfunctions, queueing problems, and processes not completed for any of many possible problems. This gives production control the information necessary to rearrange job schedules, avoid developing a backlog of production work, and to notify users of possible delays.

In order to better describe the various production control interactions within the NDPF, the functions were organized into major categories, in a sequence equivalent to the daily operations. In that way it was possible to follow typical jobs through from start to finish in the proper sequences.

These production control interactions have been developed to handle NDPF operations as conceived in the phase B/C study. During phase D, any changes to the mode of operations or data flow in the NDPF will affect production control. Therefore, production control procedures must be developed in consonance with system development and be modified as necessary to provide a viable and interactive capability when the GDHS becomes operational.

The functions and their logical sequence of events follows, for the bulk and request modes of operation:

Bulk Mode:	Request Mode:
User job control (1)	User job control (1)
Telemetry and DCS processing (1), (2)	Information management (2)
Image conversion and geometric correction	Pre-process imagery (includes digitizing, mensuration, transformations) (1)
Photo lab processing	Digital image processing (geometric and photometric corrections) (2)
Screen/select/index (1)	
Image set correlation	
Photo lab processing	Photo lab processing
User job control	User job control

(1) Direct interface with information management processing function.
(2) Major computer processing functions.

As noted above there are four major functions requiring extensive computer processing or interaction: telemetry and DCS processing, bulk image conversion and geometric correction, information management, and digital image processing. Production control must schedule all processing around these four functions, since it is required that large blocks of time be "reserved," in a multi-processing environment, each day for their processing.

Because of the large amount of core storage required to do digital image processing, it is envisioned that no bulk image conversion nor telemetry processing can be performed while digital image processing is taking place. However, the NDPF operating system and information management programs will be resident in core at all times; the operating system to service the entire system, and the information management capabilities to service user requests, file updates, input/output terminal interactions, and production control reporting.

Scheduling occurs at two levels of detail. Block scheduling is required to process all imagery and related data through the bulk mode. It is estimated that once all inputs are received at the NDPF, e.g., video tapes, telemetry, updated orbital ephemeris, there will be a 6-day cycle needed to complete the processing. Individual job scheduling of normal computer room activities occurs within the framework of the block schedule.

Each day a new 6-day cycle begins, so in effect all functions are performed daily, but in support of various levels of the 6-day cycles, as shown in Table 4.4-1.

Table 4.4-1. 6-Day Cycle Data

Inputs Received	Day 1	Day 2	Day 3	Day 4	Day 5	Day 6
Day 1	Process telemetry and DCS data	Convert and process all bulk imagery (LBR and photo lab)	Screen, select, index all imagery	Correlate all images in a set (PPR)	Reproduce all film for distribution (photo lab)	Assemble all bulk imagery and data for packaging and shipping
Day 2		Process telemetry and DCS data.	Convert and process all bulk imagery (LBR and photo lab)	Screen, select, index all imagery.	Correlate all images in a set (PPR)	Reproduce all film for distribution (photo lab)

└──►continued through Day 6

4.4.4.1 Bulk Mode

In the bulk mode it is possible to trace the steps of a typical 6-day cycle, as the production control function follows the job through the various functions. Outlined below are the production control actions within each step. Production control abbreviated as P. C. for brevity of the bulk mode.

<u>User Job Control</u> (action required prior to Day 1 processing)

- Label tape (telemetry, video, ephemeris) and create transaction card identifying time and/or orbit (tape contents).

- Submit transaction card and tape to library for storage until all tapes for a particular day are received.

- Log tape into library and add library accession number to card -- send card back to P. C.

- P. C. enters tape status into P. C. status file.

- P. C. runs daily query to determine status of tapes received and to create work order if all tapes have been received--one copy to job control to initiate 6-day cycle; one copy to library to retrieve desired tapes.

- For DCS tape received, label tape and create transaction card identifying DCS tape contents.

- Submit DCS tape to library for future process scheduling.

- Log DCS tape into library and add library accession number to card--send card back to P. C.

- P. C. enters tape status onto file.

The interactions of user job control with production control and the library are detailed in the individual production control flow charts, Figures 4.4-5 through 4.4-11.

<u>Telemetry and DCS Processing</u>

- Query alerts P. C. when telemetry is to be processed.

- Job is scheduled, and a transaction card prepared for each major step in the process.

- Submit transaction card to P. C. when initial spacecraft reference tape has been built.

- Submit transaction card to P. C. when attitude history tape has been built.

- Submit transaction card to P. C. when final spacecraft reference tape is completed.

- Submit transaction card to P. C. when annotation and index tapes are built.

- Submit transaction card to P. C. when master digital data tape has been compiled.

- For each of above-received cards P. C. updates status file.

- All tapes are sent to the library (annotation, index, attitude history, master digital). The annotation tape is saved for the image conversion function; the index tape is saved for updating the index/abstract file in the information management function; the other tapes are stored for future requests.

- For DCS processing P. C. generates a work order and schedules job.

- P. C. has computer room run entire DCS job (includes all DCS re-formatting, editing, and merging, and information management update).

- Upon DCS job completion, transaction card submitted to P. C.

- P. C. updates status file.

- P. C. sends tapes to library and audit listings to DCS file analyst.

The production control flows for these processes are contained in Figure 4.4-5.

Image Conversion and Geometric Correction

- Query alerts P. C. when bulk image conversion is to be scheduled.

- P. C. creates work order and transaction card for each unique input tape flowing through the operation.

- As each card is returned to P. C. the status file is updated.

- Each output film and a transaction card is sent to the photo lab, where internal control procedures require transaction card outputs at various key stops in the photo lab process.

- For each unique film output photo lab submits transaction card to P. C.

- P. C. updates status file with each input.

- Photo lab sends film to library and notifies P. C.

- The work order remains active for further processing.

Figure 4.4-6 depicts the production control interactions for bulk image processing.
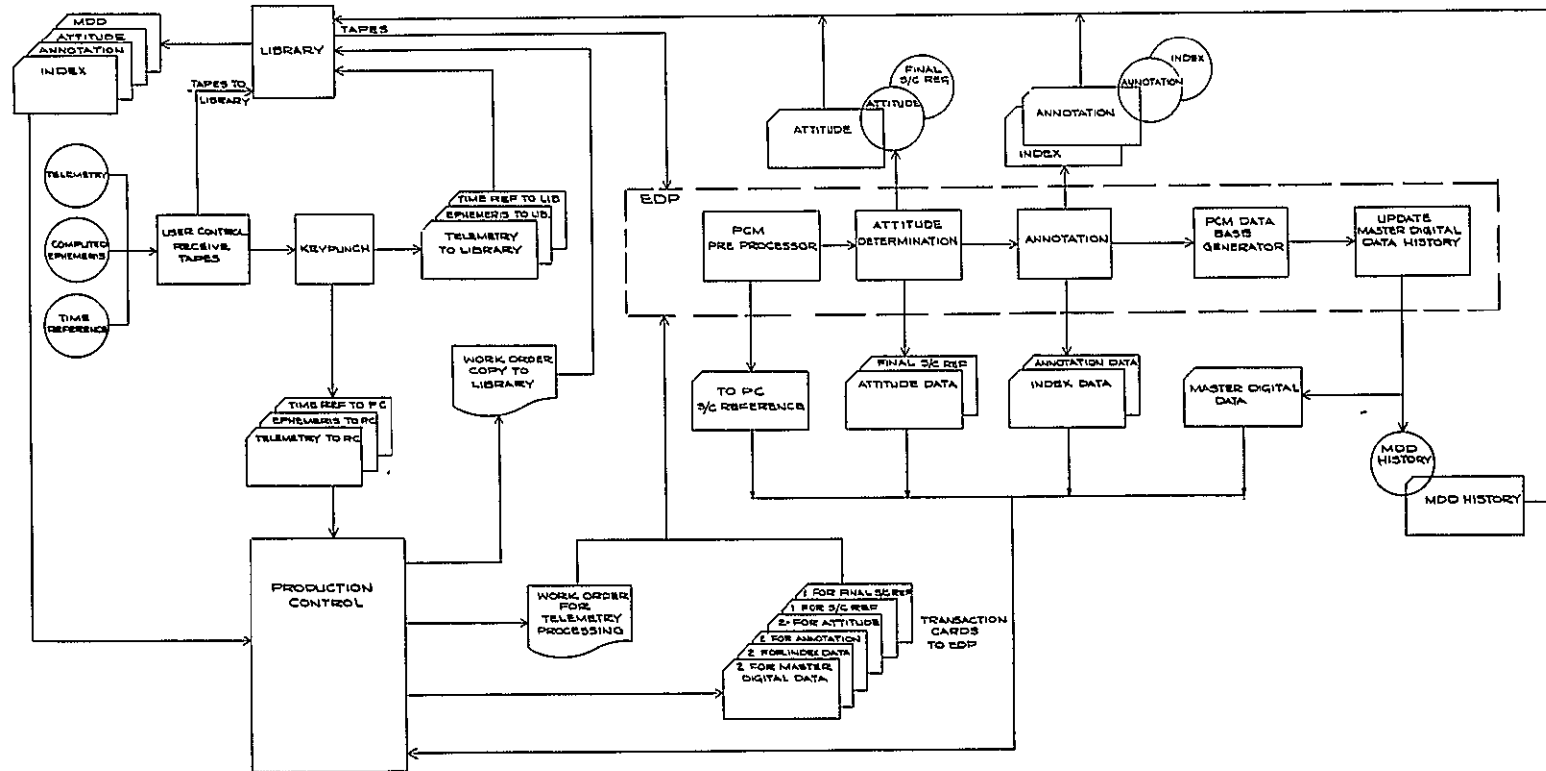
Figure 4.4-5

PRODUCTION CONTROL for telemetry processing

4-74.
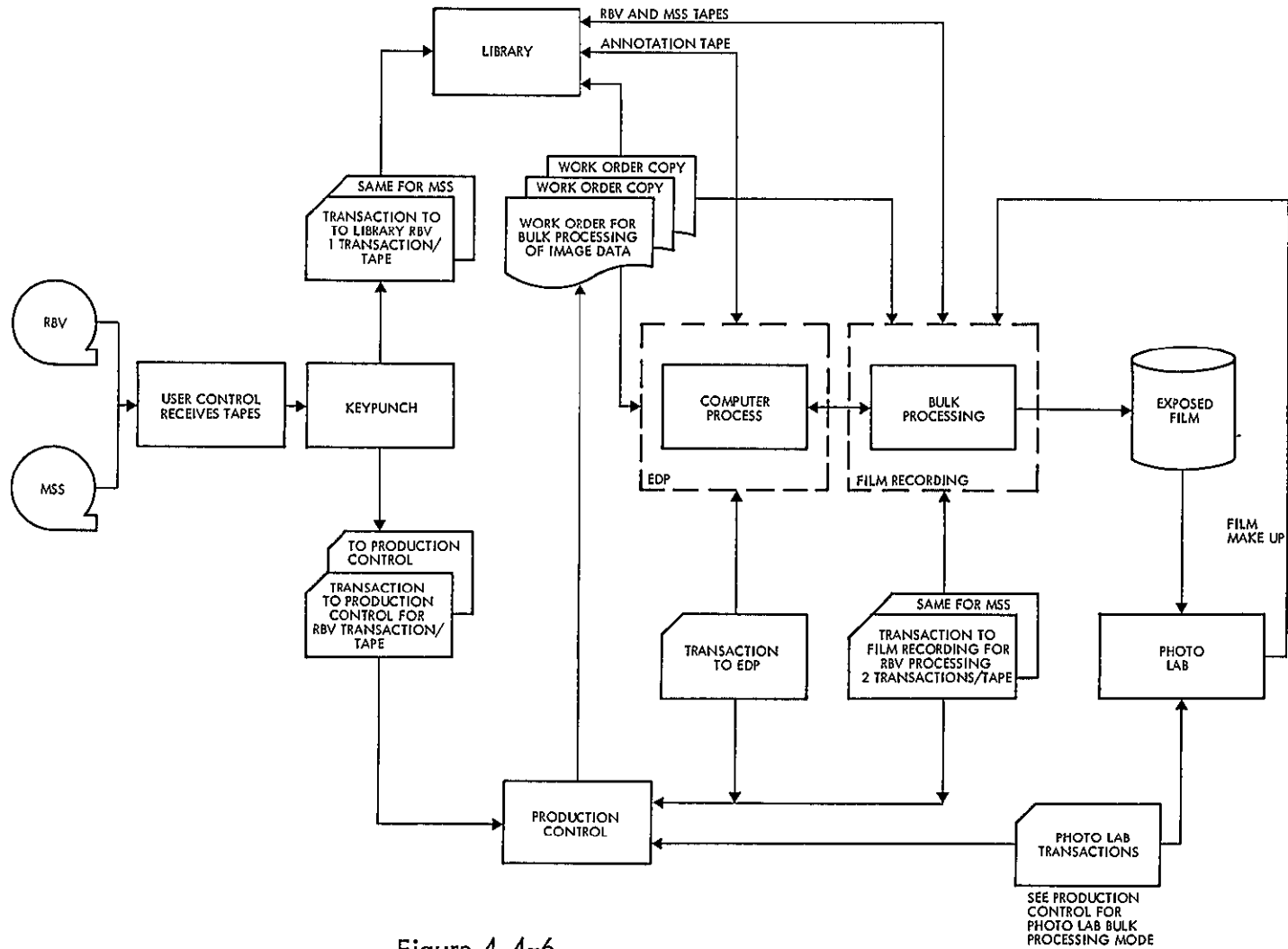
Figure 4.4-6

PRODUCTION CONTROL for bulk image processing
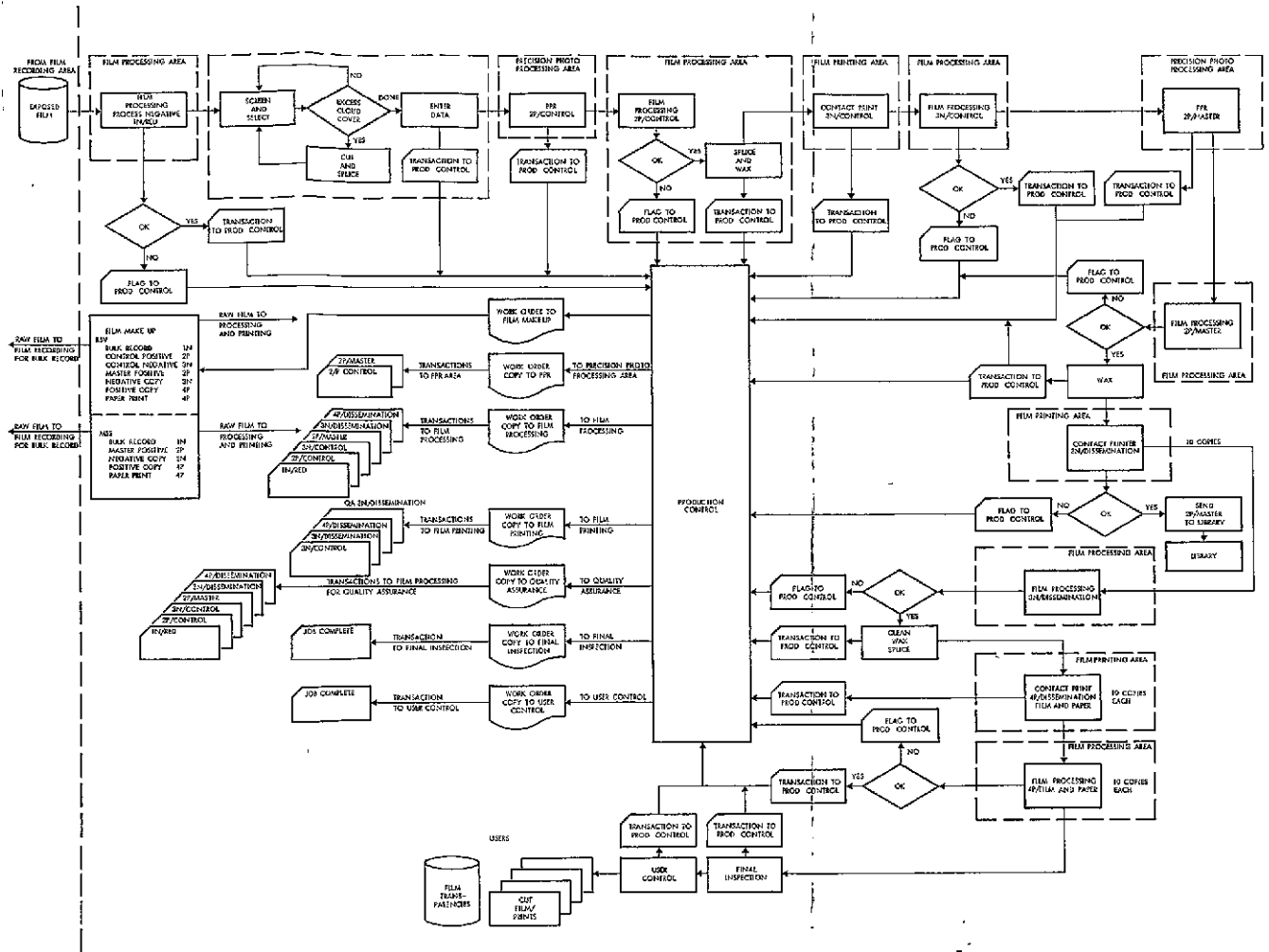
Figure 4.4-7

PRODUCTION CONTROL for photographic
laboratories bulk processing mode
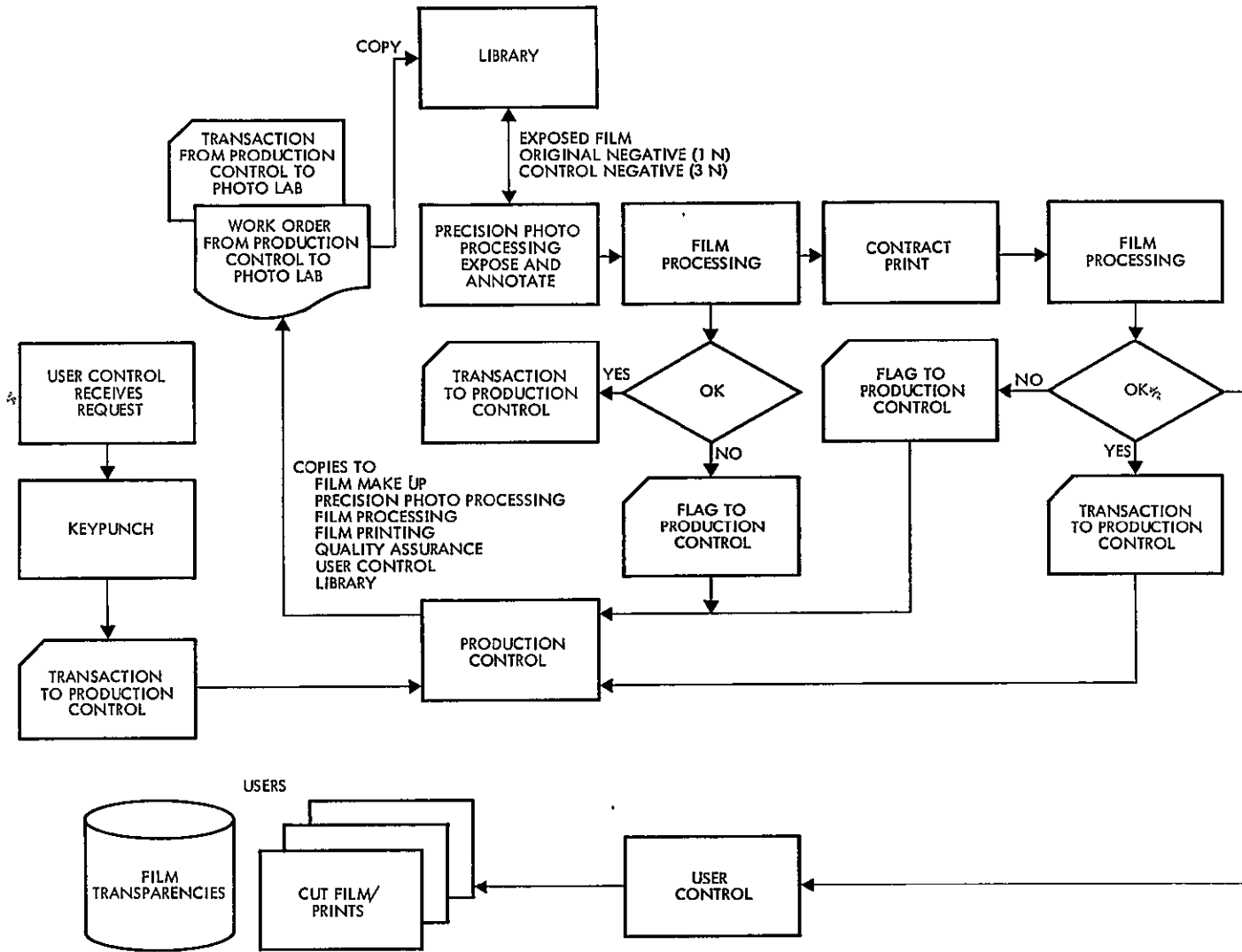
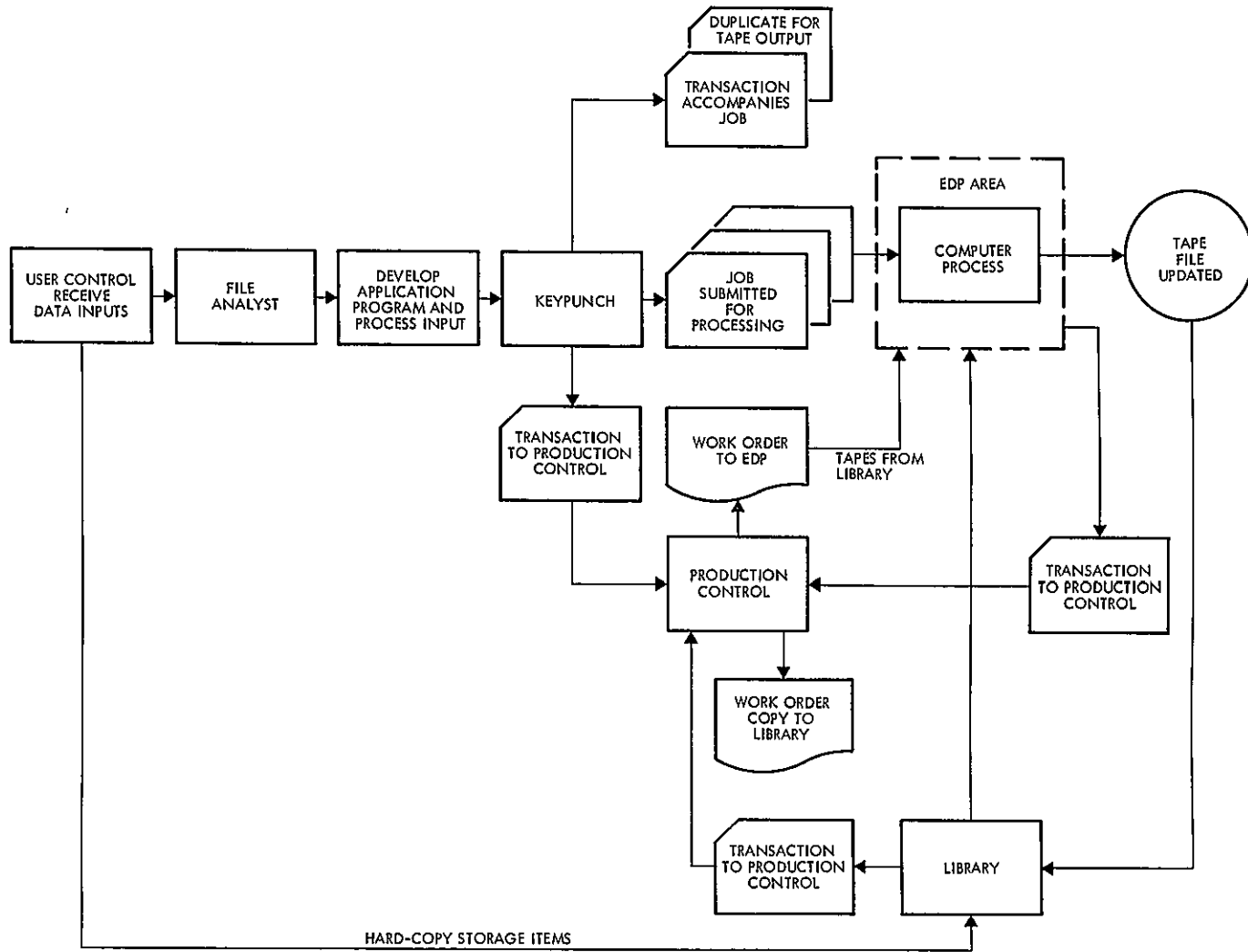Figure 4.4-8

PRODUCTION CONTROL for color film processing

Figure 4.4-9

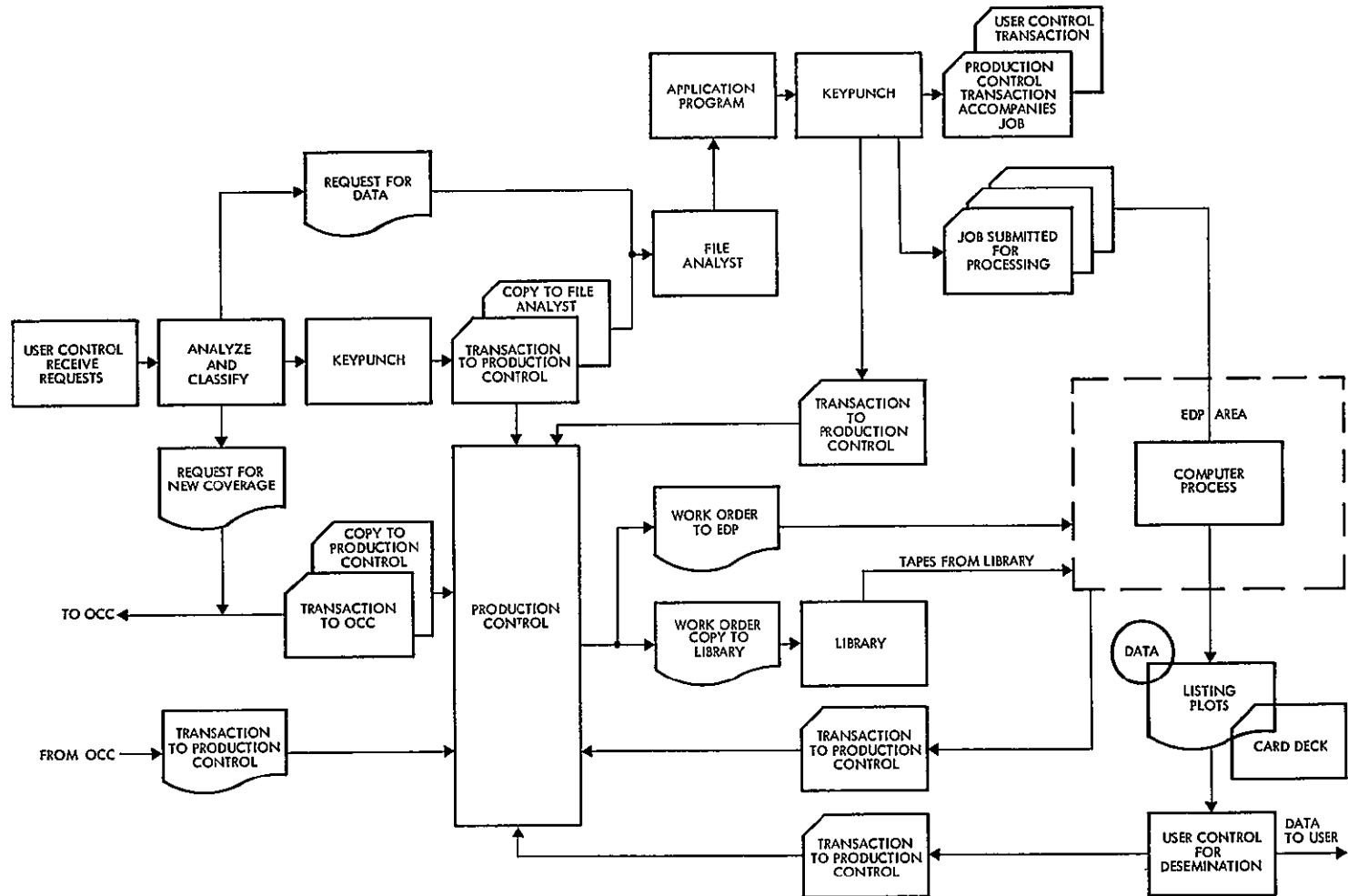PRODUCTION CONTROL for processing data inputs to
NDPF from external sources

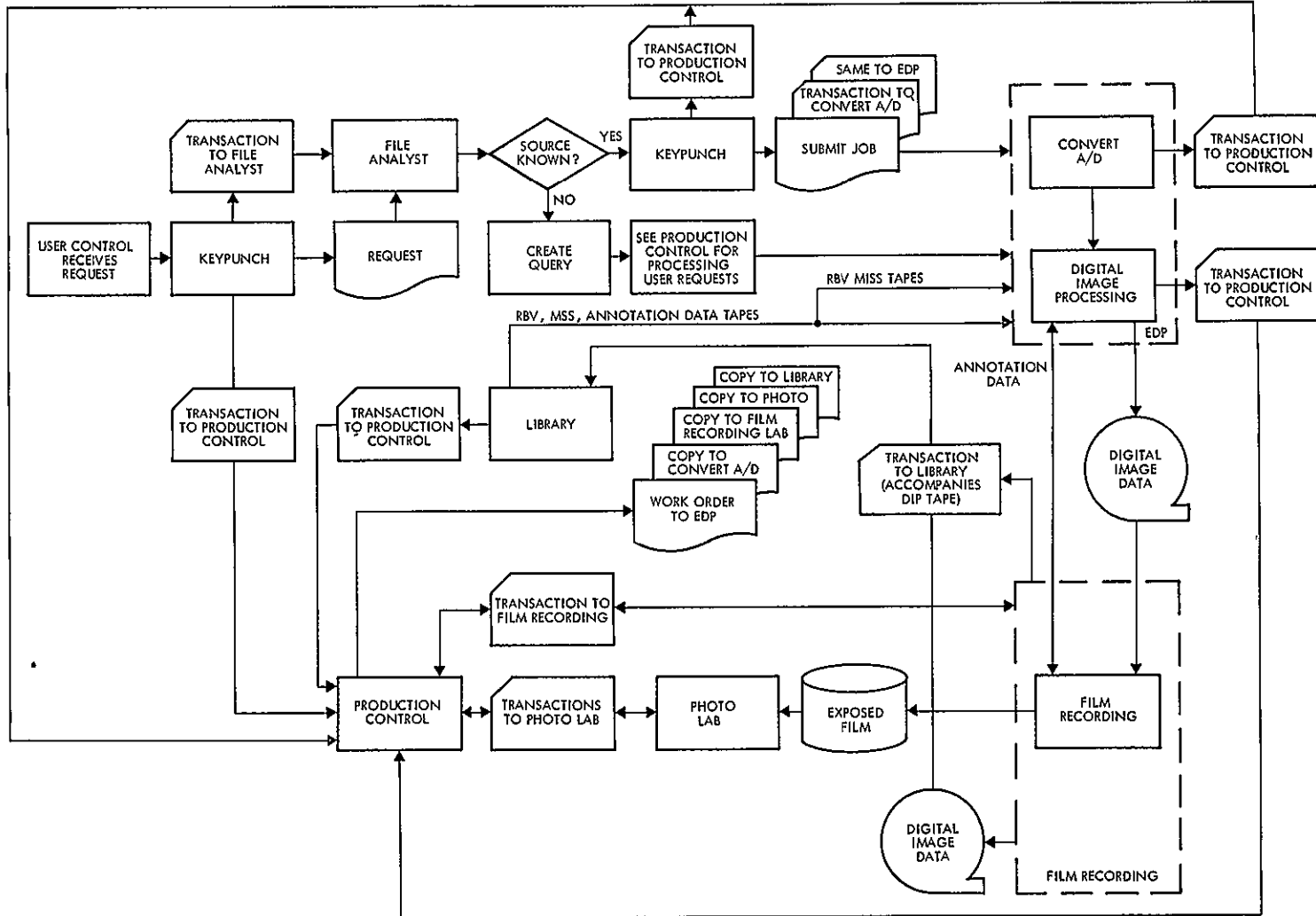Figure 4.4-10
PRODUCTION CONTROL for processing user requests

Figure 4.4-11

PRODUCTION CONTROL for digital image processing
(no ground reference data)

Screen/Select/Index Bulk Imagery

- P. C. schedules the screening unit and re-activates work order.

- After screening unit updates index/abstract file, file analyst submits transaction card to P. C.

- After processing one roll of film, or as directed by work order, screening unit submits transaction card to P. C. and sends job on to photo correlation unit.

- P. C. updates status file.

Image Set Correlation

- After all necessary control copies are exposed on film by the precision photo restitutor (PPR), a transaction card is submitted to P. C. and the film is sent to the photo lab.

- P. C. updates status file.

- After photo lab processes all control copies, submits cards to P. C.

- P. C. updates status file.

- P. C. schedules image correlation for rest of frames in sets.

- After correlation, unit submits card to P. C. and sends film to photo lab.

- P. C. updates status file.

- Photo lab submits card to P. C. when masters are processed, and again when user copies are completed. Lab sends masters to library and output film to user job control.

- P. C. generates work orders and transactions to cover each major functional area in the processing of film from its initial recording to its final printing and dissemination to users. The work orders and transactions generated by production control and those submitted back to P. C. are illustrated in Figure 4.4-7.

- Exposed film is processed and inspected. P. C. notified whether or not the results are adequate.

- Processed film is viewed. Frames with too much cloud cover are deleted, all other frames are classified for cloud cover and quality. P. C. notified when job is completed.

- Film sent to photo restitution area where a control copy is made. P. C. notified when job is completed.

- Control film is processed. P. C. notified whether or not the results are adequate.

- Processed film is exposed. P. C. notified.

- Exposed film is processed. P. C. notified whether or not the results are adequate.

- Processed film sent to photo restitution area where a master positive is made for storage and reproduction purposes. P. C. notified.

- Master positive is processed. P. C. notified whether or not the results are adequate.

- Processed film is exposed. P. C. is notified if any problems exist.

- Exposed film is processed. P. C. is notified whether or not the results are adequate.

- Processed film is exposed to make transparencies and prints for dissemination. P. C. notified when job is done.

- Transparencies and prints are processed. P. C. notified whether or not the results are adequate.

- A final inspection is made of products to users. P. C. notified.

- User job control receives film for shipment to users. P. C. notified when data shipped.

Figure 4. 4-8 depicts the production control flow for processing color composites.

User Job Control (For output)

- As output film and montages are completed in the bulk mode P. C. receives transaction cards.

- Products are packaged and shipped to users via the mail-out room.

- Mail-out room returns card to P. C. after shipment.

- P. C. updates status file.

- P. C. produces status reports.

4. 4. 4. 2 Request Mode

In the request mode, the primary functions in continual daily operation are the activities of precision image processing and information management. Since bulk and precision image processing cannot be scheduled to run concurrently, production control must provide a job

schedule which effectively utilizes the computer and other ADP resources to handle the daily processing requirements for each functional task. The daily activities of information management, whether supporting the bulk or request mode, would be either internally scheduled for batch processing or would involve on-line processing. The major production control interactions with the functions of the request mode are discussed below.

User Job Control (External inputs and requests)

● For external inputs, e.g., data for files, maps, other hard-copy, etc., data is routed directly to either the library for storage or to a file analyst for subsequent information management processing. (See Figure 4.4-9.)

● For user-generated coverage requests, creates coverage request transaction cards, one to the OCC for scheduling, the other to update P. C. status file.

● After OCC schedules, notifies P. C. by submitting card.

● P. C. updates status file and notifies user of schedule.

● For data and/or imagery requests, creates transaction cards for each job type, sends request and card to file analyst and P. C.

● P. C. updates status file, as appropriate.

Figure 4.4-10 covers production control interaction for processing user requests.

Information Management Processing (applies to both bulk and request modes)

● For file update and/or request query, P. C. receives job from file analyst who has assembled the job package.

● P. C. creates work order and transaction card for each job, schedules job for computer processing, and orders tape(s) from library.

● P. C. submits job to computer room and updates status file.

● After job is completed, P. C. returns job to file analyst.

● P. C. updates status file with job completion transaction card.

● For internally-generated update and/or request query, P. C. generates new work order and transaction card, schedules job, and orders tapes from library.

● P. C. submits job and card to computer room.

- After job is completed P. C. updates status file with card, sends tapes to library and outputs, products and audit listings, to file analysts.

- File analyst submits outputs to user job control.

Pre-process Imagery for Precision Processing (includes Digitization, mensuration, transformations, etc.)

- P. C. generates work order and transaction card, schedules job, orders tapes, and submits job to either viewing/mensuration unit or computer room.

- If a mensuration job, transaction cards follow through process, returning to P. C. when measuring is completed and again after transformation computations are completed. Work order remains active for future precision processing.

- If mensuration and transformation effects data content of index file, P. C. notifies file analyst for subsequent information management update job; could be continuation of active work order or new work order when scheduled by P. C.

- P. C. updates status file

- If a digitization job, P. C. receives completed job transaction card and updates status file.

- Completed tapes are sent to user job control for distribution to users.

- User job control mails tapes and sends transaction card to P. C.

- P. C. updates status file.

- If further precision processing is involved, work order remains active.

Digital Image Processing

- If pre-processing was involved, work order remained active, and P. C. schedules job, order tapes from library, and submits job and transaction card to computer room.

- If no pre-processing was needed, P. C. creates work order and transaction card, schedules job, orders tapes from library, and submits job and card to computer room.

- Upon job completion, card returned to P. C., and output is forwarded to either job control, if a digital tape, or to the LBR unit or photo lab, if further processing is needed.

- P. C. updates status file.

- LBR unit submits card to P. C. when job is completed.

4-86

- Photo lab submits card to P. C. when job is completed--output film is sent to user job control for distribution, retention film to library.

- Library and user job control submit card to P. C. to indicate job is complete.

- P. C. updates status file.

Production control flow for digital image processing is presented in Figure 4.4-11.

Photo Lab Processing

- Exposed film is received from the film recording area.

- Exposed film is processed. P. C. is notified.

- Processed film is exposed for developing dissemination copies. P. C. is notified.

- Exposed film is processed. P. C. is notified.

- Processed film is exposed for transparencies and prints. P. C. is notified.

- Transparencies and prints are processed, examined and sent to user job control. P. C. is notified.

- User job control receives film for shipment to users. P. C. notified when data is shipped.

User Job Control

- As film, tapes, listings, are completed in the request mode, P. C. receives transaction cards.

- Products are packaged and shipped to users via the mail-out room.

- Mail-out room returns card to P. C. after shipment.

- P. C. updates status file.

- P. C. produces status reports.

CONTENTS

5. PHOTO PROCESSING

5.1 PRINCIPAL FUNCTIONS

The principal functions of the photographic laboratory segment of the data services laboratory are to reproduce, in accordance with standardized procedures, the imagery exposed in the telemetry and image data processing on the laser beam recorders and precision photo restitutors, and to respond to users' requests for nonstandard photographic reproduction. The standard and nonstandard products include black and white positive and negative film reproductions and positive paper prints and color transparencies and prints. The photographic laboratory also prepares photo montages depicting the coverage obtained by the RBV's and the MSS in each 18-day cycle.

The photographic laboratory will:

- Develop the film exposed in the laser beam recorder and the PPR

- Expose and develop intermediate film negatives and positives

- Expose and develop black and white and color film and paper reproductions for dissemination to the users

- Respond to user requests for special photographic products (e.g., nonstandard color reproduction, enlargements, additional copies)

- Perform quality assurance tests on all materials it produces

- Produce photographic montages depicting the coverage obtained by the ERTS sensors

- Maintain photographic equipment.

5.2 ORGANIZATION

The organization of the photo lab is shown in Figure 5.2-1. Principal responsibilities of each element are as follows.

- Supervisor. Manages all aspects of the operation. Coordinates with telemetry and image data processing and data services laboratory management.
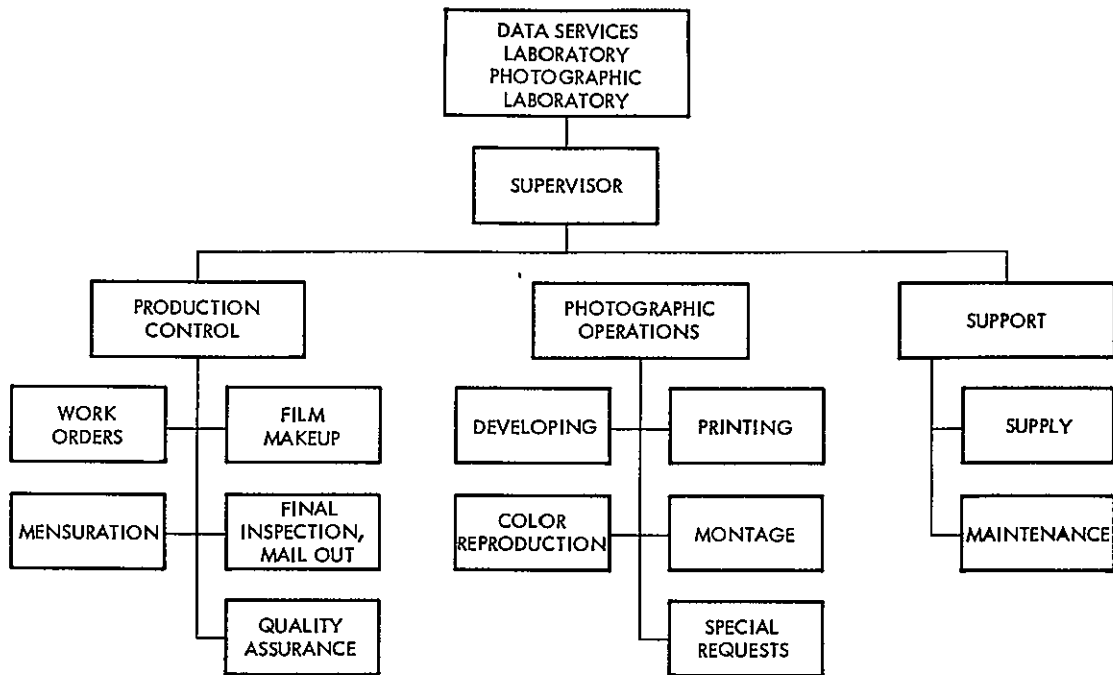
Figure 5.2-1

PHOTOGRAPHER LABORATORY ORGANIZATION

- Production Control. Prepares work orders. Prepares raw film and paper in lengths tailored to requirements of each processing operation. Measures ground truth data. Performs final inspection of materials; prepares them for dissemination. Performs quality assurance tests.

- Photographic Operations. Operates continuous developing machines. Prepares chemical solutions. Inspects developed film and paper for visually detectable defects. Prepares sensitometric curves for evaluating processed film. Cleans and waxes film. Operates continuous photographic printers. Produces color composite negatives, positive transparencies, and paper prints. Responds to users' requests for special photo products. Prepares photo coverage montages.

- Support. Procures, warehouses, and dispenses expendable supplies. Performs routine maintenance on photo lab equipment.

5.3 QUALITY ASSURANCE

The photographic laboratory will establish and maintain densitometric/ sensitometric and chemical analysis procedures which will ensure the utmost in quality assurance. The basic precept will be to ensure that any differences in tonal or spectral responses in the photographic materials can be attributed only to differences in the ground scene, the illumination, the atmosphere, or performance of nonphotographic elements of the ERTS.

Sensitometric step wedges will be exposed on the head and tail of each roll of film to be exposed and developed. Following development, these wedges will be read on an Itek recording densitometer which automatically produces a sensitometric curve. Experienced operators can determine from this curve the nature and magnitude of changes that must be made in the exposure or chemical processing of the film.

Sensitometric tests will be made when raw film of a new batch number is received by the photographic laboratory. Tests will be made by exposing a step wedge on a sample of the new film, processing the sample in a sensitometric processor, reading the wedge on a densitometer, and converting the resulting sensitometric data into modifications of the printing and processing procedures for film of that batch.

A modification of the sensitometric testing procedures can be used on RBV calibration images, if they are available, as a check on computer processing. After these images have been processed in the usual way, and the head and tail sensitometric step wedges read and recorded, a number of locations in the uniformly exposed image area will be read and recorded on the densitometer. These locations will be chosen to provide information on shading and blemish areas as well as to get average image density. The sensitometric/densitometric data, along with the value of the calibration exposure, as determined by precalibration and telemetered data, provide the basis for calculating sensor responsivity, including localized effects, at the time of the exposure. Data from calibration exposures at different levels give limited effective gamma information.

All chemical solutions will be analyzed in the mixing room before the mix is certified for use. Samples taken from the processing machine during a run, and especially prior to starting up after a prolonged shut down, will also be analyzed. The principal tests will be to ensure standard pH, bromide content, and total alkalinity of the solutions. Special tests may be run to determine causes of unexpected film response.

These sensitometric/densitometric and chemical tests are thoroughly documented by the manufacturers of sensitized materials, chemicals, and photographic equipment. Quality assurance personnel will be selected on the basis of previous experience in high-precision photographic laboratory quality assurance work.

The processing machines will be scratch tested and chemically certified at the beginning of each day, or following a prolonged shutdown. The scratch test involves running a strip of fogged film through the processor and examining it for scratches or abrasions that might be caused by a buildup of foreign materials (e. g. , dried gelatin) on the rollers. The chemical certification involves processing a sensitometric strip in the machine and reading the results on a recording densitometer.

The processed film will be cleaned and waxed on a Kodak model JB-CW2 waxer before it leaves the processing section. This is especially important in the case of archival materials and of positives or negatives that must be used several times in a printer as, for example, in the exposure of 10 duplicates from a single film.

In the final inspection section, the materials will again be visually inspected (Richards light table, Bausch & Lomb Zoom 70 stereomicroscope) for quality and for adherence to the work order. Defective materials will be recycled to produce acceptable delivery products. This section may also be responsible for sorting the output materials for distribution to the archives or the users.

5.4 DSL PHOTO LAB OUTPUT

5.4.1 Processing Modes

During each day of operation, the sensor systems can produce an estimated maximum of either 45 sets of imagery per day (case A) or 165 sets per day (case B). A set of imagery in case A consists of three

RBV frames and four equivalent MSS frames. In case B, a set of imagery consists of three RBV frames and five MSS frames (the fifth frame is the thermal infrared channel record). The imagery produced in case A will be processed in the telemetry and image data processing and data services laboratory photographic laboratory on the basis of a 5-day, 40-hour week; processing of case B imagery may require a 7-day, 168-hour week.

Two processing requirements have been established: 100 percent of the imagery will be processed in the bulk mode, and in response to user requests, an estimated 5 percent of the imagery will be processed in the precision mode. Color transparencies will be produced from 20 percent of the bulk imagery and from all the precision imagery. Copies of the bulk imagery (negative and positive film and positive paper prints) will be delivered to each of 10 users; copies of precision imagery will be delivered to the requesting user.

Two variations of bulk processing are available.

Bulk processing mode I converts 100 percent RBV and MSS data to photographic form with some photometric correction accomplished in the laser beam recorder, but with little or no geometric correction. The film records are exposed in the laser beam recorder. The records are reproduced for dissemination with no further corrective treatment. All video data go through this mode as the first step in any processing mode. A simplified flow diagram is shown in Figure 5.4-1.
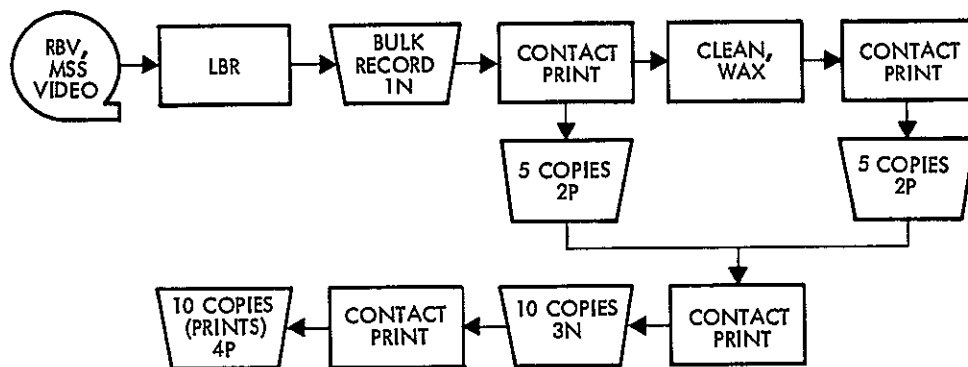

Figure 5.4-1

BULK MODE I

Bulk processing mode II converts 100 percent RBV and MSS data to photographic form with some photometric correction (in the laser beam recorder) and limited geometric correction (in the precision photo restitutor). This is accomplished by subjecting the output from bulk mode I to further treatment in the precision photo restitutor. The output is corrected by instructions computed from transformation data which are in turn derived from reseau measurements and known spacecraft positional and ephemeral data. Figure 5.4-2 is a simplified flow diagram of this mode.
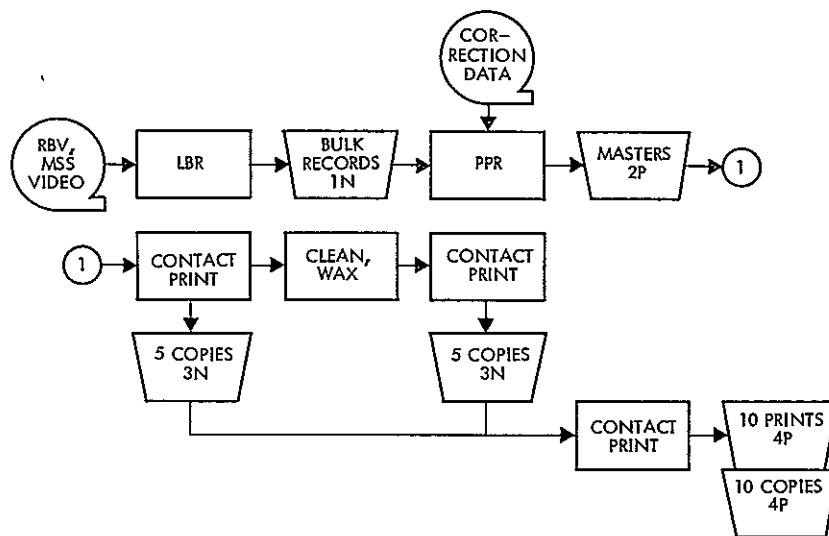

Figure 5.4-2
BULK MODE II

Precision processing converts selected data to photographic form with improved photometric and geometric corrections. A flow diagram is shown in Figure 5.4-3.

Color production converts selected sets of data to false color positive transparencies and paper prints (see Figure 5.4-4).
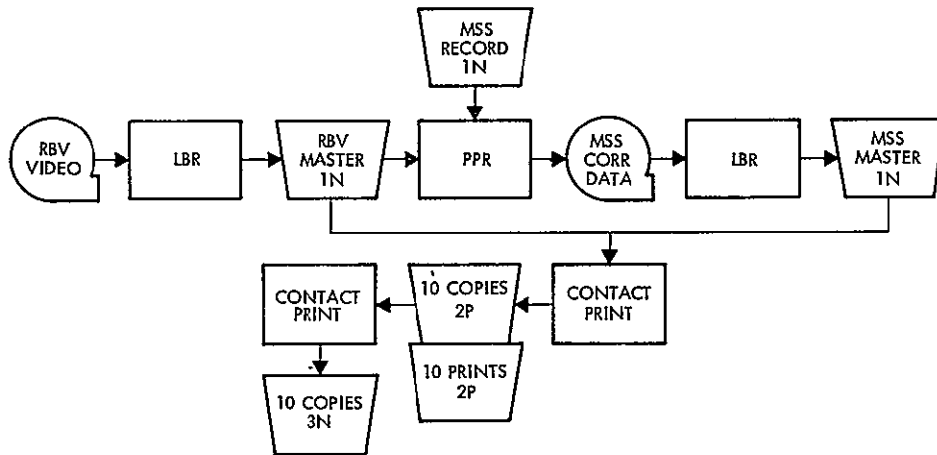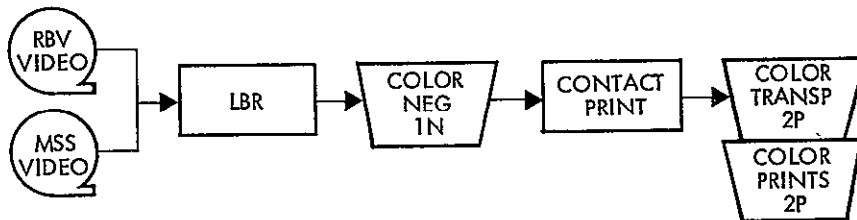
Figure 5.4-3
PRECISION MODE

Figure 5.4-4
COLOR PRODUCTION

5.4.2 Output Quantities

Production quantities in bulk mode I are:

	Case A	Case B
Frames per day (7-day week)	315 (135/180)	1,320 (495/825)
Sets per day (7-day week)	45	165
Sets to be processed per day	63	165
Bulk records (1N)	441 (375 feet)	1,320 (1,100 feet)
Copy positives (2P)	4,410 (3,750 feet)	13,200 (11,000 feet)
Copy negatives (3N)	4,410 (3,750 feet)	13,200 (11,000 feet)
Copy prints (4P)	4,410 (3,750 feet)	13,200 (11,000 feet)
Color negatives	39 (35 feet)	99 (85 feet)
Color positive transparencies	390 (350 feet)	990 (850 feet)
Color prints	390 (350 feet)	990 (850 feet)

Production quantities in bulk mode II are.

	Case A	Case B
Frames per day (7-day week)	315 (135/180)	1,320 (495/825)
Sets per day (7-day week)	45	165
Sets to be processed per day	63	165
Bulk records (1N)	441 (375 feet)	1,320 (1,100 feet)
Masters (2P)	441 (375 feet)	1,320 (1,100 feet)
Copy negatives (3N)	4,410 (3,750 feet)	13,200 (11,000 feet)
Copy positives (4P)	4,410 (3,750 feet)	13,200 (11,000 feet)
Copy prints (4P)	4,410 (3,750 feet)	13,200 (11,000 feet)
Color negatives	39 (35 feet)	99 (85 feet)
Color positive transparencies	390 (350 feet)	990 (850 feet)
Color prints	390 (350 feet)	990 (850 feet)

Precision mode I or II production volume is

	Case A	Case B
Sets per day (7-day week)	2.25	2.25
Sets to be processed per day	4	9
RBV masters (1N)	12 (15 feet)	27 (30 feet)
MSS masters (1N)	16 (20 feet)	36 (40 feet)
Copy positives (2P)	28 (25 feet)	63 (60 feet)
Copy prints (2P)	28 (25 feet)	63 (60 feet)
Copy negatives (3N)	28 (25 feet)	63 (60 feet)
Color negatives	12 (15 feet)	27 (30 feet)
Color positive transparencies	12 (15 feet)	27 (30 feet)
Color prints	12 (15 feet)	27 (30 feet)

5.4.3 Variety of Outputs

The standard outputs of the photographic laboratory for dissemination to the users are:

- Black and white negatives

- Black and white positive transparencies

- Black and white positive paper prints

- Color positive transparencies

- Color positive prints.

Nonstandard outputs, in response to users' requests, may include:

- Black and white and color enlargements or reductions

- Glass plates

- Special color composites.

Other standard products include:

- Negatives and positives required in various processing steps

- Coverage montage negatives.

All standard black and white products for dissemination will be on 9.5-inch roll film or paper. Standard color transparencies may be on either 9.5-inch roll film or 10 x 10-inch sheet film. Standard color prints will be on 10 x 10-inch paper. Coverage montage products are described later in this section.

The generations of intermediate and output materials are shown in the figures in Section 5.

5.5 PHOTOGRAPHIC REPRODUCTION PROCESS

The transfer of information through an imaging system, whether it is a photographic, television, or direct viewing optical system, is accompanied by degradation of the information content by the inherent characteristics of the system. Generally, such systems are designed to display an image for direct viewing by a human observer; therefore, the observer must be considered as a component of the system.

The system may be designed to compensate in part for the degradation of information caused by the characteristics of the observer's eye and brain. Image enhancement techniques can be used to increase or change various characteristics of the input information as required to ease the task of the photointerpreter in detecting, recognizing, and identifying objects from their images in the output display.

In most imaging systems, the quality criterion is that the imagery be pleasing to the observer. Those qualities that present a pleasing appearance are determined by the characteristics of tonal reproduction, sharpness (as contrasted with resolution), and, in color reproduction systems, the color balance or fidelity both in hue and purity. In general, a pleasing reproduction of a scene is one that the observer feels is a reasonable likeness of the original.

For scientific work, the criteria are more stringent. The data received from the imaging system must be capable of interpretation with precision and repeatability of position within the image field (geometry), intensity of the reflected radiance with regard to object characteristics, both spectral and intensity, and the characteristics of the radiating source, modified by the characteristics of the transmission path (atmosphere, radiometry). The edges of objects seen in the image must be sharply defined.

The term gamma, from its origin in photography, denotes the slope or gradient of a characteristic (D-log E) curve plotted on log-log paper. For signal changes of a small percentage, the value of gradient or gamma is the ratio of relative output to relative input. For example, when a gradient of 2.0 is specified for a given point in the characteristic curve, a 2 percent change in input will cause a 4 percent change in output. If the characteristic curve that describes the dynamic transfer function of log radiance input to log radiance output is a straight line, the gamma will be a constant at all points. This does not occur in practical systems, so that gamma refers only to the slope of straight line portion curve. The term gradient should be applied to describe the derivative of the curve at all other points. Thus, the measure of gamma is a measure of the enhancement or reduction of contrast of a reproduction relative to the original. If the gamma is greater than unity, contrast differences in the object are increased in the reproduction. If gamma is lower than 1, contrast is reduced. When gamma is unity, the reproduction system is linear.

The characteristic curve of most image reproduction systems has an S-shaped characteristic, so that the gradient in the low light, or toe, and the high light, or shoulder, of the curve is considerably less than the maximum gradient or gamma that is measured in the middle of the curve.

This lowering of gradient causes a compression of gray step values at these points. This generally is considered beneficial because it permits fitting a relatively large input dynamic range into a somewhat more restricted dynamic range of the reproducing system.

A typical tone reproduction cycle which closely resembles that which might be obtained with ERTS photography is shown in Figure 5.5-1.
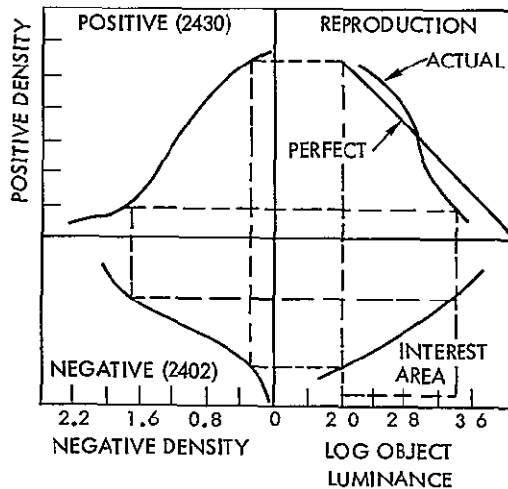

Figure 5.5-1
TYPICAL TONE REPRODUCTION CYCLE

A multispectral acquisition system provides a means of enhancing differences in recorded imagery by breaking the spectrum of an object into several component bands. This allows increased information discrimination. Tonal differences that may exist in narrow spectral bands are often masked when integrated over a broad spectral range. For a multispectral band acquisition system, the system should be balanced to acquire the maximum amount of information discrimination in each individual band. Tests have indicated that this condition is satisfied within the dynamic range.

The ERTS system will use tonal change detection to improve the ability to detect and recognize earth resources information. Since multispectral change detection is the main goal, the system should be precalibrated for maximum information acquisition for nominal image acquisition conditions. When these conditions have been established, they should be fixed, and, at least in bulk mode reproduction, should reflect the same system parameters. In this way, any tonal or color changes in the final output imagery will reflect changes in the satellite sensor, telemetry, or

reproduction systems. In special cases, such as in the precision mode, it may be advantageous to deviate from this fixed tone reproduction standard.

Because of atmospheric attenuation and scattering, one would expect the dynamic range of the multiband records to be different. Atmospheric scattering, often referred to as haze or atmospheric radiance, is basically a wavelength-dependent function and varies from being completely selective to being almost totally nonselective depending on the types and concentrations of particles in the atmosphere. For a pure Rayleigh atmosphere, the scattering is inversely proportional to the fourth power of wavelength. For a hazy atmosphere with large concentrations of water vapor and smoke, the scattering is almost wavelength-dependent. Some authorities have stated that a typical atmosphere combining both Rayleigh and Mie scattering goes approximately as a function inverse to the 1.6 power of wavelength. In any case, the nominal conditions for scattering are predominantly in the ultraviolet and blue region of the spectrum and fall off significantly in the red and infrared regions of the spectrum. For the ERTS case, the apparent contrast in the red band is expected to be higher than that in the green, and that in the infrared to be higher than that in the red.

Test results at Itek have indicated that the best results are obtained when the density ranges of the individual spectrum records are approximately equal. If the densities of the records are equivalent, the printing and color balancing of the resulting additive color records are simplified. A nominal dynamic range of about 10·1 (equivalent to a density range of 1.0) has been found ideal for making additive color records. Most color reproduction materials have a fairly high gamma with a relatively narrow exposure latitude. Too high a contrast in the separation records can result in a loss of information because the color reproduction material is not able to record the entire tonal range of the input imagery. The density range should also be kept down to make exposure and color balancing easier in the additive color process.

The individual separation records can be dynamically balanced to some extent either in the satellite or in the ground handling equipment. Some correction may be possible in the satellite by adjusting the gain control on the individual RBV cameras. Thus, it may be possible to telemeter

equivalent signal ranges for each RBV. This would alter the apparent scene contrast range in one or more of the records to produce a near balance. This would be done in a calibrated fashion so that the actual apparent object radiance could be reconstructed if desired. After this calibration is set, the RBV responses should not be changed during the life of the system. Uncontrollable system changes that result from aging and temperature variations can be determined by calibrated reference standards within the satellite.

The input dynamic range can also be altered in the initial printout state. The taped input data for each channel can be computer analyzed and a corrected signal can be fed to the laser beam recorder. In this manner, the dynamic range for each record can be either raised or lowered to a prescribed level to produce a nominal standard equivalency. When this condition has been established for the bulk mode, it should remain constant.

For the precision mode, it might be desirable to deliberately deviate from this standard. For example, there might be three possible atmospheric conditions. heavy haze, moderate haze, and clear. Specific precalibrated correction functions can be stored in the computer for these three cases. The computer would input these input specifications to the laser beam recorder to balance the dynamic ranges of the individual records for each specific condition.

A third possible way to correct the contrasts of the multispectral black and white records is by processing each individually to different gammas. However, this is not recommended, since the control and repeatability of such a process would be a complex process with a high potential error. The major tone reproduction corrections should be made in the computer and laser beam recorder stages of the reproduction process.

Itek's experience has shown that, in multiple duplication stages, a near ideal tone reproduction produces best results. This occurs at a process gamma of 1.0 at which there is 1·1 correspondence between log exposure range and density range. After the film type and processing conditions have been established to achieve the optimum nominal condition,

they are held constant to ensure repeatable results in all future reproductions.

A calibrated reference step wedge will be generated in the laser beam recorder. This will provide the best process control and color balancing of the imagery. This step wedge can be used as a process control standard for subsequent production stages. By monitoring the densities reproduced on the wedge, proper exposure and photographic processing control can be assessed. The three integrated calibrated step wedges on the RBV records should produce a neutral black and white tone. Deviation from a neutral tone would indicate an improper balancing of one or more of the multispectral print channels used to produce the additive color record.

Neutral tone balancing has been used as a standard in color printing for many years. In spectral cases, balancing to a neutral tone for certain types of images may not produce optimum results. In the precision mode, the balance can be altered to produce records that meet the optimum needs of a user, but this would be a nonstandard process.

5.6 RADIOMETRIC ACCURACY OF A PHOTOGRAPHIC PROCESS

The ERTS imagery will extract radiometric data from the ground scene, so it is necessary to carefully consider the accuracy of photographic materials used as quantitative radiation sensors. A well controlled photographic process can produce remarkably accurate and repeatable radiometric and photometric data.

Several types of errors can occur when film is used as a radiometer. One error is caused by the nonuniformity of sensitivity in the typical photographic material. Any nonuniformity in sensitivity across the film web will produce errors in the developed imagery. However, the uniformity of the quality films made today is exceptionally good, and sensitivity variations are less than 5 percent as a result of manufacturing tolerances. As long as the film is stored in a suitable environment, uniform sensitivity is maintained until the film is used. The absolute sensitivity of photographic materials can vary with each batch. However, batch variations can be determined and corrected for in a quality-control sensitometric operation so that essentially uniform results can be obtained from batch to batch.

The largest radiometric error generally occurs in film processing. To achieve good radiometric results, the uniformity of the processing will be well controlled. Each part of the film will receive the same chemical treatment. This requires uniform agitation and uniform temperature as well as constancy of developing solutions. Processing uniformity of 95 percent or better can be achieved in precise sensitometric processing. However, in a normal well-controlled production processing operation, variations might be slightly greater. These variations would be the total across the format and not the point-to-point variation between adjacent detail.

The size of the object or objects being evaluated influences radiometric accuracy. Photographic film is composed of small grains of silver. These grains represent the noise in the photographic process. When a large area is being evaluated, the noise level of the system is exceeded and the radiometric accuracy will be very good. However, as smaller objects are evaluated, the area of the grain noise of the system is entered and density fluctuations as a function of this grain noise begin to appear. Accuracy is lost as the signal-to-noise level increases. The film that has been selected for ERTS duplication, EK-2430, has the lowest granularity (8.9) of currently available production duplicating materials, and it will have a minimal effect on the radiometric accuracy of the system.

Exposure variations also affect photographic materials used as quantitative radiation sensors. However, quality printing devices ensure exposure accuracies of within a few percent.

The possible reciprocity effect that results from large exposure variations could cause error. However, this problem should not occur in the ERTS system because extraordinarily large ranges are not anticipated.

Latent image decay is another potential source of radiometric error. Significant time lag between exposure and processing is not anticipated, and no error will occur from this source.

The ERTS photographic process will be well controlled; good sensitometric calibration and control procedures will maintain a radiometric accuracy of 95 percent or better for objects whose images are in

the size range of a millimeter and larger. Objects whose images approach the grain noise limit of the film will have larger errors.

5.7 IMAGE QUALITY

The ERTS baseline system involves several photographic reproduction stages. A potential loss in image quality is encountered in going from generation to generation. Since a primary goal of the ERTS system is to retain a maximum of spatial and geometric integrity in the imagery, the baseline system will produce the initial hard copy image on 9-1/2-inch film. The actual pictorial image will be enlarged 7.3 times from the image at the sensor.

The maximum performance of RBV cameras in the ERTS program will be on the order of 80 line pairs per millimeter at the vidicon surface. This imagery will be enlarged to a 7.3-inch format on the laser beam recorder on 9-1/2-inch film, a resolution of 8 to 10 lines per millimeter will be achieved in the laser beam recorder image output. This is a low resolution value for the photographic film used. The possibility of image quality losses in further reproduction steps is significantly reduced. High quality duplication equipment can reproduce resolutions from 100 to 400 lines per millimeter.

A general photographic rule is that if the resolution capability of the reproduction process is 10 times better than the resolution of the input imagery, there will be no significant image degradation. Thus, we are well above this limit.

Kodak type 2430 fine grain duplicating film will be used for all duplications. This film has a resolution capability of over 300 line pairs per millimeter, and its transfer function is high (see Figure 5.7-1). At the nominal resolution for laser beam recorder imagery (10 cycles per millimeter), the modulation transfer function of this film is approximately 0.95. If the modulation transfer functions are cascaded, the system modulation can be theoretically calculated through a number of generations, using type 2430 film in each of the reproduction stages.

As presently conceived, the telemetry and image data processing baseline system will require three duplication steps to produce the final dissemination black and white transparencies. To determine the resultant
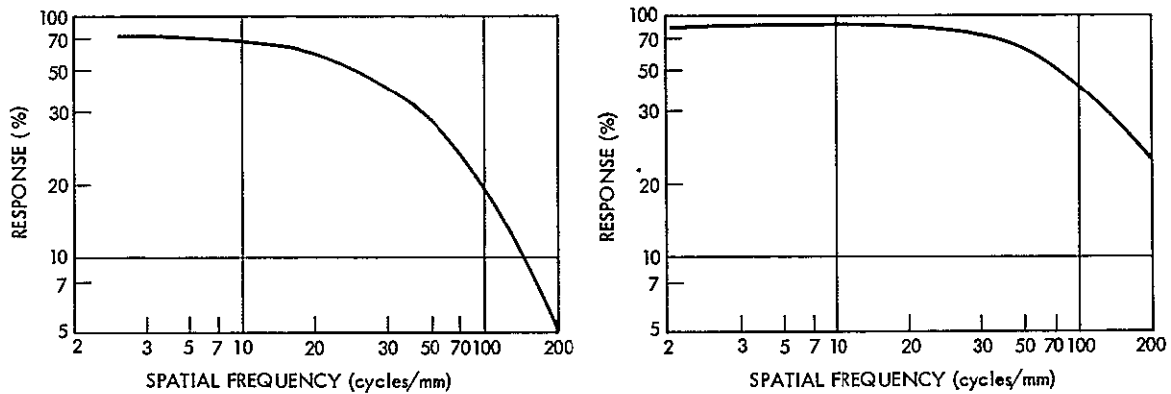
Figure 5.7-1

MODULATION-TRANSFER FUNCTION CURVES
for Kodak 2402 and 2430 film

modulation transfer loss for three generations, the modulation transfer
value is cubed. The resulting modulation transfer response is 0.86.
Using type 2430 film at this modulation transfer results in very little loss.
At the ERTS level, a modulation reduction of 0.14 maximum is considered
insignificant. The higher loss in the lower frequency information, which
is the bulk of the picture, is significantly less than this.

The anticipated quality of the false color prints and transparencies
that will be produced from the black and white spectral records should also
be considered. It has been theoretically and practically demonstrated that
by superimposing identical images, i. e., images whose geometry is
intrinsically the same, image quality can be improved. If multiple images
are reproduced and integrated by superimposition on black and white film,
the resolution of the resulting print increases as the square root of the
number of integrations. This is accompanied by an increase in edge
definition.

When a color material is used to record the integrated records, the
results are less straightforward because the images do not truly integrate,
because they are formed on the three emulsion layers. However, since
part of the addition is due to hue and color differences, there will be some
degree of image enhancement, especially in areas that reproduce in a
more or less neutral tone. Thus, even though the image quality of the

color reproduction material is intrinsically lower than that of equivalent black and white duplicating materials, the resulting color imagery should be equivalent or superior in spatial resolution to black and white imagery.

5.8 PHOTOGRAPHIC PRINTING EQUIPMENT AND TECHNIQUES

Comparing system modulation transfer functions shows that the best response is obtained when the ERTS sensor images are reproduced throughout at an image size of 7.3 x 7.3 inches on 9.5-inch film. Table 5.8-1 illustrates this comparison. Data for the figure were derived from Kodak Publication No. M-29, "Kodak Data for Aerial Photography," and from the following assumptions or computations.

Film Width	Image Size	Cycles/mm
70 mm	2 x 2 inches	36
5 inches	3.85 x 3.85 inches	19
9.5 inches	7.3 x 7.3 inches	10

Cycles/ mm	Modulation Transfer (% Response)		
	2402 Film	2430 Film	Optics
36	56	87	75
19	70	92	85
10	80	95	95

Table 5.8-1 shows the percent response achieved in each of the following reproduction cycles·

- a) Contact printing through four generations (1N through 4P)

- b) Enlarging a 2P from either 70 mm or 5-inch to a 7.3-inch 3N.

- c) Contact printing the enlarged 3N to a 4P

- d) Reducing the 7.3-inch 2P to a 70 mm 3N.

Table 5.8-1. Comparison of Modulation Transfer

Film Width	Cycles per mm	Percent Response						
		1N	2P	3N	4P	Enlarge 2P to 7 3 inch 3N	Contact 7 3 inch 3N to 4P	Reduce 7 3 inch 2P to 2 inch 3N
70 mm	36	56	49	43	37	32	28	--
5 inch	19	70	64	59	54	50	46	--
9 5 inch	10	80	76	72	68	--	--	68
Film Type		2402				2430		

The values in the first cycle are derived by cascading the film responses (e.g., 2402 film has a response of 56 percent and 2430 of 87 percent at 36 cycles/mm). Assuming that the laser beam recorder input is 100 percent, the values in the first four columns of the 70 mm row of Table 5.8-1 are.

$$1.0 \times 0.56 = 56\% \ (1N)$$
$$0.56 \times 0.87 = 49\% \ (2P)$$
$$0.49 \times 0.87 = 43\% \ (3N)$$
$$0.43 \times 0.87 = 37\% \ (4P)$$

The fifth value includes the MTF of the optics, thus $0.49 \times 0.87 \times 0.75 = 32\%$ (2P to 3N). The sixth value is $0.32 \times 0.87 = 28\%$ (3N to 4P).

The response of the 9.5-inch film is higher in each generation than the responses of either of the other two films, and the loss in resolution is therefore relatively less in the 7.3-inch images.

If a 70 mm or 5-inch 2P is optically enlarged to a 9.5-inch 3N, the responses again are less than the response of the contact printed 3N (32, 50, and 72 percent respectively). Similarly, if the enlarged 3N's are contact printed to a 4P (third cycle), the responses are also lower than the response of the contact printed 4P (28, 46, and 68 percent respectively).

If the 9. 5-inch 2P is optically reduced to a 70 mm 3N (fourth cycle), the resulting image has a response of 68 percent, compared to the 43 percent response of a contact printed 70 mm 3N. Contact 4P's made from the reduced 3N will have a response of .56 percent (not shown in Table 5.8-1) compared to a 37 percent response in the contact printed 70 mm 4P.

This analysis shows that system response using 9. 5-inch film (7.3 x 7.3-inch image) is in all cases superior to the responses of either 70 mm film (2 x 2-inch image) or 5-inch film (3. 85 x 3. 85-inch image).

A further consideration is the thickness and type of base required to maintain dimensional accuracy in the reproduction process.

The data in Table 5. 8-2 are from Kodak Publication No. M-29. They indicate a slightly better dimensional stability in films coated on 7. 0 mil Estar than on 4. 0 Estar. However, the additional cost of 7. 0 mil base, and the additional storage space and spool diameter, are not justified by the ERTS requirements. Cellulose acetate is entirely unsuitable.

Table 5. 8-2. Dimensional Change Characteristics

Film Base	4 0 mil Estar	7 0 mil Estar	5 2 mil Cellulose Acetate
Coefficient of linear expansion, % per 1 % RH	0 0025	0 0015	0 0075 L 0 0080 W
Coefficient of linear expansion, % per degree F	0 0010	0 0010	0 0040 L 0 0045 W
Processing dimensional changes, %	-0 01	-0 01	-0 01 L -0 02 W
Shrinkage, %, 7 days at 120 F, 20% RH	0. 04	0. 02	0 10 L 0 10 W
Shrinkage, %, 1 year at 78 F, 60% RH	0 03	0 02	0 10 L 0 10 W

After the superiority of the 9.5-inch film was established, and a decision made to expose all standard products in a contact printer, selection of the printer was the next consideration.

To produce film and paper copies of RBV and MSS imagery for distribution, continuous printers capable of exposing approximately 8000 feet of film and 4000 feet of paper per shift are required. Three printers were considered: the Kodak Niagara, Log Etronic model SP-10/70, and Miller-Holzwarth model EN-6A. The Niagara was rejected because it exceeds the throughput requirement and is the most expensive of the three candidates. The Niagara operates at a constant rate of 100 feet per minute, exposing 36,000 feet in a 6-hour operating period; its cost is over $50,000. The model EN-6A was rejected because it does not represent the best in the state of the art.

The Log Etronic SP-10/70 can reproduce 200 lines/mm. It has a variable throughput rate that depends on the density of the input negatives and on the output material. An average rate of 25 feet per minute for film and 15 feet per minute for paper is estimated; thus, two model SP-10/70's are required to expose either case A or case B copies. The estimated capability of two printers exceeds the throughput requirements, thus providing a backup capability for peak loads and/or machine downtime.

The SP-10/70 is relatively simple to operate and maintain. The electronic circuitry is modularized, so that most breakdowns can be rapidly corrected by exchanging plug-in components. As with any printing device, the SP-10/70 is sensitive to vibration. However, suitable damping mounts can minimize this problem.

The imagery from the seven or eight RBV and MSS sensors will be recorded first by a laser beam recorder. In bulk mode I, the bulk record (1N) will be printed on the SP-10/70 to produce 10 copies of the 2P positive transparencies and the 2P paper prints. The 2P transparencies will be printed to produce 10 copies of the 3N. The film transparencies (positive and negative) will be reproduced on Kodak type 2430 film. The paper prints will be made on Kodak Varicontrast waterproof paper.

The exact exposure parameters will be determined initially during the prelaunch integration and acceptance period. Adjustments will be made during the immediate postlaunch period, based on sensitometric/densitometric tests. Tone reproduction charts similar to that illustrated in Figure 5.5-1 will be constructed to aid in selecting the standard procedures to be followed. The goal will be to achieve a 1.1 correspondence between input and output.

The printing process in the bulk mode will not be allowed to cause uncontrolled variations in the tonal reproduction process. The inherently high (99 percent or better) modulation transfer function of the contact printing process will ensure that the only loss in resolution from generation to generation will be that caused by the modulation transfer function response of the films. Losses in resolution that are inevitable in optical (i. e. , enlarging or reducing) printing will be avoided.

In the precision (request) mode, it may be desirable to deviate from the standard printing process to provide separation negatives and/or positives especially designed to emphasize features of interest to the user (e. g. , to alter the maximum or minimum density or the gamma of a specific spectral record to emphasize geological, agricultural, or hydrographic features in an area). Experimentation in the photographic laboratory, on advice of the requesting user, will be necessary to establish the nature and magnitude of required deviations from standard procedures. Specially exposed films may be made on either the Log Etronic SP-10/70 or on the Miller Holzwarth 1119; the latter would probably be used for most special request printing. The 1119 is a manual one-at-a-time printer with excellent resolution (approximately 200 lines/millimeter). The output film would be 10 x 10-inch sheets.

In addition to contact prints (on film or paper), users may request enlargements of all or portions of a frame or set. A Durst V-184 enlarger has been selected to satisfy this requirement. The Durst has a resolving power of about 100 lines/millimeter. A complete set of lenses and condensers will be provided to permit enlargements of 10 x 10-inch negatives up to 20 diameters.

Two Miller Holzwarth model 1119 contact printers are provided. This is a step and repeat (i.e., noncontinuous) printer. It will accept sheet or roll film input and output materials. It is a point light source printer and is rated at 140 lines/millimeter at 2:1 test object contrast. Variable contrast filters are provided for use with variable gamma paper or with panchromatic film. Dodging is provided by a system of adjustable mirrors. The printer is equally usable for black and white or color printing.

A Morse model A-14 contact printer is used in the montage darkroom for exposing the reduced copy negatives made from the 7.3 x 7.3-inch prints. This is a step and repeat sheet paper printer of adequate resolution.

Color printing techniques are discussed in Section 5.10.

In their original proposal to TRW, Itek suggested that their RS^{TM} sensitized material might prove useful in the annotation process. This suggestion was based on the fact that the RS "emulsion" can be applied to processed photo film, then exposed (by a CRT or other means) and developed without affecting the existing photographic image. The need for such a means of accommodating changes in the annotations was eliminated during the study by the decision to expose the annotations in the LBR and the PPR using the laser beam and/or a CRT in the LBR, and a CRT in the PPR. No further consideration was given to RS or any other similar sensitized material.

5.9 FILM PROCESSING

Approximately 8000 linear feet of film and 4000 feet of paper must be developed in an 8-hour shift, either case A or case B. Developing equipment to handle this quantity of film was selected by comparing throughput time, simplicity of operation and maintenance, proven ability to produce high quality output, initial cost, and availability. The Kodak Versamat model 11-CM, Houston Fearless HTA-3, PakoRol model 48/1, and Itek Transflo model 1207 were considered. The Versamat was selected. The HTA-3 was rejected because of high initial cost, long procurement lead time, and complexity. The PakoRol and Transflo were rejected because of their slow throughput rate.

The Versamat is simple to operate and maintain. However, it must be carefully prepared for use and must be cleaned thoroughly when it is to be shut down for any appreciable period. The Versamat is in widespread use; parts and manufacturer service are readily available. It is self-threading, and will accept film or paper in short lengths, as small as 4 x 5 inches, or rolls up to 1000 feet long. Environmental and utilities requirements are minimal, it has a hot air exhaust requirement of only 250 CFM compared to the HTA requirement of 1700 CFM. It also has considerably smaller requirements for water input and drain.

A nominal throughput rate of 15 FPM and an operating period of six hours per 8-hour shift is a realistic planning figure. This equates to 5400 feet of film per machine per shift. Each shift is required to process approximately 8000 feet of film and 4000 feet of paper. Three Versamats are required to accommodate this workload. A fourth Versamat is recommended to handle peak workloads and special requests and to serve as a backup in the event of malfunction.

Several chemistries are available for processing film in the Versamat. A final decision as to which chemistry produces the best results will not be made until tests are conducted in which imagery closely resembling that expected from the laser beam recorder and PPR is processed. TRW believes that Itek's proprietary PC-5 chemistry, developed especially for use in the Versamat, will prove to be superior to chemistries offered by other vendors. This is based on the extended dynamic range of imagery developed in PC-5 (better information content in the highlights and shadows), faster throughput time, lower replenishment requirements (less chemistry expended), and suitability for use with almost any silver halide film or paper.

The chemical solutions used in the photographic laboratory will be prepared in a chemical mixing room suitably sealed from the rest of the facility to preclude contamination of the air by chemical dust. Solutions will be prepared in transportable 50-gallon mixing tanks. Solutions may be piped to the processing stations or may be delivered in the mixing tanks.

The Versamats may be equipped with self-contained silver recovery units. Alternatively, the waste solutions may be piped to a central station for recovery of silver and treatment prior to being discharged into a sewer system.

5.10 COLOR REPRODUCTION

Color composites made from ERTS imagery are not intended to reproduce the visual appearance of the colors in the scene. The spectral bands do not coincide with those used in normal true color photography. The purpose of the ERTS color photos is to provide the user with an image in which the color of an object provides some desired information about the object. The process of producing a color composite must therefore be designed to faithfully record spectral signatures as they are seen by the ERTS sensors and as they are recorded by the laser beam recorder on black and white color separation negatives.

In normal color duplication processes, rather elaborate precautions are taken to correct the color balance, contrast, and density. These precautions are less import in producing color materials from the ERTS imagery. It is probably not desirable to introduce into the processing cycle any of the techniques used to correct the colors in the conventional process, because the hue and chroma of the final color reproduction is unimportant; what is important is that any given color of an object should always mean the same thing about the object, or, conversely, that a given object condition should always reproduce as the same color.

This establishes the requirement that each step in the color process must always convert the same combination of black-and-white tones (in the black and white separations) to a specific color in the final composite color transparency or print. To achieve this, several precautions must be taken, and each step in the color process must be standardized. The necessary precautions are:

1) The black and white separations must be exposed and processed to produce densities and contrasts which faithfully reflect the reflected illumination from the scene as modified by the atmosphere and the transmission/recording system.

2) The composite color materials must be exposed by illumination of standard color temperature and intensity for a standard exposure time.

3) A standard set of filters must be used during exposure of the color negative.

4) The color film or paper must be calibrated against a standard negative, and color correction filters must be selected which will ensure a standard response when the preceding precautions have been observed.

5) The color materials must be stored and otherwise handled in such a manner that temperature and other variables do not alter the color response.

6) The time between exposure and processing should be as nearly uniform as possible.

7) Processing must be standardized.

The production of composite color negatives from black and white separation positives or negatives involves the additive color printing process. In this process, a single sheet of color film is successively exposed by blue, green, and red light modulated by the corresponding black and white separation films; exact registration of the three exposures is mandatory. Special effects may be produced by varying the combinations of filter and separation image. For example, it may be desirable to modulate the blue light with a red filter and vice versa to accentuate some feature in the imagery. It may also be desirable for some special cases to use a negative separation for one color and positives for the other two.

The following filters are the standard filters used in additive color printing: Wratten No. 25 (red), No. 99 (green), and No. 98 (blue). Neutral density and color correction filters may also be required to modify the exposure and to balance the color material to the standard.

Tungsten operating at 3000° K will produce the desired energy levels with adequate evenness of intensity distribution. The Sylvania BVA tungsten halogen lamp and the Sylvania FCS tungsten halogen lamp are more than adequate to produce the energy levels required within the desired spectral regions. The extra energy produced by both lamps will allow any future changes in the system that may be necessary.

In all three-color systems, a certain ratio of energy inputs to the three sensors is specified as neutral or gray. As the intensity of the input energy is increased while the specified ratio is maintained, the luminance

of the reproduction increases (lighter grays) toward white. A change in the ratio will produce color. Adjustments of the three RBV camera systems to maintain gray-scale tracking over the range from black to white is critical if spectral signatures are to be reproducible in the false color hard copy output of the system.

Nonlinearity of the responses of each camera and associated video amplifier and differences in black level setting affect the tracking capability of a three-color vidicon camera system. If the system is adjusted for correct tracking of large area gray steps, errors in small area gray steps at the black end may still exist because of flare light addition. Since the photo-conductor of the vidicon may exhibit increased transparency toward the red end of the spectrum, this flare increases for the red as compared with the blue-green. Before flight, the RBV system should be calibrated for black level shifts in small area blacks as a function of the average irradiation reaching each sensor. Some correction can be made in the image recorder by resetting the black level of the recorder for each spectral band.

The color control system will be based on the use of one or more standard negatives. These negatives will include imagery typical of the scenes to be photographed by the RBV and MSS, both as to terrain and color. A neutral gray area will be included on each negative. One negative will be the primary control for calibrating new color materials; the others will be secondary controls for special lighting, terrain, or other conditions. The control negatives will be used for comparing its printing characteristics with those of other color negatives, for comparing the color responses of different emulsion coatings (batches) for checking processing, and for determining which color correction filters are required in the printing process.

An additional control will be available in the gray scales exposed on the separation negatives in the laser beam recorder. The densities of the gray step on each separation corresponding to the gray area of the control negative will be read. These will be used, in conjunction with red, green, and blue densities of the gray card on the control negative, to determine the cyanmagenta, and yellow filters necessary for accurate color rendition.

The recommended color reproduction system is based on the Kodak
Aero-neg System. The basic elements of this system are shown in
Figure 5.10-1. The Aero-neg system was selected because of its
versatility and the ready availability of sensitized materials and chemicals.

```
              ┌─────────────────────┐
              │     EXPOSURE        │
              │ KODAK TYPE SO-151   │
              │    EKTACHROME       │
              └─────────────────────┘
                         │
              ┌─────────────────────┐
              │    DEVELOP TO       │
              │   NEGATIVE OR       │
              │     POSITIVE        │
              └─────────────────────┘
                         │
   ┌──────────┬──────────┼──────────┬──────────┐
```

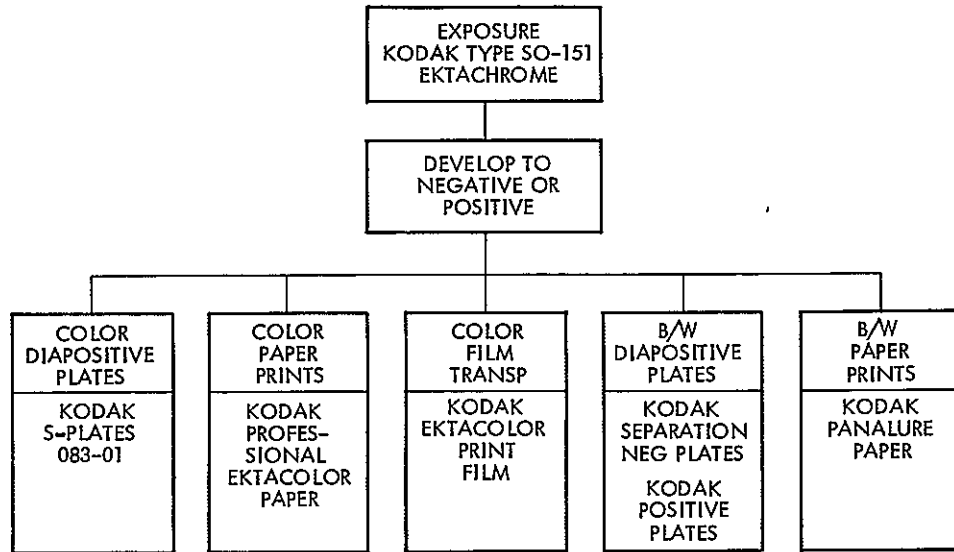| COLOR DIAPOSITIVE PLATES	COLOR PAPER PRINTS	COLOR FILM TRANSP	B/W DIAPOSITIVE PLATES	B/W PAPER PRINTS
KODAK S-PLATES 083-01	KODAK PROFESSIONAL EKTACOLOR PAPER	KODAK EKTACOLOR PRINT FILM	KODAK SEPARATION NEG PLATES KODAK POSITIVE PLATES	KODAK PANALURE PAPER

Figure 5.10-1

KODAK AERO-NEGATIVE COLOR SYSTEM

No high production additive color printer is commercially available.
Itek has developed two experimental devices, but neither in its present
configuration will accept 7.3 by 7.3-inch images. One (an additive color
viewer-printer) is being used successfully at NASA, Houston, to produce
color materials from Apollo and other multiband photographic projects.
This device produces 8 by 10-inch reproductions from the central 1 by
1-inch portion of the input separations. A considerable design and engi-
neering effort would be required to adapt it to the ERTS requirements.

The other Itek instrument is an integrating enlarger originally
designed to superimpose on one output film image from three negatives
identical in all respects except their random grain pattern. The super-
imposition, by reinforcing the grain pattern in the output, achieves

substantial image enhancement and produces much sharper image edges than could be obtained from any single negatives. The instrument also can superimpose the images from three color separations, either on a viewing screen or on a sheet of color film. Filters in the optical train can be manipulated to produce almost any color response desired. In its present configuration, the enlarger accepts 35-millimeter inputs and produces 8 by 10-inch color negatives or positives. Engineering design changes, which would enable this instrument to be used as a color printer for the ERTS program, would involve enlarging the instrument and refining some of its features. The design effort can be lessened by the use of a reduction printer (such as a Bausch & Lomb diapositive printer) to photographically reduce the 7.3 by 7.3-inch ERTS images to approximately 3.5 by 3.5 inches. This would minimize the size of the enlarger and simplify the optical design. Registration of the images would be achieved by visual alignment of the registration marks on the projected imagery. Development costs of approximately $100, 000 would be required to make the enlarger suitable for ERTS use.

While no partially or fully automated additive color printer exists which is suitable for use with ERTS imagery, a reliable and accurate manual method is available, and will be used. The presence of registration marks on the ERTS imagery considerably reduces the time required for conventional manual registration, since it is much easier to line up these marks than to rely on image detail. About 12 minutes per set are required for registration and exposure; two registration stations are capable of handling either Case A or Case B requirements. The method consists of the following steps:

1) The three color separation positives are visually registered on a light table, using the registration marks produced in the precision photo restitutor. After registration, the positives are taped together.

2) A Condit registration punch is used to punch two holes simultaneously in the border of the three registered separations.

3) In a darkroom, a sheet of color film is placed in position on a Condit registration board. One of the three separations is placed in contact with the film. The registration board provides two pins, carefully matched to the holes produced on the registration punch. An exposure is made through the separation positive; the illuminant is a point light source with an appropriate filter.

4) The first separation is removed, the second is positioned on the registration board, and an exposure is made through an appropriate filter.

5) The third separation is similarly exposed.

6) The color film is developed to produce a positive or negative transparency, which is then used in a color contact printer to produce copies.

Tests conducted by Itek on a Kodak registration punch and registration board, which have been in use for several years, have shown that registration is achieved to within 0.0005 inch.

The color negatives produced manually will be processed in a Carr Model 195-2WM color processing unit. Contact prints will be made on a Miller-Holzwarth Model 1119 printer (see Section 5.8). A Kodak rapid color processor, Model 16K, will handle special request or small quantity color paper processing. The color printing and processing section will be equipped with a Macbeth color analyzer, Model EP-1000, for use in maintaining color balance in the color materials.

Although no existing printer is immediately available for use in the ERTS program, the precision photo restitutor can be used for this purpose. Only one feature is added to the basic PPR to permit exposure of the color negative: a provision for inserting color filters in the optical path. In this mode, the precision photo restitutor operates as follows:

1) A color separation negative is positioned on the input stage and unexposed color film on the output stage. The PPR is operated in the open loop mode and the image of the input negative is exposed (through a color filter) on the output film.

2) The second separation negative is positioned on the input stage and similarly exposed through its filter, in precise registration with the previous image. The third separation is exposed in the same way. The output film is not moved until all three images have been exposed.

3) The annotations are exposed by the CRT. Note that the annotation cathode-ray tube must operate in a dark line mode to produce colored annotations against a clear background. If this is not desirable, i.e., if a bright line cathode-ray tube is preferable, the inputs to the precision photo restitutor must be positives rather than negatives.

4) The color film is developed to a negative by reversal if the inputs are negative, or it is developed directly to a negative if the inputs are positive.

A Log Etronic color printer Mark III was selected for exposing color transparencies and prints from the color negatives. This instrument is widely used by aerial photography firms and is readily available. A competitive instrument is the Kodak Rainbow which was rejected because of cost and long procurement lead time.

Several continuous color developers were considered for the data services laboratory photographic laboratory requirement. A color Versamat, Model 1411, was selected because of its established reputation and also because of commonality of parts with the black and white machines. Only one color Versamat is required to satisfy the throughput requirements. Either roll film or sheet film may be processed on this instrument. Similarly, the Versamat will accept either film or paper without a change of chemistry or other major operational adjustments.

Shading variations that are acceptable in a black and white reproduction may not be acceptable in a three-color system. Differences in the responses of the three TBV tubes as a function of position on the photoconductor when exposed to a uniform spectrally neutral field may cause noticeable departures from neutrality in the reproduction when printed onto color material. Variations noticeable as color shading of reproduction of a gray field will indicate the need for further shading correction beyond the correction that is inserted in each RBV camera system. If this is a problem in the ERTS color reproduction system, correction may be applied by using positive silver masks in the duplication stage or by dodging. Both the Miller Holzwarth 1119 and the Log Etronic Mark III have this capability. The 1119 uses a set of adjustable mirrors; the Mark III uses incremental exposure control.

5.11 COVERAGE MONTAGE

The principal map series that covers the United States at a scale of 1:1,000,000 are the World Aeronautical Charts. More than 50 of these charts, each 22 by 29 inches, are required to cover the United States and Alaska. The mechanical difficulties of producing the montages on these charts discourage their use.

The geological survey map of the United States is a single sheet, 42 x 65 inches, on a Lambert conformal projection, at a scale of 1:3,168,000. The map contains the outlines of the individual states, the locations of major cities, and the major drainage systems. It appears to be the best choice for the montages to minimize production problems (especially in view of the requirement for 1000 copies of the montage).

The photographs must be reduced from 7.3 by 7.3 inches to approximately 2.27 x 2.27 inches to conform to the map scale. Prints at 1:1,000,000 (made from the bulk processed negatives) will be affixed to a baseboard (matching detail in the 10 percent overlap), and copies on an 8 by 10-inch film sheet. Three sets of four prints may be copied on one 8 x 10-inch negative. As many prints as necessary for an orbit will be copied in this manner. The negatives will be contact printed. After the prints are trimmed and affixed to the base map, matching detail to the map and to the overlap, the montage will be recopied at a reduction of approximately 2.7X. Four 20 by 20-inch negatives will be required to include the entire map with a 1-inch overlap between the negatives, both vertically and horizontally.

When the resulting negatives are reproduced by photolithography at a 1:1 scale, the images of the ERTS photographs will be slightly less than 1 by 1 inch. Although the individual frames will be quite small, it is possible to annotate each frame with an identification legend that will enable the user to determine the identity of any frame he wishes to retrieve for special processing. As an adjunct to the montage, a textual description (date, time, and sensor) of the frames available in each pass may be produced that would simplify the annotation of individual frames by permitting the use of only pass and frame numbers on the montage prints.

NASA specifies that separate montages shall be prepared for the RBV and the MSS imagery. This may not be necessary to provide information regarding coverage by either of the two sensors (except possibly coverage by the thermal infrared channel of the MSS). If coverage of an area is available from both sensors, only one RBV frame is needed to prepare the montage. If either sensor is inoperative, or if the imagery of one sensor is lost in the transmission or recording processes, a single letter code on the montage print or in the textual data can indicate the operational sensor.

The montages should be reproduced by the Government Printing Office or by some other agency equipped to reproduce large cartographic products. This would obviate the need for the NDPF to procure and operate large lithographic presses and ancillary equipment that would be used only twice monthly. The montage pages should also be bound by this reproduction facility.

CONTENTS

6. FUNCTIONAL AND TIMELINE ANALYSIS

6.1 INTRODUCTION

During system operations there are specific activities which must occur on a daily basis. These have been defined generally in other volumes and follow here in more detail. As with any large data processing system there are operations which can occur in parallel and others which must occur serially, awaiting the results of one set of data before processing the next. It is also apparent that some functions are either totally manual or require only off-line operation, with little or no dependency on a computer interface.

It is the purpose of a timeline or throughput analysis to determine those functions and operations which work together, to time the processing from start to finish, and to derive quantitative information which assists in specifying the hardware requirements. It has been possible to assemble throughput times for the various functions of the NDPF. Quantitative data has been assembled which provides useful information about the system, especially computer and off-line hardware timing data. Using one day as a standard, the throughput for each NDPF function has been calculated and recorded in the following tables and charts.

After some consideration, it was decided to use a flow somewhat different from that of the overall system flow (see Volume 15, Section 1, also the appendix volume). In the system master flow (Volume 15, Figure 1-1), the processing involved is in functions 19.0 and 20.0. The functions described under these headings are in user terms: for a timing analysis, it is more convenient to rework the flow to correspond to the machines and personnel of the NDPF. Another reason for the modified functional flow is that in the baseline system, MSS and RBV bulk mode data processing are handled in a quite similar fashion.

Figure 6.1-1 is a top level functional flow, and the sub-functions or activities discussed and referenced in this section are keyed to the function numbers on the functional flow chart.
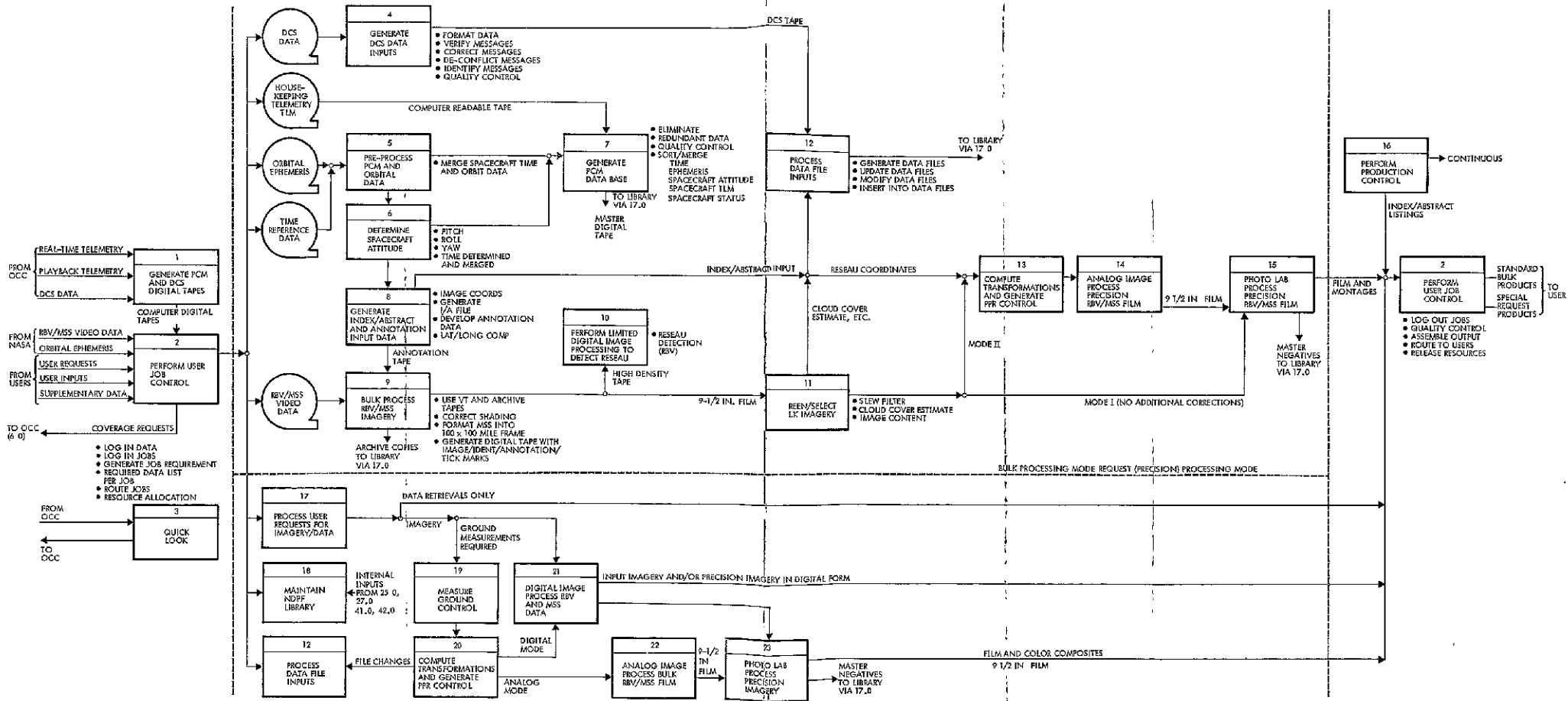
Figure 6.1-1
NDPF FUNCTIONAL FLOW

Two alternative systems are considered where applicable — a system A which is the most automated, and an alternative system B which uses manual and/or semi-automatic processes to a greater extent. The times are based on 315 frames of imagery per day for ERTS A, case A, 1315 frames per day for ERTS B, case B, request imagery as specified in the NASA design specifications, and assumptions for other request services. Throughput rates consider three alternatives where possible: a most optimistic, a most likely, and a maximum time to process the data, assuming a large, medium, and small scale computer, respectively, or a range of possibilities if the activities are manual.

A summary of the preliminary timeline results is included in Tables 6.1-1 and 6.1-2, and following in Section 6.2 are individual discussions of each function in more detail. Also included in this section are individual functional flow diagrams where applicable.

6.2 TIMELINE ANALYSIS

6.2.1 Function 2.0 — Perform User Job Control (assumes a 5-day work week)

This function, strictly manual, is actually a part of the production control activity, but activities requiring several operations can be timed for the throughput. Times are the same for both Systems A and B.

Daily Activities	Occasional Activities
3.1 - 6.2 - 12.3 hours	0.25 - 0.5 - 1.0 hour

All activities can be handled in an 8-hour day with the appropriate manning. See Figure 6.2-1 for data flow.

6.2.2 Functions 1.0, 4.0, 5.0, 6.0, 7.0, 8.0 — PCM Processing

These functions are grouped together because they are interrelated, comprising the computer operations of PCM telemetry and DCS processing. Not allowing for set-up times and production control delays between functions it can be seen that a "likely" CPU processing time is 104 minutes (1.7 hours) to process the telemetry and DCS data per day. Input/output time is estimated to be an additional 1.25 hours, for a total of 2.95 hours.

Table 6.1-1. NDPF Computer Time Requirements (Elapsed time per day, in hours)

| | ERTS A Case A | | | ERTS B Case B | | | | | | | | |
| | 5 days | | | 5 days | | | 6 days | | | 7 days | | |
	360/65	360/75	360/85	360/65	360/75	360/85	360/65	360/75	360/85	360/65	360/75	360/85
1.0 Operating system	0 50	0 33	0 11	1 50	0.99	0 33	1 50	0 99	0 33	1 50	0 99	0 33
2 0 Telemetry processing	3 80	2 95	1 82	5 70	4 22	2 24	5 70	4 22	2 24	5 70	4 22	2 24
3 0 Information management	0 30	0 20	0 07	0 50	0 40	0 15	0 50	0 40	0 15	0 50	0 40	0 15
Total non-image process	4 60	3 48	2 00	7 70	5 61	2 72	7 70	5 61	2 72	7 70	5 61	2 72
4 0 Process control	0 03	0 02	0 01	0.11	0 07	0 03	0 10	0 06	0 02	0 08	0 05	0 01
5 0 Image digitizing	0 35	0.35	0 35	1 40	1 40	1 40	1 17	1 17	1 17	1 01	1 01	1 01
6 0 Image calibration	0 73	0 49	0 21	0 73	0.49	0 21	0 61	0 41	0 18	0 52	0 34	0 15
7.0 Bulk mode 2**												
7 1 Baseline	3 35	2 38	1 02	12 67	9 10	3 87	10 75	7 60	3 22	9 29	6 50	2 76
7.2 Option A	3 44	3 07	2 40	12 61	11 26	8 80	10 52	9 39	7 33	9.01	8 04	6 28
7 3 Option B	--	--	1 40	--	--	5 14	--	--	4 28	--	--	3 66
8.0 Precision mode 1	2 45	1.72	0.74	9 16	7 13	3 05	8 49	5 96	2 56	7 30	5 12	2 19
Total image process	7 00	5.65	3 71	25 01	20 35	13 49	20 89	16 99	11 26	17 92	14 56	9 64
Total Time (Baseline A)	11 60	9 13	5 71	32 71	25 96	16 21	28 59	22 60	13 98	25 62	20 17	12 36

---

*Timing data is based on worst case loads including ERTS-B with 3 RBV and 5 MSS channels

** 7 1   Baseline includes reseau detect and computational support of PPR doing TBV and MSS images

7 2   Option A is computer time for doing all RBV images all digital

7 3   Option B is same as Option A except that the addition of a second high speed channel would allow cutting input/output times in half This is only available on System 360/85 and 95   This channel has been configured with the 1 5 megabyte/second disks for reseau detect and precision modes   A 3 0 megabyte/second disk is also available for growth capability.

Table 6.1-2.   NDPF Off-line and Manual Time Requirements

	Hours per Day	
	Case A (5-day week)	Case B (7-day week)
Off-line Processes		
Analog PPR processing (bulk and request modes)	18.7	55.6
Screening without reseau measurements	5.4	16.2
Ground mensuration (request mode)	4.0	12.0
Recording imagery on high density tape (bulk mode)	6.6	19.8
LBR processing (bulk mode)	2.5	7.5
LBR processing (request mode)	0.1	0.3

Manual Applications	Hours per Day
User job control	6.2
Process data file inputs	5.3
Process user requests	2.8
Maintain library	continuous
Production control	continuous

This figure is shown in Table 6.1-1 as representing the CPU and input/output time for a 360/75 in case A.   See Figures 6.2-2, 6.2-3, 6.2-4, 6.2-5, 6.2-6, and 6.2-7.   See Table 6.2-1 for timing details.

6.2.3   Function 9.0 — Bulk Process RBV/MSS Imagery (assumes a 5-day work week)

Computer time is nominal in this function, supporting process control digitizing, inserting annotation, and processing calibration imagery to correct for shading.   This amounts to about 0.69 hours per day in case A and 1.79 hours per day in case B.   There is additional time required to mount and de-mount tapes, this also nominal, and to process LBR film in the photo lab.
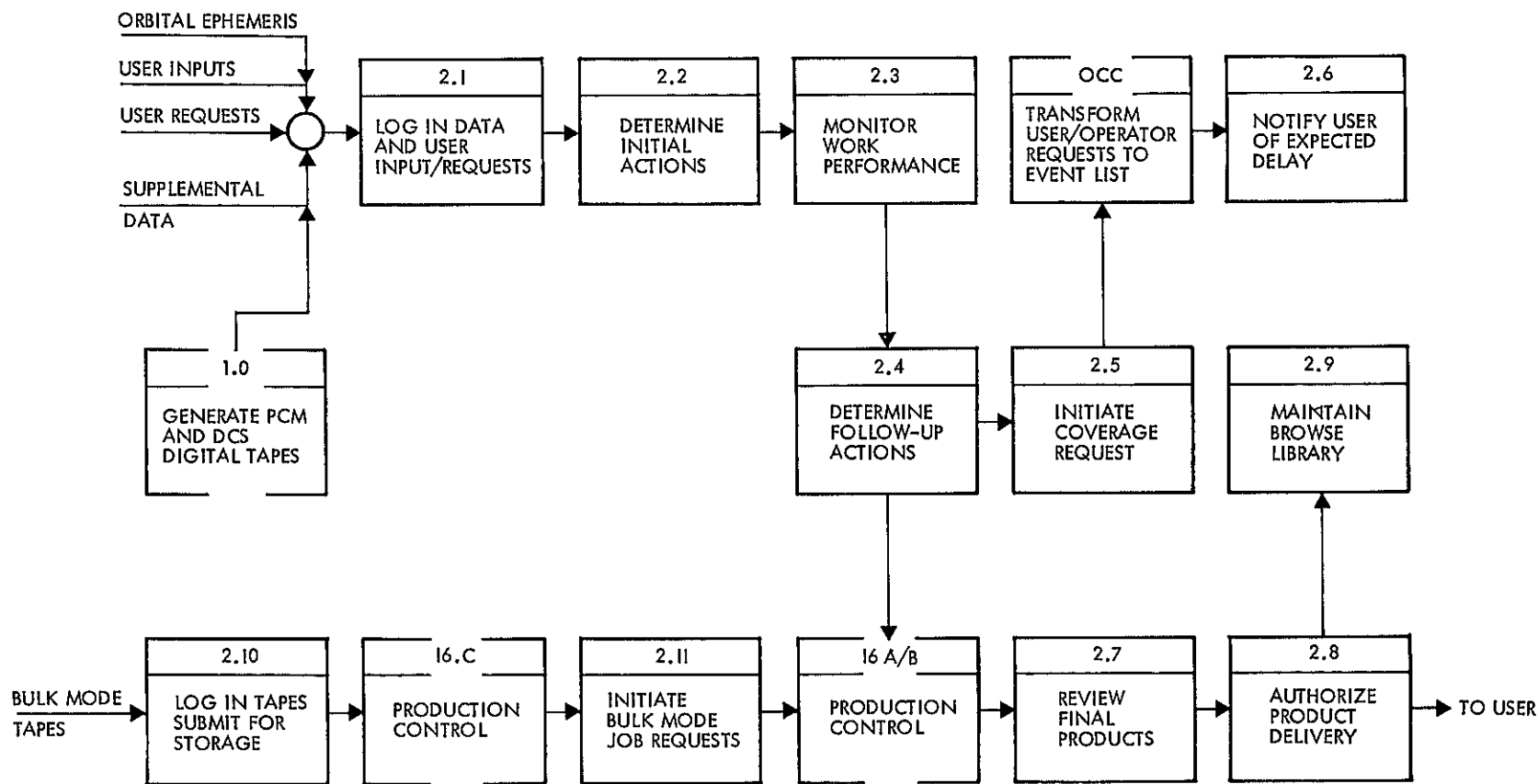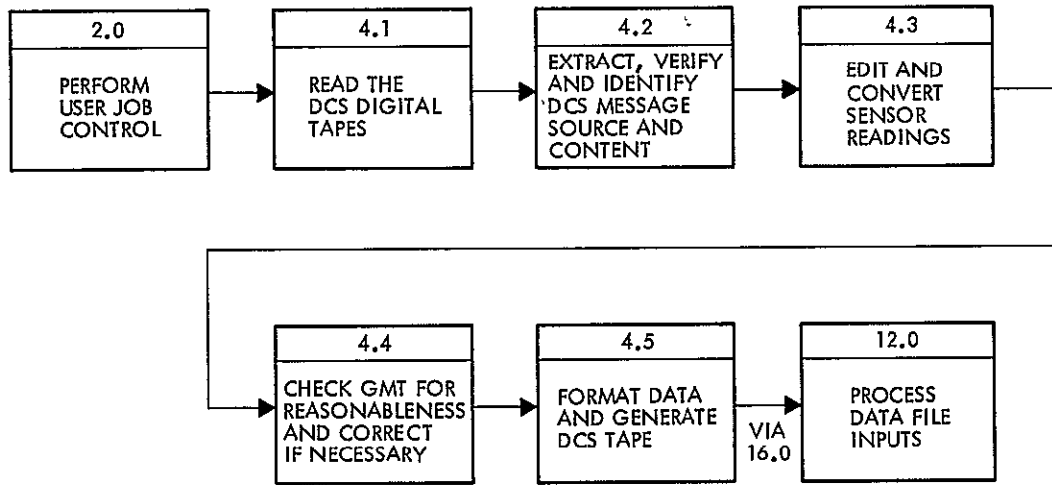
Figure 6.2-1

PERFORM USER JOB CONTROL

2.0		4.1		4.2		4.3
PERFORM USER JOB CONTROL	→	READ THE DCS DIGITAL TAPES	→	EXTRACT, VERIFY AND IDENTIFY DCS MESSAGE SOURCE AND CONTENT	→	EDIT AND CONVERT SENSOR READINGS

4.4		4.5		12.0
CHECK GMT FOR REASONABLENESS AND CORRECT IF NECESSARY	→	FORMAT DATA AND GENERATE DCS TAPE	VIA 16.0	PROCESS DATA FILE INPUTS

Figure 6.2-2

GENERATE DCS DATA INPUTS

2.0		5.1		5.2
PERFORM USER JOB CONTROL	→	IDENTIFY AND CORRECT PCM GMT DISCREPANCIES	→	MERGE ORBIT PARAMETERS WITH CORRECTED GMT

7.0
GENERATE PCM DATA BASE

5.3		5.4	
INITIALIZE SPACECRAFT REFERENCE FILE	→	GENERATE TIME HISTORY AND PCM DIGITAL TAPE SCHEDULE	VIA 16.0

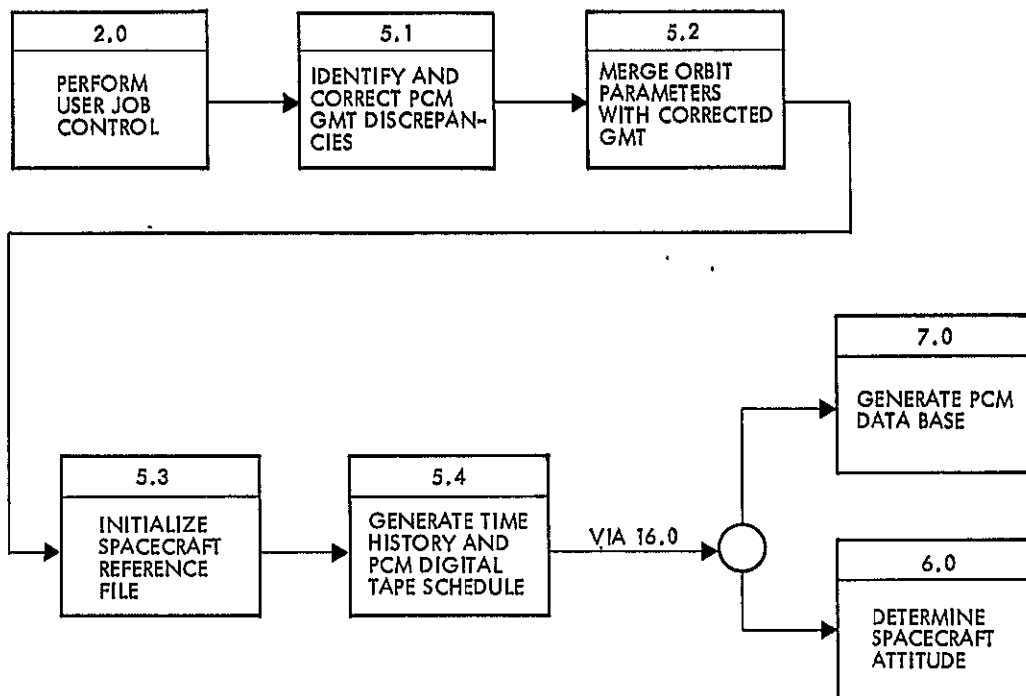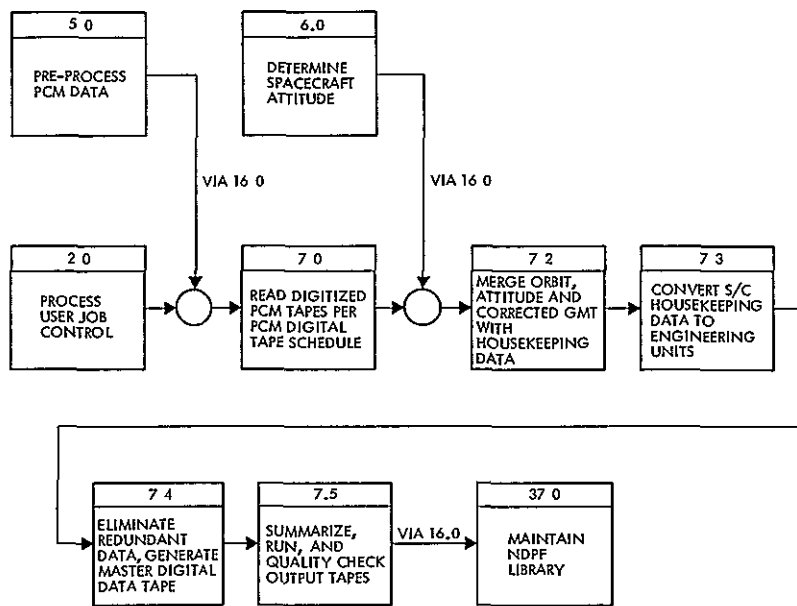| 6.0 |
|---|
| DETERMINE SPACECRAFT ATTITUDE |

Figure 6.2-3

PRE-PROCESS PCM AND ORBITAL DATA

Figure 6.2-4
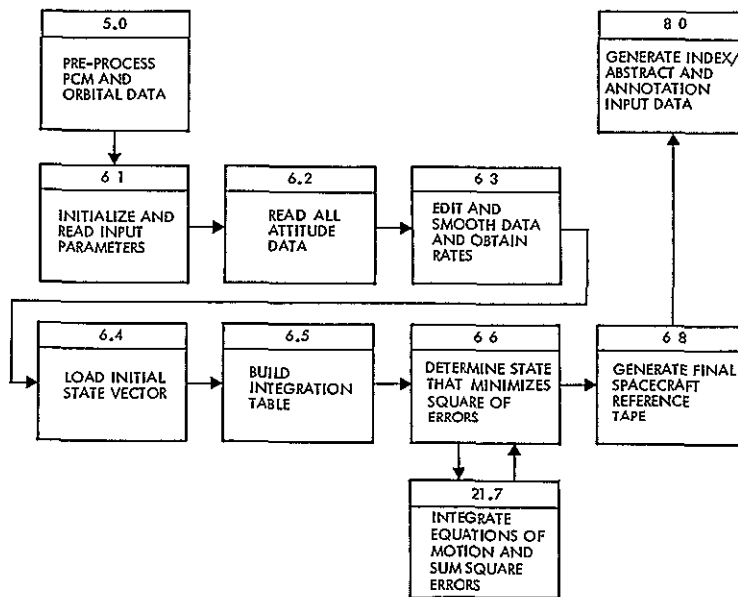
GENERATE PCM DATA BASE

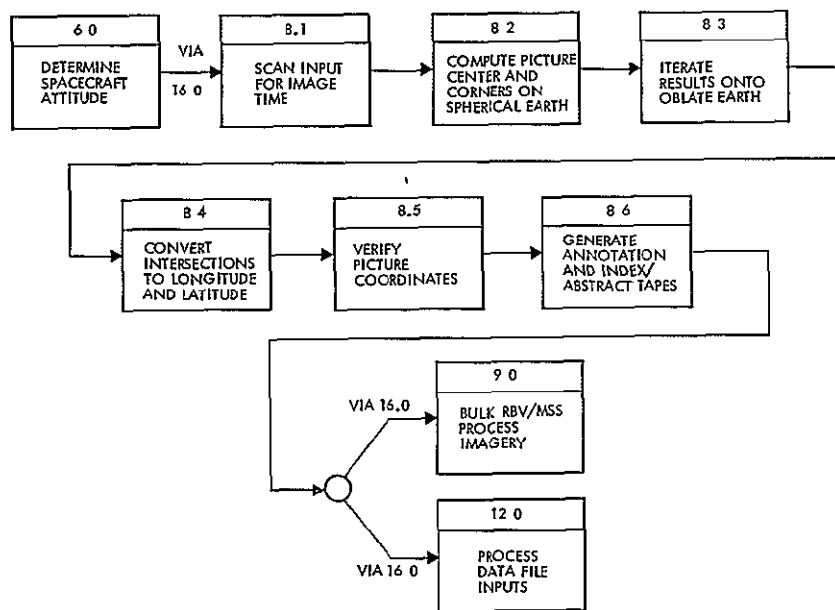

Figure 6.2-5

DETERMINE SPACECRAFT ATTITUDE
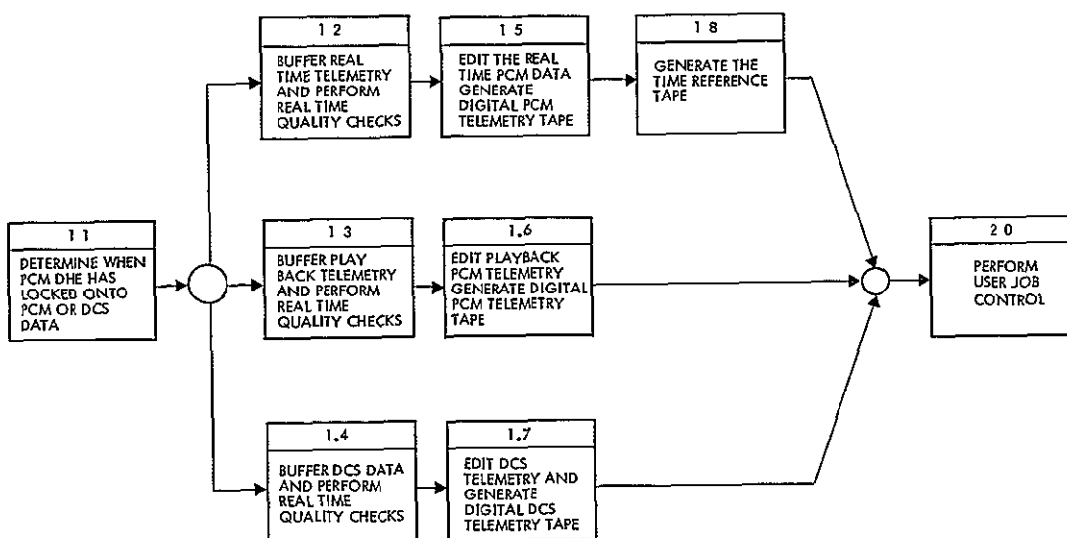
Figure 6.2-6

GENERATE INDEX/ABSTRACT AND ANNOTATION

Figure 6.2-7

GENERATE PCM AND DCS DIGITAL TAPES

Table 6.2-1. PCM and DCS Timing

Function	Description	CPU Timing (minutes)		
		Minimum	Likely	Maximum
1.0	Generate PCM and DCS tapes	5	15	60
4.0	DCS data generation	1	4	10
5.0	Pre-process PCM/orbital data	1	8	20
6.0	Determine attitude	5	40	80
7.0	Master digital data generation	8	35	90
8.0	Index-abstract/annotation	0.5	2	4

Two additional timing figures are significant off-line functions which use special hardware recording the imagery and annotations on tape, and converting the imagery to film via the LBR. Recording imagery on high density tape requires 52 seconds per image for RBV data, and 56 seconds per image for MSS data. Film recording time, using the laser beam recorder, requires 14 seconds per RBV image and 7.5 seconds per MSS image. See Figure 6.2-8 for the bulk process RBV/MSS imagery data flow. Tables 6.2-2 and 6.2-3 summarize these times, for both Case A and Case B.

6.2.4 Function 10.0 — Perform Limited Digital Image Processing to Detect Reseau

The digital image processing uses a limited amount of time in the analog support mode (approximately 0.3 hours per day in case A and 1.3 hours in case B). Figure 6.2-9 shows the data flow.

6.2.5 Function 11.0 — Screen and Select Bulk Imagery (assumes a 5-day work week)

The activities in this function have been timed for designs A and B. In design A additional time for input/output terminal processing, classifying and abstracting, has been included, at the same time reducing time
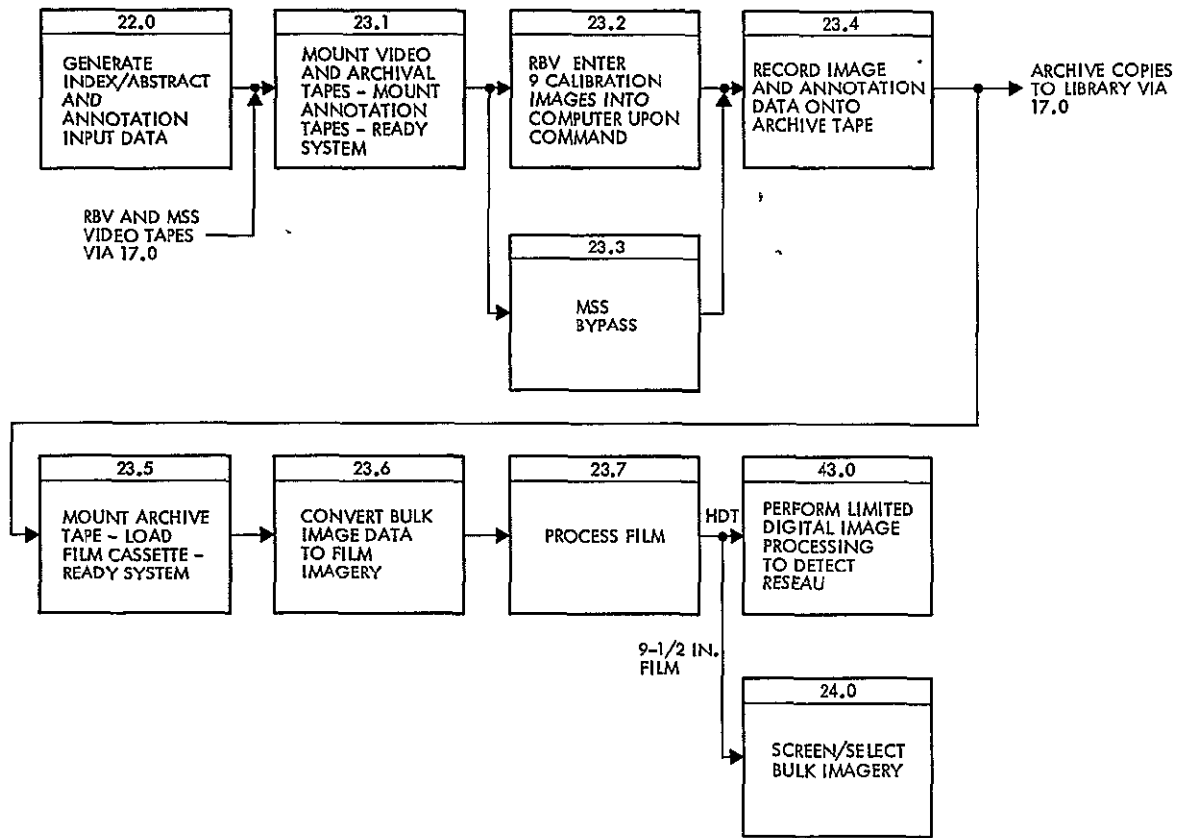
22.0
GENERATE INDEX/ABSTRACT AND ANNOTATION INPUT DATA

23.1
MOUNT VIDEO AND ARCHIVAL TAPES - MOUNT ANNOTATION TAPES - READY SYSTEM

23.2
RBV ENTER 9 CALIBRATION IMAGES INTO COMPUTER UPON COMMAND

23.4
RECORD IMAGE AND ANNOTATION DATA ONTO ARCHIVE TAPE

ARCHIVE COPIES TO LIBRARY VIA 17.0

RBV AND MSS VIDEO TAPES VIA 17.0

23.3
MSS BYPASS

23.5
MOUNT ARCHIVE TAPE - LOAD FILM CASSETTE - READY SYSTEM

23.6
CONVERT BULK IMAGE DATA TO FILM IMAGERY

23.7
PROCESS FILM

HDT

43.0
PERFORM LIMITED DIGITAL IMAGE PROCESSING TO DETECT RESEAU

9-1/2 IN. FILM

24.0
SCREEN/SELECT BULK IMAGERY

Figure 6.2-8

BULK PROCESS RBV/MSS IMAGERY

Table 6.2-2. High Density Tape Recording Times

Recording on High Density Tape (hours per day)	RBV	MSS	Total
ERTS A, case A, 5 days	2.7	3.9	6.6
ERTS B, case B, 5 days	10.0	17.9	27.9
6 days	8.3	14.9	23.2
7 days	7.2	12.8	20.0

Table 6.2-3. LBR Recording Times

Recording on Film via LBR (hours per day)

ERTS A, Case A

- 5 days (40 hours)

| Sensor | Bulk Mode* | | Request Mode | | Total Time per day |
	Frames per day	Time per day	Frames per day	Time per day	
RBV	189	88.0 min.	9	2.8 min.	
MSS	252	63.0 min.	13	3.3 min.	
		2.5 hours		0.1 hour	2.6 hours

ERTS B, Case B

- 5 days (more than 40 hours)

RBV	693	5.4 hours	35	16.3 min.	
MSS	1,148	4.8 hours	57	14.3 min.	
		10.2 hours		0.5 hour	10.7 hours

- 6 days

RBV	578	4.5 hours	29	13.5 min.	
MSS	956	4.0 hours	48	12.0 min.	
		8.9 hours		0.4 hour	9.3 hours

- 7 days

RBV	495	3.8 hours	25	11.7 min.	
MSS	820	3.4 hours	41	10.3 min.	
		7.2 hours		0.4 hours	7.6 hours

*Refer to Figure 6.2-8 for the bulk processing data flow.

```
┌─────────────────┐      ┌─────────────────┐      ┌─────────────────┐
│      23.0       │      │      43.1       │      │      43.2       │
├─────────────────┤      ├─────────────────┤      ├─────────────────┤
│  BULK PROCESS   │─────▶│  READ           │─────▶│  DETECT         │
│  RBV/MSS        │      │  DIGITIZED      │      │  RESEAU         │
│  IMAGERY        │      │  IMAGE          │      │                 │
│                 │      │  DATA           │      │                 │
└─────────────────┘      └─────────────────┘      └─────────────────┘
```

```
        ┌─────────────────┐      ┌─────────────────┐
        │      43.3       │      │      44.0       │
        ├─────────────────┤      ├─────────────────┤
        │  STORE          │─────▶│  COMPUTE TRANS- │
        │  RESEAU         │      │  FORMATIONS AND │
        │  COORDINATES    │      │  GENERATE       │
        │                 │      │  PPR CONTROL TAPE│
        └─────────────────┘      └─────────────────┘
```
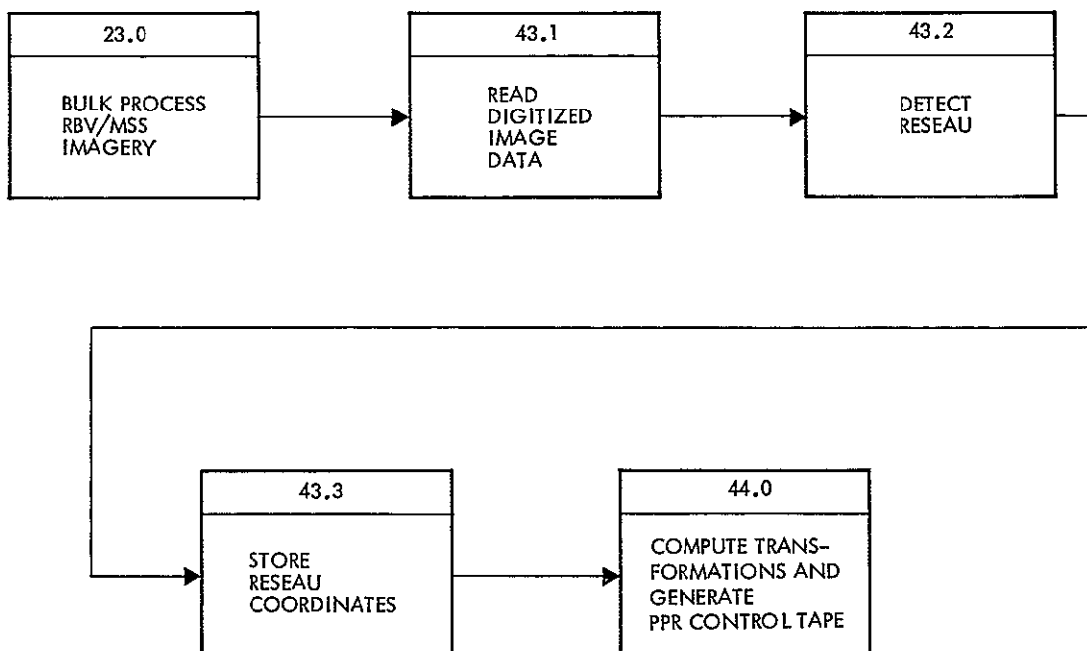
Figure 6.2-9

PERFORM LIMITED DIGITAL IMAGE PROCESSING
to detect reseau

to account for software detection of reseau points. The figures assume
5 minutes per frame to classify and abstract. Design B assumes manual
reseau detection.

● Design A — does not include any reseau measurements, only
  mounting, demounting, viewing, classifying, abstracting, and
  input/output terminal interactions.

    ERTS A, Case A

    324 minutes per day

    5.4 hours per day

● Design B — includes manual reseau measurement of selected
  control copy frames.

    ERTS A, Case A   ERTS B, Case B

    642 minutes per day   1,613 minutes per day
    10.7 hours per day   ˙   26.9 hours per day

For design B, manual reseau measurement, timing assumes a
maximum of 9 frames measured per day. Four screening stations would
be required to meet case B. This would also impose an added screening

load in the request mode in order to measure reseaus not measured in this function.

For design A, automatic reseau measurement by the computer, times are given assuming all frames are previously measured. Considering prime shift operation only there would be a need for three screening stations to provide reasonable backup. See Figure 6.2-10 for the screen/ select and measure bulk imagery data flow.

6.2.6 Function 12.0 — Process Data File Inputs (assumes a 5-day work week)

Except for the actual updating activity, which requires computer software, this function is primarily manual. The times shown are total time per day to process all data file inputs.

System A	System B
Manual steps 2.7 - 5.3 - 10.5 hours	3.1 - 6.1 - 12.2 hours

Figure 6.2-11 shows the file input data flow.

6.2.7 Functions 13.0, 19.0 and 20.0 — Measure Ground Control, Compute Transformations, and Generate PPR Control

In this bulk mode limited transformations are computed prior to PPR control processing. This is shown in Figure 6.2-12. In the request or precision mode the same PPR control processing would take place in the analog process, with an additional need for ground data measurement of the imagery. The ground measurement function is shown in Figure 6.2-13, and the request mode transformations are shown in Figure 6.2-14.
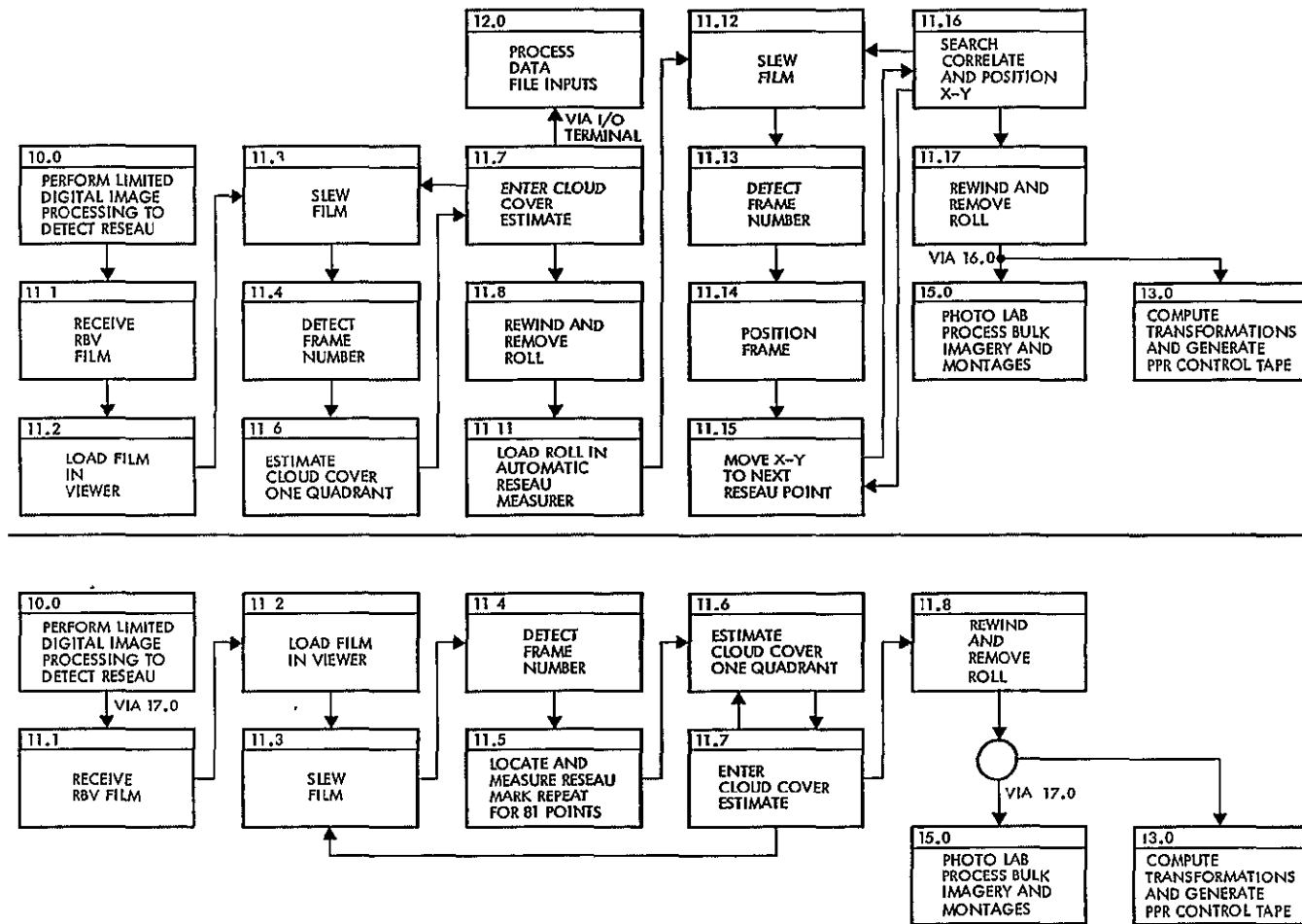
Figure 6.2-10

SCREEN/SELECT AND MEASURE BULK IMAGERY
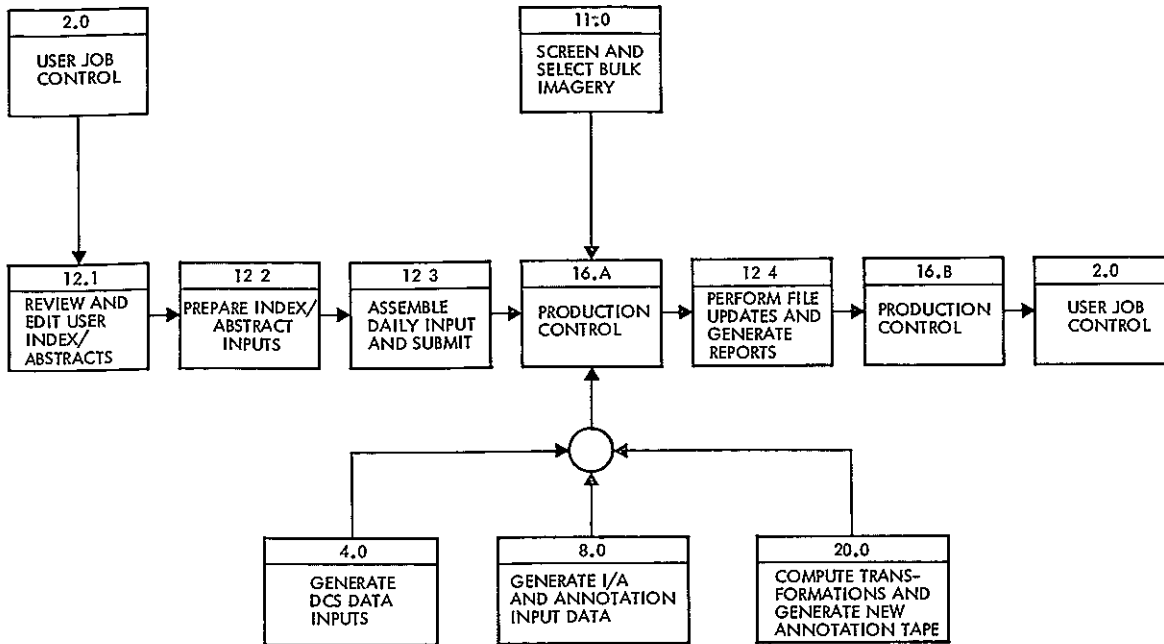
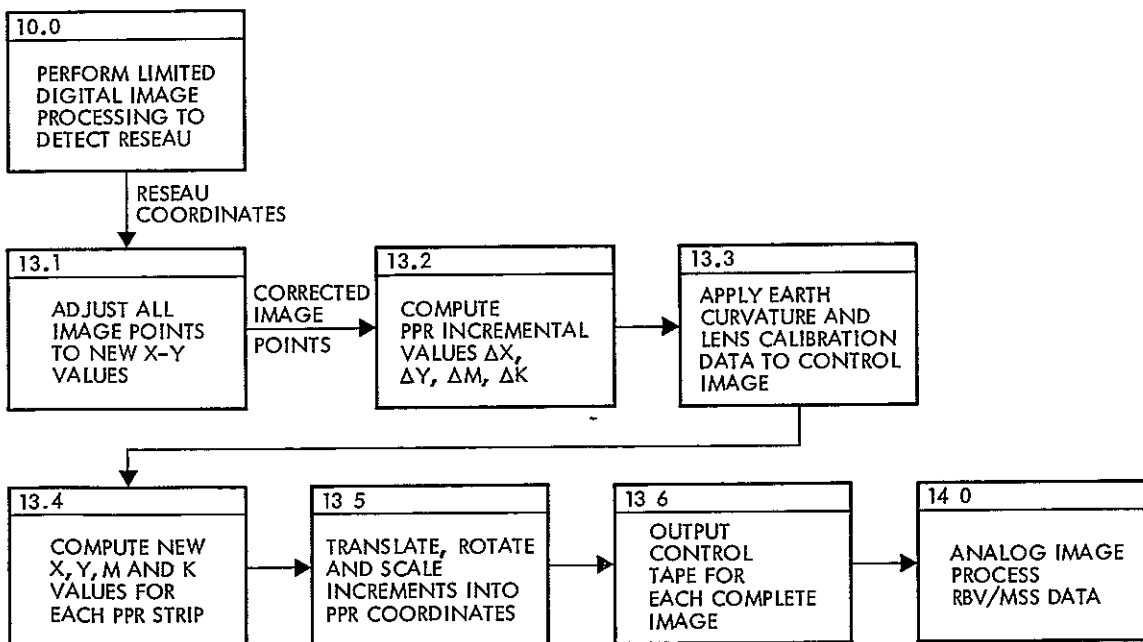Figure 6.2-11

PROCESS DATA FILE INPUTS

Figure 6.2-12

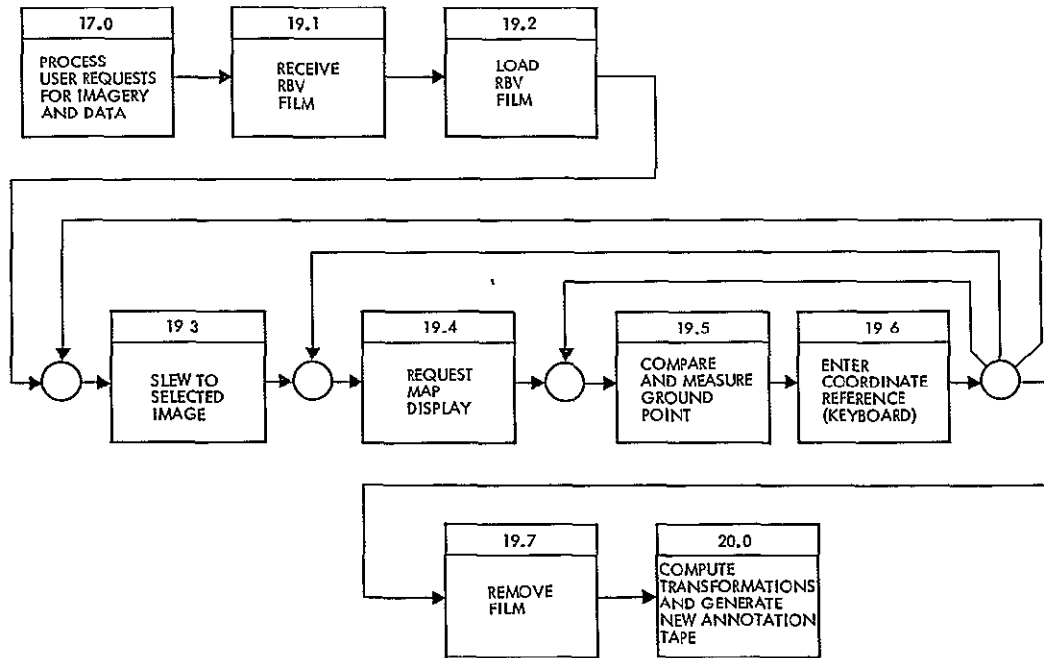COMPUTE TRANSFORMATION AND GENERATE PRR CONTROL

Figure 6.2-13

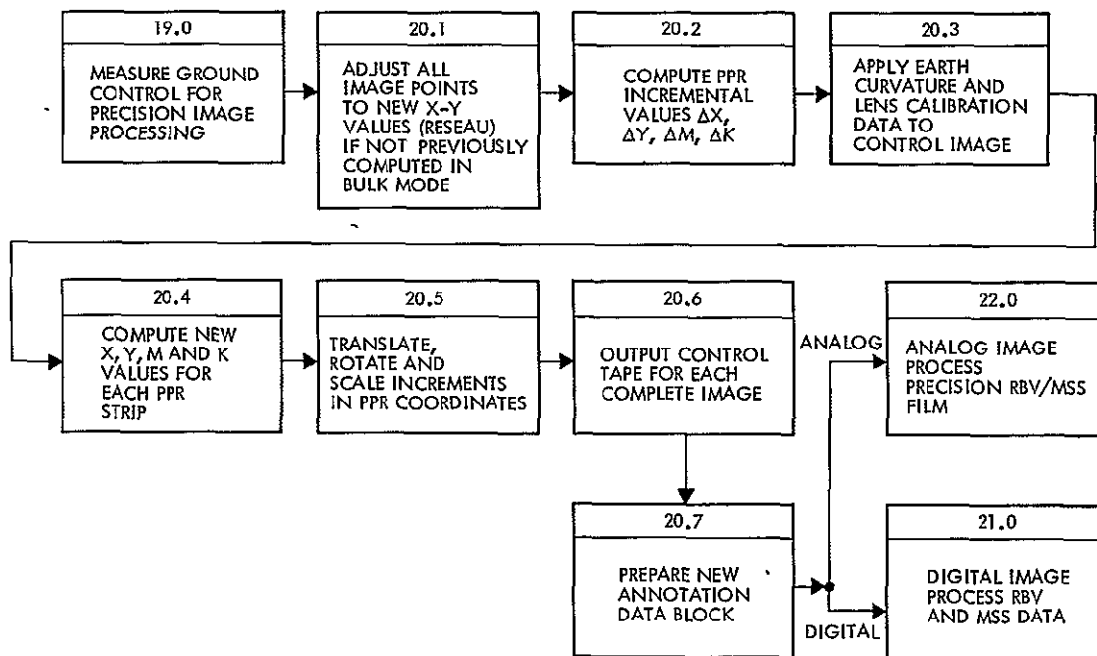MEASURE GRAND CONTROL for precision image processing

Figure 6.2.14

COMPUTE TRANSFORMATIONS and generate new annotation tape

Computer times needed, total elapsed time, to support all the mensuration and PPR control is summarized in hours per day in Table 6.2-3.

Table 6.2-3. Computer Times

	ERTS A, Case A	ERTS B, Case B		
		5 days (hours)	6 days (hours)	7 days (hours)
Least	0.66 hour	2.58	2.14	1.84
Most likely	2.0 hours	7.73	6.45	5.52
Maximum	3.0 hours	11.59	9.68	8.37

To meet ERTS B, case B volumes it is obvious from the figures that a large computer (e.g., 360/85) would be required in order to reduce the processing time to approximately 2 hours per day.

Ground control measurement is a time consuming off-line function. The following times assume a 5-day work week.

- Design A — assumes all reseau points were automatically measured in bulk mode, and 5 percent of bulk imagery must be processed, at 1-hour per frame

ERTS A, Case A

3.2 hours per day

ERTS B, Case B

11.6 hours per day

For Design A, one or two ground control measurement stations are required.

- Design B — assumes only 9 frames per day originally reseau-measured manually in bulk mode, thus imposing additional time in this function to measure both the reseaus and ground control for 5 percent of the bulk imagery. Because of the selection of design A further analysis of design B was curtailed.

6.2.8 Functions 14.0 and 22.0 — Analog Image Processing

The PPR functional analysis indicates the activity timing per image as 2.5 minutes for bulk II mode. For precision processing, it is possible

to switch to a smaller slit for greater accuracy. In this case, a processing time of 4 minutes is indicated. The time line analysis for each type of processing, e.g., control, RBV, color, was completed.

Table 6.2-4 indicates production requirements for each type of processing, cases A and B. The input requirements are based on a 5-day work week for case A and a 7-day work week for case B.

Based on the requirements given in Table 6.2-4, the PPR machine usage is given in Table 6.2-5. The total production of both bulk mode II and precision mode output can be accomplished with four PPR machines running 6.8 hours per day for case A and 17.5 hours per day for case B. Since this maximum rate will rarely be imposed because of cloud cover, it is possible to consider only three PPR machines for the entire processing modes, using overtime to cover peaks in production requirements. If the PPR approach is used only for bulk mode II processing, three PPR machines are required, since case B machine hours total 49.3.

Figure 6.2-15, in two parts, shows the data flow through the bulk mode analog image processing. Figure 6.2-16, also in two parts, shows the flow through the request mode.

Table 6.2-4. PPR Processing Requirements

Processing Mode	Case A			Case B		
	5-Day Week Images per Day	Rolls	Time, Minutes	7-Day Week, Images per Day	Rolls	Time, Minutes
Control (RBV, red band)	63	1	165	165	1	423
RBV (2)	126	1	326	330	2	845
MSS (4)	252	2	650	660	4	1,690
Bulk total	441	4	1,144	1,155	, 7	2,958
Request color						
RBV	13	1	108	33	1	258
MSS	26	1	205	66	1	505
Request color total	39	2	313	99	2	763
Precision control	3	—	22	8	—	42
RBV	6	—	34	16	—	74
MSS	12	—	58	32	—	138
Color						
RBV	3	—	22	8	—	42
MSS	6	—	34	16	—	74
Precision total	30	—	170	80	—	370
Total production	510		1,627	1,334		4,091
Machine hours per day			27.1			68 2

Table 6.2-5. PPR Machine Requirements

	Case A 5-Day Week	Case B 7-Day Week
Total production		
Machine hours	27.1	68.2
PPR machines required, hours per day	4 for 6.8 3 for 9.3	5 for 15.7 4 for 17.5 3 for 22.7
Bulk production only		
Machine hours	19.1	49.3
PPR machines required, hours per day	3 for 6.4	3 for 16.4
Request color production		
Machine hours	5.2	12.7
Bulk and request color		
Machine hours	24.3	62.0
PPR machines required, hours per day	3 for 8.1	3 for 20.6

6.2.9 Function 17.0 — Process User Requests for Image/Data
(assumes a 5-day work week)

This function involves the manual processing of user requests, the actual computer retrieval times, and the "programming" times needed to modify or create queries and/or special user report formats.

Manual steps	1.3 - 2.8 - 6.5 hours per day
Computer	Not specified but minimal
Programming	1/2 - 2 - 5 days turnaround

Figure 6.2-17 shows the data flow for this function.
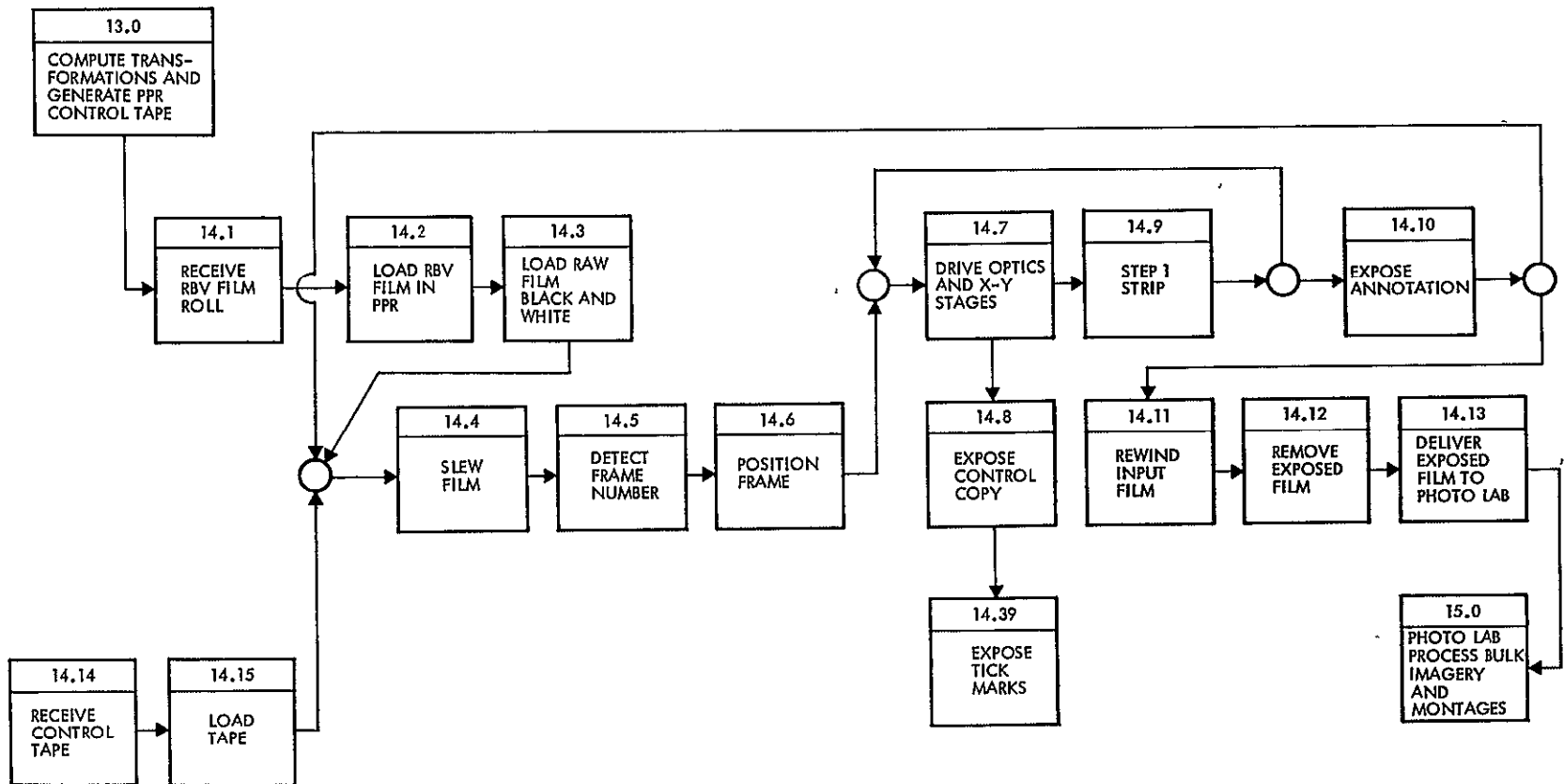
Figure 6.2-15

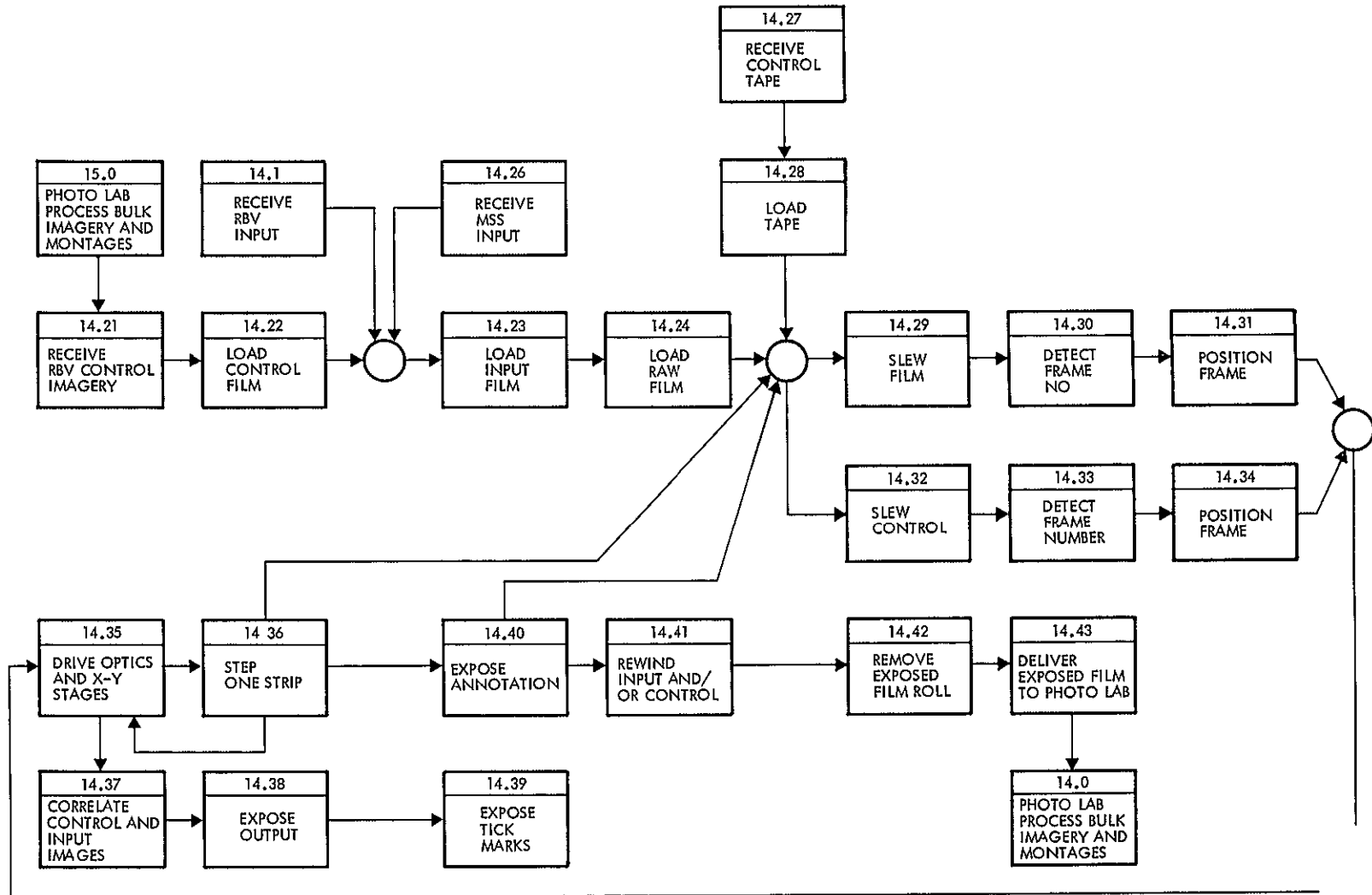ANALOG IMAGE PROCESS RBV/MSS DATA (bulk mode) – control copy preparation

Figure 6.2-15

ANALOG IMAGE PROCESS RBV/MSS DATA   (bulk mode) – control copy preparation (continued)
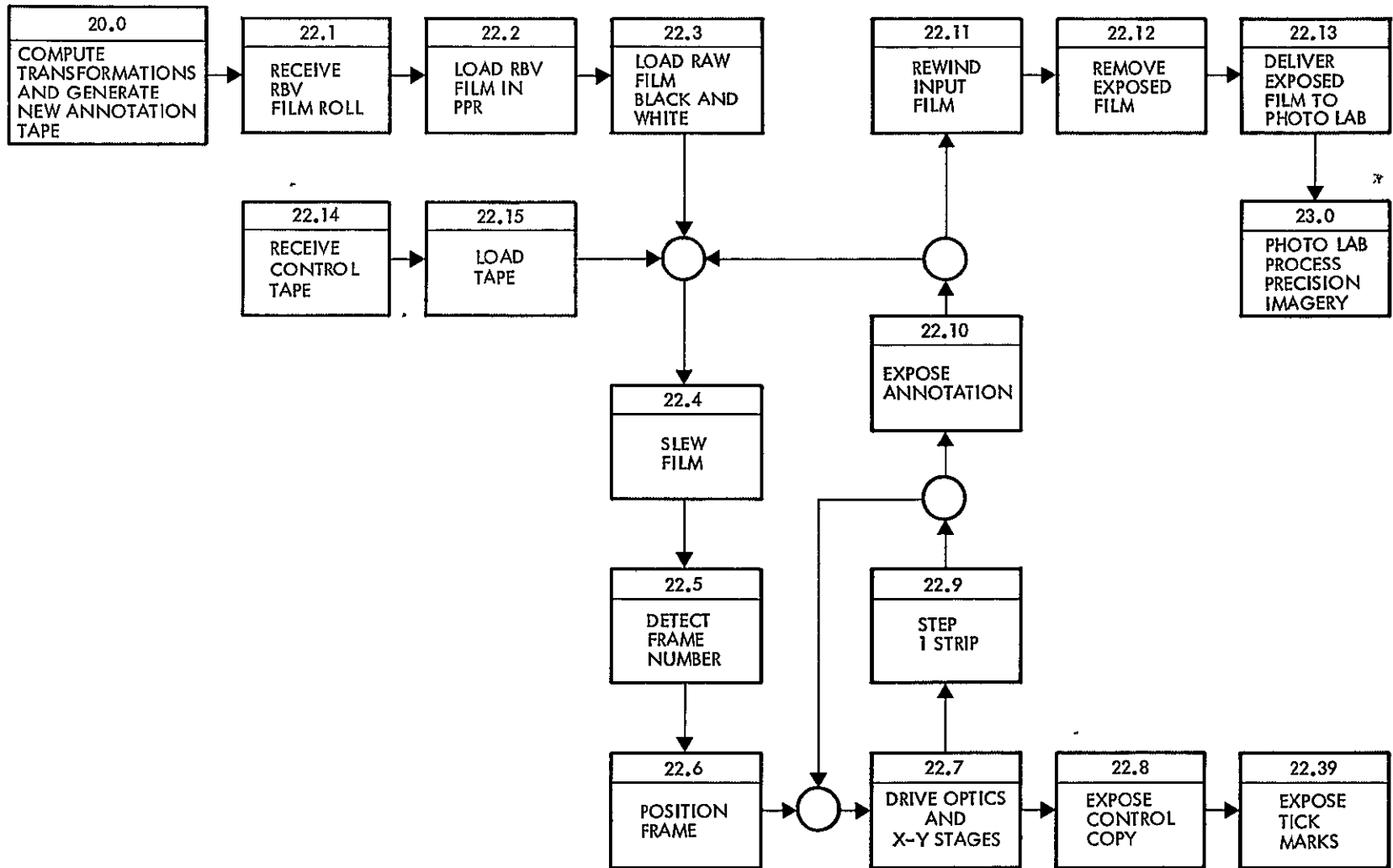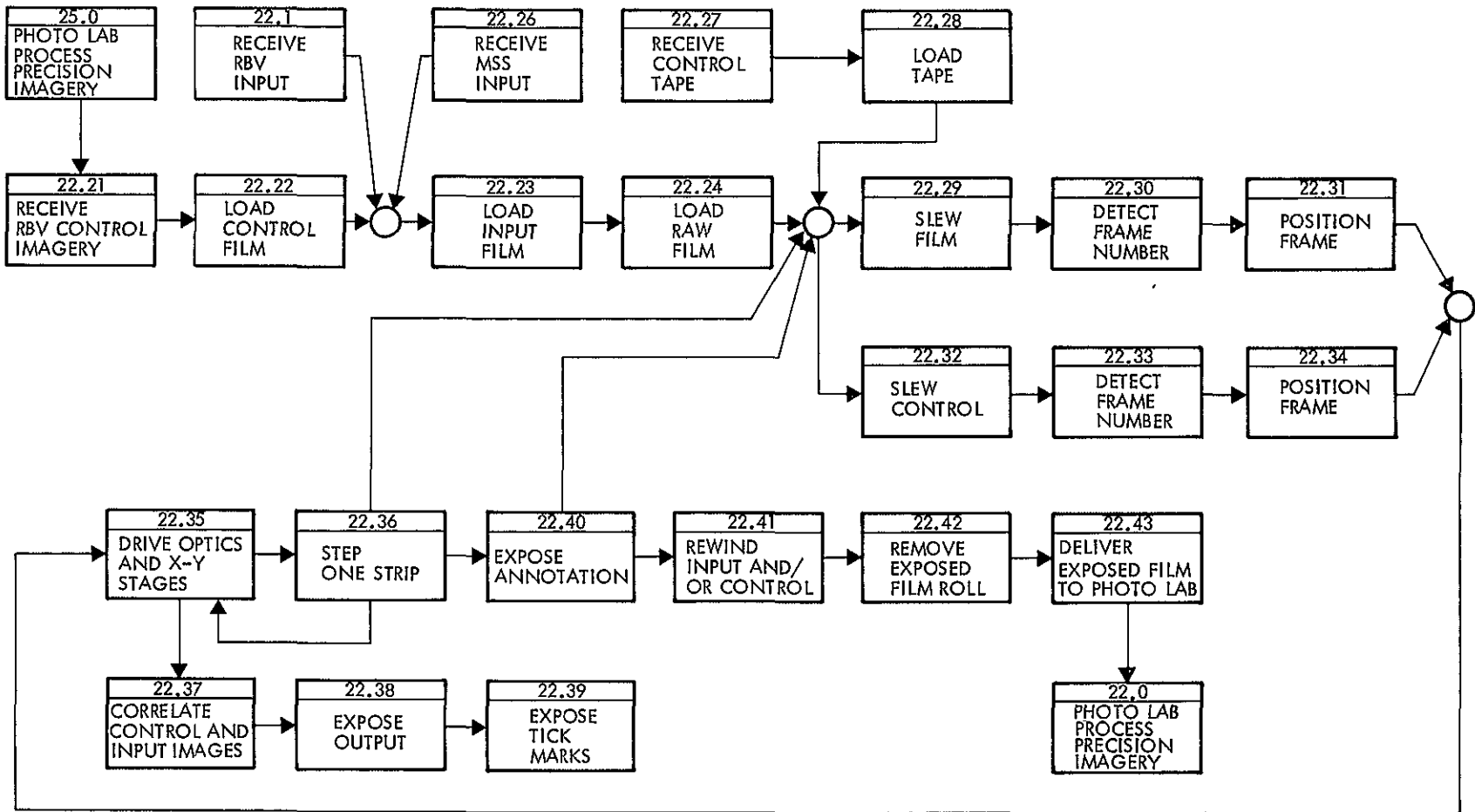
20.0		22.1		22.2		22.3			22.11		22.12		22.13
COMPUTE TRANSFORMATIONS AND GENERATE NEW ANNOTATION TAPE		RECEIVE RBV FILM ROLL		LOAD RBV FILM IN PPR		LOAD RAW FILM BLACK AND WHITE			REWIND INPUT FILM		REMOVE EXPOSED FILM		DELIVER EXPOSED FILM TO PHOTO LAB

Figure 6.2-16

ANALOG IMAGE PROCESS RBV/MSS DATA (request mode) control copy preparation

22.14 RECEIVE CONTROL TAPE

22.15 LOAD TAPE

23.0 PHOTO LAB PROCESS PRECISION IMAGERY

22.10 EXPOSE ANNOTATION

22.4 SLEW FILM

22.5 DETECT FRAME NUMBER

22.9 STEP 1 STRIP

22.6 POSITION FRAME

22.7 DRIVE OPTICS AND X-Y STAGES

22.8 EXPOSE CONTROL COPY

22.39 EXPOSE TICK MARKS

Figure 6.2-16

ANALOG IMAGE PROCESS RBV/MSS DATA (request mode) image correlation (continued)
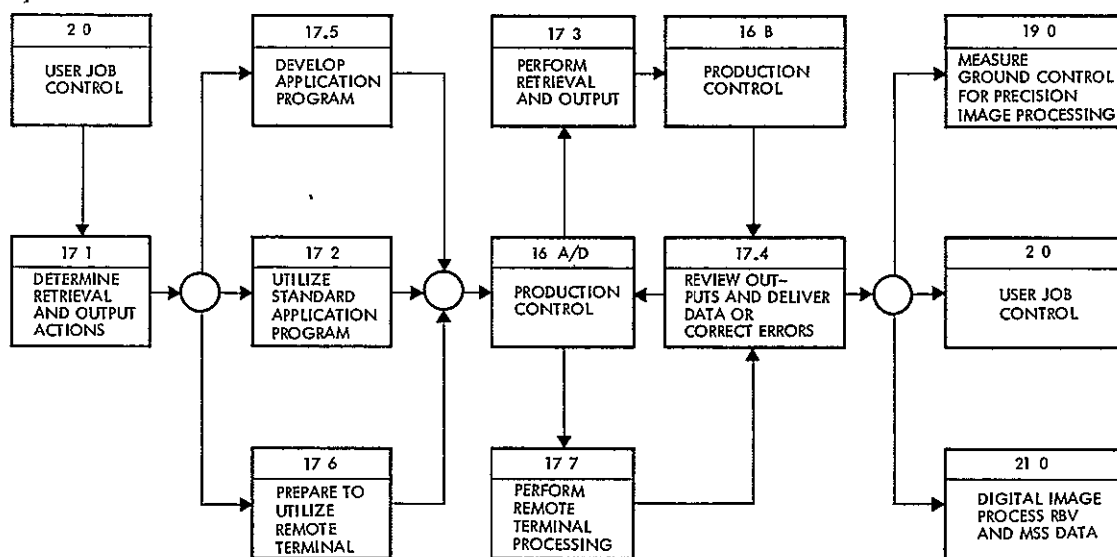
Figure 6.2-17

PROCESS USER REQUESTS FOR IMAGERY/DATA

6.2.10 Function 18.0 — Maintain NDPF Library

The wide range of activities performed in the NDPF library do not require large blocks of time, but the frequency of requests could cause certain activities to be repeated a number of times. Figure 6.2-18 shows the data flow.

6.2.11 Function 41.0 — Digital Image Process RBV and MSS Data (assumes a 5-day work week)

- Design A — assumes "precision" image processing of 5 percent of the bulk inputs. It also includes writing digital tapes of input images. Throughput times vary depending upon the types of corrections made, and according to the output mode selection. See Figure 6.2-19.
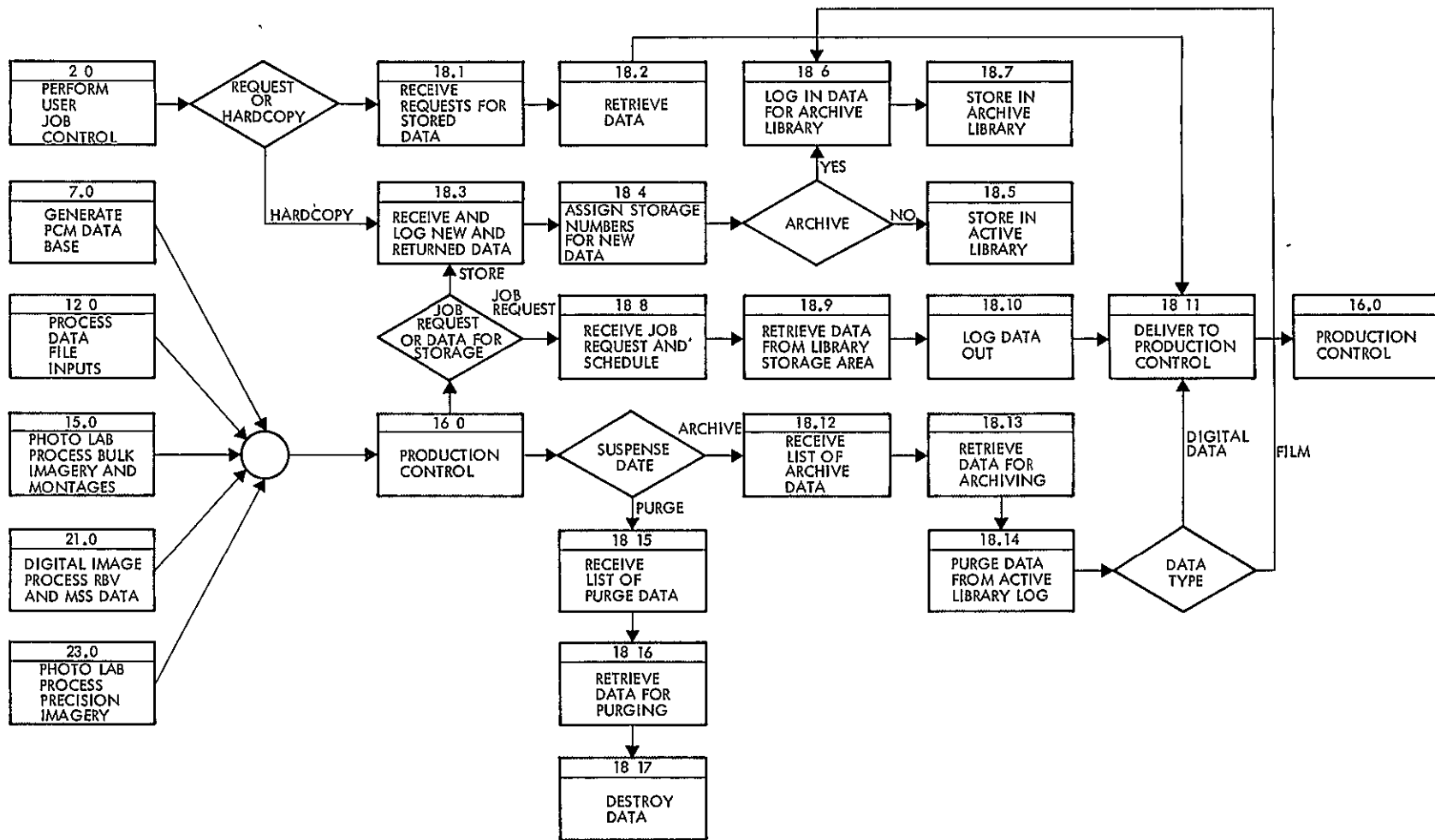
Figure 6.2-18

MAINTAIN NDPF LIBRARY
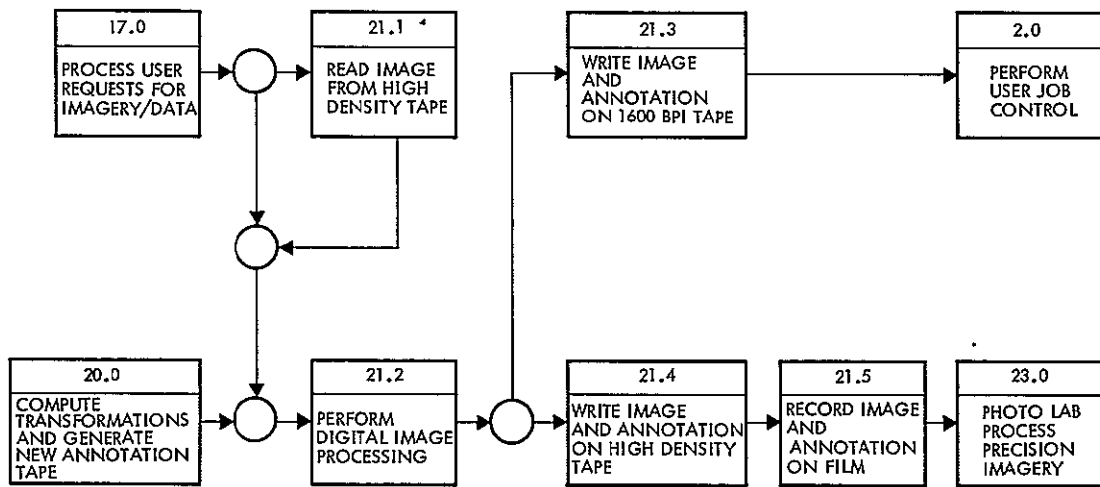
Figure 6.2-19

DIGITAL IMAGE PROCESS RBV AND MSS DATA

7. Correlation of DCS Data
   With Imagery

CONTENTS

7. CORRELATION OF DCS DATA WITH IMAGERY

7.1 INTRODUCTION

In the ERTS spacecraft, the DCS receiver and the imaging sensors are quite distinct. They collect different sorts of data, often at different times. In particular, DCS data is often collected from areas not in view of the cameras.

The hardware separation does not hold with the users. There are many cases in which users must correlate DCS data with image data. The requirements for such correlation, and the means to achieve these have been analyzed.

7.2 REQUIREMENTS

There are three distinctive cases where correlation is required.

- DCS data is needed to help interpret imagery
- Imagery data is needed to interpret DCS data
- Unified experiments are being conducted.

Each of these cases has been examined.

7.2.1 DCS Aids to Imagery Interpretation

In some applications of ERTS, there is a need for ground truth. This may serve one of two purposes.

- Provide data to develop signature recognition schemes
- Provide additional data to aid in interpretation.

As an example of the first purpose, we consider the problem of estimating salt water intrusion into fresh water reservoirs. There is some evidence to indicate that color signatures may be useful for this. To test and develop the concepts, ground truth is needed. This includes data from river or estuary flow gauges, tide sensors, rainfall gauges, etc. Insofar as this data is available from the DCS, it must be made available.

After such a technique has become operational, the same DCS data would be supportive to analysis. This is an example of the second purpose.

Another example might be the determination of sea state near an offshore station by the percentage of white foam on the surface. This must be correlated with sea state data for analysis of the utility of the techniques.

7.2.2 Imagery Aids to DCS Interpretation

In some cases, RBV or MSS data can be very useful in interpreting DCS data. An example might be in water resource studies. DCS sensors might be set to measure the content of deep water tables.

To interpret such data over a period of time, it may be useful to have data on surface water; ERTS imagery may be able to provide such data.

7.2.3 Unified Experiments

A good example here is estimating the amount of water locked up in a snow pack; imagery can give the extent of the pact. Properly placed DCS sensors can give snow depth, estimate snowfall rates, and monitor air temperature.

The combination of detailed spot measurements with imagery together provide a superior estimate of water content than can either sensor system alone.

7.3 CORRELATION REQUIREMENTS

From the applications analysis, it is fairly clear what sorts of things must be done to properly correlate ERTS imagery with DCS data. This involves:

- Retrieval for DCS data
- Imagery annotation requirements.

7.3.1 DCS Data Retrieval Requirements

DCS data must be retrievable on three keys:

- Geographical location
- Time span
- Type of sensor data available.

One must be able, for example, to find all DCS data within the boundary of a given RBV frame, taken in the month of August, where the observing station measures both air temperature and ground moisture.

7.3.2 Imagery Annotation Requirements

It is, at least in some circumstances, most desirable to have imagery annotated with the location of DCS stations. There are several ways to handle this.

- Include locations as a part of the image annotation

- Provide maps, or map overlays, of the location of DCS stations, to the same scale as the imagery.

The object of such annotation is to alert users of the imagery that potentially useful DCS data is available.

It should be noted that DCS users presumably know where their stations are located; the montage catalog can be used to alert them to potentially useful imagery.
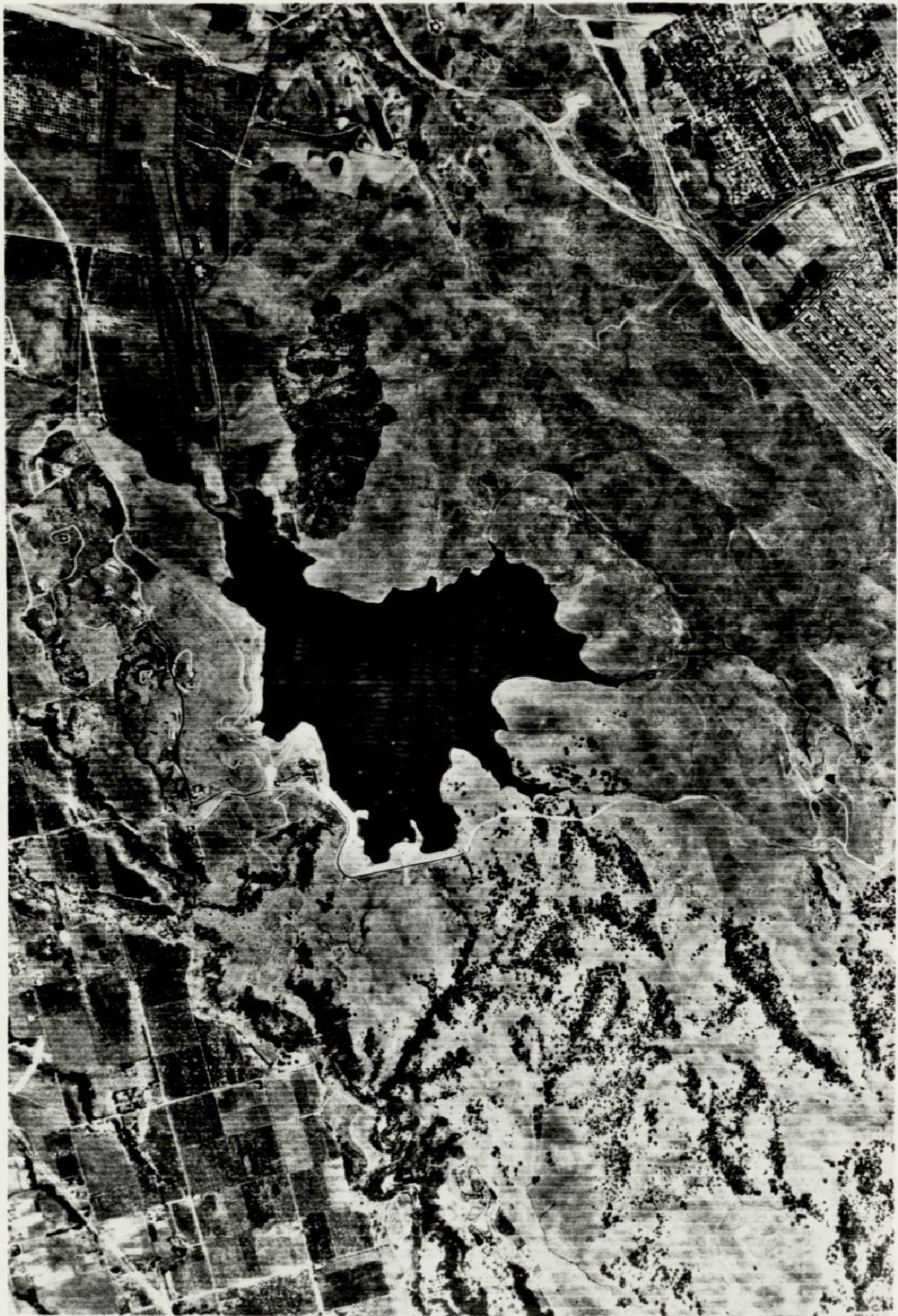
Figure 2.4-15

PORTION OF ORTHOPHOTOGRAPH OUTPUT FROM STEREOMAT IV;
SOURCE MODEL IS 6-INCH FRAME PHOTOGRAPHY (SCALE, 1:24,000)
NEAR POMONA, CALIFORNIA

Figure 2.4-16

SAMPLE ORTHOPHOTOGRAPH FROM AS-11C; SOURCE MODEL IS 6-INCH
FRAME PHOTOGRAPHY (SCALE, 1:48,000) NEAR FORT SILL, OKLAHOMA

Figure 2.4-17

ORTHOPHOTOGRAPH WITH SUPERIMPOSED 40-FOOT
CONTOURS OF FORT SILL, OKLAHOMA, MODEL;
OUTPUT SCALE IS 1:50,000

Figure 2.4-18

ORTHOPHOTOGRAPH PRODUCED BY ZEISS GZ-1 WITH PROFILE DATA
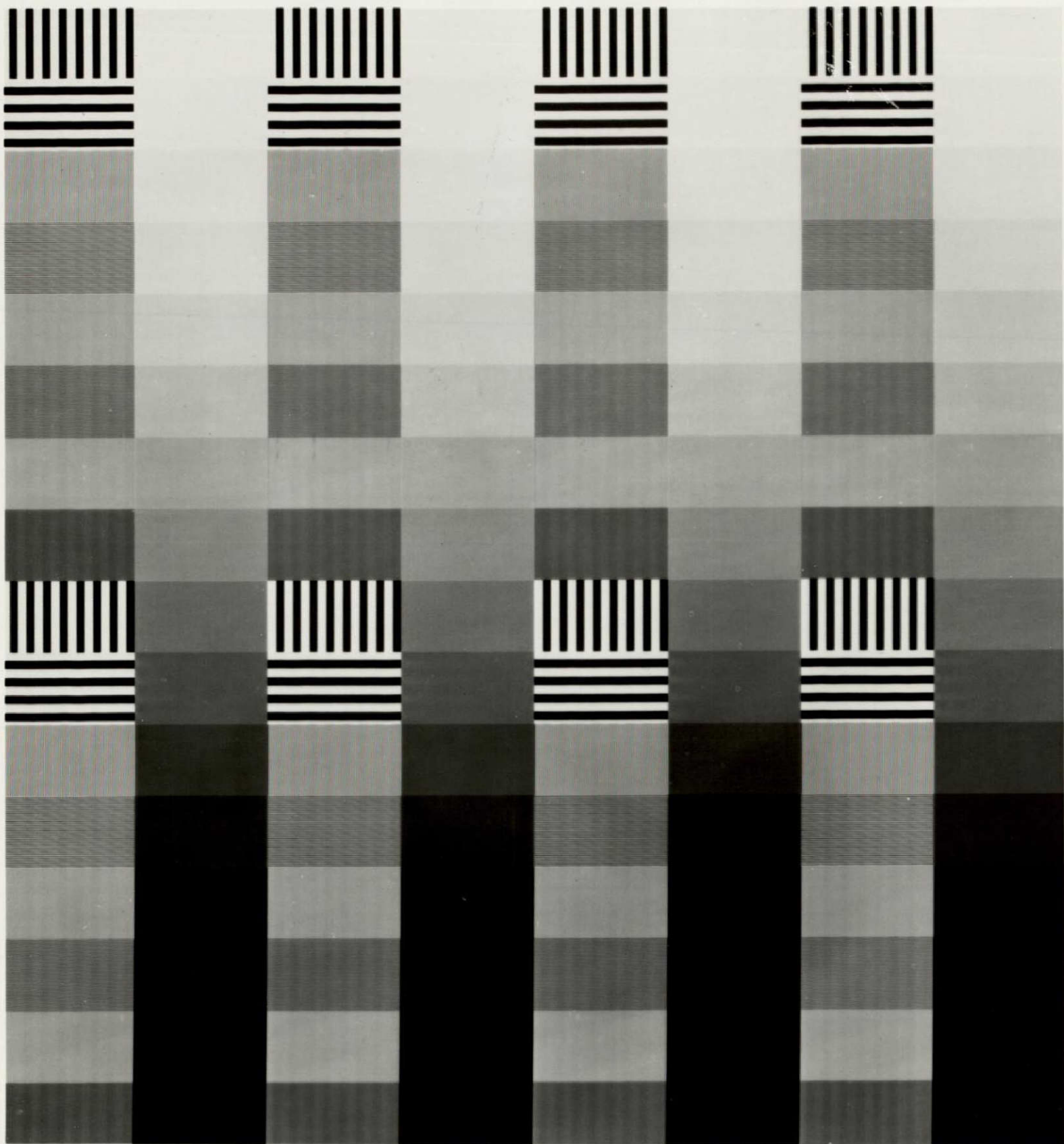BY ITEK EC-5/PLANIMAT

Figure 2.8-1

TEST PATTERN PRODUCED ON RCA ENGINEERING
MODEL LASER BEAM RECORDER